DOE/NASA/0096-1
NASA CR-159868

THERMAL ENERGY STORAGE SYSTEMS USING FLUIDIZED BED HEAT EXCHANGERS

Tom Weast
Larry Shannon
Midwest Research Institute

June 1980

Prepared for
NATIONAL AERONAUTICS AND SPACE ADMINISTRATION
Lewis Research Center
Under Contract DEN 3-96

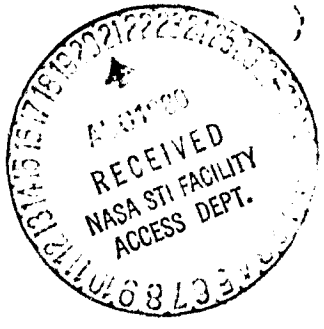

for
U.S. DEPARTMENT OF ENERGY
Office of Solar, Geothermal, Electric and Storage Systems
Division of Energy Storage Systems

NOTICE

DOE/NASA/0096-1
NASA CR-159868

THERMAL ENERGY STORAGE SYSTEMS USING FLUIDIZED BED HEAT EXCHANGERS

Tom Weast
Larry Shannon
Midwest Research Institute
425 Volker Boulevard
Kansas City, Missouri 64110

June 1980

Prepared for
National Aeronautics and Space Administration
Lewis Research Center
Cleveland, Ohio 44135
Under Contract DEN 3-96

for
U.S. DEPARTMENT OF ENERGY
Office of Solar, Geothermal, Electric and Storage Systems
Division of Energy Storage Systems
Under Interagency Agreement EC-77-A-31-1034

1 Report No	2. Government Accession No	3 Recipient's Catalog No
DOE/NASA 0096-1 NASA CR-159863		

4 Title and Subtitle	5 Report Date
THERMAL ENERGY STORAGE SYSTEMS USING FLUIDIZED BED HEAT EXCHANGERS	June 1980
	6 Performing Organization Code

7 Author(s)	8. Performing Organization Report No
Tom Weast and Larry Shannon	
	10 Work Unit No

9 Performing Organization Name and Address	11. Contract or Grant No
Midwest Research Institute 425 Volker Boulevard Kansas City, Missouri 64110	DEN3-96
	13 Type of Report and Period Covered Contractor Final Report January 1979 - January 1980

12. Sponsoring Agency Name and Address	14. Sponsoring Agency Code
NASA-Lewis Research Center 21000 Brookpark Road Cleveland, Ohio 44135	

15. Supplementary Notes

Final Report. Prepared under Interagency Agreement EC-77-A-31-1034. Project Manager, D. G. Perdue, Transportation Propulsion Division, NASA Lewis Research Center, Cleveland, Ohio 44135.

16. Abstract

The purpose of this study was to conduct a technical and economic assessment of the use of fluid bed heat exchangers (FBHX) for Thermal Energy Storage (TES) in applications having potential for waste heat recovery. A large number of industrial processes and solar power generation were considered to determine the applicability of a FBHX for TES. The potential applications were grouped on a unit operations basis so that if the system was applicable to one industry it may also be adaptable to other industries having similar unit operations. The rotary cement kiln and the electric arc furnace were chosen for evaluation using a variety of screening criteria.

Numerous potential FBHX configurations were evaluated to identify the most effective types for TES systems and ranked according to operating parameters such as efficiency of heat recovery, heat transfer rate, system pressure drop, environmental problems, stability of bed operation, etc. In order to maximize the system's effectiveness while minimizing parasitic power requirements, multistage shallow bed FBHX's operating with high temperature differences were identified as the most suitable for TES applications.

The technical feasibility of FBHX for TES systems has been verified by analysis of the two selected conceptual systems. Each technical evaluation included establishing a plant process flow configuration, an operational scenario, a preliminary FBHX/TES design, and parametric analysis. A computer model was developed to determine the effects of the number of stages, gas temperatures, gas flows, bed materials, charge and discharge times, and parasitic power required for operation.

The maximum national energy conservation potential of the cement plant application with TES is 15.4×10^6 barrels of oil or 3.9×10^6 tons of coal per year. For the electric arc furnace application the maximum national conservation potential with TES is 4.5×10^6 barrels of oil or 1.1×10^6 tons of coal per year.

Present time-of-day utility rates are near the breakeven point required for the TES system. Escalation of on-peak energy rates due to critical fuel shortages could make the FBHX/TES applications economically attractive in the future.

17. Key Words (Suggested by Author(s))	18. Distribution Statement
Thermal Storage Fluidized Beds	Unclassified - Unlimited Star Category - 44 DOE Category UC-94a

19. Security Classif. (of this report)	20. Security Classif. (of this page)	21. No. of Pages	22. Price*
Unclassified	Unclassified	215	

* For sale by the National Technical Information Service, Springfield, Virginia 22161

NASA-C-168 (Rev. 10-75)

FOREWORD

The work described in this report was sponsored by NASA-Lewis Research Center under Contract No. DEN 3-96 and was conducted by Midwest Research Institute (MRI). Several members of MRI participated in the program under the direction of Dr. K. P. Ananth. Principal authors of this report are Mr. Tom Weast and Dr. Larry Shannon.

MRI would like to acknowledge the assistance of Dr. Frederick Zenz, Consultant to MRI on the program, and the guidance provided by Messrs. Don Perdue, Larry Gordon, and Bert Phillips of NASA-Lewis Research Center during the conduct of this program.

Approved for:

MIDWEST RESEARCH INSTITUTE

L. J. Shannon, Executive Director
Engineering and Applied Sciences

TABLE OF CONTENTS

LIST OF FIGURES

LIST OF FIGURES (continued)

LIST OF FIGURES (concluded)

LIST OF TABLES

LIST OF TABLES (concluded)

EXECUTIVE SUMMARY

This systems study was conducted to determine the viability of using Fluidized Bed Heat Exchangers (FBHX) for Thermal Energy Storage (TES) in applications with potential for waste heat recovery.

The development of efficient TES systems is necessary for many energy conservation programs to be technically and economically attractive. By utilizing the mass of a fluidized material for thermal energy storage, the energy transfer and storage functions can be integrated into a common FBHX/TES system. The objective of this project was to identify and analyze operating characteristics and economics of potential FBHX/TES systems when used for waste heat recovery and utilization. The conceptual study formulated to address this objective was divided into two major tasks. Task I defined potential FBHX concepts and identified potential applications into which TES can be efficiently integrated. Task II evaluated the technical and economic feasibility of the two most promising systems identified in Task I and recommended one application for additional study or demonstration.

FBHX Concept Definition

Since the TES medium is the mass of the FBHX bed material, it was necessary to evaluate the various FBHX configurations for identification of the most effective types for TES systems. Numerous configurations of fluidized bed heat exchangers are possible. The various potential fluidized bed heat exchanger/ storage configurations were ranked according to such operating parameters as efficiency of heat recovery, heat transfer rate, system pressure drop, environmental problems, stability of bed operation, etc.

Based on the review of FBHX configurations, multistage shallow bed systems with external storage of nonfluidized solids was chosen as the most promising system.

TES Application Identification

A large number of industrial processes, solar power generation, and HVAC systems were considered for potential application of FBHX for TES. Due to the large number of potential applications, they were grouped by unit process with similar waste stream characteristics. Thus, a selected FBHX/TES system for a unit process in one industry may also be adaptable to other industries with similar unit processes. Flow charts were obtained for the unit processes and energy balances performed in order to evaluate the potential for energy recovery.

Integration and Selection

In order to reduce the potential applications to the most promising systems for a more detailed review, a number of criteria were selected for the processes. Of the candidate applications screened, Cement Plant Rotary Kilns and Steel Plant Electric Arc Furnaces were identified, based on the chosen selection criteria, as having the best potential for successful use of FBHX/TES system.

The process flow configuration for the two applications are similar in that the TES charge cycle for both designs uses hot exhaust gases to heat the bed material (sand) in a counter flow multistage, shallow FBHX. The hot solids are then stored in an insulated structure until the multistage shallow FBHX is used to heat low temperature gases for a waste heat boiler. The cooled solids are stored in another insulated structure to await the next charge cycle. The electric arc furnace application also includes a buffer FBHX/TES to smooth the short duration (2 to 3 hr) periodic variations in gas temperature before proceeding to the long-term FBHX/TES described above.

Technical Evaluation

The technical analysis included a parametric analysis to determine the optimum FBHX/TES design. A computer model was developed to determine the effects of the number of stages, gas temperatures, gas flows, bed materials, charge discharge times, and parasitic power required for operation.

For the two industrial process applications that were studied in detail, significant quantities of energy can be recovered via a waste heat boiler and turbine-generator set. The inclusion of thermal energy storage increases the flexibility of operation of the selected applications, however, the parasitic power required to operate the TES system and the thermal losses which occur when the thermal energy is stored and retrieved results in a net reduction in useful energy output. The resulting trade-offs between total useful power recovered and flexibility of operation depend on the operating scenarios selected for potential applications.

For the cement plant application the operating scenarios consisted of a 12-hr charge mode with 80% of the kiln exhaust gases going directly to the waste heat boiler while the remaining 20% goes to the TES system. The 12-hr discharge mode completes the scenario with 100% of the kiln exhaust gases going directly to the waste heat boiler plus 20% of the cooled boiler exhaust which is reheated by the TES system. The energy recoverable without storage is 132 kwh/ton of cement. With TES, the net energy recoverable is reduced 5%, however, the TES gives an 18% energy shift from the charge to discharge mode.

For the steel plant application the operating scenario consisted of a 12-hr charge mode with all the electric arc furnace exhaust gases going to the TES system. The 16-hr discharge mode which completes the scenario has all of the electric arc furnace exhaust gases going directly to the waste heat boiler plus an additional 50% which is reheated by the TES system. The energy recoverable without TES is 116 kwh/ton of steel. With TES the net energy recoverable is reduced 20%, however, the TES system gives a 44% energy shift from the charge to discharge mode.

Without TES, the model cement plant would have an energy savings potential of 364 barrels of oil per day or 92 tons of coal per day. The model electric arc furnace steel plant would have an energy savings potential of 152 barrels of oil per day or 38 tons of coal per day. The maximum potential energy savings with 100% of all plants participating is 16.3×10^6 barrels of oil or 4.1×10^6 tons of coal per year for the cement plant applications, and 5.7×10^6 barrels of oil or 1.4×10^6 tons of coal per year for the steel plant application.

With TES, the model cement plant would have an average energy savings potential of 345 barrels of oil per day or 88 tons of coal per day. The energy shift from TES charge to TES discharge is equivalent to 32 barrels of oil per day or 8 tons of coal per day. On a national level the potential energy savings are 15×10^6 barrels of oil per year or 4×10^6 tons of coal per year, while the energy shift from TES charge to TES discharge is equivalent to 1.4×10^6 barrels of oil per year or 0.4×10^6 tons of coal per year.

The model electric arc furnace would have an average energy savings potential of 720 barrels of oil per day or 30 tons of coal per day. The energy shift from TES charge to TES discharge is equivalent to 54 barrels of oil per day or 14 tons of coal per day. On a national level the potential energy savings are 4.5×10^6 barrels of oil per year or 1.1×10^6 tons of coal per year, while the energy shift from TES charge to TES discharge is equivalent to 2.0×10^6 barrels of oil per year or 0.5×10^6 tons of coal per year.

Economic Evaluation

In the economic analysis the estimated capital investment costs, annual operating costs, and unit energy costs to construct and operate each model system were determined. Capital investment costs represent the total investment required to construct a new system and will include direct costs, indirect costs, contractor's fees, and contingency. Annual operating costs represent the variable, fixed, and overhead costs required to operate the systems. Unit energy costs for each model system are the annual operating cost of the system divided by the annual energy savings. All costs associated with the waste heat boiler system and the fluidized bed heat exchanger TES system were determined separately.

When the energy recovery system does not include TES the cost of on-site generated power must be sufficiently less than the cost of equivalent purchased power to pay for the waste heat boiler and turbine generator and provide an attractive return on investment. The recovery systems without storage would be feasible in many parts of the country with present utility rate structures. The economic analysis revealed that the system economics with TES are extremely sensitive to the differential price of the displaced purchased utility power during the TES charge and discharge modes. This is due to the parasitic power and thermal losses associated with TES which reduce the net recoverable energy slightly. Therefore, the economic advantage of the energy shift which is available with TES must be large enough to recover the value of the net energy reduction as well as the investment required to provide TES.

Examination of several time-of-day utility rate structures was encouraging. If sufficient differentiation occurs between on-peak and off-peak energy rates as peaking fuels such as oil become more expensive, then TES via FBHX may offer significant economic advantages. The minimum differentiation for a break-even operation of the TES without capital recovery requires the ratio of on-peak to off-peak energy charges to be 1.76 for the cement kiln application and 1.92 for the electric arc furnace application. In order to recover the incremental capital investment required for TES and provide a return on their incremental investment the ratios would have to be significantly higher. For example, doubling of the above ratios results in a simple pay back of approximately 15 years at present utility rates.

Most utilities do not presently differentiate between the power demand charge for regular customers and the standby power demand charge for operators of waste energy recovery systems. Reduced demand charges for the waste heat recovery systems would provide additional economic benefits and increase the economic feasibility of FBHX/TES.

Recommendations

Specific R&D areas which could be pursued in the near term are:

1. Collection of data for the cement kiln application to determine the electrical load profile and waste heat available in specific plants which might be candidates for TES installation and demonstration.

2. Detailed technical and economic evaluation of the electric arc furnace application with only the TES/buffer.

3. Analysis of current utility rates and prediction of future trends in time-of-day utility pricing which could make FBHX/TES more economically attractive.

1.0 INTRODUCTION

Energy conservation is an important component in any plan to reduce energy use in the United States. One area for energy conservation that has promise is the utilization of thermal energy recovery and energy storage technology in selected applications.

All thermal energy storage (TES) concepts have one common problem, i.e., the application of highly efficient and economical heat exchangers. Systems used for recovery of sensible heat generally consist of conventional tubular type exchangers or involve direct contact of a working fluid with the storage media. The major concerns of these concepts are requirements for large heat transfer surface areas or plugging of the flow by loose particles. In latent heat transfer, serious problems with the accumulation and removal of salt deposits on heat transfer surfaces may be encountered. As a means for overcoming these problem areas, a number of heat exchanger designs have been and are being investigated, including fluidized bed heat exchangers (FBHX).

Fluidized solids have been used for heat transfer since the first catalytic cracking units were constructed for the petroleum industry in the early 1940's. Numerous experimental studies of gas, liquids and solids flow and of heat transfer in fluidized beds have been reported. The results obtained on heat transfer in general, and on heat transfer to and from surfaces in fluidized beds, indicate that heat transfer coefficients are intermediate between gas and liquid values for the same velocities of flow. The increased heat transfer rates realized with fluidized solids make a fluidized bed heat exchanger an attractive concept for integration into thermal energy storage systems. However, as with any heat exchanger/energy storage/application combination, technological uncertainties and potential component/system integration problems exist which must be analyzed before the overall technical and economic feasibility can be defined.

Under NASA Contract No. DEN 3-96, Midwest Research Institute (MRI) conducted a study to identify and parametrically analyze the operating characteristics and the economics of potential thermal energy storage applications utilizing fluidized bed heat exchangers. Two major tasks comprised the study: Task I - Application Identification, Fluidized Bed Concept Definition, and Integration of Applications with Fluidized Bed Concepts, and Task II - Technical and Economic Evaluation of Selected Applications and Fluidized Bed Concepts.

In Task I, industrial processes, solar power generation and building and community heating ventilating and air conditioning (HVAC) systems were first screened to identify potential applications. Both high temperature (> 250°C) and low temperature (< 250°C) thermal energy storage applications were considered. Six potential applications for thermal energy storage which could utilize fluidized bed heat exchangers were identified. Following selection of the applications, fluidized bed concepts were developed and evaluated for subsequent

integration with the potential applications. The final activity in Task I involved the selection of two of the six potential applications/fluidized bed heat exchanger concepts for further technical and economic evaluation in Task II.

In Task II a technical analysis and an economic evaluation were performed for the two applications selected in Task I. Each application was parametrically analyzed and evaluated. This techno-economic assessment included: (a) system thermocycle efficiency; (b) estimates of physical size and system component costs; (c) qualitative and quantitative benefits; and (d) estimates of capital, operation and maintenance costs with appropriate contingency for development processes and uncertainties.

The following sections of this report present a discussion of the activities conducted in Tasks I and II, the conclusions which were reached and recommendations for future R&D efforts. Four appendices are also included with the report. Appendix A presents schematic flow diagrams of the applications considered in the study; Appendix B illustrates typical hand calculations for determining the basic FBHX/TES design and operating parameters; Appendix C presents the computer program developed for the more detailed final design of fluidized beds and the parametric analysis; and Appendix D gives the equations for a special multistage buffer design for one of the selected applications.

2.0 APPLICATION IDENTIFICATION, FLUIDIZED BED HEAT EXCHANGER CONCEPT DEFINITION, AND INTEGRATION OF APPLICATIONS WITH FLUIDIZED BED CONCEPTS (Task I)

Activity on this task consisted of three major subtasks preceded by an information acquisition step. The major subtasks were: (a) identification of potential applications of fluidized bed heat exchangers for TES systems; (b) definition of potential concepts of fluidized bed heat exchangers applicable to TES; and (c) matching of heat exchanger concepts with potential applications.

The information acquisition step included:

* Computerized literature searches covering information on (a) thermal energy utilization and losses in process industries, (b) solar energy power generation systems, (c) energy systems for building and community complexes, and (d) electric power plants, etc.

* Computerized literature searches covering fluidized bed technology, heat transfer by fluidized beds, modeling of fluidized beds, energy storage via fluidized beds, etc.

* Review of Department of Energy (DOE) reports on waste energy recovery, energy storage, energy conservation and/or consumption.

* Review of the Environmental Protection Agency (EPA) technical reports related to effluent or emission guidelines for industries to obtain proces flow diagrams, primary energy balances, and effluent characteristics.

The type of data collected consisted of (a) characteristics of waste energy streams such as quantities and forms of energy discharged, pressure, temperature, etc., and (b) characteristics of various fluidized bed systems and factors that determine their compatibility for TES applications. These data were then utilized in the conduct of the three major subtasks which are discussed in detail in the following sections of this report.

2.1 APPLICATION IDENTIFICATION AND SELECTION

A wide range of candidate applications for the use of fluidized bed heat exchangers were reviewed in order to identify the applications which would be studied in detail. Specific activities involved in the application identification effort are discussed next.

2.1.1 Application Identification

The review of applications focused on three broad categories: industrial processes, power generation (including solar Brayton cycle) and furnaces and boilers used for HVAC purposes.

2.1.1.1 Industrial Process Applications--

A wide variety of industrial manufacturing processes was reviewed to identify potential waste energy streams for which fluidized bed heat exchangers might be used for energy recovery and storage. Table 1 presents a list of potential applications.

In addition to the industries delineated in Table 1, we also searched for applications in the chemical and allied products industries.* The chemical and allied products industries manufacture thousands of products, many of which are manufactured with totally different technologies. Opportunities for waste energy recovery clearly exist, but specific applications for fluidized bed heat exchangers are difficult to define because of the myriad of processes and process options and the lack of available process information and waste energy stream data. General opportunities identified are:

1. Rejected heat in hot air from compressors.

2. Waste heat from process streams.

3. Waste heat in stack gases.

4. Waste heat in exhaust streams from furnaces, dryers, reactors, and distillation columns.

The petroleum refining industry presents the same type of problem as encountered in the chemical and allied products industry--a wide range of waste energy recovery possibilities, numerous process options, and limited data on waste energy streams. A further complication is the lack of information available on the extent of energy recovery already practiced in the industry.

Processes used in petroleum refineries were studied in some detail to identify possible energy recovery opportunities. Because there are so many different processes used in different ways in hundreds of petroleum refineries, it is impossible to define the average refinery. Our analysis, therefore, focused on general opportunities for waste energy recovery, and the principal opportunities we identified are:

1. Waste heat in various process streams.

2. Stack gases from distillation columns, catalytic cracking units, fractionation units, etc.

---

* Category includes such diverse segments as Organic and Inorganic Chemicals, Drug Industry, Soap and Detergent, Gum and Wood Chemicals, Coal Tar Chemicals, Paint and Varnish, etc.

TABLE 1

PRELIMINARY LIST OF WASTE ENERGY STREAMS FOR WHICH FLUIDIZED BED HEAT EXCHANGERS MIGHT BE USED FOR ENERGY RECOVERY AND STORAGE

Industry	Waste Energy Stream
Iron and Steel	1. Sinter and Pellet Machine/Cooler Stack Gases 2. Electric Arc Furnace Exhaust Gases 3. Soaking Pit Stack Gases 4. Reheating Furnace Stack Gases 5. Annealing and/or Forging Furnace Stack Gases
Iron Foundry	1. Cupola Exhaust Gases 2. Electric Arc Furnace Exhaust Gases
Steel Foundry	1. Electric Arc Furnace Exhaust Gases
Ferroalloy	1. Electric Arc Furnace Exhaust Gases[a/]
Nonferrous Foundry	1. Electric Arc Furnace Exhaust Gases 2. Reverberatory Furnace Exhaust Gases[b/] 3. Crucible Furnace Exhaust Gases
Primary Copper	1. Concentrate Roaster Exhaust Gases 2. Reverberatory Furnace Exhaust Gases 3. Matte Converter Exhaust Gases 4. Copper Refining Furnace Exhaust Gases
Primary Aluminum	1. Rotary Kiln Exhaust Gases 2. Hot Alumina Stream 3. Electrolysis Cell Exhaust Gas Stream 4. Heat Treating/Remelting Furnace Exhaust Gases
Primary Zinc	1. Roaster Furnace Exhaust Gases 2. Sinter Machine Exhaust Gases
Primary Lead	1. Sinter Machine Exhaust Gases 2. Blast Furnace Exhaust Gases 3. Reverberatory Furnace Exhaust Gases 4. Softening Furnace Exhaust Gases
Secondary Nonferrous Smelting and Refining	1. Electric Arc Furnace Exhaust Gases 2. Reverberatory Furnace Exhaust Gases 3. Blast Furnace Exhaust Gases
Alkalies and Chlorine	1. Lime Kiln Exhaust Gases[c/]

TABLE 1 (concluded)

Industry	Waste Energy Stream
Inorganic Pigments (Zinc Oxide)	1. Roaster, Refinery Furnace, and Kiln Exhaust Gases
Cement	1. Cement Kiln Exhaust Gases 2. Cement Cooler Exhaust Gases
Lime	1. Lime Kiln Exhaust Gases 2. Lime Cooler Exhaust Gases
Phosphate Fertilizer	1. Phosphate Rock Dryer or Kiln Exhaust Gases 2. Product Dryer Exhaust Gases 3. Product Cooler Exhaust Gases
Nitrogen Fertilizer	1. Rejected Heat in Exhaust Gases from Furnaces, Turbine Compressors, Air Coolers, etc. 2. Product Dryer Exhaust Gases
Clay or Ceramic Products	1. Dryer Exhaust Gases 2. Kiln Exhaust Gases
Petroleum Refining	1. Rejected Heat in Stack Gases from Heaters, Boilers, Furnaces, Flares, etc.
Pulp Mill	1. Boiler Exhaust Gases 2. Recovery Furnace Exhaust Gases 3. Lime Kiln Exhaust Gases
Asphalt Paving Plants	1. Rotary Dryer Exhaust Gases
Glass	1. Rejected Heat in Exhaust Gases from Furnaces 2. Annealing Tunnels or Oven Exhaust
Food Processes	1. Rejected Heat to Boiler Exhaust Gases 2. Heat from Hot Water Waste Streams
Textiles	1. Rejected Heat from Boiler Exhaust Gases

a/ High CO content of gas stream may prohibit usage except as a direct fuel.
b/ Many plants use waste-heat boilers or recuperators to recover waste heat from this stream. Extent of application may be limited.
c/ Lime kiln used in sodium carbonate manufacture.

There are numerous applications of fluidization in the petroleum refining industry for product production, but the extent to which fluidized bed heat exchangers may have been considered for energy recovery is an open question. In view of the industry's familiarity with this technology, the industry might be expected to have looked at the possibility of using fluid beds. This point was discussed with Dr. Zenz, our consultant, and with knowledgeable industry personnel. We were not able to identify any significant use of fluid bed units in the industry for heat recovery/storage purposes. We believe that the reasons the industry probably has not taken a hard look at fluid bed heat exchangers are that (a) the existing heat balances are already quite good (i.e., the processes are efficient enough), and (b) that there is not enough economic incentive to install such equipment and systems.

An examination of the waste energy streams listed in Table 1 and discussed in the preceding paragraphs discloses a considerable degree of commonality in unit processes or operations. This commonality suggests a grouping based on the unit process or operation rather than by industry. Table 2 presents one such grouping.

A significant advantage results from this approach. Namely, if a fluidized bed heat exchanger/energy storage system can be shown to be technically feasible for a specific unit process or waste stream common to several industries, implementation in several industries might occur.* The approach can be illustrated by considering the similarity in the characteristics of exhaust gases from kilns used to calcine mineral materials such as limestone, bauxite, etc. Table 3 presents representative data on the characteristics of exhaust gas streams from various mineral calcining kilns. The overall similarity of the individual streams is apparent, and one can expect that if a fluidized bed heat exchanger/energy storage system were shown to be technically feasible for one industry it would also be feasible for the others.

* Economic feasibility is likely to be industry specific and involve a careful study of economic factors peculiar to a given industry.

TABLE 2

POTENTIAL INDUSTRIAL APPLICATIONS OF FLUIDIZED BED HEAT EXCHANGERS AS A FUNCTION OF UNIT OPERATIONS OR WASTE ENERGY STREAMS

Unit Process/Waste Energy Stream	Application
1. Kiln Exhaust Gases	Cement Lime Sodium Carbonate Pulp Mill Zinc Oxide Primary Aluminum Clay and Ceramic Products Phosphate Fertilizer
2. Clinker Cooler Exhaust Gases	Cement Lime Phosphate Fertilizer
3. Sinter and Pellet Machine/ Cooler Exhaust Gases	Iron and Steel Primary Zinc Primary Lead
4. Electric Arc Furnace Exhaust Gases	Iron and Steel Iron Foundry Steel Foundry Ferroalloy Nonferrous Foundry Secondary Nonferrous Smelting and Refining Refractories
5. Reverberatory Furnace Exhaust Gases	Primary Copper Primary Lead Nonferrous Foundry Secondary Nonferrous Smelting and Refining
6. Blast Furnace Exhaust Gases	Primary Lead Secondary Nonferrous Smelting and Refining
7. Mineral Dryer Exhaust Gases	Phosphate Fertilizer Clay and Ceramics Products Asphalt Paving
8. Compressor Exhaust Air	Chemical and Allied Products Pneumatic Machinery Compressed Gas Chillers

TABLE 2 (concluded)

Unit Process/Waste Energy Stream	Application
9. Distillation Column Exhaust Streams	Chemical and Allied Products Petroleum Refining
10. Internal Combustion Engine Exhaust Gases	Prime Movers, Standby Electric Power Generation, Municipal Power Plants, Irrigation
11. Wash Water Drains	Food Processing Textiles
12. Cupola Exhaust Gases	Foundry
13. Boilers	Industrial Plants Space Heating

TABLE 3

REPRESENTATIVE DATA ON THE CHARACTERISTICS OF EXHAUST GAS STREAMS FROM MINERAL CALCINING KILNS

Industry	Temperature °C (°F)	Flow Rate	Chemical Composition (% volume)	Moisture Content (vol. %)
Cement Kiln	66-454 (150-850)	0.016-212 m^3/sec (34-450,000 acfm) 0.042-293 m^3/sec (90-620,000 acfm)/ton of product	CO_2: 17-25 O_2: 1-4 CO: 0-2 N_2: 75-80	1-40
Lime Kiln	316-982 (600-1800)	0.024-94.4 m^3/sec (50-200,000 acfm)/ton of product	CO_2, O_2, N_2, H_2O SO_2	-
Pulp Mill Lime Kiln	204-482 (400-900)	0.003-23.6 m^3/sec (7-50,000 scfm)	CO_2: 16-22 CO: 0-0.7 O_2: 0.3-5 N_2: 77-78	-
Bauxite Kiln (Primary Aluminum)	121-399 (250-750)	0.012-63.7 m^3/sec (25-135,000 scfm)	CO_2, O_2, N_2, H_2O	40-50
Sodium Carbonate Lime	260 (500)	-	CO_2, O_2, N_2, H_2O	-

2.1.1.2 Solar Power Generation Applications--

The generation of electrical power by solar systems for commercial consumption is an emerging technology. Design data for flow rates, temperatures, heat transfer rate, heat flux, interruption times, turbine sizes, etc., as well as proposed thermodynamic cycles and media were used to evaluate the possibilities for using fluidized beds for heat exchangers for TES in solar Brayton cycles.*

2.1.1.3 Boilers Used for HVAC--

Waste energy streams from boilers used for HVAC needs in various types of buildings represent a broad class of potential applications for fluidized bed heat exchangers. Steam boilers of various types and sizes are utilized in residential, commercial, and industrial applications. All boilers have similar operating characteristics and the recoverable energy from any type or size will generally be limited to removing energy from the stack gases. The two general classifications of boilers can be described as custom (on-site constructed) and package boilers.

Custom (on-site constructed) units are water tube boilers having a steam delivery capacity of 7,560 kg/sec (100,000 lb/hr) or more (2,800 and up boiler horsepower,** BHp). The large majority of these boilers are designed and constructed with economizers, heat recovery or preheater systems which make use of stack gas energy. As a result, there is little, if any, recoverable energy remaining in this gas. It is possible to use the fluidized bed heat exchanger concept as a heat recovery device in new boilers; however, boiler manufacturers believe that they are not cost competitive with other known heat recovery techniques. Current designs of these boilers operate in the efficiency range of 90 to 95%.

Packaged boilers can be of either the water tube or fire tube design. Water tube boilers range in size from 130 to 1,890 kg/sec (17,250 to 250,000 lb/hr) (500 to 7,200 BHp). Operating pressures range from 1.7 to 32.4 MPa (250 to 4,700 psig), and these boilers operate in the efficiency range of 80 to 85%. New boilers in this classification may or may not be equipped with economizers. Most designs will use sufficient passes of hot gas through the tube bundles to obviate the need for economizers and other heat recovery devices. Information obtained from boiler manufacturers is summarized in Table 4. The information given in this table was used to assess the potential of these boilers for fluidized bed heat exchanger/ storage applications.

2.1.2 Application Selection

A multivariate analysis technique was used to screen the unit operations shown in Table 2. The methodology for the multivariate screening analysis is shown schematically in Figure 1. This methodology was used to identify six unit operations which represent the best potential for thermal energy storage using fluidized bed heat exchangers.

* Design data were taken from preliminary designs for proposed systems.

** One boiler horsepower can deliver 33,475 Btu/hr.

TABLE 4

SUMMARY OF INFORMATION FOR HVAC AND PROCESS BOILERS

Type	Fuel	Size Range[a]	Normal Pressure (psi)[a]	Exhaust Gas Temperature	Volume Exhaust Gas	Efficiency (%)	Excess Air (%)[a]
Custom	Coal Oil Gas	> 1,890 kg/sec > 250,000 lb/hr (> 1,000 BHp)	2.1-34.4 MPa (300-4,700)	38-121°C (100-250°F)[c] above sat. steam temperature	21.88-25 / min.kg steam; 12-14 cfm/ BHp; 0.35-0.40 cfm/lb steam	90-95	25 17 15
Water tube	Coal Oil Gas	130-1,890 kg/sec (17,250-250,000 lb/hr) (10-1,000 BHp)	1.7-34.4 MPa (250-4,700 psi)	38-121°C (100-250°F)[c] above sat. steam temperature	21.88-25 / min.kg steam; 12-14 cfm/ BHp; 0.35-0.40 cfm/lb steam	78-88	25 17 15
Fire tube	Coal Oil Gas	2.5-261 kg/sec (345-34,500 lb/hr)	0.1-1.7 MPa (15-250 psi)	38-121°C (100-150°F)[c] above sat. steam temperature	21.88-25 / min.kg steam; 12-14 cfm/ BHp; 0.35-0.40 cfm/lb steam	80-88	25 17 15

a/ Varies somewhat with manufacturers.
b/ Is included in exhaust gas volume. Minimum exhaust temperature is at or above dewpoint of fuel used. Most manufacturers limit to 185-204°C (365-400°F) to prevent corrosion.
c/ Higher exhaust gas temperatures are coal-fired boilers.

METHODOLOGY FOR CONDUCTING MULTIVARIABLE SCREENING

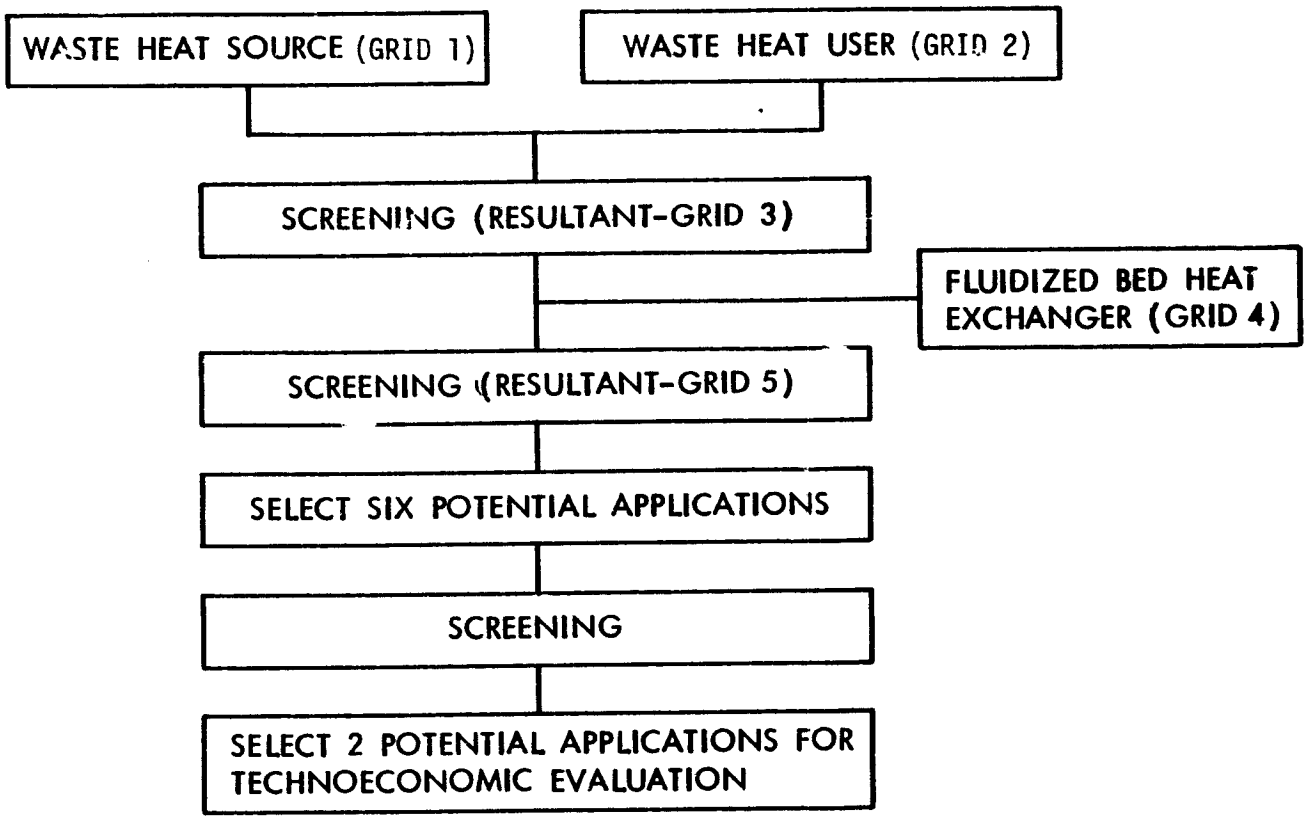

Figure 1 - Multivariable Analysis Flow Diagram

The first step in the screening process was to develop a grid to evaluate the unit operations on the basis of waste stream characteristics. Table 5 lists the elements of this grid. The unit operations were then ranked using the elements in Table 5.

Important characteristics of potential uses (e.g., feed material preheat, preheat of fuel and air, power generation) of the waste heat recovered from the unit operations were next defined via a second grid. Table 6 presents the elements of this second grid.

Next, grids 1 and 2 were matched to screen and evaluate applications and uses. Many of the elements of the grids did not provide a clear differentiation between applications, and it was necessary to select specific criteria to achieve the requisite screening. Five elements were finally selected from grids 1 and 2 as being the key criteria:

- Temperature of waste stream $\geq$ 38°C ($\geq$ 100°F)
- Flow rate of waste stream gas $\geq$ 4.2 m^3/sec ($\geq$ 10,000 cfm) or liquid $\geq$ 0.012 m^3/sec (200 gpm)
- Total annual waste available for recovery > 10^{15} J (> 10^{12} Btu/year)
- Need for energy storage
- Proximity of source to use

For example, if a unit operation (i.e., energy source) has a temperature of 38°C (100°F) or more, it fulfills the first criterion. Similarly, the other criteria are considered. The resulting grid based on screening with the five criteria is shown in Figure 2 (grid 3). In this screening process, the following unit operations were eliminated:

* Periodic Kilns (low flow rate)
* Dryers (waste energy available low, no need for storage)
* Air compressor (waste energy available low)
* IC engines (waste energy available low)
* Distillation column exhaust (low flow rate, no need for storage)
* Boilers (low flow rate, no need for storage)

The next step required the matching of the screening grid for energy source and use with a grid defining key elements for fluidized bed heat exchangers. The elements used for the fluidized bed heat exchanger grid were:

TABLE 5

ELEMENTS OF GRID USED TO EVALUATE UNIT OPERATIONS

1. Quantity of Waste Heat Available
   - > 20% input
   - 10-20% input
   - 3-10% input
   - < 3% input

2. Temperature
   - > 538°C (> 1000°F)
   - 316-538°C (600-1000°F)
   - 177-316°C (350-600°F)
   - < 177°C (< 350°F)

3. Stream Media
   - Single phase
   - Two phase
   - Three phase

4. Flow Rate
   - Continuous and steady
   - Continuous but variable
   - Intermittent but steady
   - Intermittent but variable

5. Seasonal Operation
   - Nonseasonal
   - Long season
   - Medium season
   - Short season

6. Corrosive
   - Noncorrosive
   - Slightly corrosive
   - Fairly corrosive
   - Extremely corrosive

7. Stream Hazards
   - Toxic
     - Nontoxic
     - Slightly toxic
     - Fairly toxic
     - Extremely toxic

TABLE 5 (concluded)

7. Stream Hazards (continued)
    - Explosive
        - Nonexplosive
        - Low order
        - Medium order
        - High order

8. Compatibility with Fluid Bed Heat Exchanger
    - Very
    - Fairly
    - Somewhat
    - Not

TABLE 6

ELEMENTS OF GRID USED TO DEFINE USE CHARACTERISTICS

Proximity (source to application)
- Within 61 m (200 ft)
- Within 61-152 m (200-500 ft)
- Within 152-305 m (500-1,000 ft)
- Over 305 m (1,000 ft)

Use Factors
- Temperature
  - Initial and final less than source (T_i and $T_f < T_s$)
  - Initial is less than source which is less than the final need ($T_i < T_s < T_f$)
  - Initial is less than source which is much less than final need ($T_i < T_s << T_f$)
  - Wide excursions of source or need for application
- Quantity of Energy Supplied
  - > 20% of needs
  - 10-20% of needs
  - 3-10% of needs
  - < 3% of needs
- Storage Time Required
  - Short (< 24 hr)
  - Medium (24-96 hr)
  - Long (96-960 hr)
  - Very long (> 960 hr)

Potential Energy Savings
- Very high
- High
- Medium
- Low

Energy source	Energy use	Screening criteria[a/] Temp. ≥ 38°C (≥ 100°F) 1	Q ≥ 4.2 m³/sec (≥ 10,000 cfm) 2	Waste energy ≥ 10^{15} J (≥ 10^{12} Btu/yr) 3	Need for storage 4	Proximity source-use 5
Rotary kiln/clinker cooler (cement)[b/]	Power boiler, feed preheat	X	X	X	X	X
Periodic kiln (ceramics)	Drying, kiln preheat	X	0	X	X	X
Sinter/iron ore (iron)	Mix preheat, boiler	X	X	X	X	X
Electric arc furnace (iron and steel)	Boiler	X	X	X	X	X
Reverberatory furnace (copper)	Boiler	X	X	X	X	X
Blast furnace systems (iron)	Boiler	X	X	X	X	X
Dryer (fertilizer)	No end use can be identified	X	X	0	0	X
Air compressor (chemicals, cryogenics)	Process hot water	X	X	0	X	X
Internal combustion engine (utility, industry, transportation)	No end use can be identified	X	X	0	X	X
Distillation column exhaust (chemicals, refining	Process hot water/steam	X	0	X	0	X
Washdown water (food)	Water preheat	X	X	X	X	X
Cupola exhaust (iron)	Blast air preheat, hot water	X	X	X	X	X
Boilers (industrial, commercial, residential)[c/]	Air/feedwater, preheat	X	0	X	0	X
Solar receptor (Solar Brayton Electric power plant)	Steam turbine, gas turbine	X	X	X	X	X
Coke oven (iron)	Boiler, charge preheat	X	X	X	X	X

Legend: X = Criterion fulfilled.
0 = Criterion not fulfilled.

a/ Criterion No. 1: Temperature of waste heat source stream--if ≥ 38°C (≥ 100°F), then X.
Criterion No. 2: Volumetric flow rate of the waste stream--if ≥ 4.2 m³/sec (≥ 10,000 cfm), then X.
Criterion No. 3: Potential energy content in the waste stream--if ≥ 10^{15} J (≥ 10^{12} Btu/year) equivalent, then X.
Criterion No. 4: Need for energy storage--if the supply does not match demand relative to time and quantity, then there is a need for storage and, hence, X.
Criterion No. 5: Proximity of source to user--if source and user are within reasonable distance, then X.

b/ A representative industry in each unit process is selected for criteria evaluation.

c/ Utility boilers eliminated because of their large size, efficiency of economizers, etc.

Figure 2 - Grid 3 - Integration of Energy Source and Energy Use

* Fluid media (gas preferred).*

* Waste stream temperature ≥ 260°C (≥ 500 F).

* Unique aspects of fluidized bed heat exchangers for storage (i.e., pollutant removal potential, advantages over packed beds, etc.).

The selection of these elements resulted from the review of fluidized bed heat exchangers discussed in Section 2.2. A gas media is preferred to liquid media for a fluidized bed heat exchanger, both for high temperature (> 250°C) and low temperature (< 250°C) applications. In general, fluidized bed heat exchangers become more attractive as the temperature differential between the fluidizing media and the bed material increases. For this reason, the minimum temperature criterion of the waste stream was raised to 260°C (500°F). Pollutant removal potential and mobility of the bed material are advantages of fluidized beds in comparison to packed beds.

The result of matching the fluidized bed heat exchanger grid with the screening grid for energy source and use is shown in Figure 3 (Grid 5). During this screening step, the following unit operations were eliminated:

* Blast furnace - low gas temperature

* Washdown water - liquid media

The unit operations which remain after the screening by the criteria in Grid 5 are presented in Table 7. The total waste energy available for recovery from these unit operations in various industries is also indicated in this table. Total waste energy available was estimated based on waste stream energy content per unit weight of the product and the production for the reference year (1976).

Based on the available waste energy data shown in Table 7 and the screening procedures, the six most promising unit processes were selected. Table 8 presents the unit processes and the industry chosen for the application. Two of the applications, dry quenching for coke ovens and solar Brayton power plant, represent technology not currently in use in the United States. Process flow diagrams for the selected applications are presented in Appendix A.

Dry quenching of coke is being used abroad and new coke oven batteries constructed in this country might use the dry quenching technique depending upon economic factors. The potential for energy recovery from this process is significant, and since the technology may be implemented in this country in the future, we included the process among the six most promising.

Although no solar Brayton power plants exist at this time, they represent a promising alternate energy source for the future as well as a potential application for fluidized bed heat exchanger/energy storage technology. The solar power plant is included in the group for these reasons.

* See Section 2.2. for a discussion of this point.

Energy Source	Energy Use	Screening Criteria[a/]			
		Media - Gas Preferred 1	Exhaust Temp. T ≧ 260°C (≧ 500°F) 2	Unique Aspects of Using Fluidized Bed 3a	3b
Rotary kiln/clinker cooler (cement)[b/]	Power boiler, feed preheat	X	X	X	X
Sinter/iron ore (iron)	Mix preheat, boiler	X	X	X	X
Electric arc furnace (iron and steel)	Boiler	X	X	X	X
Reverberatory furnace (copper)	Boiler	X	X	X	X
Blast furnace systems/coke oven (iron)	Boiler	X	0	X	X
Washdown water (food)	Water preheat	0	0	0	X
Cupola exhaust (iron)	Blast air preheat, hot water	X	X	X	X
Solar receptor (Solar Brayton electric power plant)	Steam turbine, gas turbine	X	X	NA	X
Coke oven (iron)	Boiler, charge preheat	X	X	X	X

Legend: X = Criterion fulfilled.
0 = Criterion not fulfilled.

a/ Criterion No. 1: X if the waste heat is gaseous; 0 if liquid.
Criterion No. 2: Temperature of waste heat source stream--if ≧ 260°F, then X.
Criterion No. 3: Unique aspects of using fluidized bed heat exchanger in the recovery/storage system--
(a) pollution removal potential--X if there is such potential;
(b) advantages over state-of-the-art high temperature storage system--X if such advantages exist.

b/ A representative industry in each unit operation is selected for criteria evaluation.

Figure 3 - Grid 5 - Integration of Energy Source, Energy Use, and FBHX

TABLE 7

REMAINING UNIT PROCESSES FROM THE MULTIVARIATE ANALYSIS AND THE ENERGY CONTENT OF THE WASTE STREAMS

Unit Operation	Applications	Annual Energy in Waste Stream 10^{15} J (10^{12} Btu/yr)
Rotary kiln and clinker cooler	Cement	149
	Lime	40.5
	Zinc oxidation	4.3
	Primary aluminum	8.3
	Clay and ceramic	17.2
	Phosphorus	1.8
Sinter and pellet machine	Iron and steel	44
	Zinc	0.7
	Lead	0.3
Electric arc furnace	Iron and steel	7.2
	Iron foundry	0.1
Reverberatory furnace	Copper	67
	Lead	1.1
	Secondary aluminum	3.9
Cupola	Iron foundry	1.5
Solar receptor	Solar Brayton power plant	*
Coke oven (dry quench)	Iron and steel	66.5

* According to our definition, the term "quantity of energy in waste stream" is not applicable in this case since total power generated in 1976 using solar receptors is negligible. Also, the hot gas stream from the solar receptor is the primary output rather than a waste stream. However, the proposed concept has the long range potential to replace conventional power plants.

TABLE 8

SELECTED APPLICATIONS FOR THERMAL ENERGY STORAGE USING FLUIDIZED BED HEAT EXCHANGER

	Unit Process	Application	Annual Energy in Waste Stream 10^{15} J (10^{12} Btu/year)
1.	Rotary kiln/clinker cooler	Cement	149
2.	Sinter and pellet machine	Iron and steel	44
3.	Electric arc furnace	Iron and steel	7.2
4.	Reverberatory furnace	Copper	67
5.	Coke oven (dry quench)	Iron and steel	66.5
6.	Solar receptor	Solar Brayton power plant	Not applicable

In order to select two of the six applications for a detailed techno-economic evaluation in Task II of the project, two approaches were considered. The first approach involved reexamination of the previous selection factors and weighting and prioritization of each criterion. The multivariate screening analysis would be repeated and each of the six potential fluid bed applications would be scored. The two best scores would then be recommended for further study. This approach was abandoned because the selection of weighting factors for the previous criteria was deemed to be too subjective. Also additional examination and attempted ranking of some criteria such as media or proximity would prove to be meaningless or lacking in sufficiently detailed information for evaluation.

The approach which was chosen involved the use of additional criteria and a final screening step. Since the initial screening process had already determined that the six final candidate applications were suitable for fluid bed heat exchanger/storage systems, the additional criteria focused on those aspects that were not considered previously.

The additional criteria considered were:

* Adaptability to candidate process

  + easily adapted--i.e., add on unit

  o some physical modification or process alteration required

  - extensive physical modification or process modification or no units presently in service

* Growth potential of candidate process

  + number of plants or process units increasing

  o stable industry

  - plants or process units decreasing due to alternate process, foreign competition, declining market, etc.

* Relative simplicity of operation

  + Simple controls and existing personnel

  o Moderate controls and retrained personnel

  - Complex controls and specialized personnel

* Timeliness

  + Short-term

  o Mid-term

  - Long-term

* Acceptability to candidate industry

  + Willing to try and invest in new ideas and equipment

  o Might try but reluctant to invest in new ideas and equipment

  - Reluctant to try and invest in new ideas and equipment

The results of the final screening process are presented in Table 9.

As a result of the screening process, the following candidate fluid bed heat exchanger/energy storage applications were selected:

* Cement Plant - Rotary Kiln/Clinker Cooler

* Steel Plant - Electric Arc Furnace

A brief summary which highlights the positive and negative factors which led to the selection of the cement plant-rotary kiln/clinker cooler and the steel plant-electric arc furnace as the recommended candidates for further evaluation and the elimination of the other four candidates is presented in the following paragraphs.

Cement plant - rotary kiln/clinker cooler - The cement plant-kiln/clinker cooler application was chosen because of the following favorable factors:

TABLE 9

EVALUATION OF ADDITIONAL FACTORS FOR THE SIX CANDIDATE APPLICATIONS

	Unit Operation	Application	Adaptability	Growth Potential	Simplicity	Timeliness	Acceptability
1.	Rotary kiln/clinker cooler	Cement	+	+	o	+	+
2.	Sinter and pellet machine	Iron and steel	o	o	+	+	o
3.	Electric arc furnace	Iron and steel	+	+	o	+	+
4.	Reverberatory furnace/converter	Copper smelting	+	-	o	+	+
5.	Coke oven (dry quench)	Iron and steel	-	-	-	o	o
6.	Solar receptor supplement	Solar Brayton power plant	-	+	o	-	-

1. There are a large number of units in operation in a growing industry.

2. The total recoverable energy, considering the total United States, is larger than any other application.

3. Fluid bed heat exchanger/storage systems can be integrated into cement plants without major plant modification.

4. The technology can be used in other industries which have calcining operations.

5. The cement industry is healthy and capital may be available to invest in plant modifications if economics are favorable.

6. There is a ready use for the recovered energy at a cement plant.

Steel plant - electric arc furnace - The steel plant-electric arc furnace application was chosen because of the following favorable factors:

1. There is a large number of units in operation and this number is increasing.

2. The recovery system can be integrated into the total system without major plant modifications; manufacturing process is not altered.

3. There is a ready use for the recovered energy at the steel plant.

The only major negative factor which might inhibit the acceptance of fluidized bed heat exchangers in the steel industry is the following:

1. The U.S. steel industry faces keen competition and may be reluctant to invest much capital unless savings are very favorable. This aspect can only be determined after a detailed economic assessment of the total system.

Copper smelting - reverberatory furnace/converter - The copper smelter-reverberatory furnace/converter application received the following favorable evaluation factors:

1. The recoverable energy potential is high.

2. The recovery system can be integrated without major plant modifications; smelting process is not altered.

3. There is a ready use for the recovered energy at the smelter plant.

The following negative factors were deemed to sufficiently outweigh the favorable factors when compared with the recommended applications:

1. There are two new competing smeltering processes. Of the 15 copper smelter operations in the United States, one already uses one of the new processes.

Adaption of fluid bed heat exchanger/storage systems to the new processes is not attractive.

2. Storage time will probably be very short, on the order of 4 to 10 min.

Steel plant - iron ore sintering - The steel plant-iron ore sintering application received the following favorable evaluation factors:

1. Recoverable waste energy is high.

2. There is a ready use for the recovered energy.

The following negative factors were deemed to sufficiently outweigh the favorable factors when compared with the recommended applications:

1. Substantial modification to sintering process will be required.

2. The modifications could alter the sintering process.

3. Less air flow will be available for controlling particulates emissions around the traveling grate.

4. Only buffer storage is required.

Steel plant - dry quench coke - The steel plant-dry quench coke application received the following favorable evaluation factors:

1. Recoverable waste energy is high.

2. Coke is a widely used material which is produced in a number of plants.

3. There is a ready use for the recovered energy at the steel plant.

The following negative factors were deemed to sufficiently outweigh the favorable factors when compared with the recommended applications:

1. Foreign coke can be purchased at a lower price than domestic coke at present which may suppress new investment in domestic coke plants.

2. Substantial changes other than the fluidized bed are required to convert the wet quench coke manufacturing process to the dry quench process which is presently not used in the United States.

Solar Brayton power plant - solar receptor supplement - The solar Brayton power plant-solar receptor application received the following favorable evaluation factor:

1. Emphasis on solar energy could result in widespread use of solar Brayton power generation.

The following negative factor was deemed to sufficiently outweigh the favorable factor.

1. No solar Brayton power plants are presently in use or contemplated in the near future.

2.2 FLUIDIZED BED HEAT EXCHANGER CONCEPT DEFINITIONS

Various fluidized bed heat exchanger concepts were studied to define those concepts suited for integration with potential applications. First, a general overview of concepts was performed, followed by a more detailed evaluation of the concepts deemed suitable for use in energy storage applications. The general overview and detailed evaluation are discussed in the following subsections.

2.2.1 General Overview of Gas Fluidized Bed Heat Exchangers

Fluidized bed concepts reviewed included single stage and multistage designs, counter flow and cross flow designs, fluidized beds with internal heat exchangers, and spouted beds. Each is briefly described in the following paragraphs.

2.2.1.1 Single Stage Fluid Beds--

A diagram showing the process flow in this type of heat exchanger is shown in Figure 4. Hot gas enters the base of the unit and passes through the distributor plate into the fluid bed. The upward moving gas exhausts to the atmosphere after passage through a cyclone separator which separates most of the entrained particulate. Feed particles at ambient temperature are charged to the bed on the one side of the unit, and hot particles are discharged on the opposite side as shown in the figure. Heat transfer occurs between the hot gas and the particles. The hot particles discharged from the heat exchanger can be sent to temporary storage in an insulated bin or used immediately in another fluid bed heat exchanger to heat some process material. This system depends upon heat recovery and storage in the solid particles in the fluid bed.

Due to rapid attainment of thermal equilibrium in a fluidized bed, the bed, exit gases, and the solids leaving the bed are essentially at the same temperature. Therefore, heat recovery in a single stage fluid bed is always low compared to multistage units (i.e., much heat is retained in the exiting hot gases). This type of system which offers the advantages of simplicity of design, reliable operation, and low equipment cost can be operated with either a shallow or a deep fluid bed.

An alternative single stage system arrangement using an internal heat exchanger is shown in Figure 5. In this system, a fixed quantity of solid particles can be used in the fluid bed without continuously charging and withdrawing particles. Hot gases, entering at the bottom through the distributor plate, heat the bed particles and the fluidized mass transfers heat to an internal heat exchanger. The configuration of the internal exchanger can be tailored for specific applications. Cool liquid enters at the base of the internal exchanger and hot liquid exits from the top. At optimized operating conditions, high

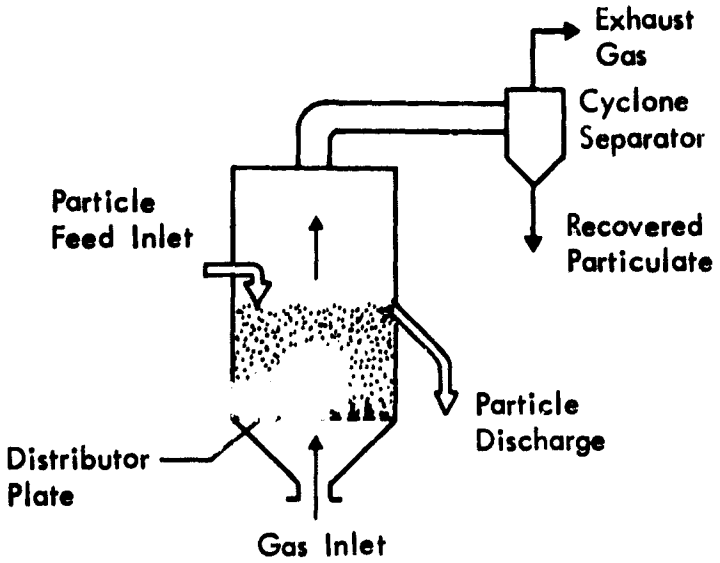

Figure 4 - Schematic Diagram of a Single Stage Counter Flow Fluid Bed Heat Exchanger

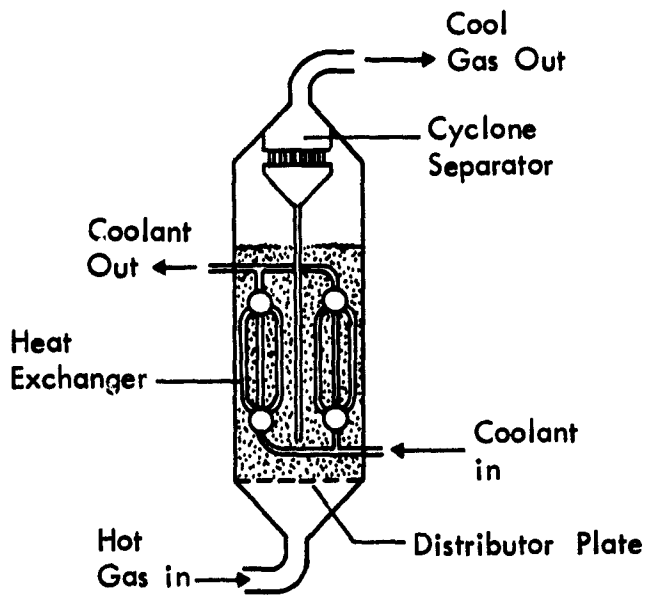

Figure 5 - Schematic Diagram of a Single Stage Fluidized Bed With an Internal Heat Exchanger

rates of heat transfer to the liquid can be realized. This type of operation is relatively simple and reliable and involves a relatively low system cost.

2.2.1.2 Multiple Stage Counter Flow Fluid Beds (Gas and Solids)--

A diagram of a multiple stage counter flow system is shown in Figure 6. The unit shown has four stages (i.e., four fluid bed sections) mounted vertically one above another. Commercial units normally have from two to four stages depending upon service requirements. These systems are most suitable for use with high temperature inlet gas streams.

In multiple stage operation, gas enters the base of the unit and passes upward successively through each stage distributor plate and fluid bed stage, and exits through the top of the unit to a cyclone separator and the atmosphere. Solids charged at the top of the unit move downward from one stage to another through downcomer pipes.

For a fixed number of stages, countercurrent contacting always has a higher thermal efficiency than a single bed unit; however, it is accompanied by a larger pressure drop and usually by a larger pumping energy requirement. Also, it is not easy to maintain a stable down flow of solids and to prevent an imbalance among the fluid beds. This system is considerably more complex and expensive than the single bed system. These systems may have either shallow or deep beds; shallow beds are most commonly used. Deep beds are more difficult to operate and control, and they involve a higher pressure drop through the system.

An alternative system arrangement involves the use of internal heat exchangers in multiple stage fluid beds. In this system, internal heat exchangers can be located in each fluid bed section as shown in Figure 7. Hot gas enters the base and moves upward through the vertically mounted fluid bed sections and exits at the top of the unit. Heat exchanger pipes, connected in series, are mounted in each fluid bed stage. Cool fluid enters the internal heat exchanger of the top fluid bed stage, flows progressively downward, and exits from the heat exchanger in the bottom fluid bed unit.

2.2.1.3 Cross Flow Fluid Beds (Gas and Solids)--

A cross flow multistage bed system for heat transfer is shown in Figure 8. Four fluid beds located at the same level are included in this unit. Portions of the same hot gas stream enter the base of each bed through a distributor plate. The combined cool gases leaving the fluid beds are discharged from the top of the unit. Solids are fed into one end of the unit, move successively through each bed, and are discharged at the opposite end of the unit. Heat exchange occurs between the hot fluidizing gas and the bed solids. After a period of retention in each bed the solids move from one bed to an adjacent bed located farther from the feed point.

As compared with the multiple stage counter flow system with the same number of stages, the cross flow system has a lower thermal efficiency but is accompanied by a lower pressure drop and usually by a lower pumping energy requirement. The cross flow arrangement has the advantages of lower power consumption, simpler equipment construction, and more reliable solids movement.

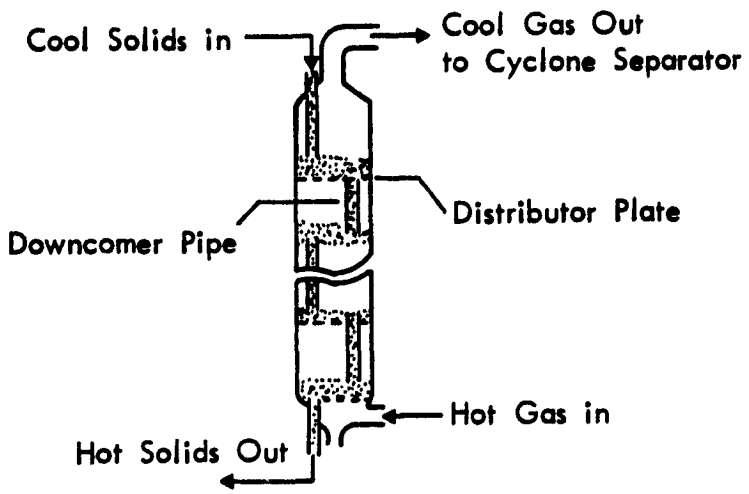

Figure 6 - Schematic Diagram of a Multistage Counter Flow Heat Exchanger

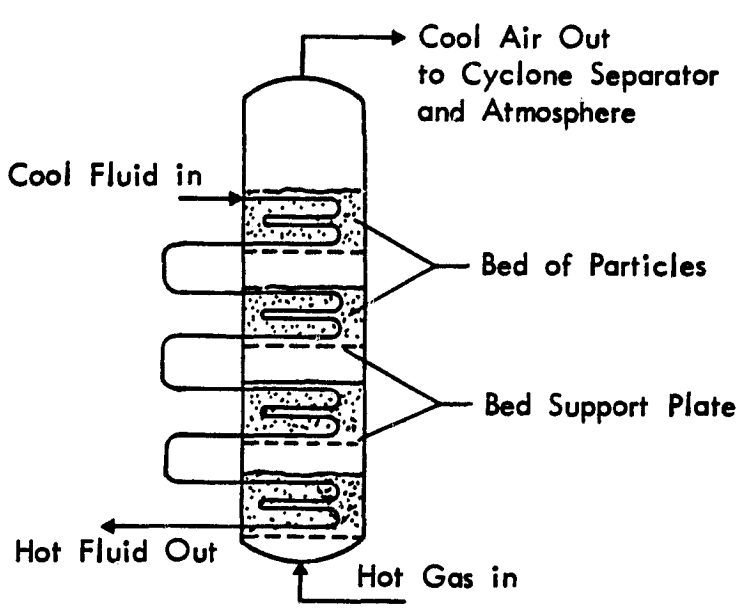

Figure 7 - Schematic Diagram of a Vertical Multistage Fluid Bed System with Internal Heat Exchanger

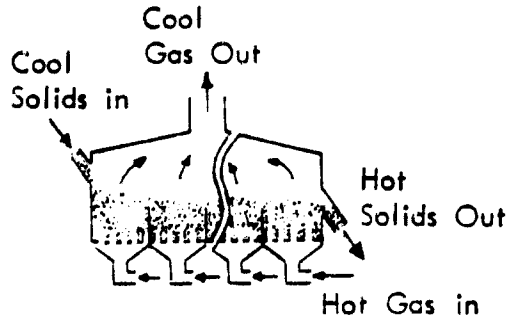

Figure 8 - Schematic for Multistage Cross Flow Fluidized Bed System

The rapid movement of particles can result in nonuniform residence times of solids in each fluid bed (e.g., short-circuiting of solids); this can result in nonuniform heating of the solids. Usually this operating problem is not a serious one. Cross flow systems can be operated with either shallow or deep beds. Since deep beds can result in excessive pressure drops and power requirement, shallow beds are more commonly used.

A single stage cross flow fluid bed unit with an internal heat exchanger is shown in Figure 9. In this system, air serves to fluidize the incoming hot solid particles, and heat is transferred to the water circulating in the heat exchanger.

2.2.1.4 Spouted Bed Systems--

For operation with large particles (larger than 20 mesh) ordinary fluidization may not be practical, and so a modified contacting scheme, the spouted bed, can be used. The spouted bed is a combination of a jetlike upward moving dilute fluidized phase surrounded by a slow downflow moving bed through which the gas percolates upwards (Figure 10).

A spouted bed is formed by penetration of a fluid jet (usually a gas) through a bed of particulate solids. Circulation of the solids is started by acceleration of the particles by a high velocity gas jet. The upward movement of particles in the spout region is the controlling factor, and solid flow downward in the annulus region follows from this movement. Gas from the axial zone leaks into the surrounding dense phase because of the axial pressure gradient generated by the relative motion between gas and solids within the spout. A distinct interface exists between the spout and the annulus. The average upward velocity of particles in the spout is one or two orders of magnitude higher than the downward velocity in the annulus. High speed particles in the spout collide with some particles on the dense-phase side of the interface and move them over into the spout. These particles then join the upward moving stream. Most of the annular solids, however, travel down to the vicinity of the gas orifice

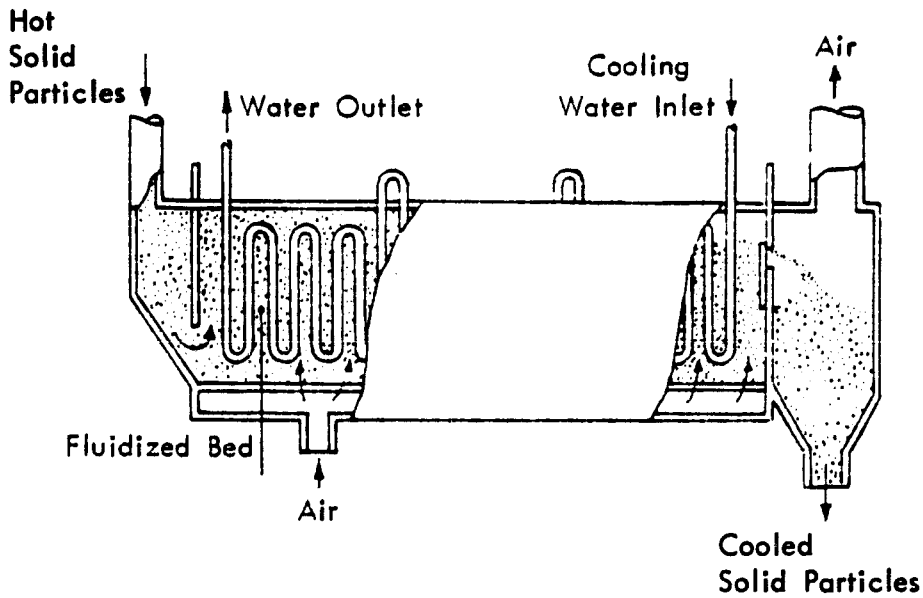

Figure 9 - Schematic Diagram of a Single Stage Cross Flow Fluid Bed Heat Exchanger

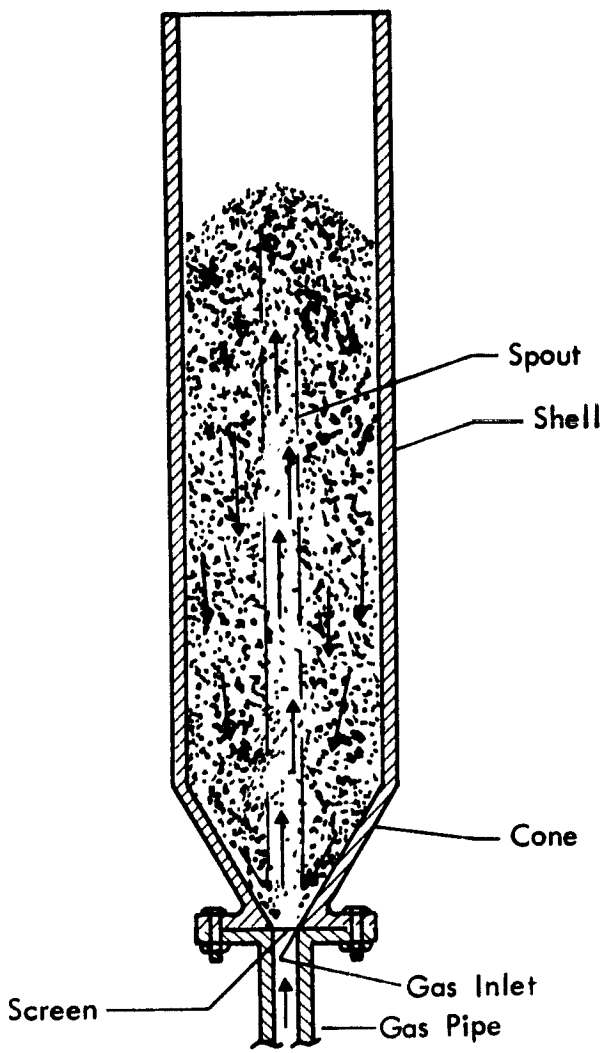

Figure 10 - Schematic Diagram of a Spouted Heat Exchanger (Batch Operation)

where they slide across the conical base and fall into the gas jet to resume their upward movement. Because of the combined effect of decreasing gas velocity and solids cross flow from the annulus, the concentration of particles in the spout increases and, beyond an initial zone of accumulation, their velocity decreases with increasing distance from the orifice. The coefficients of heat transfer in spouted beds are generally not as high as for fluidized beds.

The spouting action can be achieved with a liquid instead of a gas as the jet fluid. Liquid spouting, however, has not attracted much interest.

To date, applications of the spouted bed have been limited to a few physical operations such as the drying of grains and peas (i.e., large-sized particles).

2.2.2 General Overview of Liquid Fluidized Bed Heat Exchangers

An analysis of flow dynamics and heat transfer in liquid-fluidized beds is presented in the following paragraphs. Analogy between gas fluidized systems and liquid fluidized systems is discussed where appropriate, since the former is much more developed both in concept and practice.

2.2.2.1 Flow Dynamics--

As the fluid velocity through a bed of solid particles is gradually increased the state of incipient fluidization sets in where the fluid/particle system begins to behave like a fluid. At the onset of fluidization, the bed is more or less uniformly expanded and, up to this point, it makes little difference whether the fluid is a liquid or a gas apart from the fact that the velocity at which the bed becomes fluidized is less for a given bed particle size and density when the fluid is a liquid. Beyond this point, however, the bed behavior is markedly different. If the fluid is a liquid, the bed continues to expand uniformly with increase in the liquid velocity. If the fluid is a gas, the uniform expansion behavior is soon lost except with fine particles, the system becomes unstable and cavities or "bubbles" containing few solids are formed. In liquid-solid systems the bed voidage, ε , can be related to the superficial velocity U_f in the form,

$$\varepsilon = k\ (U_f)^n$$

where k and n are constants characteristic of the system.

The expansion characteristics of liquid- versus gas-fluidized systems lead to the difference in the type of fluidization, particulate (uniform dispersion of particles within the bed and uniform expansion) or aggregative (bed with bubbles). The magnitude of the density difference between the solids and the fluid determines whether the bed fluidizes particulately or aggregatively. The following generalization can be made:

High $(\rho_s-\rho_f)$ leads to aggregative fluidization

Low $(\rho_s-\rho_f)$ leads to particulate fluidization

Where ρ_s, ρ_f = density of solids and fluids, respectively.

There are conditions under which a liquid-fluidized system will exhibit the bubbling behavior characteristic of gas-fluidized beds. For example, lead shot/water systems fluidized aggregatively whereas glass beads/ water systems exhibit paticulate fluidization. This is consistent with the above generalization.

At high fluid velocities, whether the fluid is a gas or a liquid, a point is reached where the drag forces are such that the particles become entrained within the fluid stream and are carried from the bed. This is the state of solids transport.

2.2.2.2 Heat Transfer--

Most theoretical research on the practical application of liquid-fluidized beds has been in the proposed development of a liquid-fluidized bed nuclear reactor. Consequently, most heat transfer research has been concerned with obtaining coefficients between the fluidized liquid and the particles. Liquid fluidized beds, either small or large, operate isothermally just as gas fluidized beds do. Liquid can readily transfer a thousand times as much heat to the solid as can a gas film for a given temperature difference. Consequently, the predominant factor is heat transfer to the flowing fluid and the particles can affect the rate of transfer between the surface and the fluid in so far as they can erode away the laminar sublayer limiting transfer to the liquid. The following conclusions can be drawn concerning bed-to-wall heat transfer in liquid fluidized beds.

1. Heat transfer via a particle carrier mechanism is relatively unimportant; transfer by turbulent liquid eddies appears to be the main mechanism of heat transfer. This is in marked contrast to gas fluidized beds where the particle carrier mechanism is the dominant mode of heat transfer.

2. For a given particle size and type and a given liquid, the heat transfer coefficient is a function of bed porosity. A maximum value of the coefficient appears at a porosity of about 0.7 and its value is approximately 2 to 3 times higher than the packed bed coefficient.

3. The maximum value of the heat transfer coefficient is directly proportional to the diameter of the fluidized particles.

The above behavior can be explained as follows: as the bed porosity is increased, the relative fluid/particle velocities increase, thus reducing the limiting film thickness. Consequently, heat transfer coefficients increase.

At any given porosity, an increase in particle size also results in an increased relative fluid/particle velocity so further reducing the thickness of the limiting film, compared with the behavior with smaller particles. At the same time, larger porosities mean lower particle concentrations and the effect of the particles in reducing the film thickness through their scouring action will diminish. Because of this, the maximum in the Prandtl number at a porosity of about 0.7 to 0.75 is to be expected.

The feasibility of substituting fluidized bed shell and tube heat exchangers in the place of conventional preheaters to recover the heat from hot

geothermal brines has been studied by others (Allen, C. A., et al. Advances in Liquid-Fluidized Bed Heat Exchanger Development. Paper presented at A.I.Ch.E.-A.S.M.E. National Heat Transfer Conference, 1977 [Reference No. 77 HT 66]. Based on a review of this study and other pertinent literature the following conclusions can be drawn on the general applicability of liquid-fluidized beds:

1. The bed-to-tube surface heat transfer coefficient can be significantly increased with the used of a fluidized bed. In the above study, the coefficients were almost twice as high when the exchanger coil was exposed to the fluidized bed of sand, as when no bed was present. However, in liquid-to-liquid transfer situations where the cold-side wall-to-liquid film coefficients is limiting, increasing the hot-side film coefficient does not lead to reduction in heat transfer surface area. Generally, because of the high fluid velocity inside the tube, the cold-side coefficients are high and the hot side coefficient is limiting. Thus, in most cases use of a fluidized bed can potentially decrease the required heat transfer surface area.

2. When recovering heat from a hot liquid waste stream that is corrosive to the heat transfer surface, use of fluidized bed will offer advantages in minimizing corrosion. The continual scouring action of a fluidized bed keeps deposits off the surface.

3. Liquid-fluidized beds under most circumstances will have to operate at low temperatures, i.e., < 100°C (< 212°F), the boiling point of water. Thus, the applicability of liquid-fluidized beds is necessarily tied to the economics of recovering heat from a low level hot liquid stream.

2.2.3 Evaluation of Potential Fluidized Bed Heat Exchanger Concepts

The requirement that liquid-fluidized beds operate on low temperature liquid waste streams severely limits their applicability and they were dropped from further cosideration. The gas-fluidized bed heat exchanger concepts discussed in Section 2.2.1 were then evaluated to determine the more promising concepts for use in energy storage applications. A preliminary comparison of the characteristics of the various fluidized bed systems resulted in the following observations:

1. Single stage systems will likely be suitable only for use with low temperature inlet gas or solid streams.

2. Single stage systems offer the advantage of simplicity of design, reliable operation, and low equipment cost.

3. Multiple stage systems are most suitable for use with high temperature inlet gas or solid streams.

4. Multiple stage systems have a higher thermal efficiency and pressure drop than a single stage unit.

5. Shallow beds are more suitable for multiple stage systems than are deep beds because shallow beds are easier to operate and control, and have a lower pressure drop.

6. Multiple stage cross flow systems have lower thermal efficiency and lower pressure drop than do multiple stage counter flow systems with an equal number of stages.

7. The cross flow arrangement has the advantages over counter flow systems of lower power consumption, simpler equipment construction, and more reliable solids movement.

A more comprehensive evaluation of the fluidized bed heat exchangers was performed using screening matrices which were developed for low and high temperature applications.

In the ranking analysis, weighting factors were assigned on the basis of the anticipated relative importance of each heat exchanger parameter. These factors are shown in Table 10. The efficiency of heat recovery, which was considered to be the most important single criterion was given the maximum value of 6. The overall heat transfer rate, which is a direct function of the applicable heat transfer coefficients, was rated 5. Total pressure drop, which determines the important energy requirement, was assigned a value of 4. Capital cost, a major consideration in investment decisions, was considered to have a value of 4. Complexity of design, which contributes to difficulty of system installation and to cost was given a weighting factor of 2. Environmental problems and safety aspects, which can vary over a wide range depending on specific applications, were each assigned a value of 2. Stability of fluid bed operation was assigned a factor of 1. The state of development for a potential system was also assessed to be a consideration and was given a value of 1.

A rating rationale developed to evaluate the relative merit of different heat exchanger concepts in relationship to each heat exchanger parameter is shown in Table 11. No potentially applicable system was given a value of 0.

TABLE 10

WEIGHTING FACTORS USED IN EVALUATING FLUIDIZED BED HEAT EXCHANGER CONCEPTS

Fluidized Bed Concept Considerations	Assigned Weighting Factor
Efficiency of heat recovery	6
Heat transfer rates	5
System pressure drop	4
Capital cost	4
Complexity of design	2
Environmental problems	2
Safety aspects	2
Stability of bed operation	1
State of development	1

TABLE 11

RATING VALUE RATIONALE USED IN EVALUATING FLUIDIZED BED HEAT EXCHANGER CONCEPTS

Rating for Heat Exchanger Concept	Assigned Numerical Value
Fair	1
Good	2
Excellent	3

Note: No potentially applicable system was assigned value of 0.

The weighted rating values for each parameter as applied to a specific heat exchanger concept were developed by multiplying the assigned weighting factor by the rating value, as shown in Figures 11 and 12. The total rating value for each heat exchanger system was then obtained by adding the individual weighted rating values. Thus, the preferred ranking would begin with the highest total value (the concept deemed most suitable) and range downward to the lower total value.

2.3 INTEGRATION OF FLUIDIZED BED HEAT EXCHANGER CONCEPTS WITH POTENTIAL APPLICATIONS

The integration of fluidized bed heat exchanger concepts with potential applications was accomplished by a parametric analysis of fluidized bed systems. Flow rates, temperatures, etc., representative of waste energy streams from potential applications were used in the analysis. Details of the parametric analysis are discussed next.

2.3.1 Parametric (Engineering) Analysis

2.3.1.1 Minimum Fluidized Velocity--

As a first step in the parametric analysis, the study of flow dynamics of a fluidized bed heat exchanger was undertaken. The main operating parameter, viz., the minimum fluidization velocity, and the factors that affect this parameter were studied. The analysis was oriented toward an application area identified for the purpose of this project. As an example, the hot gas exiting a cement rotary kiln was assumed to be the heat source for utilization in a fluidized bed of solid particles. The heated particles were assumed to serve as the heat store. Tables 12 and 13 list the characteristics of the gas and particles under consideration.

	Efficiency of Heat Recovery	Heat Transfer Rates	System Pressure Drop & Energy Requirement	Stability of Bed Operation	Complexity of Design	State of Development	Environmental Problems	Safety Aspects	Capital Cost	Sum of Weighted Rating Values
WEIGHTING FACTOR	6	5	4	1	2	1	2	2	4	
HEAT EXCHANGER CONCEPTS	Rating Value Before Weighting / Rating Value After Weighting									
Counterflow System (Gas & Solids):										
Single Stage – Particle Thermal Storage										
Shallow Bed	2 / 12	2 / 10	3 / 12	3 / 3	3 / 6	3 / 3	2 / 4	2 / 4	3 / 12	66
Deep Bed	2 / 12	2 / 10	2 / 8	2 / 2	3 / 6	3 / 3	2 / 4	2 / 4	2 / 8	57
Single Stage – Internal Heat Exchanger										
Shallow Bed	2 / 12	2 / 10	3 / 12	2 / 2	2 / 4	3 / 3	2 / 4	2 / 4	2 / 8	59
Deep Bed	2 / 12	2 / 10	2 / 8	2 / 2	2 / 4	3 / 3	2 / 4	2 / 4	1 / 4	51
Multiple Stage – Particle Thermal Storage										
Shallow Bed	3 / 18	2 / 10	2 / 8	2 / 2	2 / 4	2 / 2	2 / 4	2 / 4	2 / 8	60
Deep Bed	3 / 18	2 / 10	1 / 4	1 / 1	2 / 4	2 / 2	2 / 4	2 / 4	1 / 4	51
Crossflow System (Gas & Solids):										
Single Stage – Internal Heat Exchanger	2 / 12	2 / 10	3 / 12	2 / 2	2 / 4	2 / 2	2 / 4	2 / 4	2 / 8	58
Multiple Stage – Particle Thermal Storage										
Shallow Bed	2 / 12	2 / 10	3 / 12	2 / 2	2 / 4	2 / 2	2 / 4	2 / 4	2 / 8	58
Deep Bed	2 / 12	2 / 10	2 / 8	1 / 1	2 / 4	2 / 2	2 / 4	2 / 4	1 / 4	49
Combined Counterflow & Crossflow – With Particle Thermal Storage	2 / 12	2 / 10	2 / 8	1 / 1	1 / 2	1 / 1	2 / 4	2 / 4	1 / 4	46
Liquid Fluidized Bed Systems										
Single Stage Units	2 / 12	2 / 10	2 / 8	3 / 3	3 / 6	1 / 1	2 / 4	2 / 4	1 / 4	52
Vertical Multiple Stage With Exchanger	3 / 18	2 / 10	1 / 4	2 / 2	2 / 4	1 / 1	2 / 4	2 / 4	1 / 4	51
Multiple Stage Crossflow With Exchanger	3 / 18	2 / 10	1 / 4	2 / 2	2 / 4	1 / 1	2 / 4	2 / 4	1 / 4	51
Spouted Bed Systems	2 / 12	2 / 10	1 / 4	1 / 1	2 / 4	1 / 1	2 / 4	2 / 4	1 / 4	44

Figure 11 - Master Grid - Evaluation of Fluidized Bed Heat Exchanger Concepts for Low Temperature Applications (< 250°C)

HEAT EXCHANGER CONCEPTS	Efficiency of Heat Recovery	Heat Transfer Rate	System Pressure Drop & Energy Requirement	Stability of Bed Operation	Complexity of Design	State of Development	Environmental Problems	Safety Aspects	Capital Cost	Sum of Weighted Rating Values
WEIGHTING FACTOR	6	5	4	1	2	1	2	2	4	
	Rating Value Before Weighting / Rating Value After Weighting									
Counterflow System (Gas & Solids):										
Single Stage – Particle Thermal Storage										
Shallow Bed	1/6	2/10	3/12	3/3	3/6	3/3	2/4	2/4	3/12	60
Deep Bed	1/6	2/10	2/8	2/2	3/6	3/3	2/4	2/4	2/8	51
Single Stage – Internal Heat Exchanger										
Shallow Bed	1/6	2/10	3/12	2/2	2/4	3/3	2/4	2/4	2/8	53
Deep Bed	1/6	2/10	2/8	2/2	2/4	3/3	2/4	2/4	1/4	45
Multiple Stage – Particle Thermal Storage										
Shallow Bed	3/18	2/10	2/8	2/2	2/4	2/2	2/4	2/4	2/8	60
Deep Bed	3/18	2/10	1/4	1/1	2/4	2/2	2/4	2/4	1/4	51
Crossflow System (Gas & Solids):										
Single Stage – Internal Heat Exchanger	2/12	2/10	3/12	2/2	2/4	2/2	2/4	2/4	2/8	58
Multiple Stage – Particle Thermal Storage										
Shallow Bed	2/12	2/10	3/12	2/2	2/4	2/2	2/4	2/4	1/4	54
Deep Bed	2/12	2/10	2/8	1/1	2/4	2/2	2/4	2/4	1/4	49
Combined Counterflow & Crossflow – With Particle Thermal Storage	3/18	2/10	2/8	1/1	1/2	1/1	2/4	2/4	1/4	52
Liquid Fluidized Bed Systems										
Single Stage Units	1/6	2/10	2/8	3/3	3/6	1/1	2/4	2/4	1/4	46
Vertical Multiple Stage With Exchanger	1/6	2/10	1/4	2/2	2/4	1/1	2/4	2/4	1/4	39
Multiple Stage Crossflow With Exchanger	1/6	2/10	1/4	2/2	2/4	1/1	2/4	2/4	1/4	39
Spouted Bed Systems	1/6	2/10	1/4	1/1	2/4	1/1	2/4	2/4	1/4	38

Figure 12 - Master Grid - Evaluation of Fluidized Bed Heat Exchanger Concepts for High Temperature Applications (> 250°C)

TABLE 12

CHARACTERISTICS OF THE INCOMING HOT GAS STREAM

Temperature, Tgi: 1000°F = 538°C
Volumetric Flowrate, V_F: 180,000 cfm = 85 m^3/sec
Density (air), ρ_F: 0.436 kg/m^3
Viscosity (air), μ_F: 3.57×10^{-5} kg/m.sec (3.57×10^{-6} Pa sec)
Thermal conductivity (air), k_F: 6.00×10^{-5} kJ/m.sec.°C
Specific heat (air), C_F: 1.09 kJ/kg.°C

TABLE 13

PROPERTIES OF THE SELECTED SOLIDS

Material: Dense fire clay
Average particle size, d_p: 2 mm = 2×10^3 μm = 2×10^{-3} m
Particle density, ρ_p: 2,400 kg/m^3
Specific heat, C_p: 0.94 kJ/kg.°C

The minimum fluidizing conditions in a fluidized bed has been extensively investigated. Table 14 summarizes the major correlations commonly used. Difficulties in determining minimum fluidization voidage and particle sphericity led some authors to simplify the equations using empirical relationships between these parameters and particle diameter. These simplified equations are listed in Table 15.

The minimum fluidization velocity, u_{mf}, was computed using those equations, which were compatible with the particle, gas, and bed conditions (Tables 12 and 13) under consideration. A range of values for u_{mf} was obtained. These values are listed in Table 16, along with the equations used, identified by the name of the investigator.

Table 16 shows that the predicted velocity varies over a rather wide range around the average value of 2 m/sec. Kunii and Levenspiels' prediction for large particles falls close to the average; and the average value agrees well with the minimum fluidization conditions reported by McGaw for shallow beds.

2.3.1.2 Bed Areas--

The waste energy streams from the applications selected for further study (Section 2.1) contain large volumes of gas. In order to obtain realistic bed areas for treating these large volumes of gas, the minimum fluidization velocity will have to be maximized within practical limits. This requirement would necessitate using large particles with mean diameters in excess of 100 μm. The variation of bed diameter of a single stage bed with particle diameter is presented in Figure 13 for various incoming gas flow rates and temperatures.

TABLE 14

EQUATIONS USED TO PREDICT THE MINIMUM FLUIDIZATION VELOCITY[a/]

	Equation	Range of applicability
1.	$Ga = 150 \frac{1 - \epsilon_{mf}}{\epsilon_{mf}^3} Re_{mf} + 1.75 \frac{Re_{mf}^2}{\epsilon_{mf}^3}$	Not limited
2.	$u_{mf} = \frac{(\psi \cdot d_p)^2}{150} \frac{\rho S - \rho F}{\mu F} g \frac{\epsilon_{mf}^3}{1 - \epsilon_{mf}}$	Small particles $Re_{mf} < 20$
3.	$u_{mf}^2 = \frac{\psi d_p}{1.75} \frac{\rho S - \rho F}{\rho F} g \epsilon_{mf}^3$	Large particles $Re_{mf} > 1{,}000$
4.	$G_{mf} = \frac{0.005(\psi \cdot d_p)^2}{\mu F(1 - \epsilon_{mf})} g \rho F(\rho S - \rho F) \epsilon_{mf}^3$	$Re_{mf} < 10$
5.	$G_{mf} = \frac{(\psi \cdot d_p)^2 g}{18 \mu_F} (\rho_s - \rho F) \rho F \frac{\epsilon_{mf}^5}{1 + 0.5(1 - \epsilon_{mf})}$	$Re < 2$
6.	$G_{mf} = 0.171 \psi d_p \rho F \left(\frac{\epsilon_{mf}}{1 - \epsilon_{mf}}\right)^3 \times \left(\frac{g^2 \rho S \epsilon_{mf}}{\mu F(1 - \epsilon_{mf})(1 + 0.5(1 - \epsilon_{mf}))}\right)^{1/3}$	$Re < 2$

a/ See footnote a/ - Table 15 for nomenclature.

TABLE 15

SIMPLIFIED EQUATIONS USED TO PREDICT THE MINIMUM FLUIDIZATION VELOCITY[a/]

	Equation	Range of applicability
1.	$Re_{mf} = \left(33.7^2 + 0.0408 \frac{d_p \rho_F (\rho_S - \rho_F) g}{\mu_F^2}\right)^{0.50} - 33.7$	Not limited
2.	$u_{mf} = \frac{d_p (\rho_S - \rho_F) g}{1{,}650 \mu_F}$	Small particles
3.	$G_{mf} = 1.00 \times 10^{-3} \, d_p^{\,2} \frac{\rho_F (\rho_S - \rho_F)}{\mu_F}$	$Re < 5$
4.	$u_{mf}^2 = d_p \frac{(\rho_S - \rho_F) g_c}{24.5 \, \rho_F}$	Simplified for large particles
5.	$G_{mf} = 1.4 \times 10^{-3} \frac{d_p^{1.8} [\rho_F (\rho_S - \rho_F)]^{0.94}}{\mu_F^{0.88}}$	
6.	$u_{mf} = 1.0 \times 10^{1} \frac{\mu_F}{d_p \rho_F} [(25.28^2 + 0.0571 \, Ga)^{1/2} - 25.28]$	

a/ Nomenclature:

d_p = particle (surface mean) diameter, m
g = gravitational acceleration, m/sec^2
G_{mf} = fluid mass velocity for minimum fluidization, kg/m^2.sec
u_{mf} = superficial gas velocity required for minimum fluidization, m/sec

Dimensionless groups:

$Re = u_G d_p \rho_F / \mu_F$, particle Reynolds number
$Re_{mf} = u_{mf} d_p \rho_F / \mu_F$, particle Reynolds number at minimum fluidization velocity
$Ga = g d_p^3 \rho_F \cdot (\rho_S - \rho_F) / \mu_F 2$, Galileo number
$Ar = g d_p^3 \rho_F \cdot (\rho_S - \rho_F) / \mu_F^2$, Archimedes number

Greek symbols:

ϵ_{mf} = bed voidage fraction at minimum fluidization
ψ = particle sphericity
ρ_F = fluid air density, kg/m^3
ρ_S = solids density, kg/m^3
μ_F = fluid (air) viscosity, Pa sec

TABLE 16

RANGE OF MINIMUM FLUIDIZATION VELOCITY FOR THE INPUT CHARACTERISTICS UNDER CONSIDERATION

Equation	Minimum Fluidization Velocity (u_{mf}, m/sec)
Eq. 1 of Table 14	2.14
Eq. 3 of Table 15	2.84
Eq. 4 of Table 15	2.10
Eq. 5 of Table 15	1.10
Eq. 6 of Table 15	1.65

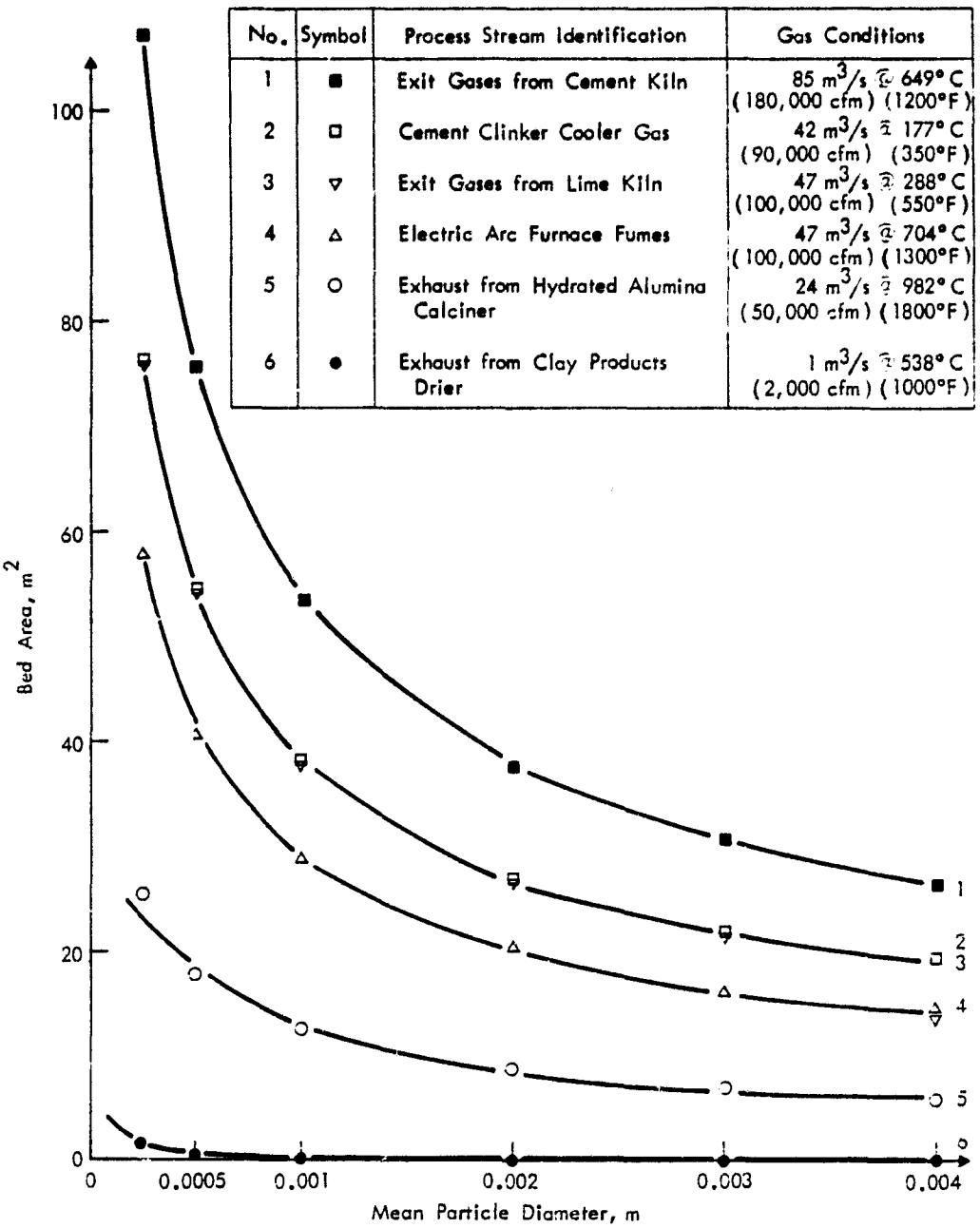

Figure 13 - Variation of Bed Area With Mean Particle Diameter

The flow rates and temperatures shown represent typical streams from industrial processes as identified in Figure 13. The bed areas are computed using u_{mf} values determined from Kunii and Levenspiel's simplified correlation. The choice of this correlation is based on the rationale discussed earlier.

2.3.1.3 Number of Stages--

The choice of either a single or multistage bed requires a careful balance between the size and cost of the fluid bed itself, the required gas-temperature recovery, the ancillary equipment, the available space, etc. Multistage beds are more expensive both in terms of first cost and operational cost. In an application where the hot inlet gas is cooled by the circulating solids, the various stages have to be of decreasing bed area from the bottom to the top of the tower to maintain a constant superficial velocity at the exit conditions of each bed stage. This structural complexity becomes more acute in cases where there is a fluctuation in the incoming gas temperature/ flow rate. However, if a high recovery of the gas temperature into the solids is desired, it can only be achieved by a multistage unit.

2.3.1.4 Design of Distribution Plate--

The quality of fluidization is strongly influenced by the type of gas distributor used. A satisfactory distributor should have the following properties.

1. It should promote uniform and stable fluidization.

2. It should minimize attrition of bed material.

3. It should be designed to minimize erosion damage.

4. It should prevent flow back of bed material during normal operation and on interruption of fluidization when the bed is shut down.

The critical nature of distributor design becomes even more important in a shallow fluidized bed. Care should be taken to prevent the feed gas from simply blowing holes through the bed at the grid ports. In deep beds, due to radial gas flow, a portion of the bed acts as its own distributor.

In general, in grid design, a compromise should be struck between pressure drop and uniformity of fluidization. Although contacting is superior when densely consolidated porous media or plates with small orifices are used, from the standpoint of large scale operations, such distributors have the serious drawback of high pressure drop. High pressure drop can also hinder the circulation of solids between two or more stages.

Orifices that are too small are liable to become clogged, whereas those that are too large may cause an uneven distribution of gas. The final selection of the combination of diameter of the orifice and the number of orifices should also consider the attrition rate and solid seepage.

2.3.1.5 Fluctuations in Incoming Fluid Flow Rate--

In fluidized beds, the flow dynamics, hence the stability of bed operation and the heat transfer rates to internal surface or the containing wall,

are all dependent on the superficial velocity of the fluid through the bed. The superficial velocity, in any case, will have to be in excess of the incipient fluidization velocity. The latter is characteristic of the fluid/particle combination. While it is advantageous to select a maximum operable velocity, the constraints in such a selection should not be overlooked. These constraints relate to particle entrainment and pressure drop.

In situations where the flow rate of incoming fluid fluctuates, the fluidized bed distributor plate is designed for the minimum flow rate to ensure fluid supply to all the holds in the grid. However, if the fluctuation is over a wide range, at the maximum fluid flow, the pressure drop due to the bed as well as the grid may be excessively high. The attrition rate of particles at the grid also increases. If the bed size is also designed to correspond to the minimum gas flow, this will result in a large entrainment when operating at the upper end of the flow rate range. If, on the other hand, the bed and grid are designed for a flow rate somewhere in the middle of the operating range, the grid should be designed to ensure that no backflow of solids or "weeping" through the grid occurs at flow rates lower than the design level. The superficial velocity at the lower end of the operating range should still be higher than the incipient fluidization velocity. Grids equipped with bubble caps prevent solids backflow, but at the cost of a higher pressure drop.

Figure 14 presents three types of flow rate versus time curves normally encountered in industrial waste streams. For the flow type 1, where only small fluctuations are encountered, an ordinary perforated plate designed for an average flow rate will suffice. But in situations where the fluctuations are large (Curve 2), or the flow is intermittent (Curve 3), bubble cap grids are preferable in order to prevent solids backflow.

In summary, when designing a fluidized bed for a fluctuating fluid flow rate, the following factors should be considered for determining the optimum design parameters:

- Superficial velocity through the bed and its effect on pressure drop, heat transfer, and entrainment.

- Grid type and its design parameters and their effect on pressure drop, attrition rate, and solids backflow.

2.3.1.6 Fluctuations in Incoming Fluid Temperature--

In recovering energy from industrial waste gases and liquids, one often encounters temperature variations in the source stream. Any system which attempts to recover heat from a waste stream should have the flexibility of handling such fluctuations in temperature. Since fluidized beds operate isothermally, large temperature changes in the incoming fluid stream lead to instability of the bed temperature and in extreme cases, a reversal of the direction of heat flow. For example, if the incoming gas is at 538°C (1000°F) at the start of the operation, on entering the bed, the gas and the solid particles attain an equilibrium temperature lower than 538°C (1000°F), say, 427°C (800°F). Now, if the incoming gas temperature changes to, say, 371°C (700°F), heat starts flowing from the bed to the gas. Consequently, the bed temperature is lowered and the exiting gas

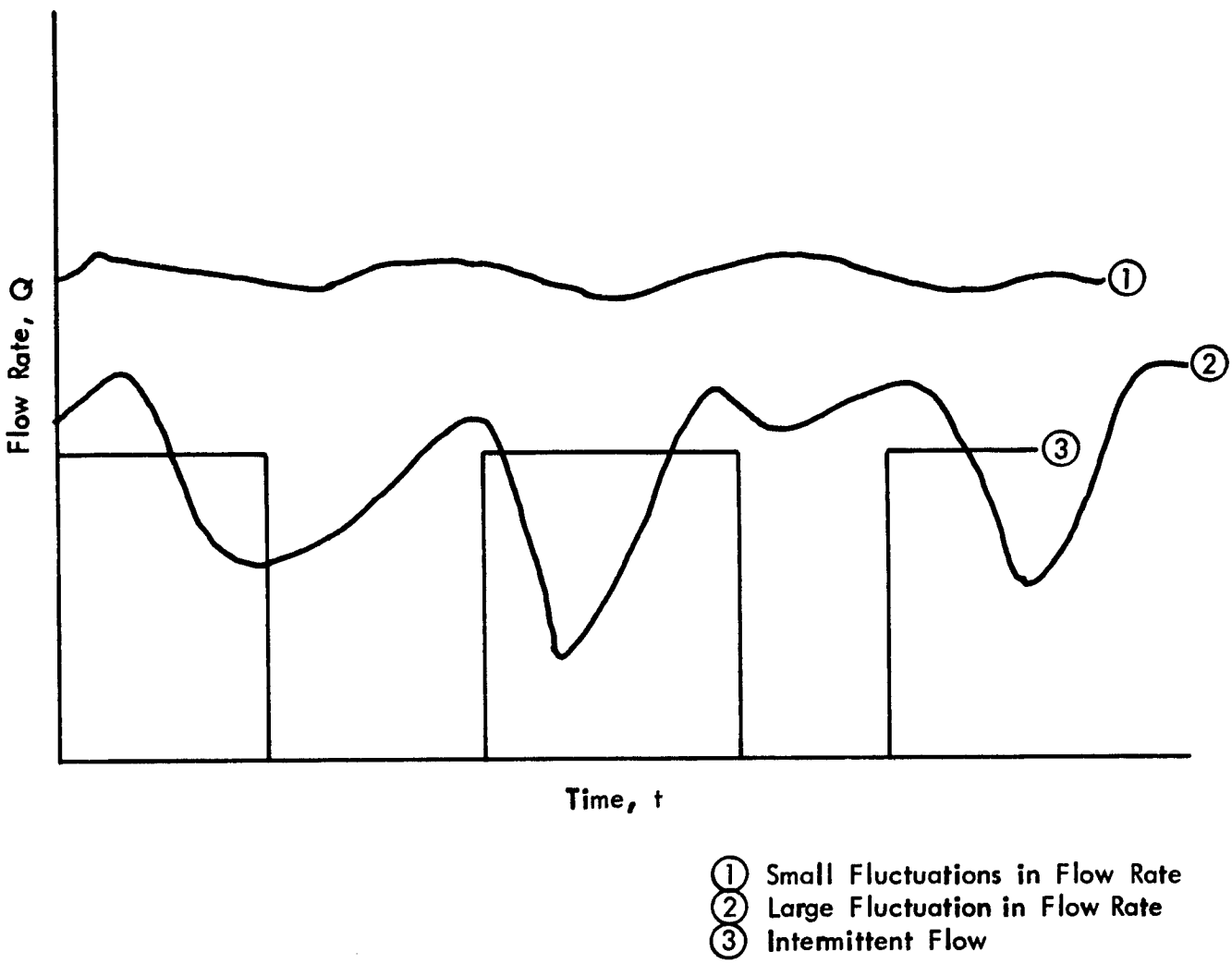

Figure 14 - Flow Rate Versus Time, Hypothetical

temperature is higher than the inlet temperature. If the fluctuation in the incoming gas temperature is small enough not to disrupt the equilibrium bed temperature (i.e., a temperature swing in T_{gi} of $\Delta T_{gi} < (T_{gi}-T_b)$, where T_{gi} = incoming gas temperature and T_b = bed temperature ($T_b < T_{gi}$), the above instability and heat flow reversal do not occur.

Temperature swings in the fluid temperature can be handled in any of the following ways depending on the system under consideration:

1. In multiple stage fluidized beds, where the gas imparts its heat to the solids circulating countercurrent to the gas flow, the incoming gas can bypass the lower stages operating at high temperatures. Each stage may be assigned an operating bed temperature range and if the gas temperature drops below this range it can be made to bypass the stage.

2. A second option is to control the circulating rate of the solids to follow the temperature excusions in the hot gas.

3. If the fluidized bed is equipped with internal heat exchangers, the flow rate of the secondary fluid through the intervals can be controlled to maintain thermal balance in each stage of the bed.

3.0 TECHNICAL EVALUATION OF SELECTED APPLICATIONS

Activity on Task II of the study involved a technical and economic evaluation of two applications selected in Task I. The details of the technical evaluations are presented in this section.

3.1 CEMENT KILN APPLICATION

The cement kiln application involves recovery of waste energy from the off-gases from the rotary kiln and the clinker cooler and subsequent use for feed preheat and power generation. A description of the overall system is presented next.

3.1.1 System Description

There are two processes used for manufacturing portland cement--the wet process in which crushed raw materials are ground with water, thoroughly mixed, and fed into the kiln in the form of "slurry," and the dry process in which the raw materials are ground, mixed, and fed into the kiln in their "dry" state. This is the only major difference between these two processes. A cement kiln is normally made of steel, lined with firebrick or special fire-resistant material, and mounted in a slightly tilted position. A large kiln may have a diameter of 7.6 m (25 ft) and a length of 228 m (750 ft). The raw material fed from the high end of the kiln is gradually heated to 1480°C (2700°F) by a forced draft burner flame located at the low end. As the raw material moves slowly from the high end to the low end, certain elements are driven off by the flame becoming part of the exhaust gases. The remaining material, grayish-black pellets about the size of marbles, is called "clinker." The hot clinker discharged from the kiln is then cooled by a clinker cooler. The clinker is fed into grinding mills where gypsum is added in the grinding process. The final grinding reduces clinker to extremely fine powder which is called portland cement.

In the dry-kiln process for the manufacture of cement, significant quantities of thermal energy are rejected to the atmosphere. Two major sources of this rejected energy are the kiln and clinker cooler exhaust gases. The kiln exhaust contains a large quantity of thermal energy at high temperature levels. The clinker cooler exhaust also contains a rather large quantity of thermal energy but at low temperatures.

As a result of the FBHX study in Task I, a multistage fluidized bed was chosen for the cement kiln application to achieve a large temperature drop in the gases going through the bed thus maximizing energy recovery. Initially, two types of multistage fluidized beds were considered (a) beds with an internal heat exchanger and (b) beds in which the bed material is circulated between hot and cold solids storage bins (Figures 6 and 7 are representative schematics of these basic bed types).

Initially, the FBHX with internals appeared to be the most attractive system because the necessity of having a seperate waste heat boiler would be eliminated and overall costs possibly reduced. This proposed system is illustrated in Figure 15. The off-gases from the rotary kiln at about 816°C (1500°F) are first used to preheat the raw blend in a single stage suspension preheater. The single stage preheater is selected in preference to (a) long rotary kiln with no preheater or (b) short kiln with a multistage preheater because of the following reasons: A rotary kiln with a preheater requires less energy for the overall calcining operation than conventional long kiln without a preheater; however, increasing the number of stages of preheating results in an alkali buildup in the clinker and affects the product quality. The exhaust gases leave the preheater at about 538°C (1000°F). These gases are then sent to a multistage fluidized bed heat exchanger. The clinker cooler off-gases at about 204°C (400°F) are used to preheat the inlet fuel/air mixture for the rotary kiln.

Preliminary sizing calculations for the FBHX with multistage deep beds and internal heat exchangers indicated that the total pressure drop through the bed would be about 275 kPa (40 psi). This high ΔP across the fluidized bed would require a high power compressor upstream of the fluidized bed where the gas is hot and particulate-laden. More importantly, the energy requirement for such a compressor would be prohibitively high and would make the overall energy recovery scheme a net energy-consuming system. This bed configuration was eliminated from further consideration.

To eliminate the high ΔP across the system, a multistage shallow fluidized bed configuration, with solids circulation, was chosen as depicted in Figure 16. During the charging mode a portion of the hot process gases are diverted to the fluidized bed storage. The remainder, if any, passes directly to the waste heat boiler. The solids are heated up during the charge phase using the hot kiln exhaust gases by circulating the cold solids from the cold solids store through the bed to the hot solids store. The reverse process takes place during the discharge mode, i.e., hot solids are circulated from the hot solids store through the bed to the cold store thus giving up the stored heat to the fluidizing cold gas. A portion of the exhaust from the waste heat boiler will be used as the fluidizing gas during the discharge phase.

3.1.2 Fluidized Bed Heat Exchanger Design

In order to design the fluidized bed heat exchanger, a realistic operating schedule for the charge and discharge cycles had to be defined. Several individuals in the cement industry, known to MRI through previous work, were contacted. In addition, a local cement plant (Missouri Portland Cement) was visited. These contacts supplemented the information previously obtained in published reports and aided in formulating typical operating scenarios for plants with fluid bed heat exchanger/thermal energy storage systems (FBHX/TES).

The rotary kiln operates continuously more than 90% of the time with approximately 5% downtime for scheduled maintenance and up to 5% downtime for unscheduled random equipment failures. Also, while most of the cement plant operates continuously, some of the equipment operate by shifts or intermittently. This situation creates variations in electrical demand. Furthermore,

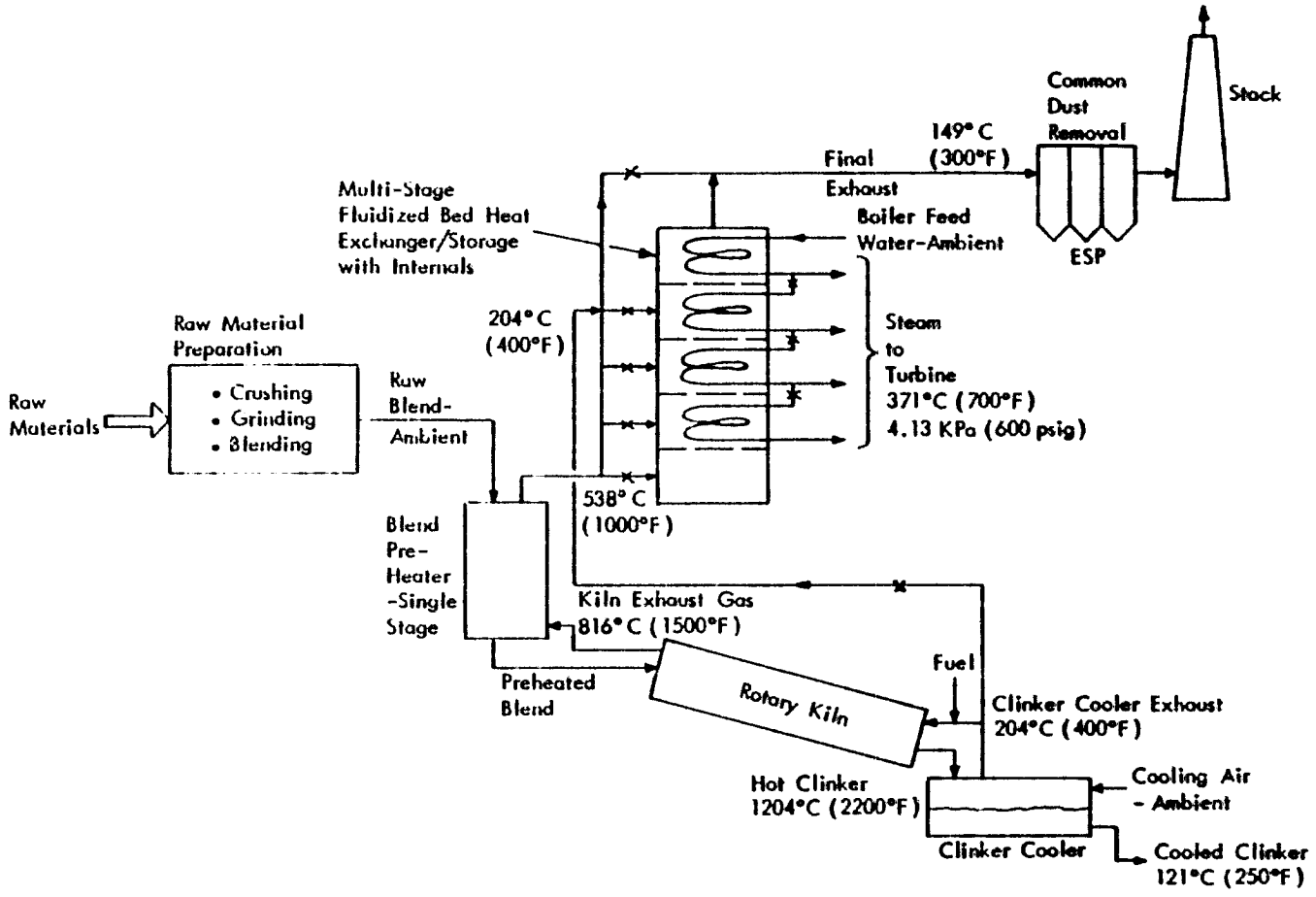

Figure 15 - Conceptual TES System Using Fluidized Bed in Cement Industry

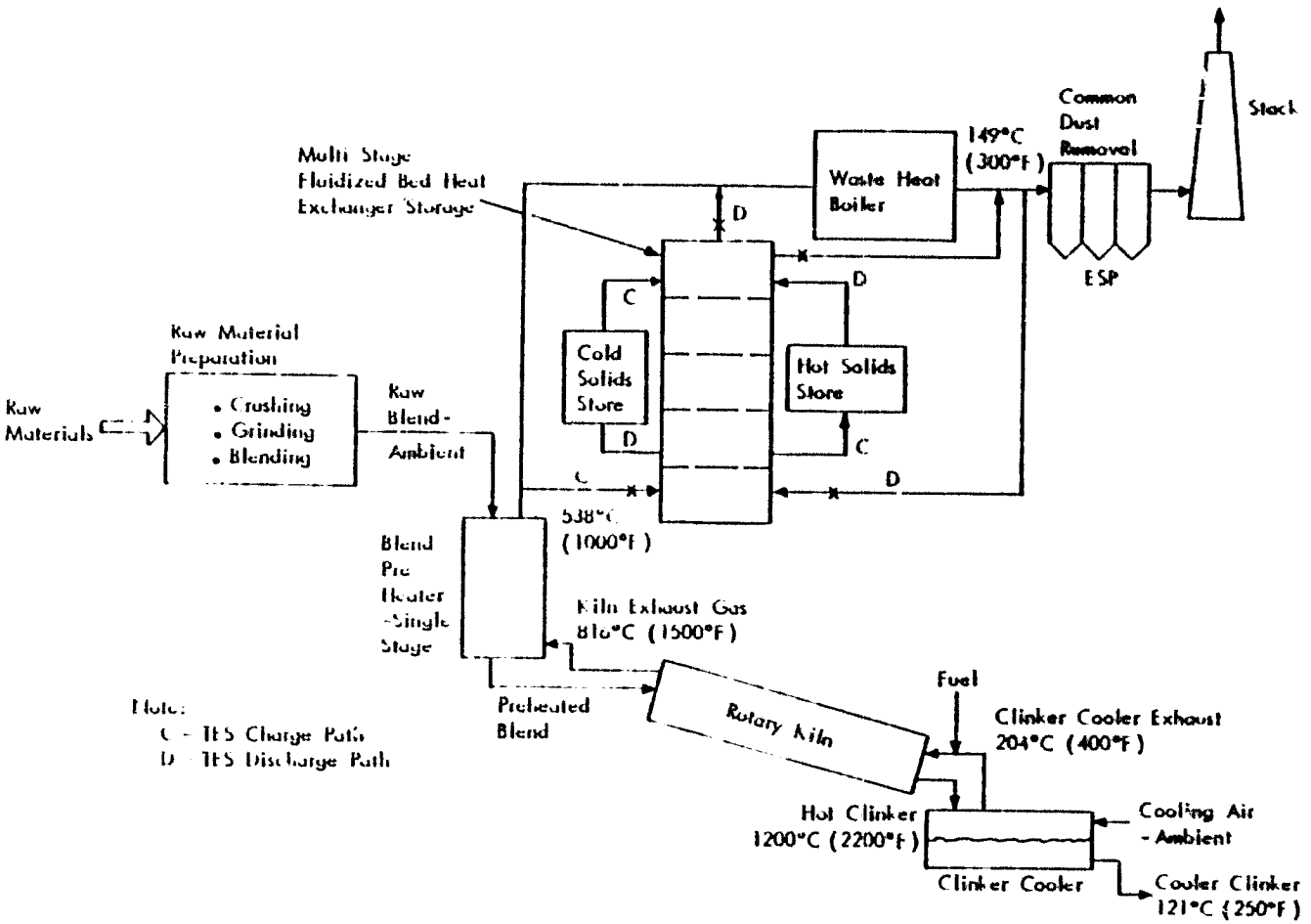

Figure 16 - Conceptual TES System Using Fluidized Bed With Solids Circulation in Cement Industry

typical electrical utility rates have on-peak demand charges based on the maximum kilowatt demand interval recorded during high load periods such as 7:00 AM through 11:00 PM. Since the rotary kiln exhaust gases provide a nearly constant energy supply, the role of the FBHX/TES system is to "smooth out" variations in electrical demand and reduce on-peak demand charges.

Based on the above considerations, the operating scenario assumed for the cement plant FBHX/TES system is to use approximately 80% of the exhaust gases for direct power generation and 20% to charge the storage system during a 12-hr period. During the following 12-hr period, the stored thermal energy would be discharged and power equivalent to 120% of the nominal waste heat available in the exhaust gases would be recovered.* This operational scenario allows up to 40% variation between maximum and minimum energy recovery which should be sufficient for effective demand peak control in most installations. Figure 17 shows the ideal selected scenario for a 24-hr cycle.

3.1.2.1 Initial Calculations for Multistage Shallow Bed Head Exchanger System--

In order to test the viability of the system shown in Figure 16 several assumptions were made to facilitate the initial hand calculations. These were:

- The mass flow of solids is such that the ΔT solids = ΔT_{gas}.
- The waste heat boiler exit temperature is 149°C (300°F).
- The cold solids store temperature is 204°C (400°F).
- No temperature rise occurs across the fans.
- The unfluidized bed depth for each stage is 0.3 m (12 in.).

The results are listed in Table 17 and depicted schematically in Figure 18a and 18b for the charge and discharge models, respectively. Details of the hand calculations are given in Appendix B. Table 18 shows a hand calculated energy balance for the initial multistage fluidized-bed design. The energy balance indicates that in the initial system design 37.8 kwh of energy per ton of clinker is forfeited during the charge mode in order to obtain 12.6 kwh of peak energy per ton during the discharge mode. More importantly the system is a net energy producer during both the charge and discharge modes and the high operational losses of the deep bed system with internals have veen mitigated by using the multistage shallow bed FBHX.

3.1.2.2 Final Calculations for Multistage Shallow Bed Heat Exchanger System--

The initial calculations for the multistage shallow bed system, which were summarized in the previous section, established the basic feasibility of the FBHX/TES system design for the cement kiln application. Attention was next directed to the optimization of the design.

* Neglecting losses in recovery of stored energy.

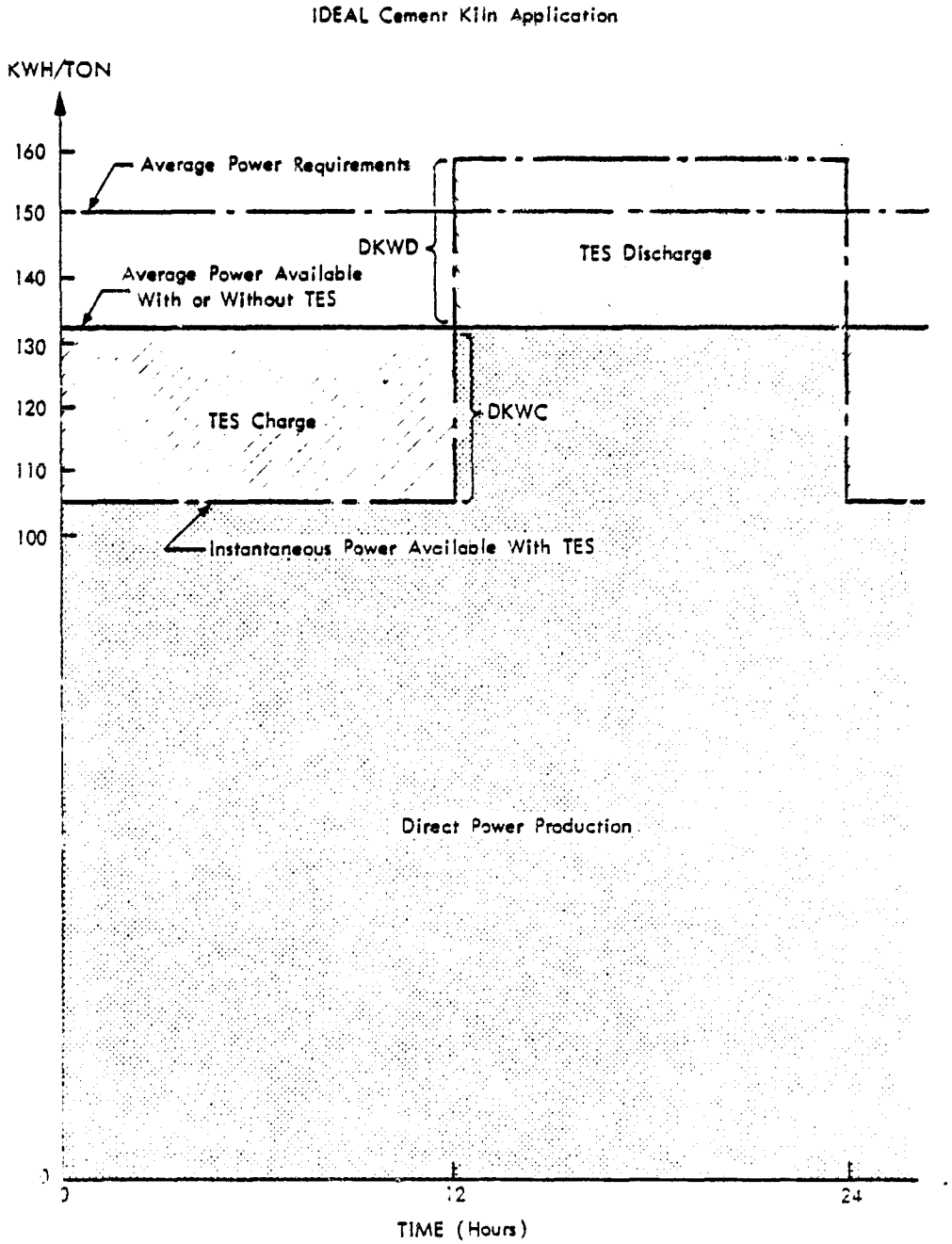

Figure 17 - Ideal Charge/Discharge Scenario for Cement Plant Rotary Kiln TES Application

TABLE 17

SUMMARY OF INITIAL FLUIDIZED BED TES DESIGN AND OPERATING PARAMETERS

Gas flow rate through the fluidized bed:

$\dot{G}$ = 13.48 kg/s = 24.1 m^3/s at 538°C, 129.6 KPa
(1.07 x 10^5 lb/hr = 51,224 acfm at 1000°F, 18.8 psia)

Solids flow rate through the fluidized bed:

$\dot{S}$ = 18.87 kg/s (1.498 x 10^5 lb/hr)

Charge:	G_{in} at 538°C (1000°F)	G_{out} at 260°C (500°F)
	S_{in} at 204°C (400°F)	S_{out} at 482°C (900°F)
Discharge:	G_{in} at 149°C (300°F)	G_{out} at 427°C (800°F)
	S_{in} at 482°C (900°F)	S_{out} at 204°C (400°F)

No. of stages: five with 55.5°C (100°F) drop across each stage

Superficial velocity of gas = 1.22 m/s (4 ft/sec)

Range = 0.63 to 1.34 m/s (2.08 to 4.41 ft/sec)

Bed diameter = 5.0 m (16.5 ft)

Total bed height including TDH = 8.8 m (29 ft)
Unfluidized bed depth = 0.3 m (1.0 ft)
Grid plate hole diameter = 6.3 mm (0.25 in.)
Total fluidized bed pressure drop = 28.3 KPa (4.1 psi)

Adiabatic fan motor power required for pressurizing the incoming gas to provide the ΔP = 783 KW (1,050 hp) during charge
= 408 KW (547 hp) during discharge

ΔP required for pneumatic transport of solids = 27.4 KPa (3.97 psi)

Adiabatic fan motor power required for the transport of solids = 24.0 KW (32.2 hp)

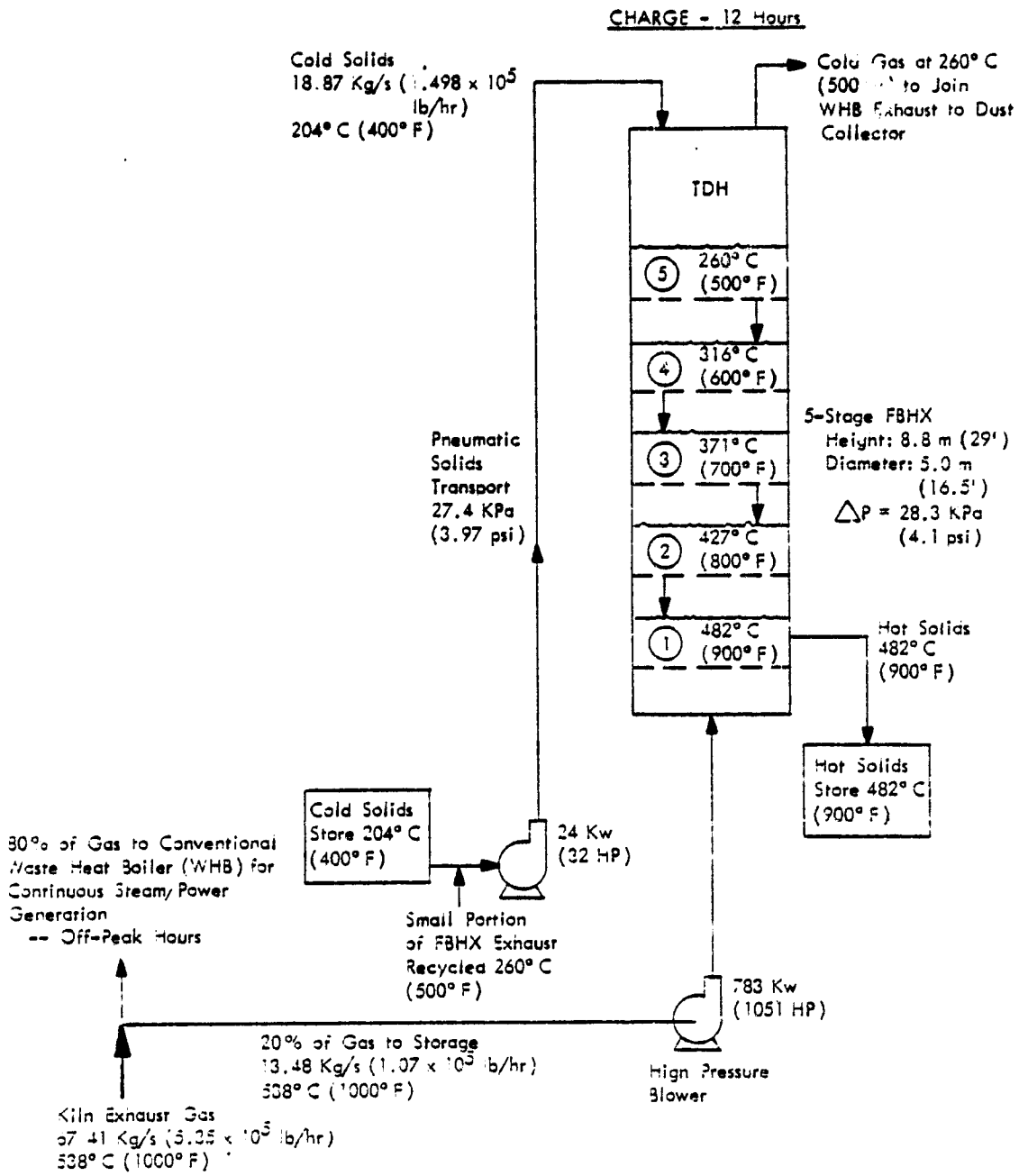

Figure 18a - Schematic Representation of the Initial Fluidized Bed TES System Design-Charge Phase for Cement Kiln Application

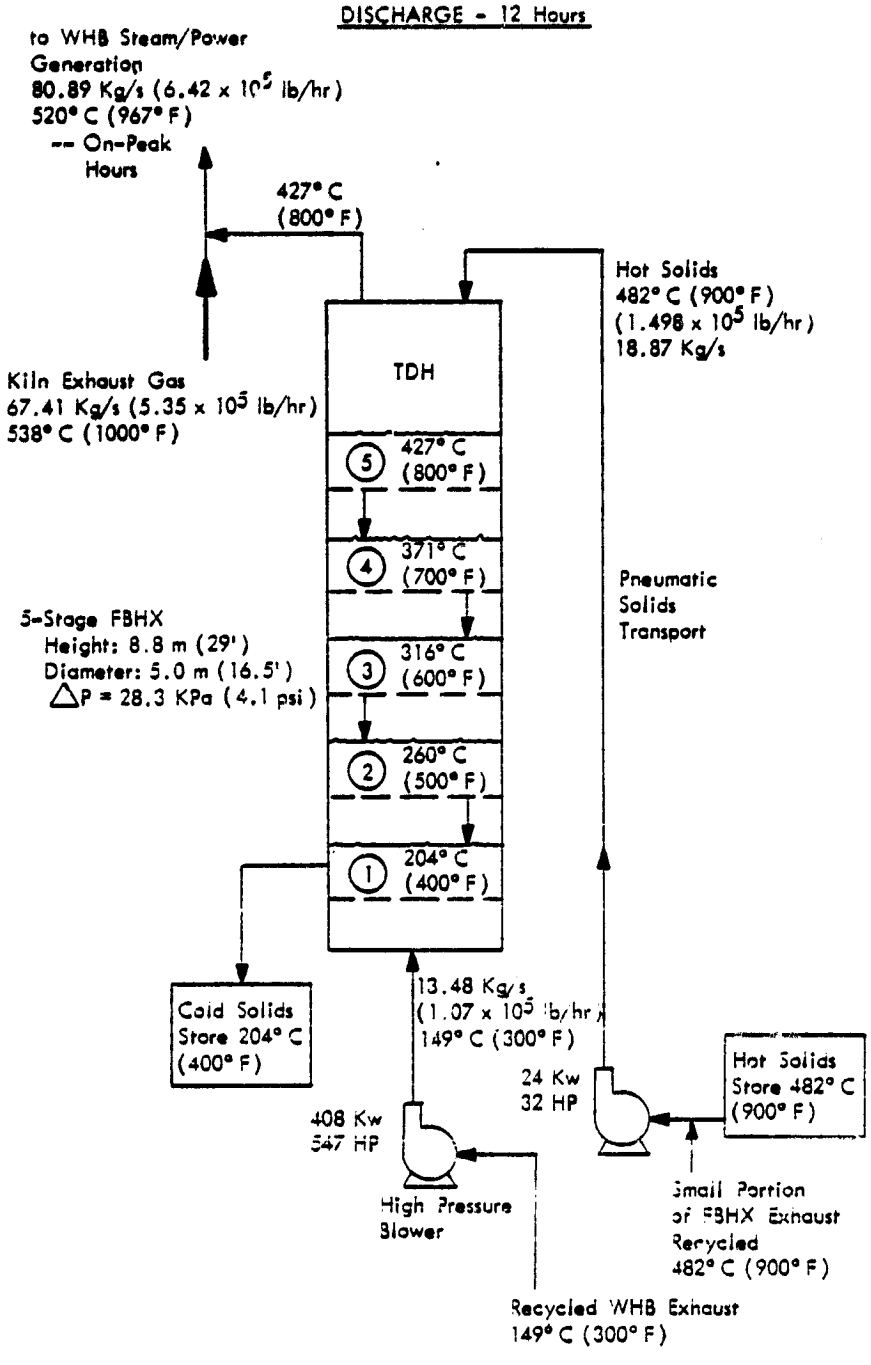

Figure 18b - Schematic Representation of the Initial Fluidized Bed TES System Design-Discharge Phase for Cement Kiln Application

TABLE 18

SUMMARY OF INITIAL ENERGY BALANCE FOR ROTARY KILN HEAT RECOVERY AND STORAGE SYSTEM

Energy available in kiln exhaust gas at 538°C (1000°F), assuming a final waste heat boiler exit temperature of 149°C (300°F):

$$\frac{5.35 \times 10^5 \text{ lb/hr} \times 0.28 \text{ Btu/lb °F} \times (1000\text{-}300)\text{°F}}{70 \text{ tons clinker/hr} \times 11{,}380 \text{ Btu/kwh}}$$

$$= 131.6 \frac{\text{kwh}}{\text{ton clinker}}$$

TES Charge

During the charging cycle, 80% of kiln exhaust goes to a conventional waste heat boiler (WHB) and 20% of kiln exhaust goes to the fluidized bed for storage. Based on this, the net energy available from the recovery system during charge cycle is:

$$E_{\text{net/charge}} = E_{\text{kiln exhaust}} - 0.2 \times E_{\text{kiln exhaust}} - E_{\text{TES operation}}$$

where $0.2 \times E_{\text{kiln exhaust}}$ represents energy charged to storage, and

$E_{\text{TES operation}}$ represents the power requirements for operating the fluidized bed TES

$$E_{\text{TES operation}} = \frac{(1{,}051 + 32) \text{ hp}}{1.341 \text{ hp/kw} \times 70 \text{ tons/hr}}$$

$$= 11.5 \frac{\text{kwh}}{\text{ton}}$$

Substituting the values in Eq. (1),

$$E_{\text{net/charge}} = 131.6 - 0.2 \times 131.6 - 11.5$$

$$= 43.8 \frac{\text{kwh}}{\text{ton}}$$

TABLE 18 (concluded)

TES Discharge

In the discharge mode, 100% of kiln exhaust and clinker cooler gas go to the WHB. In addition, the energy discharged from the storage is also available, thus resulting in a total available energy during discharge as follows:

$$E_{net/discharge} = E_{kiln\ exhaust} + 0.2 \times E_{kiln\ exhaust} \times \text{(loss factor during storage and recovery)} - E_{TES\ operation}$$

$$E_{TES\ operation} = \frac{(547 + 32)}{1.341 \times 70} = 6.2\ \frac{kwh}{ton}$$

$$E_{net/discharge} = 131.6 + 0.2 \times 131.6 \times \frac{500}{700} - 6.2 = 144.2\ \frac{kwh}{ton}$$

A computer program was prepared to aid in the calculations and add more flexibility to the analysis. The details of the computer program are given in Appendix C. This program was also used to perform the parametric analysis which is presented in Section 3.3 of this report.

The final selected design results are presented in Table 19 and are depicted schematically in Figures 19a and 19b for the charge and discharge modes, respectively. Figure 20 gives the actual operating scenario for the final design and indicates the effects of thermal effectiveness and fan power losses.

Comparison of initial values in Tables 17 and 18 with the final values shown in Table 19 indicates that considerable improvement was obtained. The final energy balance indicates that only 29.3 kwh of energy per ton of clinker must be forfeited during the TES charge mode in order to gain 16.6 kwh of peak energy per ton during the TES discharge mode. The improvements are largely due to reducing the grid hole diameter and bed depth to minimize the total pressure drop.

3.2 ELECTRIC ARC FURNACE APPLICATION

The electric arc furnace application involves recovery of waste energy from the off-gases from the furnace and subsequent use of the recovered energy for steam or power generation. A description of the overall system is presented next.

3.2.1 System Description

The production of steel in an electric arc furnace is a batch process. Cycles or "heats" range from about 1-1/2 to 5 hr to produce carbon steel and from about 5 to 10 hr to produce alloy steel. Scrap steel is charged to begin a cycle and alloying agents and slag materials are added for refining. Each cycle normally consists of alternate charging and melting operations, refining (which usually includes multiple oxygen blows of 1 to 5 min each), and tapping. Each heat requires approximately 500 kWh (1.7×10^6 Btu) per ton of molten metal.

The off-gases from a majority of the electric arc furnace installations are controlled by fabric filters; however, a few venturi scrubbers and electrostatic precipitators are also in service. In addition to the variations in control devices, there are several methods of collecting the fumes for cleaning. First is the direct shell evacuation method whereby fumes are drawn from the shell of the furnace, the carbon monoxide burned, the fumes cooled by air dilution and/or water quench, and then routed to the control device. This method has the advantage of the lowest flow rate. The air flow rate for direct evacuation furnaces averages 0.16 m^3/short ton (350 scfm/ton) of capacity although considerable variation can be found throughout the industry.

The second method incorporates a canopy hood to capture charging and tapping emissions to supplement the direct evacuation system. A greater total flow of air results. The air flow rate for these systems averages 1 m^3/short ton (2,000 scfm/ton) of capacity.

TABLE 19

SUMMARY OF FINAL FLUIDIZED BED TES DESIGN AND OPERATING PARAMETERS

Gas flow rate through the fluidized bed:

$\dot{G}$ = 13.48 kg/s = 21.4 m^3/s at 538°C, 101.4 KPa
(1.07 x 10^5 lb/hr = 51,224 acfm at 1000°F, 14.7 psia)

Solids flow rate through the fluidized bed:

$\dot{S}$ = 17.76 kg/s (1.498 x 10^5 lb/hr)

Temperature:

Charge:	G_{in} at 538°C (1000°F)	G_{out} at 270°C (519°F)
	S_{in} at 207°C (404°F)	S_{out} at 491°C (915°F)
Discharge:	G_{in} at 159°C (319°F)	G_{out} at 427°C (800°F)
	S_{in} at 491°C (915°F)	S_{out} at 207°C (404°F)

Design parameters:

No. of stages: five

Superficial velocity of gas = 0.50 to 1.04 m/s (1.68 to 3.43 ft/sec)

Bed diameter = 6.1 m (20.1 ft)

Total bed height including TDH = 5.2 m (17.1 ft)
Unfluidized bed depth = 63.5 mm (2.5 ft)
Grid plate hole diameter = 3.2 mm (0.125 in.)
Total fluidized bed pressure drop = 9.1 KPa (1.32 psi)

Adiabatic fan motor power required for pressurizing the incoming gas to provide the ΔP = 200.4 KW (269 hp) during charge
= 145.6 KW (195 hp) during discharge

ΔP required for pneumatic transport of cold solids = 8.4 KPa (1.22 psi)
ΔP required for pneumatic transport of hot solids = 6.8 KPa (0.98 psi)

Fan motor power required for the transport of cold solids = 8.1 KW (10.8 hp)
Fan motor power required for the transport of hot solids = 7.4 KW (9.9 hp)

Energy balance:

$E_{kiln\ exhaust}$ = 131.63 kwh/ton
$E_{net/charge}$ = 102.33 kwh/ton
$E_{net/discharge}$ = 148.26 kwh/ton

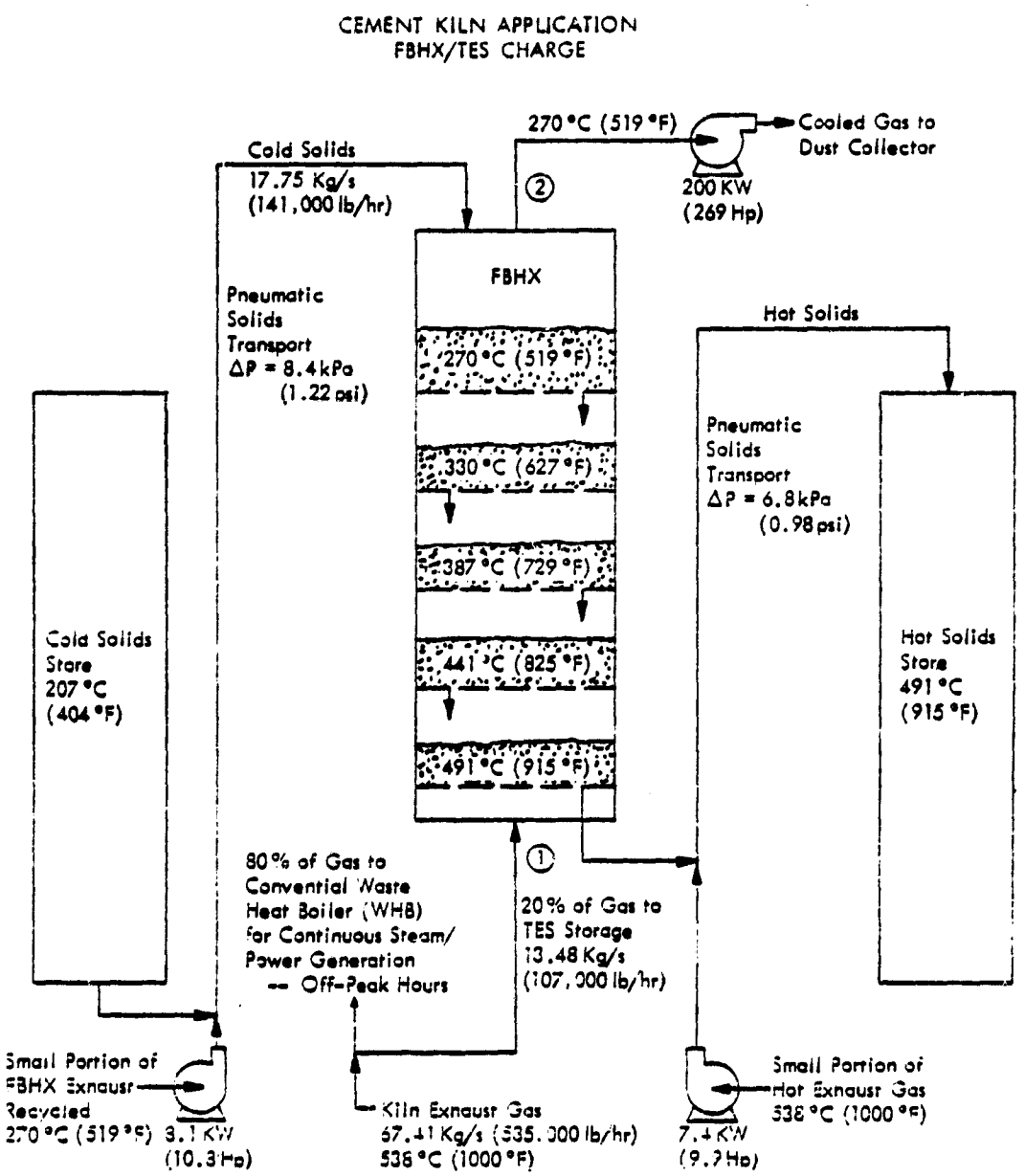

Figure 19a - Schematic Representation of the Final Fluidized Bed TES System Design-Charge Phase for Cement Kiln Application

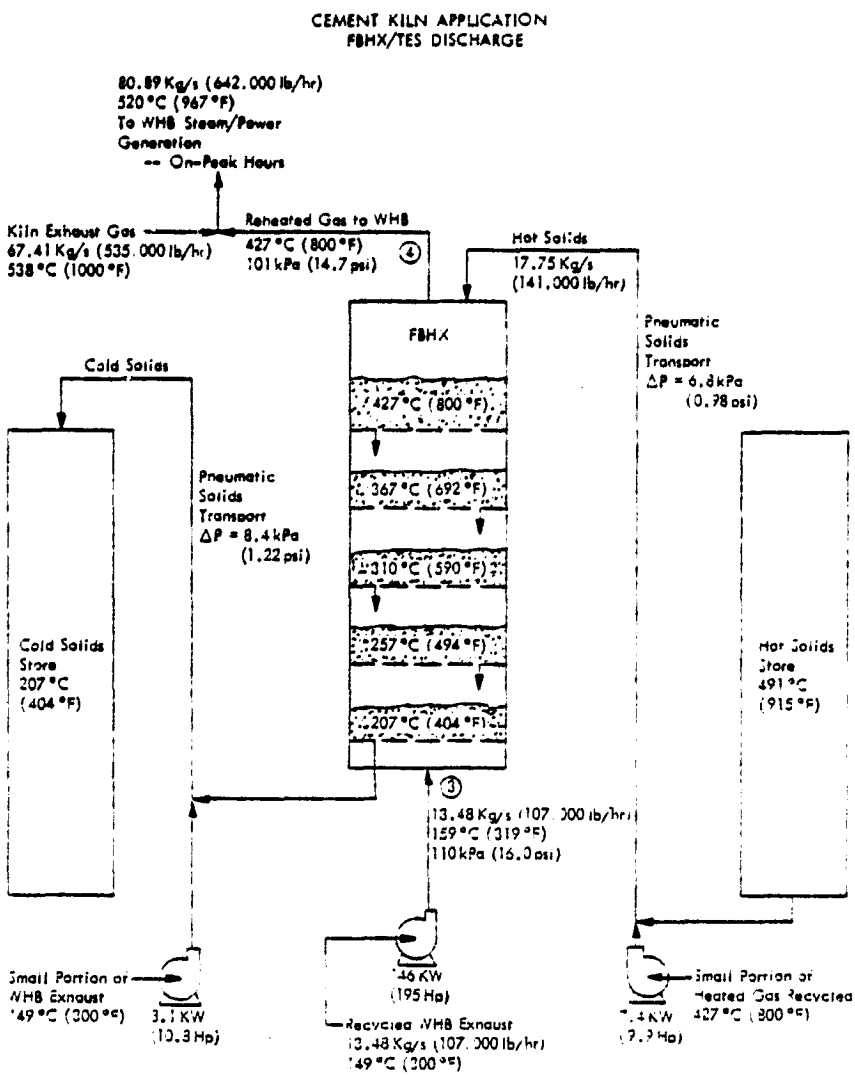

Figure 19b - Schematic Representation of the Final Fluidized Bed TES System Design-Discharge Phase for Cement Kiln Application

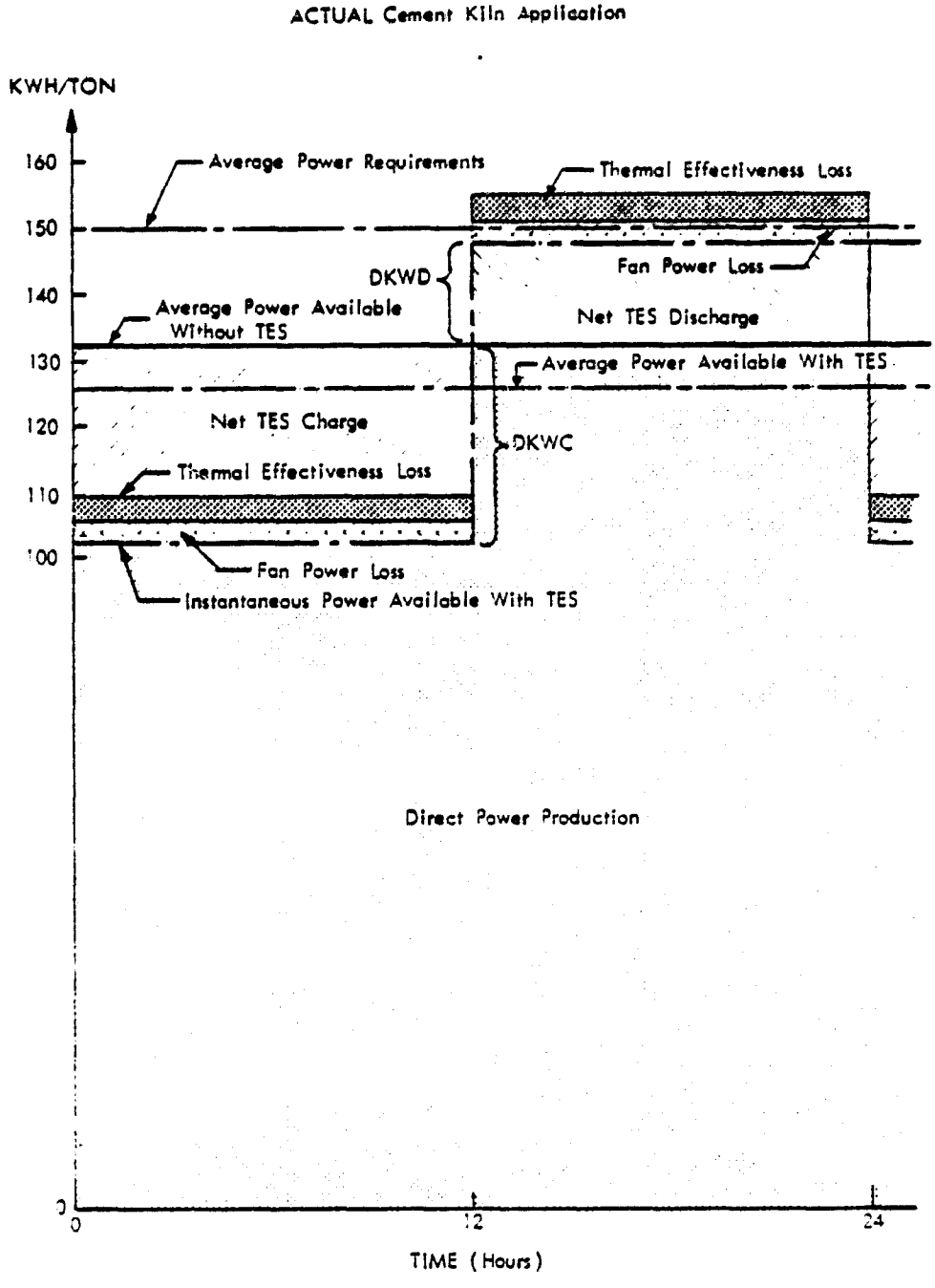

Figure 20 - Actual Charge/Discharge Scenario for Final Cement Plant Rotary Kiln TES Application

The third method is total building evacuation which results in the greatest air flow but the costs of gas conditioning are the least. The air flow for these systems averages 2.4 m^3/short ton (5,000 scfm/ton) of capacity.

In electric arc furnaces above 40-ton capacity, direct evacuation is used as the primary means to remove hot gases resulting from the process. The temperature of the primary gas stream from these furnaces varies with the cyclic operation of the furnace and may range from near ambient, 27 to 37°C (80 to 100°F) at the start of the heat to over 1650°C (3000°F) during oxygen blows. These gases, at an average temperature of approximately 700°C (1300°F), represent a good potential waste energy source if energy recovery from the gas stream occurs before the gases are quenched with dilution air and/or water and if the temperature fluctuations can be minimized.

There are two potential applications for thermal energy storage in the recovery of heat from the electric arc furnace. First, the cyclic temperature fluctuations and short-duration peaks from oxygen blows could be smoothed by an operational storage buffer through which the entire gas stream passes. This situation would result in a relatively uniform 700°C (1300°F) gas which could be used to produce steam in a waste heat boiler. Second, thermal storage could be used to accumulate energy to better match steam demand or provide peaking capabilities.

A system for recovery and storage of thermal energy from electric arc furnaces via a fluidized bed heat exchanger is shown in Figure 21. The recovered energy is converted to electric power. In contrast to the cement plant which has relatively constant energy supply (i.e., temperature and flow) in the exhaust gases, the electric arc furnace (EAF) application has a periodically variable energy supply (i.e., temperature) in its exhaust gases. Consequently, a FBHX/TES buffer was included in the proposed system to reduce the magnitude of the temperature variations. The gases leaving the buffer would then be a near constant energy supply similar to the cement plant application and more amenable for direct use or energy recovery.

3.2.2 Fluidized Bed Heat Exchanger Design

Because the energy which could be recovered from an EAF is only a fraction of the total requirements of steel production, the entire energy supply is cycled through the charge/discharge cycle of the FBHX/TES system. Electric arc furnace steel plants are typically major customers of the electrical utilities (i.e., they may constitute as much as 10% of the total utility demand) and the EAF steel plants may be subject to demand curtailments during peak load periods.

Based on these facts, the operating scenario assumed for the steel plant FBHX/TES system is to use 100% of the exhaust gases from the EAF to charge the storage system during an 8-hr off-peak period and to use the exhaust gases plus the storage discharge over a 16-hr period to generate power during on-peak periods. This operational scenario allows the peak power to be increased considerably above the amount which could be generated directly from the exhaust gases. Figure 22 shows the selected scenario for a 24-hr cycle.

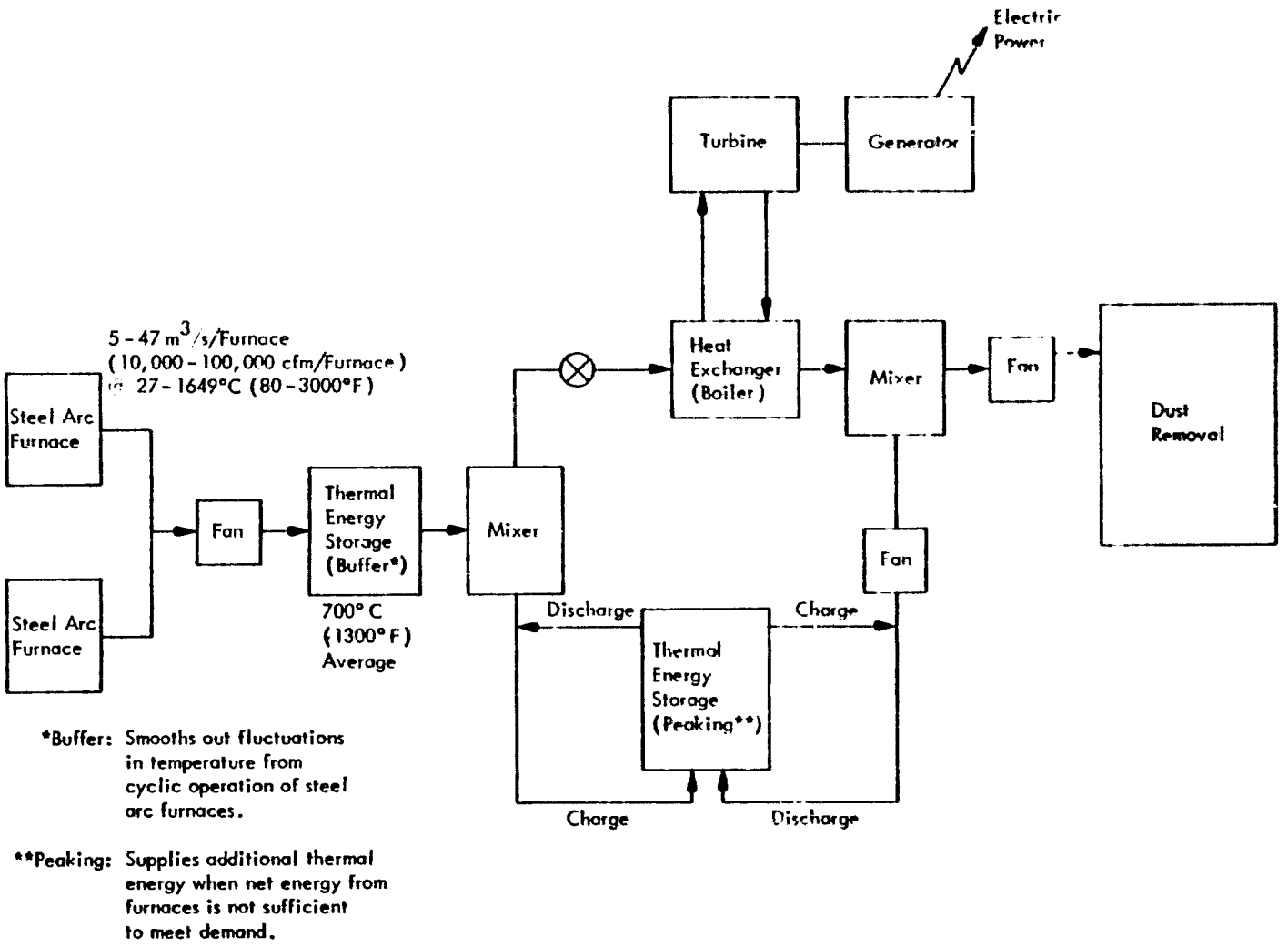

Figure 21 - Conceptual TES System Using Fluidized Beds in Electric Arc Steel Production

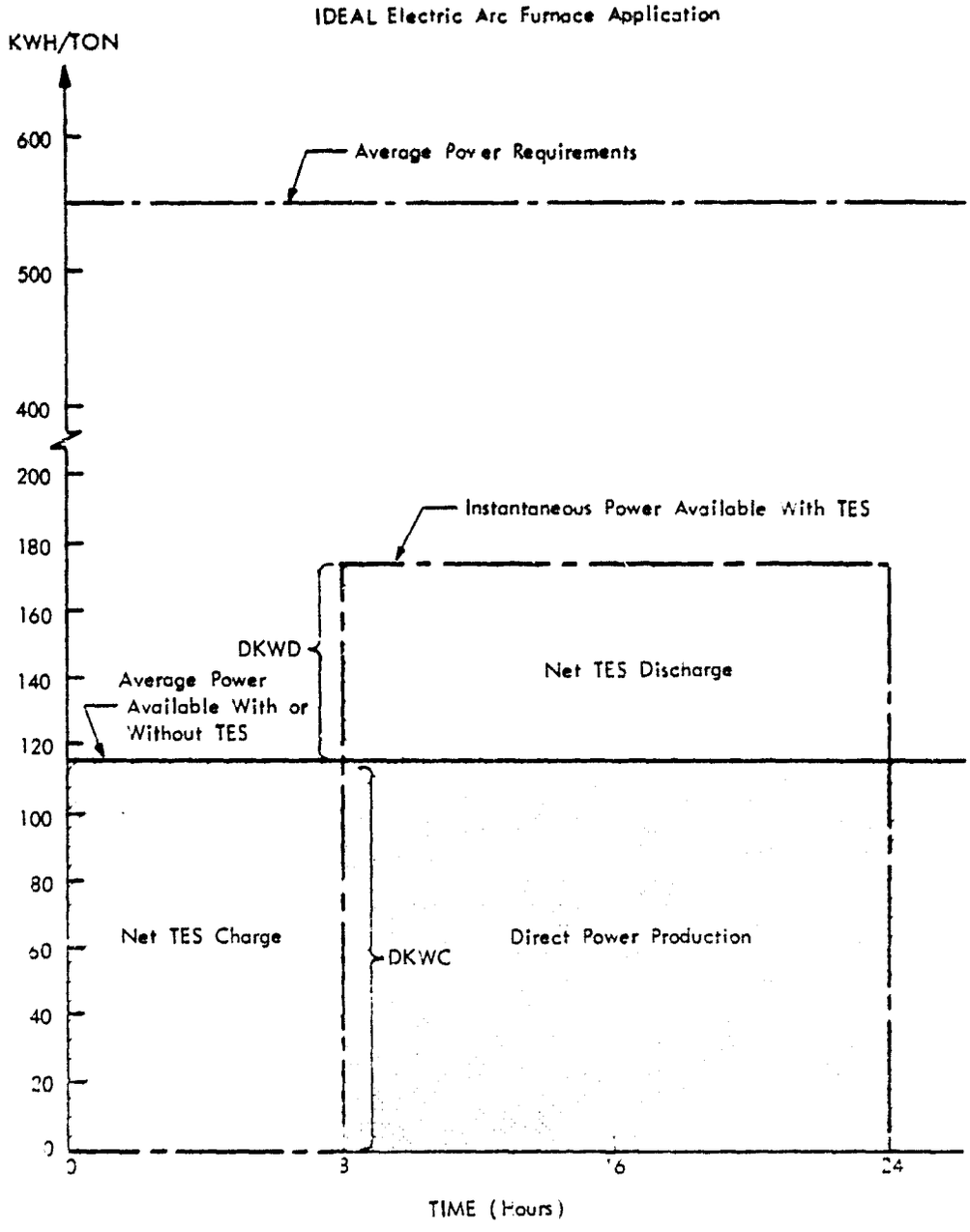

Figure 22 - Ideal Charge/Discharge Scenario for Steel Plant Electric Arc Furnace TES Application

In this application, two fluidized beds are used: one as a thermal-buffer for stabilizing the furnace exhaust gas temperature and the second as a fluidized bed heat exchanger (FBHX) to recover and use energy for power generation. The design of each of these beds is presented next.

3.2.2.1 Thermal Buffer System Design--

The exhaust gas stream from an electric arc furnace has short-term periodic temperature variations from approximately 38 to 1371°C (100 to 2500°F), with an average temperature of 700°C (1300°F). Each periodic cycle lasts approximately 3 hr. In order to effectively use or store the thermal energy available in the gas stream, it is desirable to minimize the temperature variations.

Determination of the buffer storage size requires analysis of its transient behavior. This in turn is dependent on the wave form (amplitude and period) of the inlet gas temperature variation, the desired reduction in the outlet gas temperature fluctuation, the mass flow rate and specific heat of the electric arc furnace gases passing through the bed, the specific heat of the bed material, and the number of bed stages. Appendix D presents a solution of the differential equations which result when a sinusoidal inlet temperature variation is assumed. The resulting equation for the total bed mass is:

$$M_{B_T} = \frac{N\dot{M}gC_gL}{2\pi C_B}\left(r^{-2/N} - 1\right)^{1/2} \qquad (1)$$

where M_{B_T} = total bed mass for all stages

N = number of bed stages

$\dot{M}g$ = mass flow rate of gas through the bed

C_g = specific heat of gas

C_B = specific heat of bed material

L = length of one periodic temperature cycle

r = ratio of outlet temperature amplitude to the inlet temperature amplitude

Assuming that a typical electric arc furnace has a 100-ton capacity, requires a 3-hr heat to produce steel, and exhausts 16.5 m^3/sec of gas at 700°C (35,000 scfm of gas at 1300°F) average temperature with a ± 670°C (± 1200°F) periodic temperature variation, a parametric analysis was performed to determine the buffer size. The number of stages was varied from one to five and 1/r was varied from five to 25. The results, which are presented in Table 20, indicate that the optimum number of fluid bed stages varies from two stages when 1/r = 5

TABLE 20

TOTAL MASS OF FLUID BED MATERIAL REQUIRED FOR ELECTRIC ARC FURNACE TES BUFFER WITH ALL BED MATERIAL CONTINUOUSLY FLUIDIZED

Input temperature variation = ± 667°C (1200°F)

Gas flow rate = 16.5 m^3/sec at 704°C average temperature = 19.8 kg/sec
(35,000 scfm at 1300°F average temperature = 157,000 lb/hr)

Input/Output Maximum Temperature Variation (1/r)	Output Temperature Variation °C (°F)	Total Mass of Fluid Bed Material Per Number of Fluid Bed Stages (N)				
		N = 1	N = 2	N = 3	N = 4	N = 5
5	± 133 (± 240)	167,000 kg	136,000	146,000	152,000	162,000
		(368,400 lb)	300,800	312,900	334,400	357,400
10	± 67 (± 120)	339,000	205,000	195,000	201,000	210,000
		748,200	451,200	430,500	442,300	462,300
12	± 56 (± 100)	408,000	262,000	211,000	214,000	222,000
		899,200	498,800	464,400	472,200	490,500
15	± 44 (± 80)	511,000	252,000	231,000	231,000	238,000
		1,125,100	655,600	569,300	560,500	572,000
20	± 33 (± 60)	681,000	302,000	258,000	254,000	259,000
		1,502,100	655,600	569,300	560,500	572,000
25	± 27 (± 48)	852,000	335,000	281,000	273,000	276,000
		1,878,500	738,800	619,900	601,600	609,000

to four stages when $1/r = 25$. It should be noted, if the optimum number of stages is exceeded, the total mass of all fluid bed stages will increase although the mass per stage is reduced.

A single-stage system, depicted in Figure 23, was considered first because of the relative simplicity of design and operation. However, the large mass of bed material needed to achieve significant temperature attenuation and bed pressure drop ruled out use of that design.

After additional consideration the variation of outlet temperature was chosen as ± 56°C (100°F) for the buffer storage system. For this variation in outlet temperature, a three-stage fluid bed buffer with a total of 210,650 kg (464,400 lb) of bed material is the best size. Further analysis of this bed to determine the area, depth, pressure drop, and fan horsepower required when the superficial velocity is varied from 0.15 to 1.22 m/sec (0.5 to 4.0 ft/sec) is presented in Table 21. Although the lower superficial velocities result in lower fan horsepowers, they also require much larger bed diameters which may pose air distribution and fabrication problems.

Figure 24 presents a schematic of the three-stage buffer system with a superficial velocity of 1.22 m/sec (4 ft/sec.)

Further analysis of the three-stage bed disclosed a major operational problem. Severe thermal stress will occur on the lower grid plate. As shown in Figure 24, the gas temperature exiting the first stage may vary ± 278°C (500°F). This problem was viewed as a major deterrent to the use of such a design and, as a result, an alternate design was deemed necessary.

Figures 25a and 25b show the TES buffer system which was finally chosen. This design utilitizes two solids storage containers in conjunction with a single-stage counterflow FBHX and requires that only enough bed material be fluidized at any given time to provide stable fluidization and adequate gas-solids contact, thus, minimizing the pressure drop. Since the bed temperature fluctuates only between 649 and 760°C (1200 and 1400°)F, the thermal stress on the grid plate is minimized. For the 111°C (200°F) output temperature variation illustrated, the solids flow rate varies from 0, when the inlet gas temperature is between 649 and 760°C (1200 and 1400°F), to approximately 7.7 times the gas flow rate, when the inlet gas temperature is at its maximum deviation from the 700°C (1300°F) average. The total required mass of the solids is approximately 1.16×10^6 lb for a 3-hr TES cycle and specific heats of 0.28 and 0.20 for the gas and solids, respectively.

3.2.2.2 Initial Calculations for the Peak Power System Design--

As per the operating charge/discharge scenario selected for the electric arc furnace TES, the storage system will be charged for 8 hr and discharged during the peak-demand period of 16 hr. In order to test the validity of the peak TES portion of the electric arc furnace application as shown in Figure 22 a hand calculation of the system was performed. These calculations were similar in format to the sample calculations for the cement kiln application in Appendix B. To facilitate the hand calculations a number of assumption were made. The assumptions were:

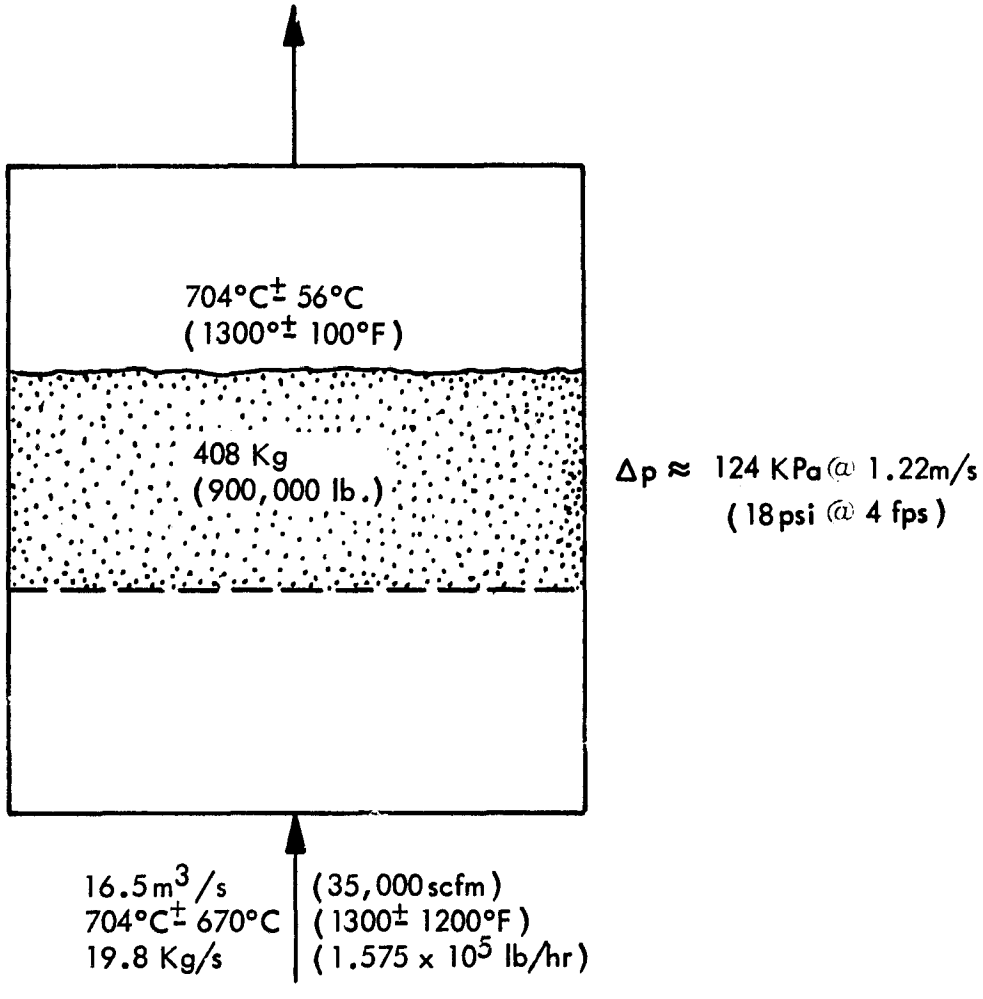

Figure 23 - Single Stage FBHX Buffer

TABLE 21

FLUID BED SIZING TRADE-OFF FOR ELECTRIC ARC FURNACE TES BUFFER

M_{B_T} = 211,000 kg (464,400 lb); N = 3; M_B = 70,000 kg (154,800 lb)

Flow rate = 16.5 m^3/s at 700°C average temperature
= 35,000 scfm at 1300°F average temperature
= 116,000 acfm at 1760°F average temperature

	Superficial Velocity m/s (ft/sec)				
	0.15 (0.5)	0.30 (1.0)	0.61 (2.0)	0.91 (3.0)	1.22 (4.0)
Bed area, m^2 (ft^2)	360 (3,872)	180 (1,926)	90 (968)	60 (645)	45 (484)
Bed diameter, m (ft)	24.1 (79.2)	17.0 (56.0)	12.1 (39.6)	9.8 (32.3)	8.5 (28.0)
Unfluidized density, kg/m^3 (lb/ft^3)	1,603 (100)	1,603 (100)	1,603 (100)	1,603 (100)	1,603 (100)
Unfluidized total depth, m (ft)	0.36 (1.2)	0.73 (2.4)	1.46 (4.8)	2.19 (7.2)	2.92 (9.6)
Unfluidized depth per stage, m (ft)	0.12 (0.4)	0.24 (0.8)	0.48 (1.6)	0.73 (2.4)	0.98 (3.2)
Bed pressure drop, KPa (psi)	5.7 (0.83)	11.5 (1.67)	22.9 (3.33)	34.5 (5.00)	45.9 (6.66)
Total pressure drop, KPa (psi)	7.4 (1.08)	15.0 (2.17)	29.9 (4.33)	44.8 (6.50)	59.7 (8.66)
I.D. fan, kw (hp)	397 (532)	773 (1,036)	1,437 (1,926)	1,967 (2,637)	2,310 (3,096)
F.D. fan, kw (hp)	398 (533)	780 (1,045)	1,077 (1,444)	2,143 (2,872)	2,749 (3,685)

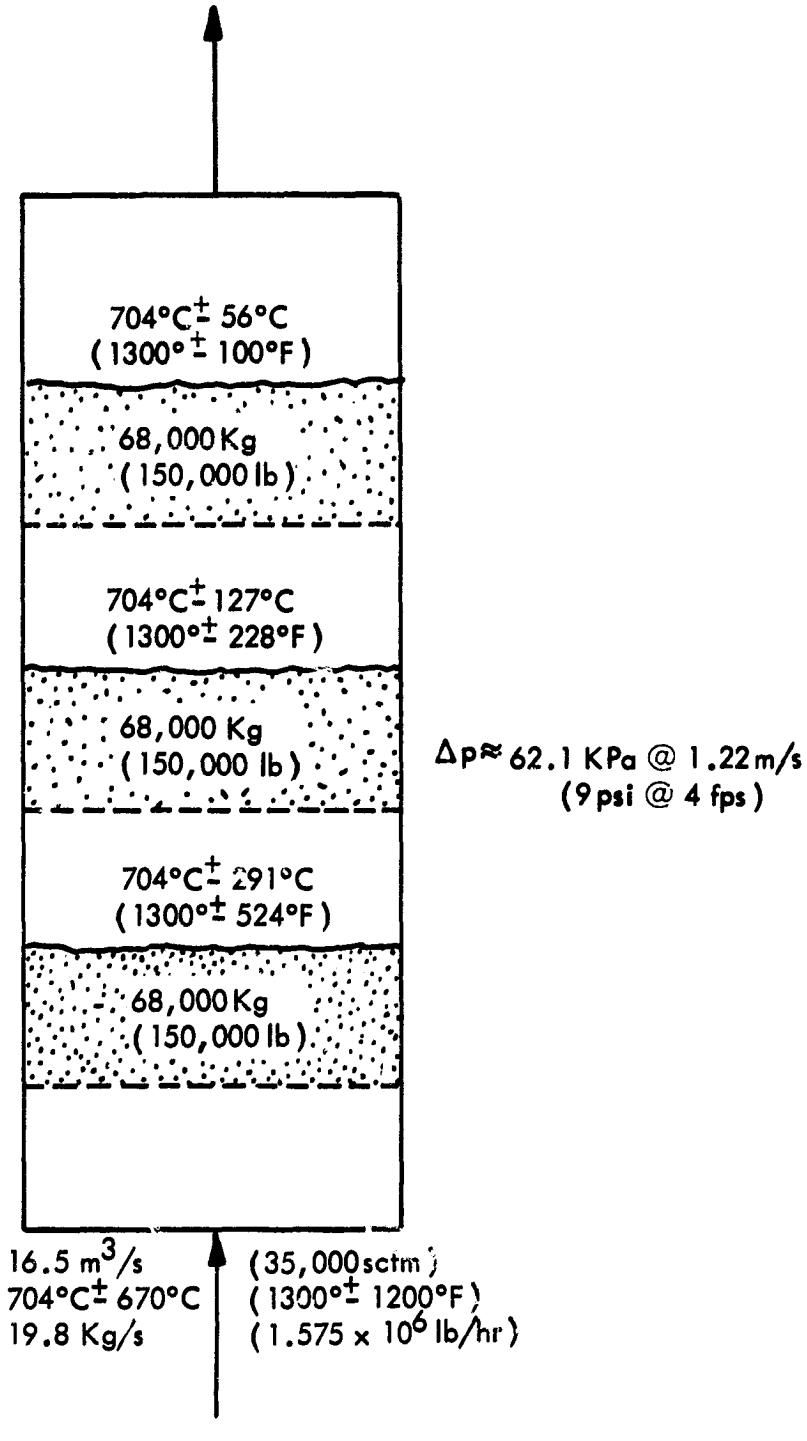

Figure 24 - Three Stage FBHX Buffer

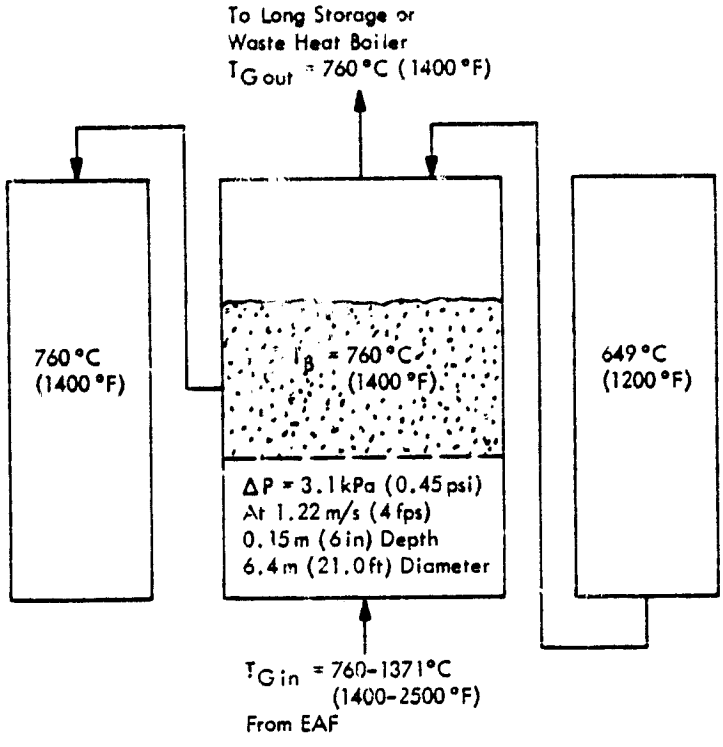

Figure 25a - Short Term Buffer TES - Charge

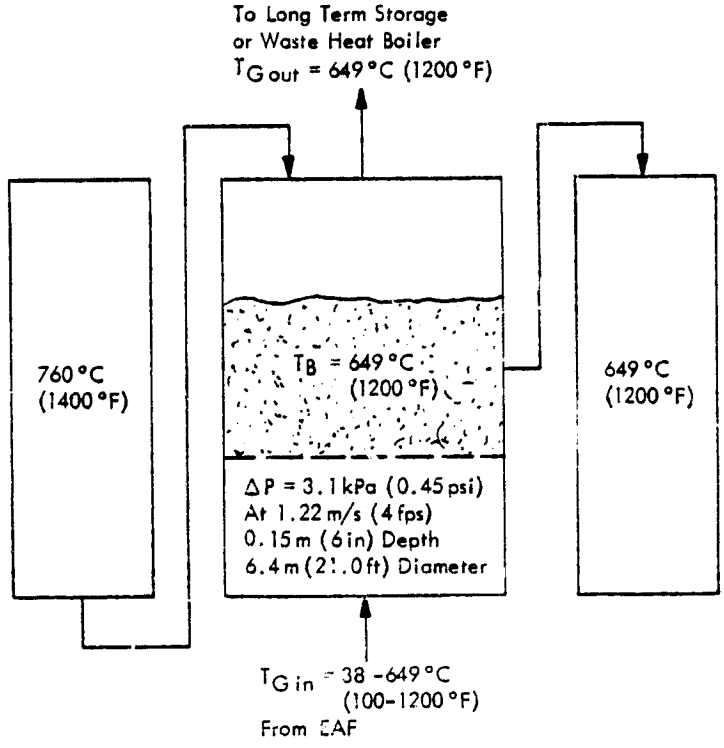

Figure 25b - Short Term Buffer TES - Discharge

- The mass flow of solids is such that $\Delta T_{solids} = \Delta T_{gas}$.
- The waste heat boiler exit temperature is 149°C (300°F).
- The cold solids store temperature is 204°C (400°F).
- There is no temperature rise across the fans.
- The unfluidized bed depth is 0.3 m (12 in.).

Table 22 summarizes the hand calculation for the FBHX initial design and operating parameters. A schematic representation of the TES system operation during charge and discharge cycle is given in Figure 26A and 26b. The design procedure is identical to that used for the cement kiln application (see Appendix C). Table 23 summarizes the hand calculated initial energy balance. The energy balance indicates that in the initial system design 179.9 kwh of energy per ton of steel is forfeited during the 8 hr charge mode in order to obtain 34.5 kwh of energy per ton during the discharge mode. This results in an overall effectiveness of 0.38 for one charge-discharge cycle.

3.2.2.3 Final Calculations for Multistage Shallow Bed Heat Exchanger System--

The initial calculations for the multistage shallow bed system, which were summarized in the preceding section, established the basic feasibility of the FBHX/TES system design for the peaking storage of the electric arc furnace application. The computer program in Appendix C was then used to optimize the design. The computer program was also used to perform the parametric analysis which is presented in Section 3.3 of this report.

The final selected design results are presented in Table 24 and are depicted schematically in Figures 27a and 27b for the charge and discharge modes, respectively. Figure 28 gives the actual operating scenario for the final design and indicates the effects of thermal effectiveness and fan power losses.

Comparison of initial values in Tables 22 and 23 with the final values shown in Table 24 indicates that some improvement was obtained. The final energy balance indicates that 146.4 kwh of energy per ton of steel must be forfeited during the TES 8 hr charge mode in order to gain 38.1 kwh of peak energy per ton during the discharge mode. This results in an overall effectiveness of 0.52 for one complete charge-discharge cycle. As with the cement plant application much of the improvement was due to reducing the grid hole diameter and bed depth to minimize the total pressure drop.

3.3 TECHNICAL ANALYSIS OF CEMENT KILN AND EAF SYSTEMS

The technical analysis of the two energy storage systems involved a detailed parametric analysis of each system. Each aspect of the technical analysis is presented in the following subsections.

TABLE 22

INITIAL FBHX DESIGN AND OPERATING PARAMETERS FOR EAF PEAK STORAGE APPLICATION

Parameter		Charge	Discharge
Gas flow: mass through FBHX, $\dot{G}$	kg/s	19.78	9.89
	(lb/hr)	(157,000)	(78,500)
volume at bed inlet,	m^3/s	38.0	8.2
	(acfm)	(80,600)	(17,400)
pressure at bed inlet,	KPa	145	145
	(psia)	(21.1)	(21.1)
Solids flow rate through FBHX, $\dot{S}$,	kg/s	27.69	13.85
	(lb/hr)	(2.205×10^5)	(1.103×10^5)
Gas temperature, in,	°C	704	149
	(°F)	(1300)	(300)
out,	°C	260	593
	(°F)	(500)	(1100)
Solids temperature, in,	°C	204	649
	(°F)	(400)	(1200)
out,	°C	649	204
	(°F)	(1200)	(400)
Range of superficial gas velocity, bottom stage to top stage,	m/s	1.9 to 1.6	0.5 to 1.2
	(ft/sec)	(6.28 to 5.18)	(1.5 to 3.83)
Number of stages (same FBHX for charge and discharge)		8	8
Diameter of bed,	m	5.0	5.0
	(ft)	(16.4)	(16.4)
Total bed height including TDH,	m	7.3	7.3
	(ft)	(24)	(24)
Unfluidized bed depth,	m	0.3	0.3
	(in.)	(1.0)	(1.0)
Grid plate hole diameter,	mm	6.3	6.3
	(in.)	(0.25)	(0.25)
Total FBHX pressure drop,	KPa	44.2	44.2
	(psi)	(6.5)	(6.5)
Adiabatic fan motor power required for pressurizing the gas to provide the ΔP,	KW	2,145	463
	(hp)	(2,878)	(621)
ΔP required for pneumatic transport of solids,	KPa	12.8	12.8
	(psi)	(1.85)	(1.85)
Adiabatic fan motor power for pneumatic transport of solids,	kw	19	19
	(hp)	(25)	(25)

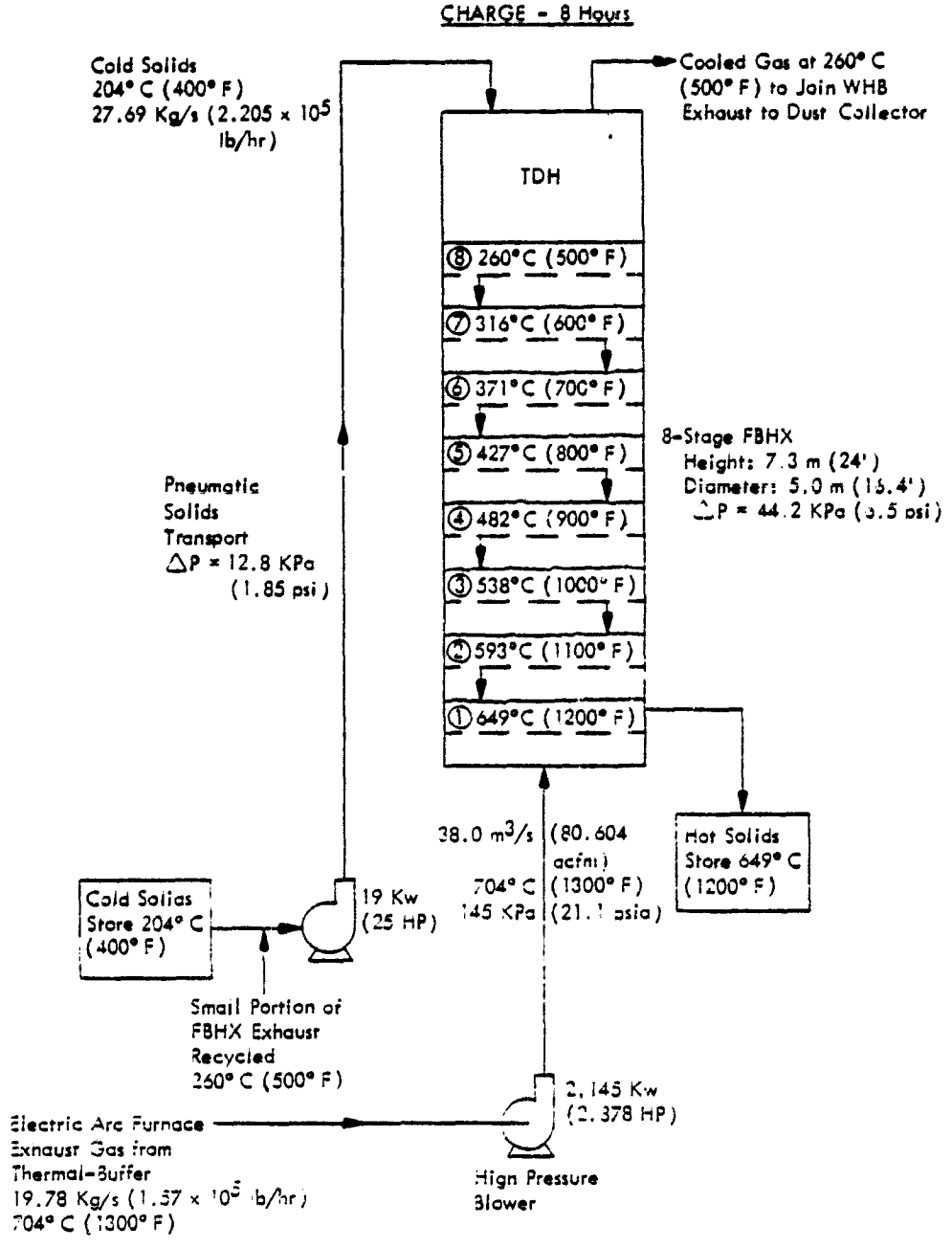

Figure 26a - Schematic Representation of the Initial Fluidized Bed TES System Design-Charge Phase for Electric Arc Furnace Application

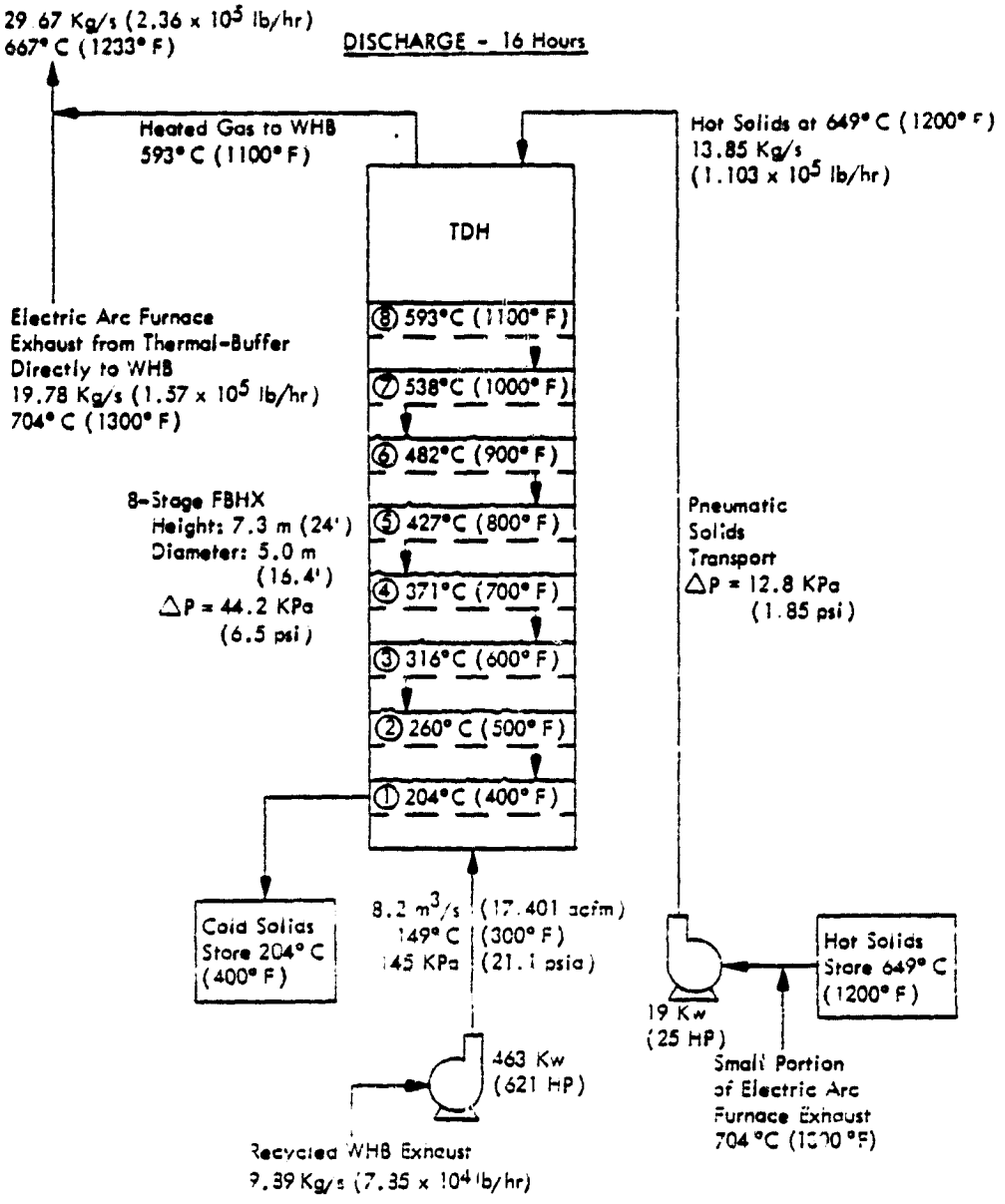

Figure 26b - Schematic Representation of the Initial Fluidized Bed TES System Design-Discharge Phase for Electric Arc Furnace Application

TABLE 23

SUMMARY OF INITIAL ENERGY AND MATERIAL BALANCE SUMMARY OF ELECTRIC ARC FURNACE TES

Basis: One electric arc furance with a capability of 100 tons/cycle operating 3 hr per cycle for a net production rate of 33.3 tons of steel per hour

Energy available in kiln exhaust gas at 704°C (1300°F), assuming a final waste heat boiler exit temperature of 149°C (300°F)

$$\frac{1.57 \times 10^5 \text{ lb/hr} \times 0.28 \text{ Btu/lb °F} \times (1300-300)°F}{33.3 \text{ tons steel/hr} \times 11{,}380 \text{ Btu/kwh}}$$

$$115.9 \frac{\text{kwh}}{\text{ton clinker}}$$

TES Charge

During the 8-hr charge cycle, the entire furnace exhaust will be sent through the buffer and the FBHX/TES system. Based on this, the net energy available from the recovery system during charge cycle is:

$$E_{\text{net/charge}} = E_{\text{buffer exhaust}} - 1.0 \times E_{\text{buffer exhaust}} - E_{\text{TES operation}}$$

where $E_{\text{TES operation}}$ represents the power requirements for operating the fluidized bed TES

$$E_{\text{TES operation}} = \frac{(2{,}878 + 25) \text{ hp}}{1.341 \text{ hp/kw} \times 33.3 \text{ tons/hr}}$$

$$= 64.9 \frac{\text{kwh}}{\text{ton}}$$

Substituting the values in Eq. (1),

$$E_{\text{net/charge}} = 115.9 - 115.9 - 64.9$$

$$= -64.9 \frac{\text{kwh}}{\text{ton}}$$

TABLE 23 (concluded)

TES Discharge

During the 16-hr discharge cycle, the furnace exhaust gas will be sent through the buffer and then directly to the waste heat boiler (WHB). In addition, a portion of the WHB exhaust equal to 50% of the furnace exhaust gas will be recycled through the FBHX thus dischargins the energy stored in the circulating solid media. The total energy available from the recovery/TES system during the discharge cycle is calculated as follows:

$$E_{net/discharge} = E_{buffer\ exhaust} + 0.5 \times E_{buffer\ exhaust} \times (\text{loss factor during storage and recovery}) - E_{TES\ operation}$$

$$E_{TES\ operation} = \frac{(621 + 25)}{1.341 \times 33.3} = 14.5\ \frac{kwh}{ton}$$

$$E_{net/discharge} = 115.9 + 0.5 \times 115.9 \times \frac{1100}{1300} - 14.5 = 150.4\ \frac{kwh}{ton}$$

TABLE 24

FINAL FBHX DESIGN AND OPERATING PARAMETERS FOR EAF PEAK STORAGE APPLICATION

Parameter	Charge	Discharge
Gas flow: mass through FBHX, G kg/s	19.78	9.89
(lb/hr)	(157,000)	(78,500)
volume at bed inlet, m^3/s	56.6	10.2
(acfm)	(120,000)	(21,600)
pressure at bed inlet, KPa	98	127
(psia)	(14.2)	(18.0)
Solids flow rate through FBHX, S, kg/s	25.86	12.93
(lb/hr)	(205,000)	(103,000)
Gas temperature, in, °C	704	174
(°F)	(1300)	(346)
out, °C	285	593
(°F)	(546)	(1100)
Solids temperature, in, °C	215	664
(°F)	(419)	(1227)
out, °C	664	215
(°F)	(1227)	(419)
Range of superficial gas velocity, bottom stage to top stage, m/s	2.7 to 2.1	0.5 to 1.2
(ft/sec)	(9.01 to 6.73)	(1.62 to 3.86)
Number of stages (same FBHX for charge and discharge)	8	8
Diameter of bed, m	5.1	5.1
(ft)	(16.8)	(16.8)
Total bed height including TDH, m	9.2	9.2
(ft)	(30.0)	(30.0)
Unfluidized bed depth, m	0.16	0.16
(in.)	(6.1)	(6.1)
Grid plate hole diameter, mm	3.2	3.2
(in.)	(0.125)	(0.125)
Total FBHX pressure drop, KPa	23.0	23.0
(psi)	(3.34)	(3.34)
Adiabatic fan motor power required for pressurizing the gas to provide the ΔP, KW	1,002	268
(hp)	(1,343)	(359)
ΔP required for pneumatic transport of solids, KPa	12.7	8.8
(psi)	(1.84)	(1.28)

TABLE 24 (concluded)

Parameter	Charge	Discharge
Adiabatic fan motor power for pneumatic transport of soilds, kw (hp)	17 (23)	8 (11)
Average energy in buffer exhaust, KWH/ton	115.88	115.88
Net energy from system with TES, KWH/ton	-30.56	153.97
Energy difference due to TES, KWH/ton	-146.44	38.09

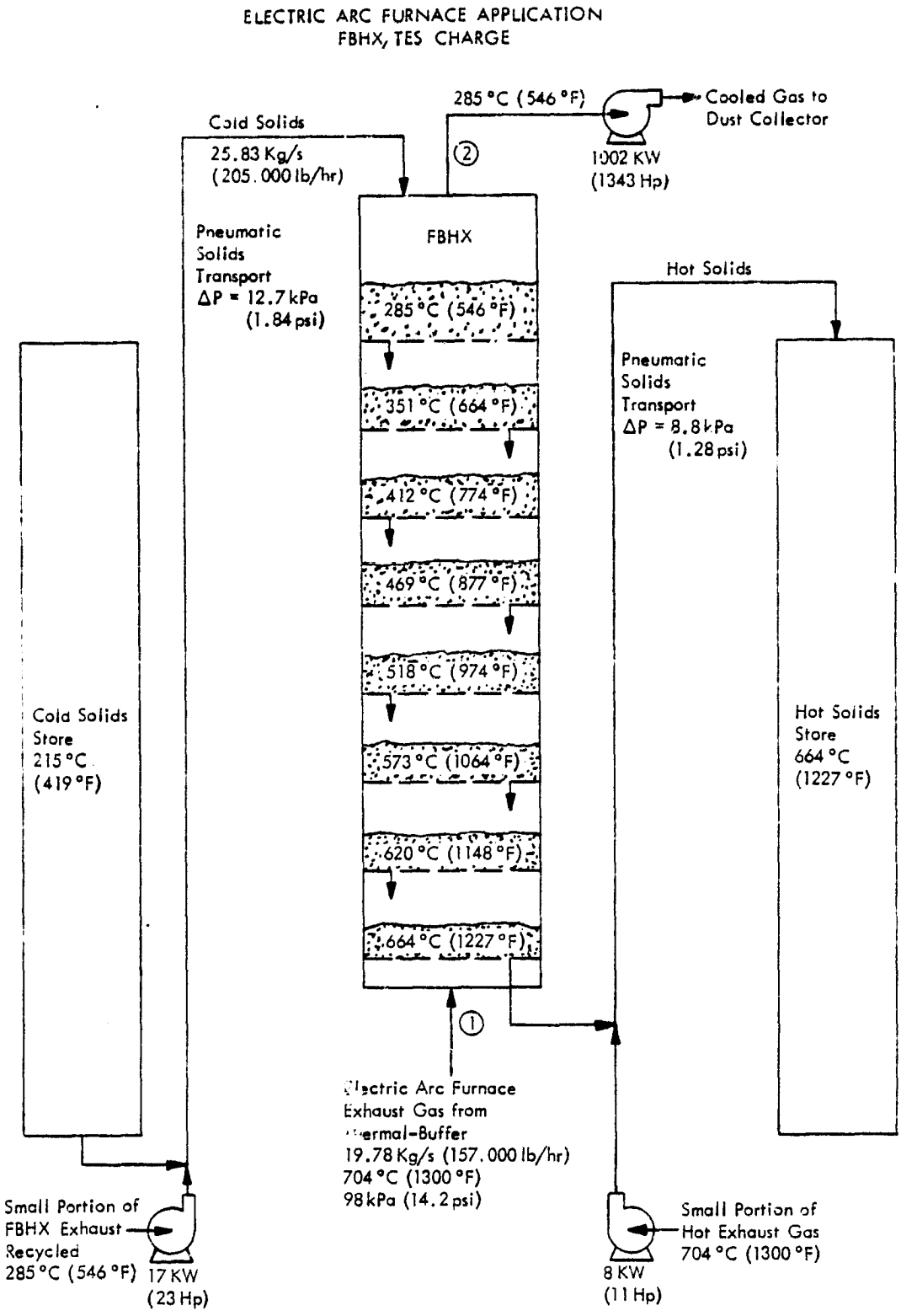

Figure 27a - Schematic Representation of the Final Fluidized Bed TES System Design - Charge Phase for Electric Arc Furnace Application

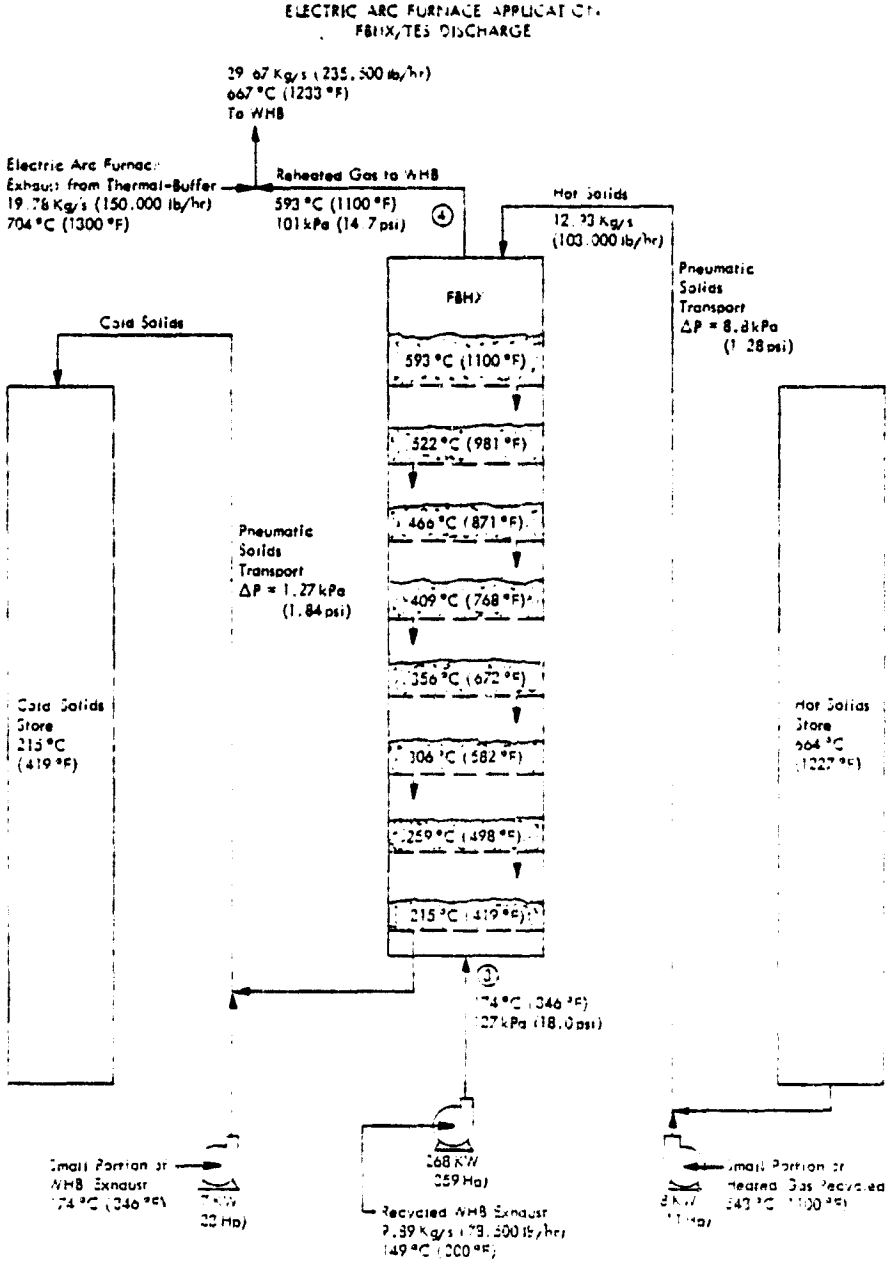

Figure 27b - Schematic Representation of the Final Fluidized Bed TES System Design-Discharge Phase for Electric Arc Furnace Application

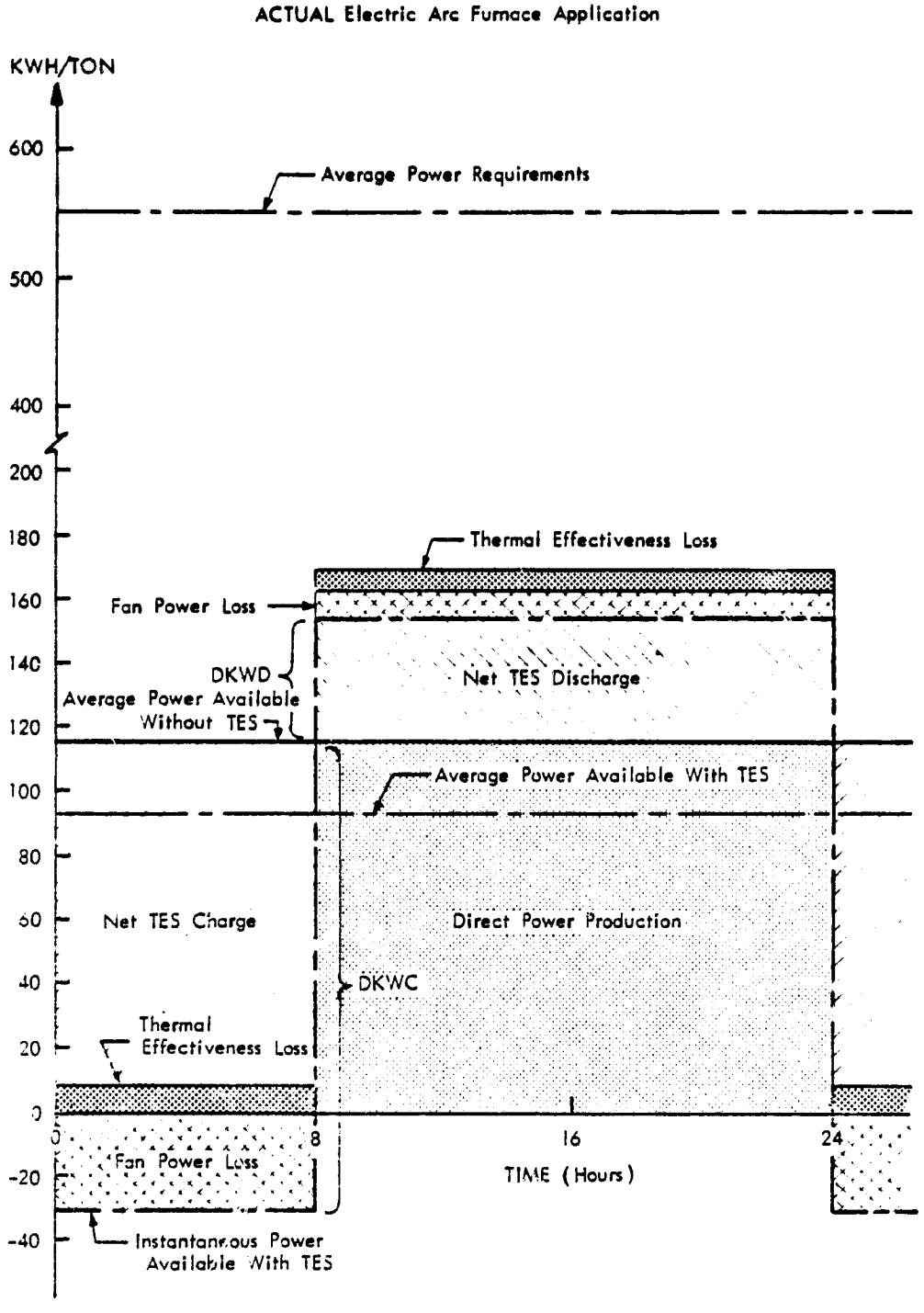

Figure 28 - Actual Charge/Discharge Scenario for Final Steel Plant Electric Arc Furnace TES Application

3.3.1 Parametric Analysis of Cement Kiln and EAF Systems

In order to perform a parametric analysis of the FBHX systems, a computer program was developed. The program was designed to be general enough to perform the design and parametric evaluation of the cement kiln, EAF, and other TES systems. The program was designed with maximum flexibility to determine the effect of major design and operating parameters on the overall eergy recovery. A general flow diagram of the computer program is presented in Figure 29. Appendix C presents the details of the program.

The major independent variables selected for program inputs include:

- General system operating parameters
- Amount and temperature of gas flow to TES during charge and from TES during discharge
- Charge-discharge cycle durations
- Particle diameter
- Fluid bed media particle and bulk densities
- Grid plate hole diameter

The major dependent variables which are calculated as program outputs include:

- Optimum number of FBHX stages
- Ratio of solids flow to gas flow
- Bed dimensions
- Bed depth
- Bed pressure drop and attrition rate
- Critical and operating gas velocities
- Horsepower required to operate the FBHX
- Horsepower required for pneumatic transport
- Net energy rate produced during charge and discharge cycles
- Net energy rate which could be produced by continuous operation without TES

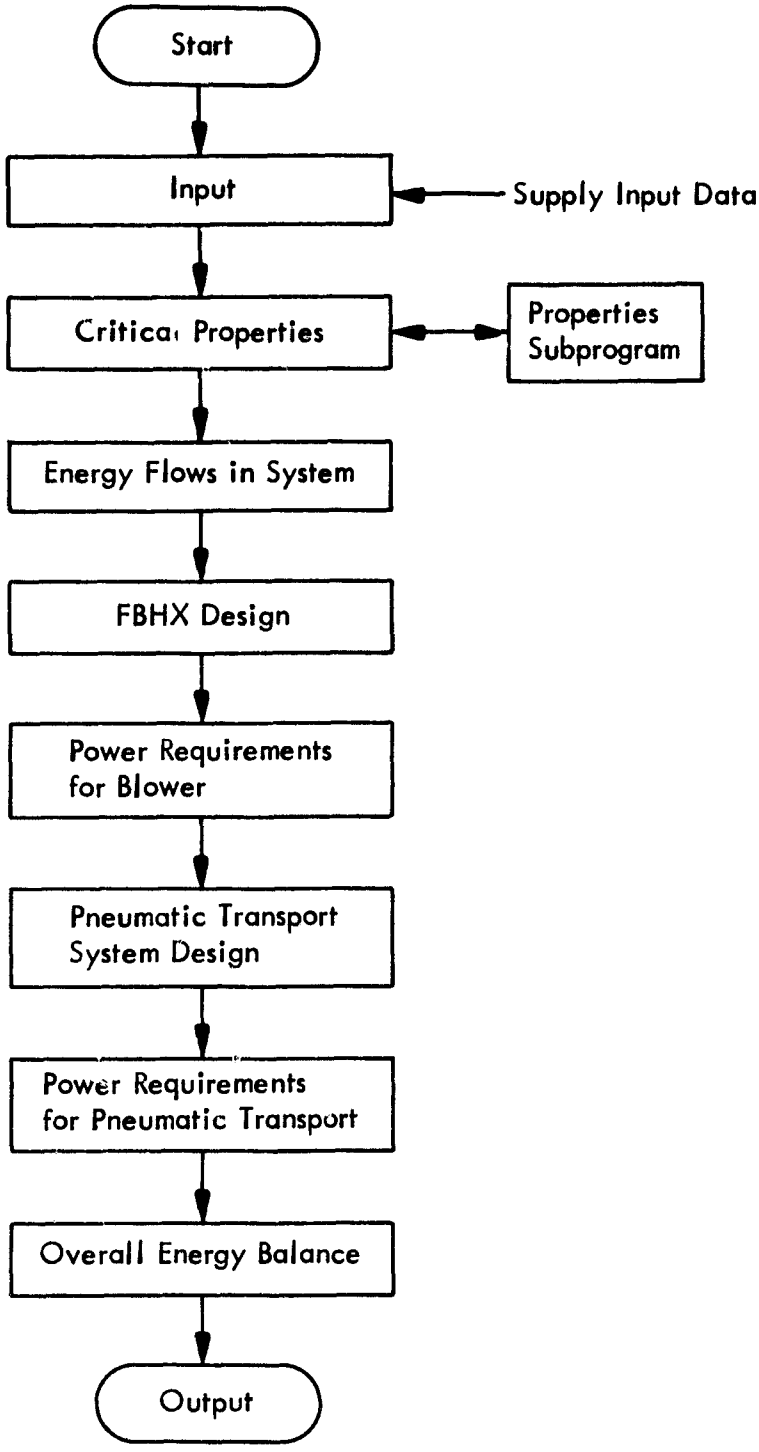

Figure 29 - Flow Diagram for FBHX TES Computer Simulation

3.3.1.1 Thermodynamic Considerations--

The first major section of the computer program examines the critical thermodynamic variables of the FBHX/TES system. These variables consist of 13 key temperature and flow parameters plus the number of fluid bed stages. These variables are:

- GFRC - the gas flow rate through the FBHX during charge
- GITC - the FBHX gas inlet temperature during charge
- GOTC - the FBHX gas outlet temperature during charge
- CHT - number of hours in the charge cycle
- GFRD - the gas flow rate through the FBHX during discharge
- GITD - the FBHX gas inlet temperature during discharge
- GOTD - the FBHX gas outlet temperature during discharge
- DCT - the number of hours in the discharge cycle
- RC - the ratio of solid flow specific heat to gas flow x specific heat during charge
- RD - the ratio of solid flow x specific heat to gas flow x specific heat during discharge
- HST - hot solids store temperature
- CST - cold solids store temperature
- N - number of FBHX stages

These 13 variables are related by the following equations which describe the thermal performance of the FBHX/TES charge-discharge system.

$$RC = \frac{GITC-GOTC}{HST-CST} \tag{2}$$

$$RD = \frac{GOTD-GITD}{HST-CST} \tag{3}$$

$$\frac{RC^N-1}{RC^{N+1}-1} = \frac{HST-CST}{GITC-CST} \quad \text{(also = ESC effectiveness during charge)} \tag{4}$$

$$\frac{RD^{N-1}}{RD^{N+1}-1} = \frac{HST-CST}{HST-GITD} \quad \text{(also = ESD effectiveness during discharge)} \tag{5}$$

$$(CFRC)(CHT)(RC) = (GFRD)(DCT)(RD) \tag{6}$$

Seven of the variables - GFRC, GITC, CHT, GFRD, GITD, GOTD, and DCT are independent input variables. This leaves six unknown variables and only five equations which makes a unique solution impossible. Rearranging the equations to eliminate HST and CST gives an equation for thermal effectiveness for the total system.

$$\frac{GOTD-GITD}{GITC-GITD} = \frac{RD}{(RD^{N+1}-1)/(RD^{N}-1)+(RC^{N+1}-1)/(RC^{N}-1)-1} \qquad (7)$$

By letting RC = RD the family of curves shown in Figure 30 was calculated to show the effect that the number of bed stages and the solid and gas flow rates have on the overall FBHX system's thermal effectiveness. Figure 30 indicates that the overall thermal effectiveness increases with the number of fluid bed stages and the optimum solid/gas energy flow ratio approaches 1.0 for two or more stages. It should be noted that for very high flow ratios the overall thermal effectiveness approaches 0.5 for any number of FBHX stages. For the two selected applications GITO is approximately 149°C (300°F). The process flow diagrams indicate that GITC is 704°C (1300°F) for the electric arc furnace application and 538°C (1000°F) for the cement kiln application. Since GITD and GITC are fixed, the thermal effectiveness and GOTD vary linearly and GOTD can easily be plotted as indicated by the righthand scales of Figure 30.

In designing the overall system it is obviously desirable to maximize the thermal effectiveness. It is also desirable to minimize the total solids which must be pneumatically conveyed and stored. Figure 31 gives the optimum operating zone to achieve maximum effectiveness with minimum solids as the number of bed stages and solid/gas energy flow rate varies. It should be noted that the one stage and two stage systems were arbitarily cut off when the energy flow ratio reaches 2.0 while all higher stage systems cut off at the maximum effectiveness. The computer program automatically selects the number of stages indicated by the criteria shown in Figure 31. Utilizing the criteria shown in Figure 31 to select the optimum number of stages for a given set of temperature inputs allows the number of unknown variables to be reduced such that there are five equations with five unknowns and unique solutions can be obtained.

Note that assumptions that RC = RD was made for the convenience of the initial investigation, however, the computer program will function when RC = RD. For a given CHT and DCT, selecting GFRC and GFRD (see Eq. 6) such that RC is approximately equal to RD resulted in near optimum energy recovery in later sensitivity studies.

The basic thermodynamic considerations above are independent of the parasitic power losses required to operate the FBHX system. Figures 30 and 31 indicate that the more FBHX stages the better, however, the next two sections examine the parasitic power and its effects on the system effectiveness for energy recovery, storage, and recycle.

3.3.1.2 Evaluation of the Cement Kiln Application--

Following the basic thermodynamic evaluation the computer program was used to examine the fluid bed design parameters and determine the FBHX/ TES system performance as a function of the input variables.

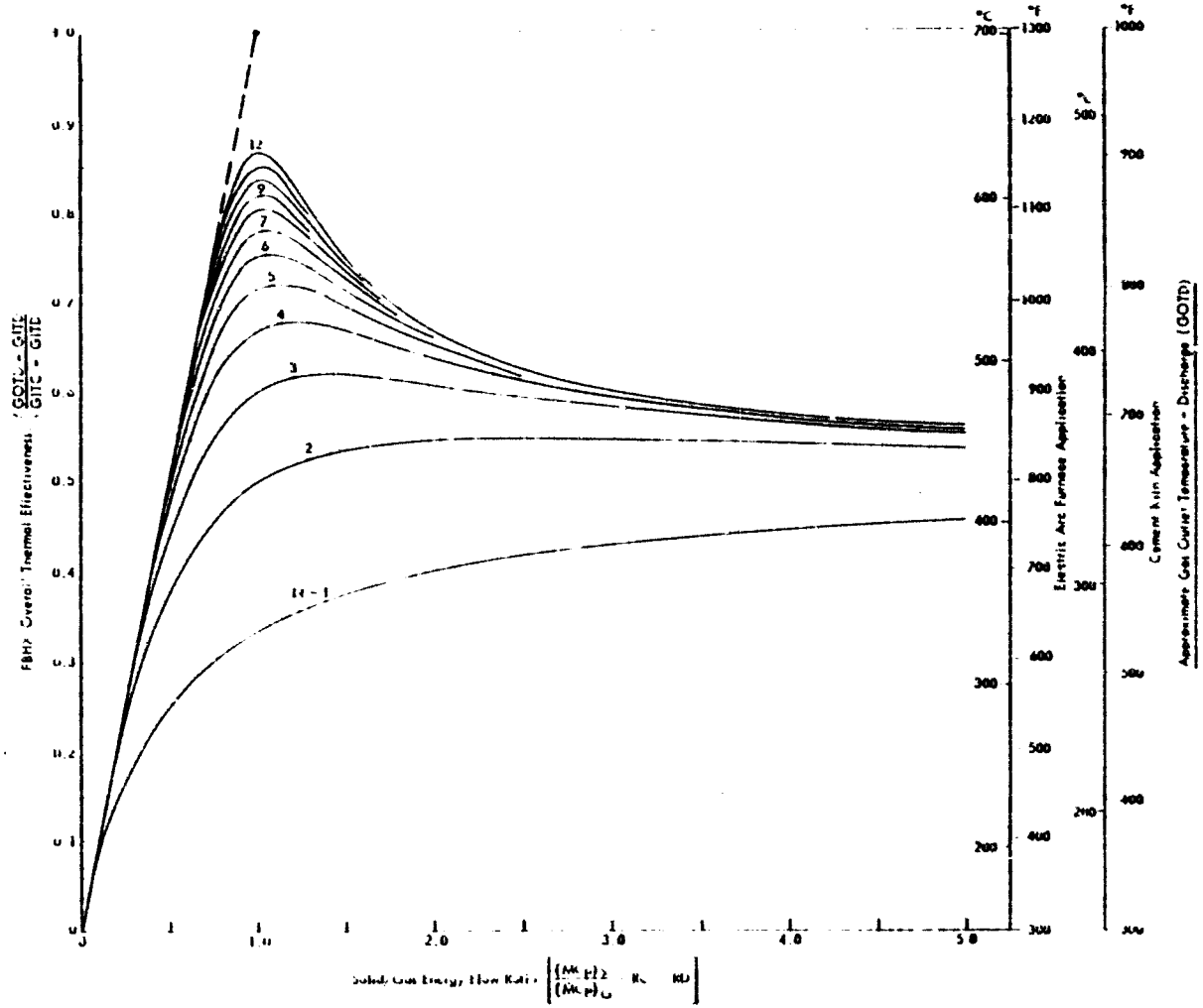

Figure 30 - Overall Thermal Effectiveness Versus Number of Bed Stages and Solid/Gas Flow

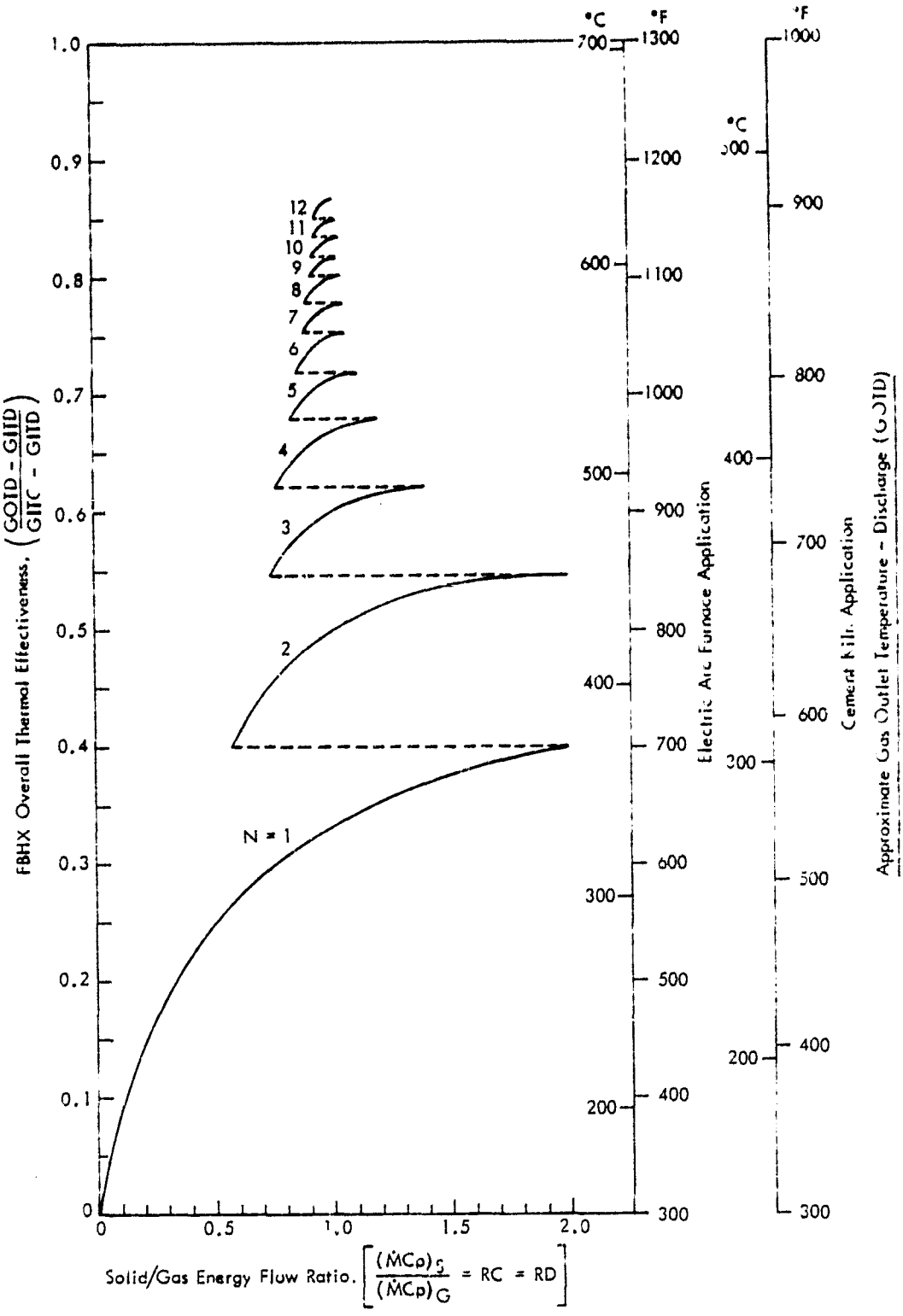

Figure 31 - Optimum Operating Zone for Maximum Effectiveness and Minimum Solids Storage

The major input variables for the cement kiln application were the production rate, the kiln gas flow rate, the FBHX flow rate during charge and discharge, the charge and discharge time, the FBHX inlet gas temperature during charge, and the FBHX gas outlet temperature during discharge. Other input parameters included the particle diameter, particle density, bulk density, and grid plate hole diameter.

Output parameters include: temperature and flows for the solid bed media, pressure drops, and horsepower requirements for the charge and discharge modes; the general fluid bed size and operating parameters including maximum and minimum fluidization velocities; attrition rate; and pneumatic transport requirements. The final output is an overall energy balance.

The interrelationships between the average peaking power and energy available during discharge, the average forfeited power and energy during charge, the gas outlet temperature during discharge, the number of charge and discharge hours, and the number of FBHX stages were investigated first.

In all the graphs which follow, the design point chosen for the model cement plant application is indicated with a circle.

Figure 32 shows the effects that the selected discharge gas outlet temperature, the number of FBHX stages, and the charge-discharge times have on the peaking power capacity and energy generation which is produced by the FBHX/TES system during the discharge mode. The average peak power capacity available is nearly proportional to the ratio of charge time to discharge time, however, the total energy generation is nearly proportional to the charge time. Figure 32 also indicates the effects of the parasitic power required for fluidization and pneumatic transport. As the number of stages increases the increasing parasitic power causes the peak power and energy to reach a maximum between 5 and 10 fluid bed stages and then decrease if additional stages are added even though the gas outlet temperature continues to decrease.

Figure 33 is similar to Figure 32, however, the ratio of peak power capacity during discharge to forfeited power capacity during charge and the ratio of peak energy generated during discharge to forfeited energy not generated during charge are plotted rather than just the discharge power capacity and discharge energy generated. The ratio of average peak power capacity available during discharge to the average forfeited power capacity during charge is nearly proportional to the ratio of charge time to discharge time. The ratio of total peak energy generation during discharge to forfeited energy not generated during charge is nearly constant for any specific number of FBHX stages or specific outlet temperature. Figure 32 also indicates the effects of parasitic power losses, however, the results are more pronounced than in Figure 31. The maximum power and energy ratios occur between four and seven FBHX stages and decrease more rapidly than previously indicated in Figure 32. The energy ratio can be considered as an overall FBHX/TES effectiveness when the parasitic losses are taken into account. Thus, the maximum FBHX/TES effectiveness is between 0.55 and 0.60 regardless of the charge-discharge times.

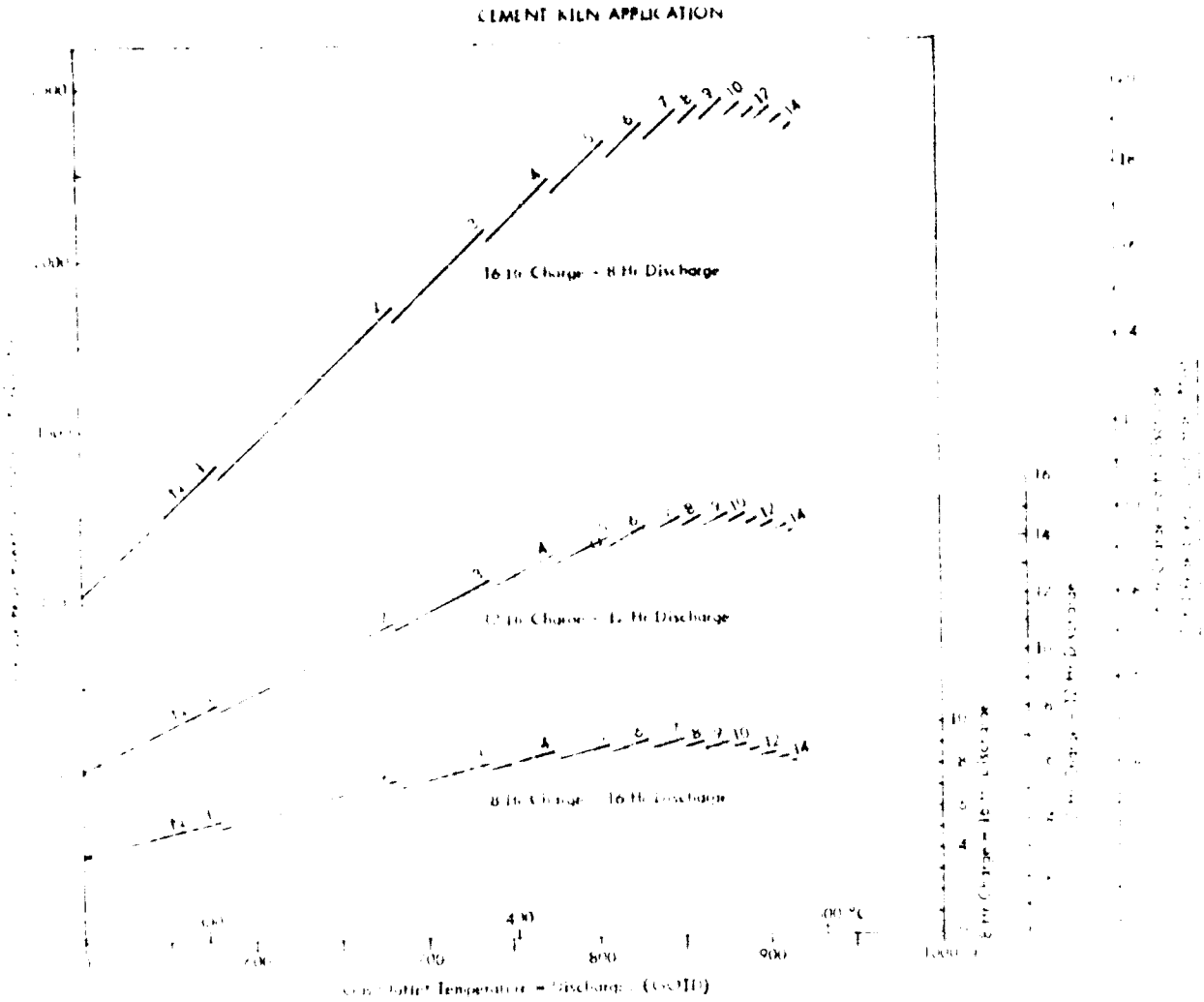

Figure 32 - Peak Power and Energy Available During Discharge as a Function of the Charge-Discharge Time - Cement Kiln Application

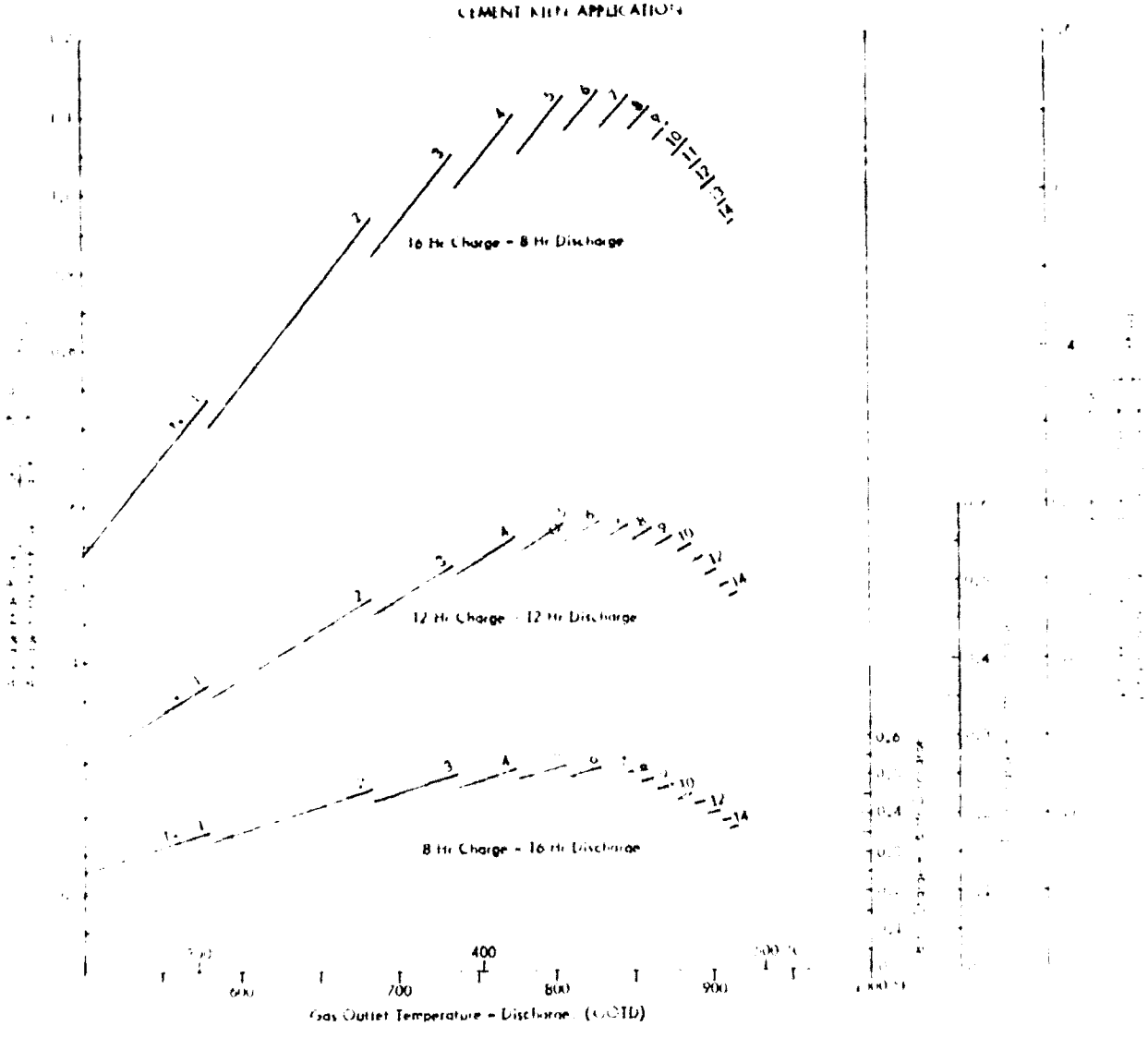

Figure 33 - Relative Power and Energy as a Function of the Charge-Discharge Time - Cement Kiln Application

By cross-plotting the average peak power during discharge from Figure 32 and the ratio of peak power during discharge to forfeited power during charge from Figure 33 the gas outlet temperature during discharge is eliminated as a parameter as shown in Figure 34. This figure dramatically shows the decreasing return obtained when the number of FBHX stages deviates from the optimum of 5 to 8 stages.

Of the other parameters investigated only the grid plate hole size and particle diameter have significant effects on the system design and performance.

The grid hole diameter is perhaps the most sensitive parameter evaluated. Figure 35 shows that the bed diameter is inversely proportional to the hole diameter while the total bed height increases with hole diameter. These effects would have a tendency to offset each other when fabricating the FBHX portion of the system.

Figure 36 shows that the number of holes required increased dramatically as the hole diameter decreases. Very small holes will lead to increased production costs because small holes are more difficult to produce as well as being more numerous. However, Figure 36 also shows that if the hole size is not minimized the fluid bed depth must be increased and consequently the bed pressure drop increased. The reason that the bed depth must be increased is to accommodate the increased jet penetration depth which results with larger holes. The effect that grid hole diameter has on the number of holes required and the pressure drop results in a trade off between high fabrication costs (i.e., many small holes) versus high operating costs (i.e., high parasitic fanpower requirements to overcome the bed pressure drop). The 3.175 mm (1/8 in.) holes selected for the model plant are believed to be a reasonable tradeoff.

Figures 37 and 38 show the indirect effects that the increased bed depth, due to large grid holes, has on the system performance. Figure 37 shows that the average peak power capacity available during discharge decreases nearly 50% while the forfeited power capacity during charge increases nearly 50% as the hole diameter and hence bed depth increase by a factor of four. The increased forfeited power capacity and reduced peak power capacity combine to give a 60% reduction in the ratio of peak energy to forfeited energy as shown in Figure 38.

Figure 38 also shows that the overall system effectiveness decreases about 10%, however, this is somewhat misleading. The overall system effectiveness parameter is the ratio of the total combined power available from the FBHX/TES and the kiln gas used directly by the waste heat boiler in the model plant compared to the power available in similar plant in which all the kiln gas goes directly to a waste heat boiler. If the model plant with the FBHX/TEX were to vent the gas which is used to charge the TES system, the overall system effectiveness would still be 90% due to the operation of the waste heat boiler. Only the difference in effectiveness can be attributed to the FBHX/TES system.

The effect of particle diameter is shown in Figure 39 which indicates that the total FBHX height is directly proportional to the particle diameter while the bed diameter decreases with increasing particle size.

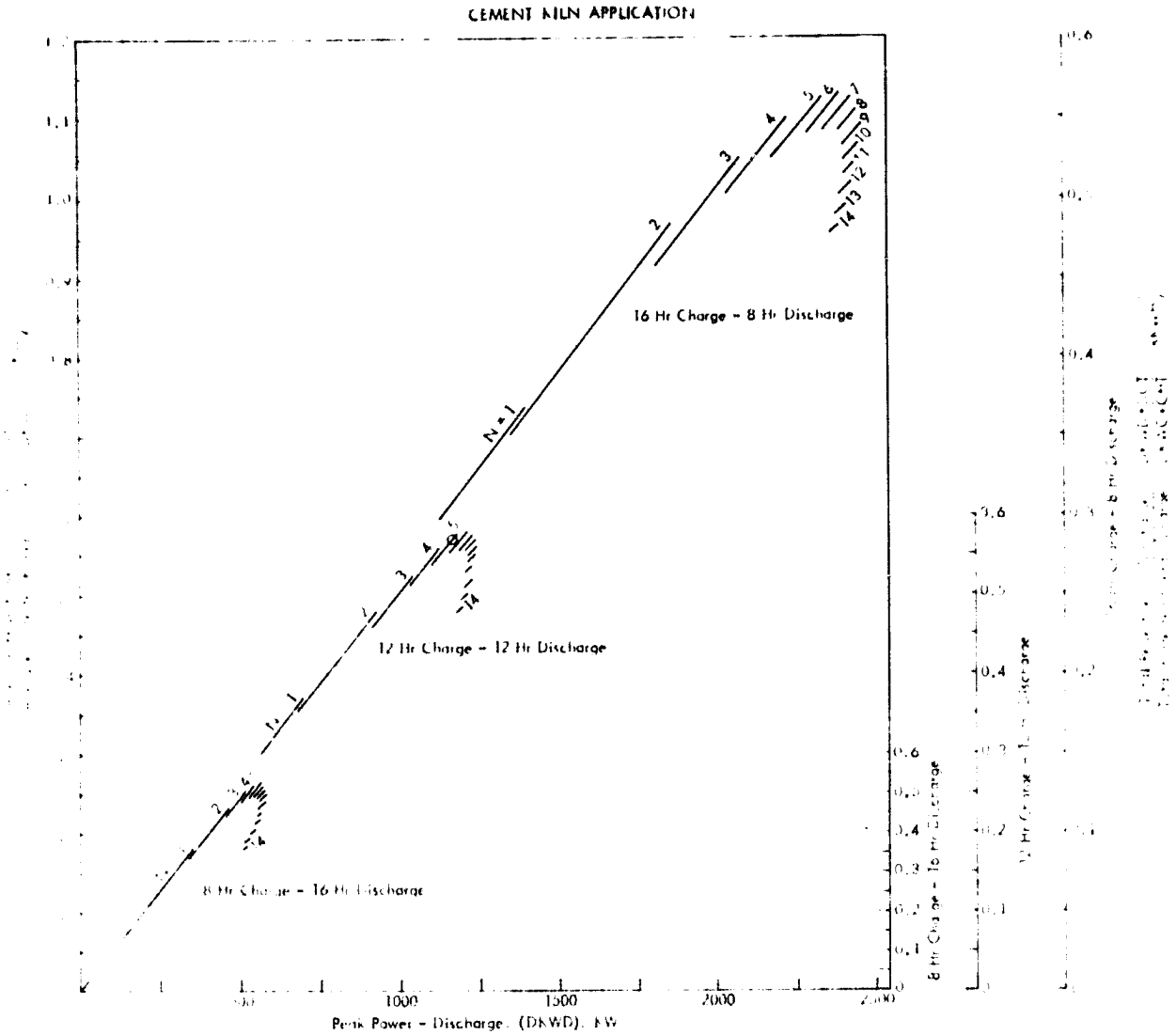

Figure 34 - Relative Power and Energy Versus Peak Power - Cement Kiln Application

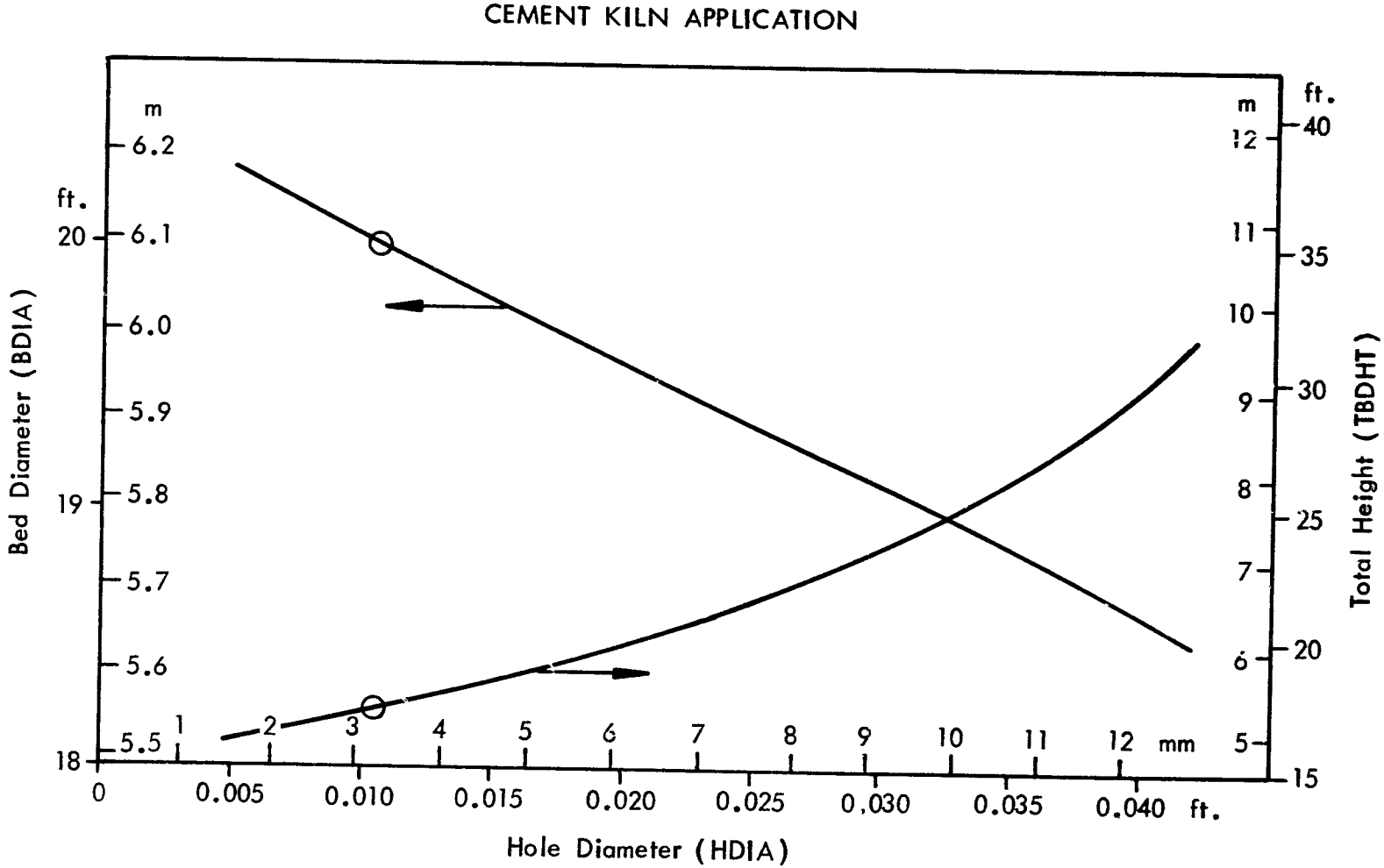

Figure 35 - Effect of Grid Hole Diameter on Bed Diameter and Height - Cement Kiln Application

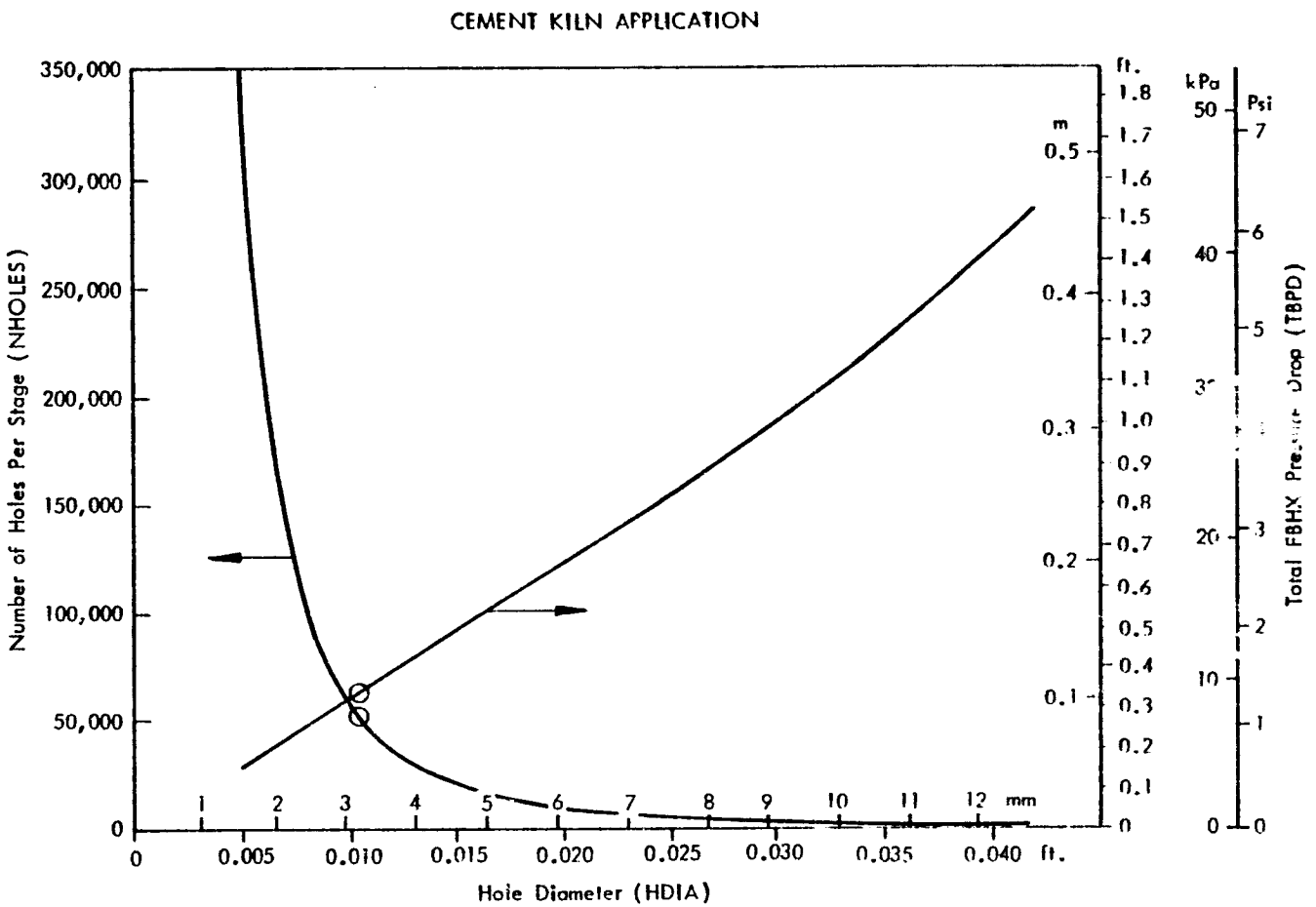

Figure 36 - Effect of Grid Hole Diameter on the Number of Holes Required, Bed Depth, and Bed Pressure Drop - Cement Kiln Application

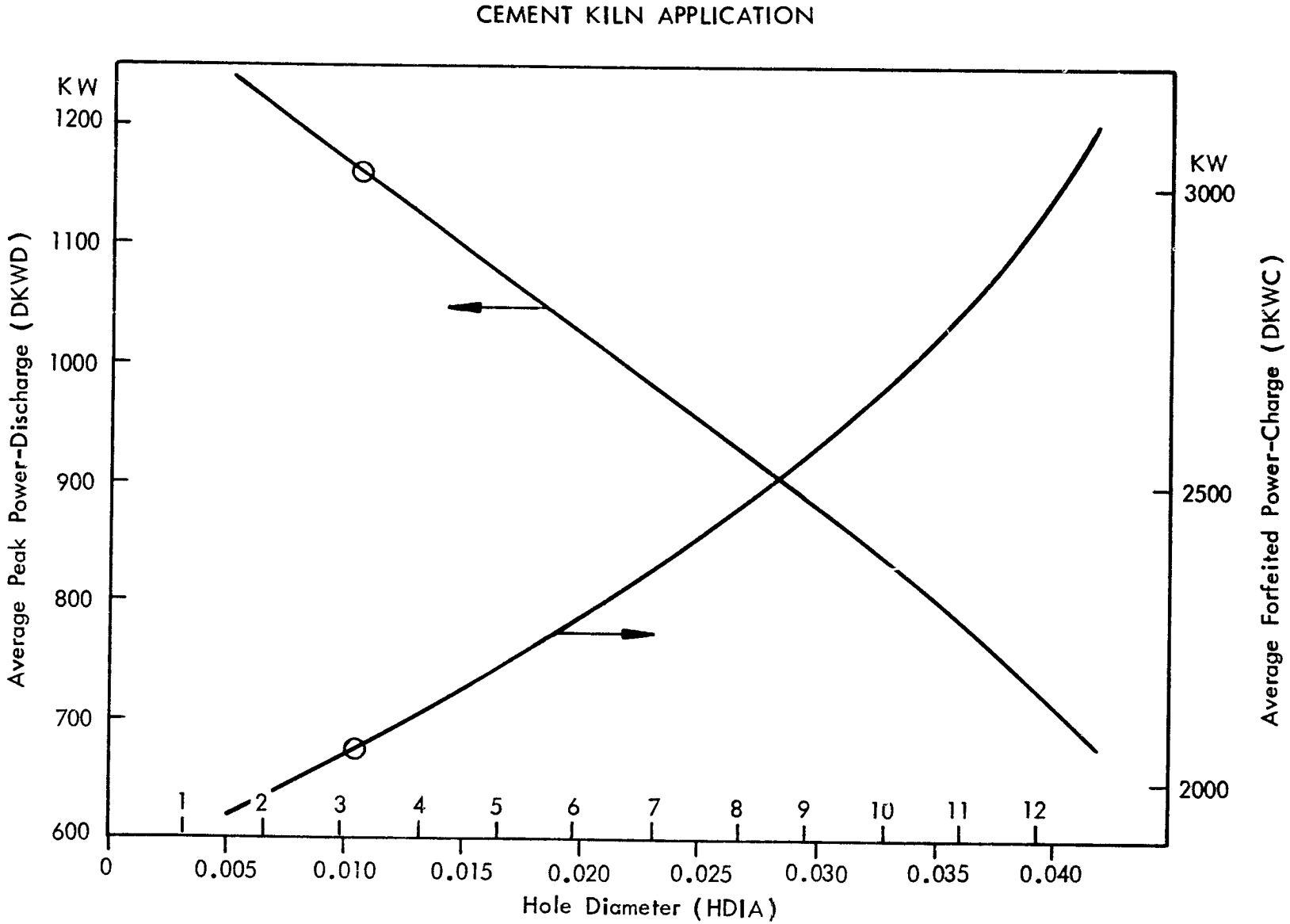

Figure 37 - Effect of Grid Hole Diameter on Average Peak Power and Forfeited Power - Cement Kiln Application

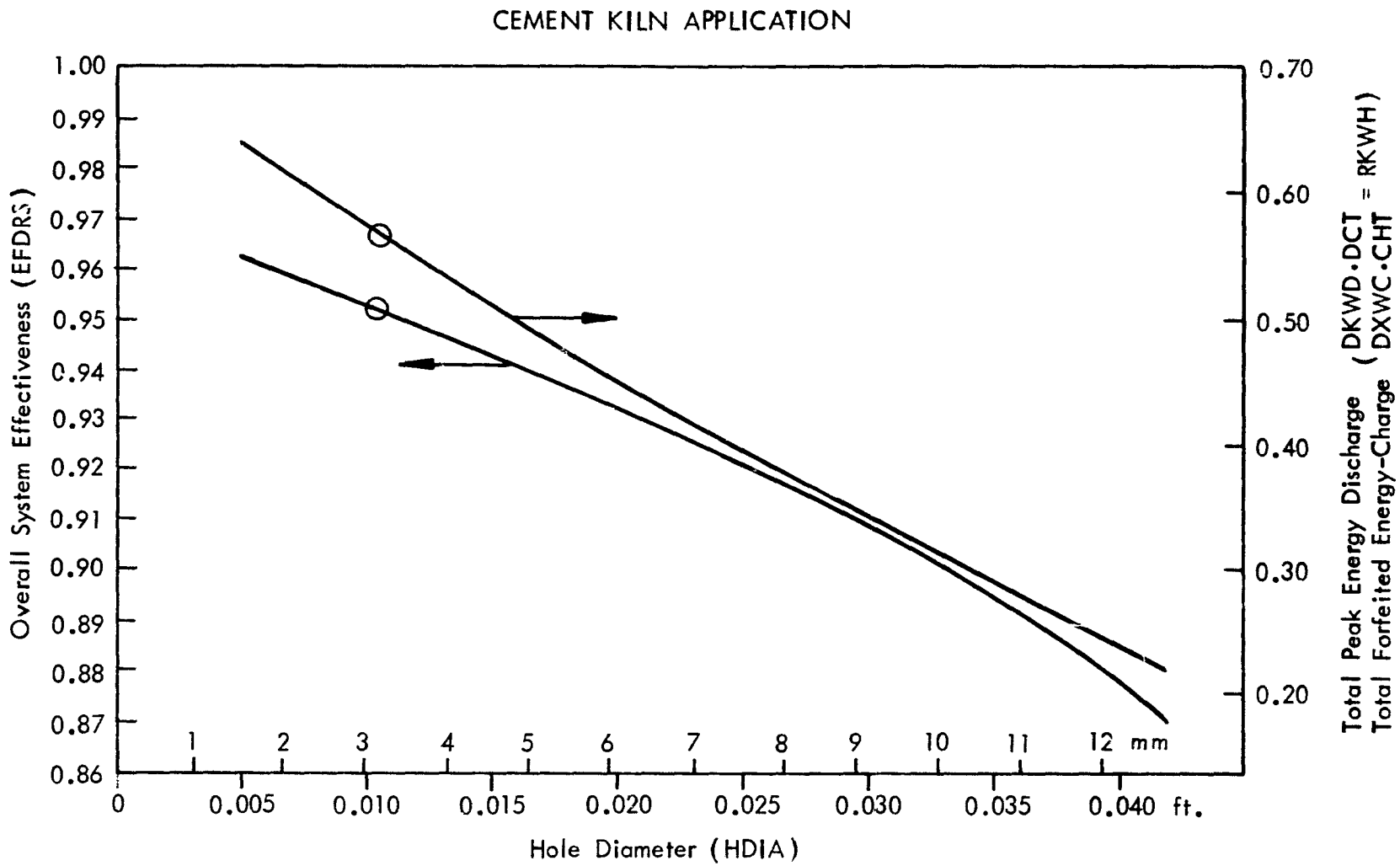

Figure 38 - Effect of Grid Hole Diameter on the Ratio of Peak to Forfeited Energy and the Overall System Effectiveness - Cement Kiln Application

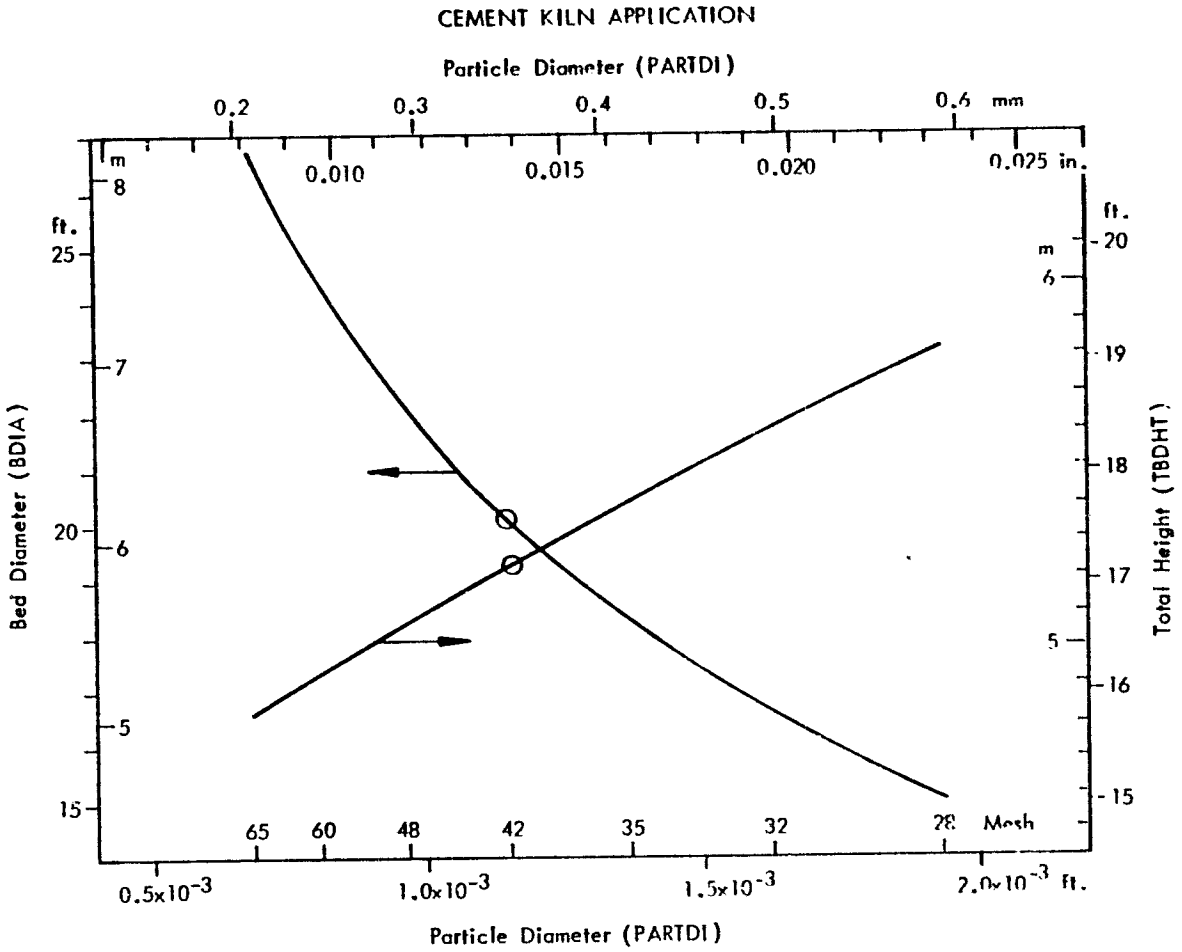

Figure 39 - Effect of Particle Diameter on Bed Diameter and Height - Cement Kiln Application

These effects are caused by the changes in minimum and maximum fluidization velocity when the particle diameter is changed. The change in particle diameter has no significant effect on the overall energy balance and results in only a fabrication cost trade off between bed diameter and total height.

The particle density was briefly examined and found to have slight effects on the FBHX/TES design and overall energy balance. However, the availability of alternate bed materials is limited and sand appears to be the best overall choice because of its price, availability, and attrition resistance. Therefore no detailed parametric evaluation was performed.

The bulk density was not evaluated in detail for the same reason. The size of the hot and cold solid storage systems are the only significant parameters affected by bulk density.

3.3.1.3 Evaluation of the Electric Arc Furnace Application--

The electric arc furnace application requires two FBHX/TES systems. The first system is a short-term thermal buffer to condition the gas temperature by attenuating periodic temperature fluctuations. The model plant design for this bed was shown in Figure 21. The other FBHX/TEX system is a long-term energy storage system similar to the cement kiln application.

For the buffer system design shown in Figure 25 there are very few parameters which can be varied significantly. A superficial velocity of 1.22 m/sec (4 ft/sec) was chosen to keep the operating velocity within the limits of the minimum fluidization velocity and terminal (entrainment) velocity of the system at the high and low extremes of the operating temperature. The 0.15 m (6 in.) bed depth was chosen to assure sufficient mixing and gas solid contact at high solids flow rates rather than to optimize pressure drop or jet penetration.

The parametric evaluation of the electric arc furnace long-term TES system is nearly identical to the cement kiln application. Figures 40 to 47 for the electric arc furnace application correspond to Figures 32 to 39 of the cement kiln application and the results depicted are similar.

The higher inlet temperature and flow rate for the electric arc furnace application results in nearly double the peak power and energy available during discharge as shown in Figure 40. The higher temperature and flow also allow additional fluid bed stages to be utilized before the diminishing return effects of pressure drop and parsitic power consumption are fully realized. Therefore, the electric arc furnace optimum peak power and energy occurs with 8 to 13 stages.

The ratios of peak power capacity to forfeited power capacity and peak energy generated to forfeited energy not generated are shown in Figure 41. These are almost exactly the same as for the cement kiln application. The only major difference is again the maximum number of stages which is 6 to 10 in the electric arc furnace application. The same also is true for the average peak power versus the power and energy ratios shown in Figure 42.

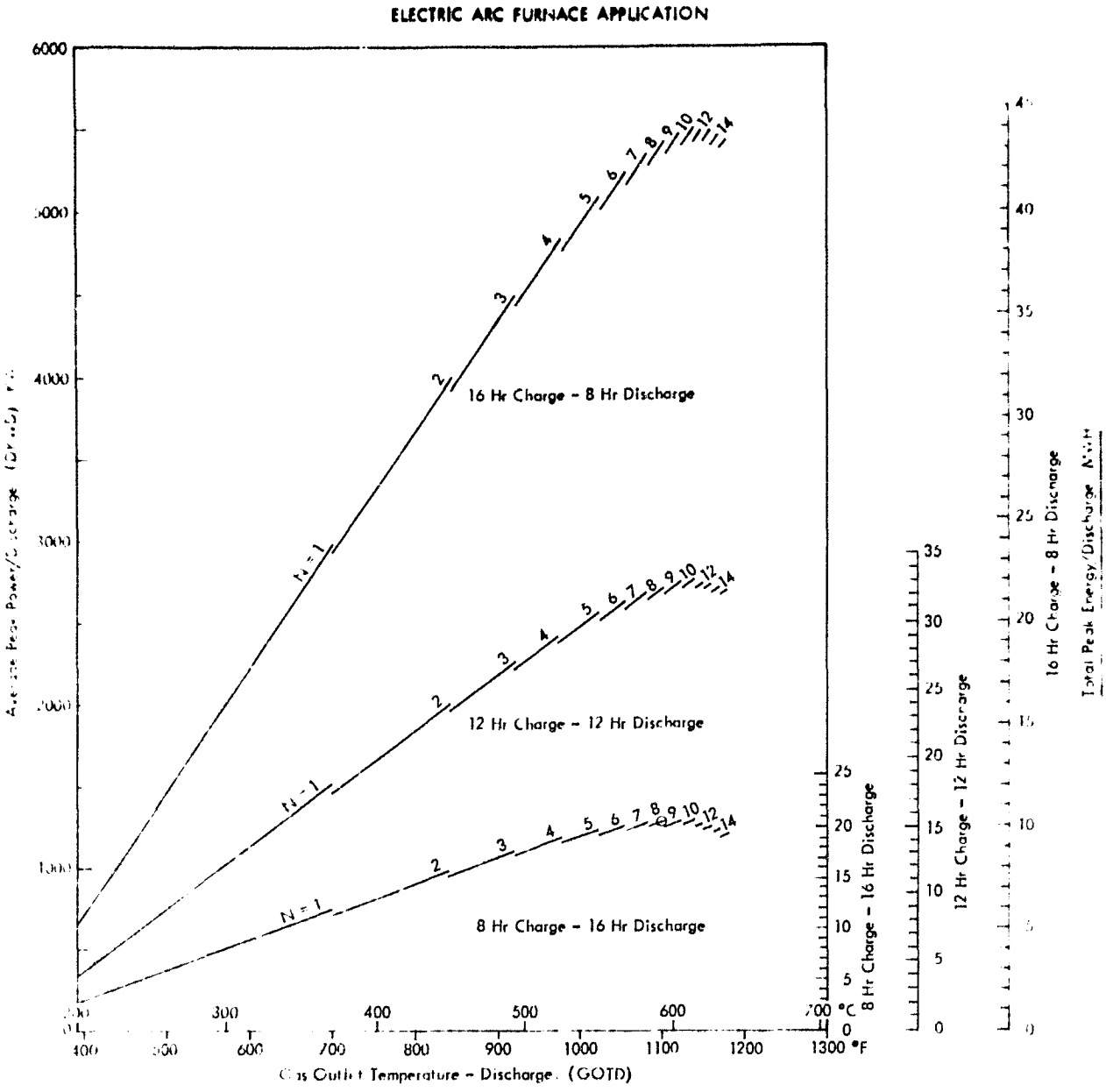

Figure 40 - Peak Power and Energy Available During Discharge as a Function of Charge-Discharge Time - Electric Arc Furnace Arc Furnace Application

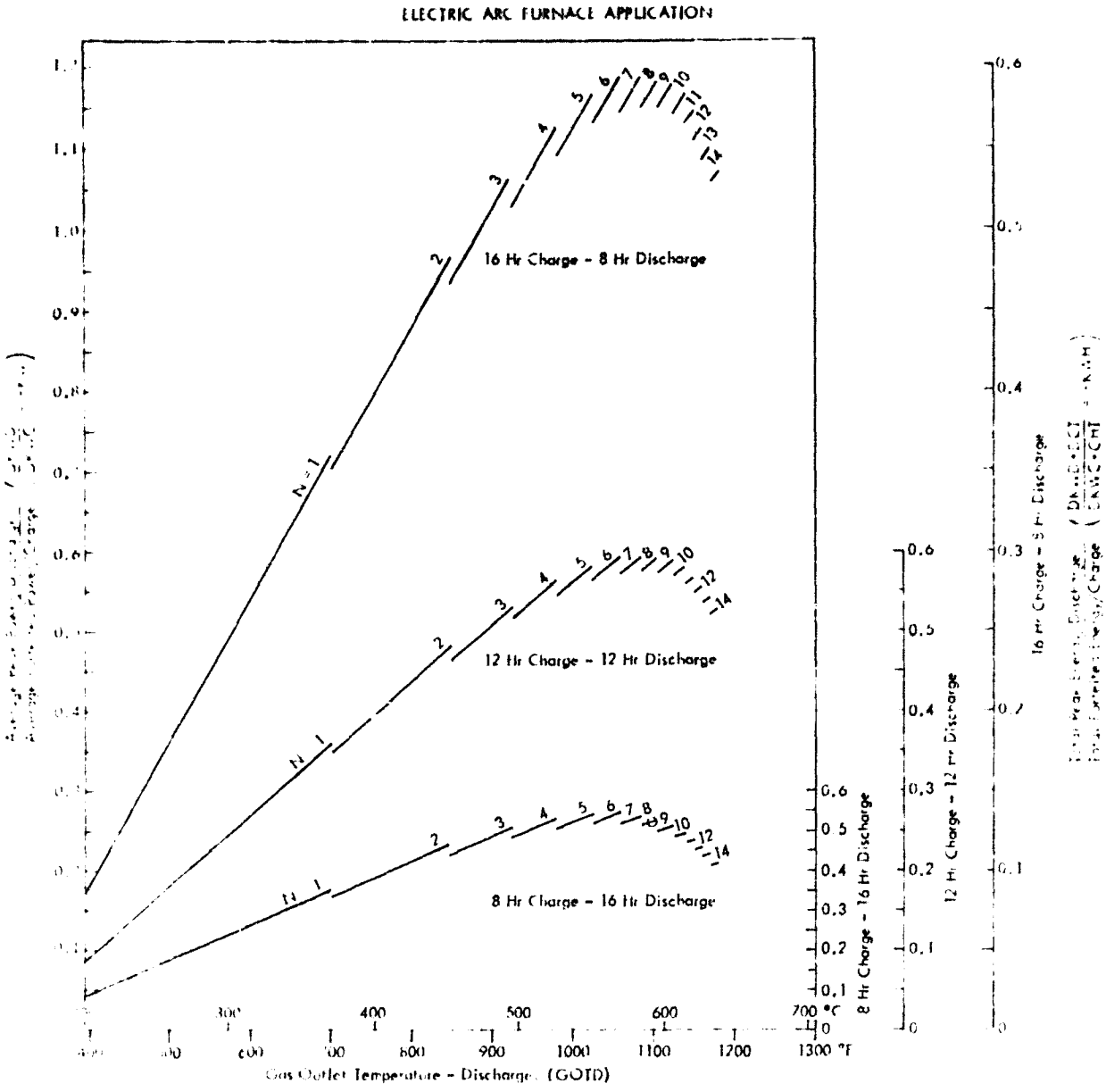

Figure 41 - Relative Power and Energy as a Function of Charge-Discharge Time - Electric Arc Furnace Application

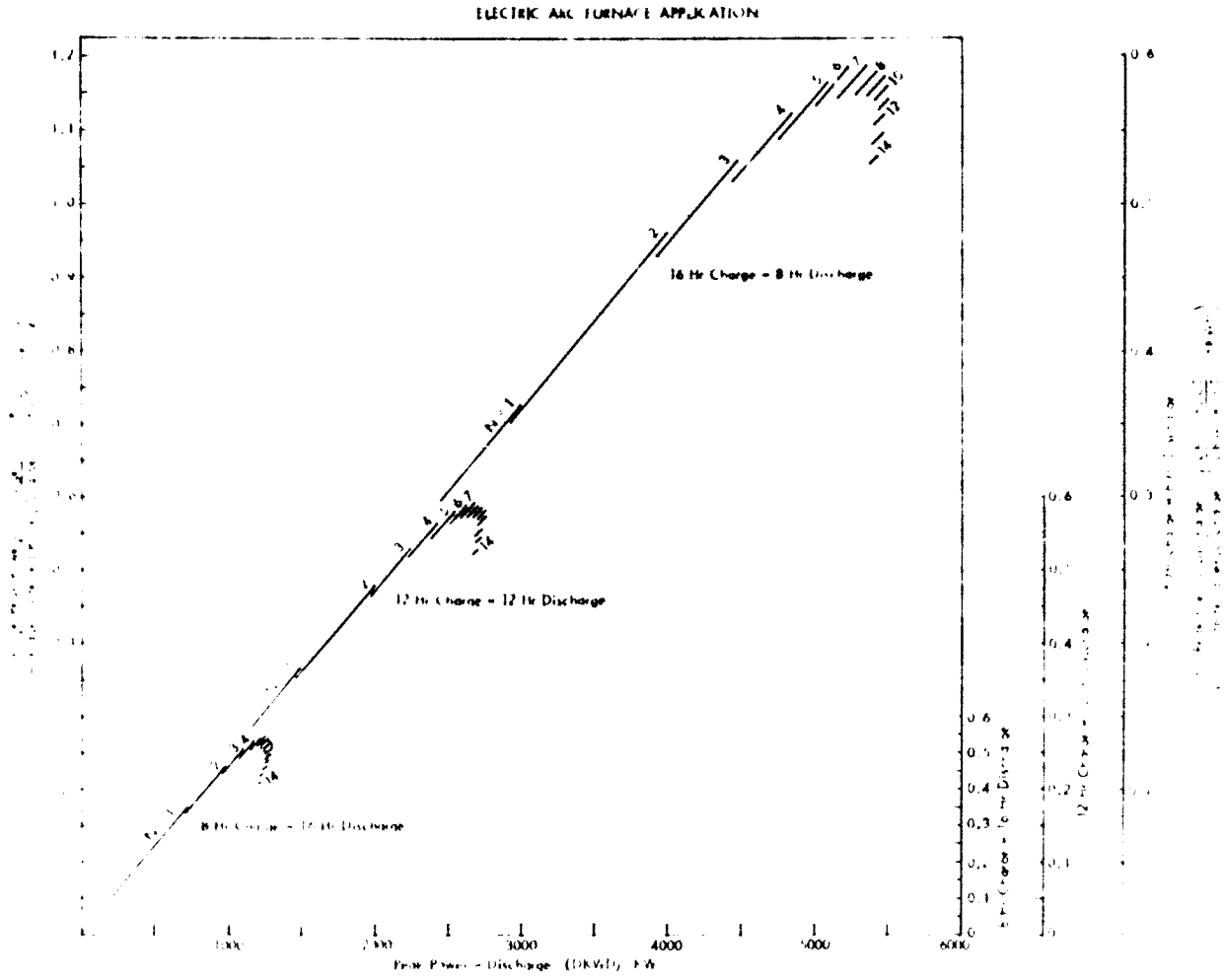

Figure 42 - Relative Power and Energy Versus Peak Power - Electric Arc Furnace Application

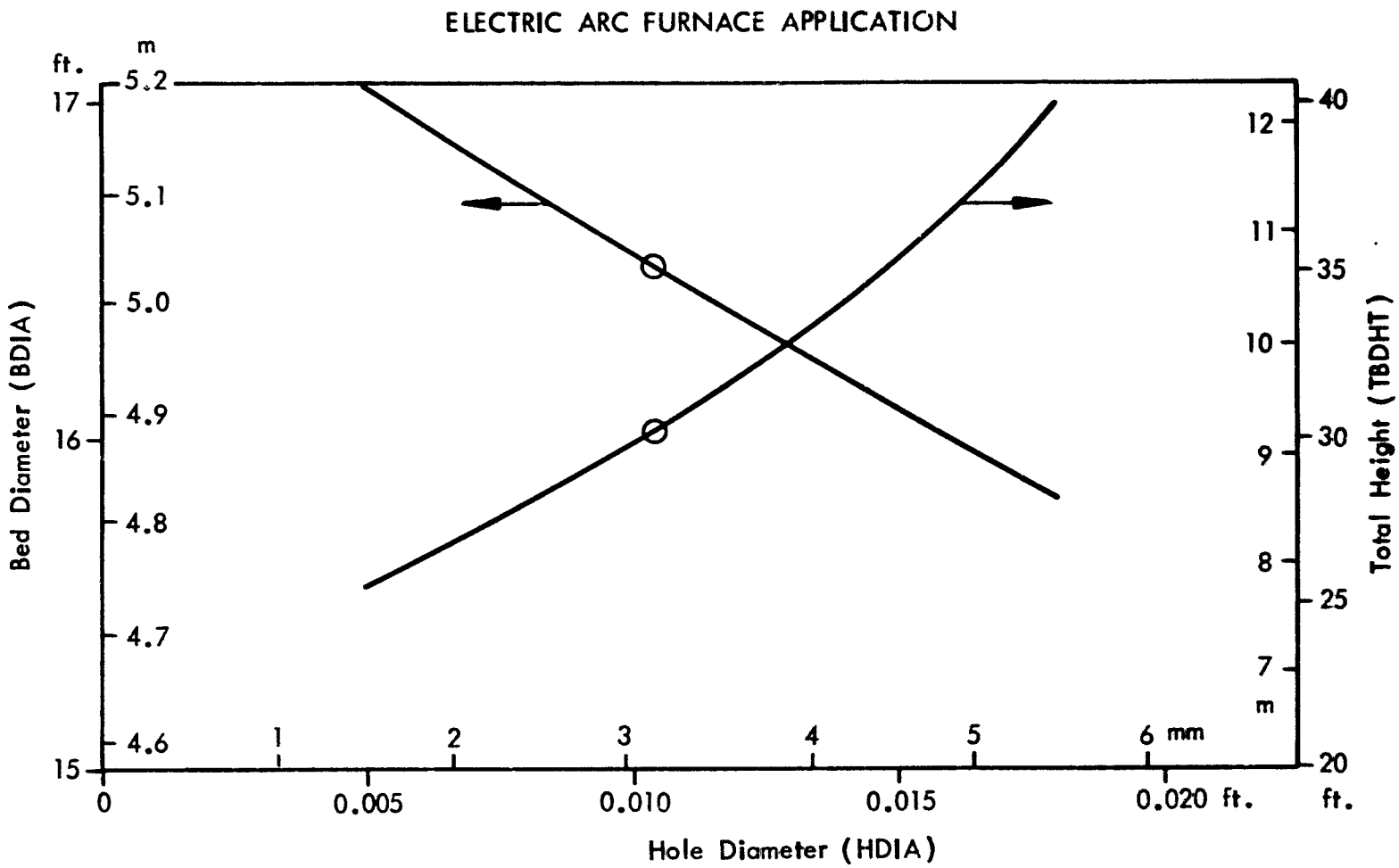

Figure 43 - Effect of Grid Hole Diameter on Bed Diameter and Height - Electric Arc Furnace Application

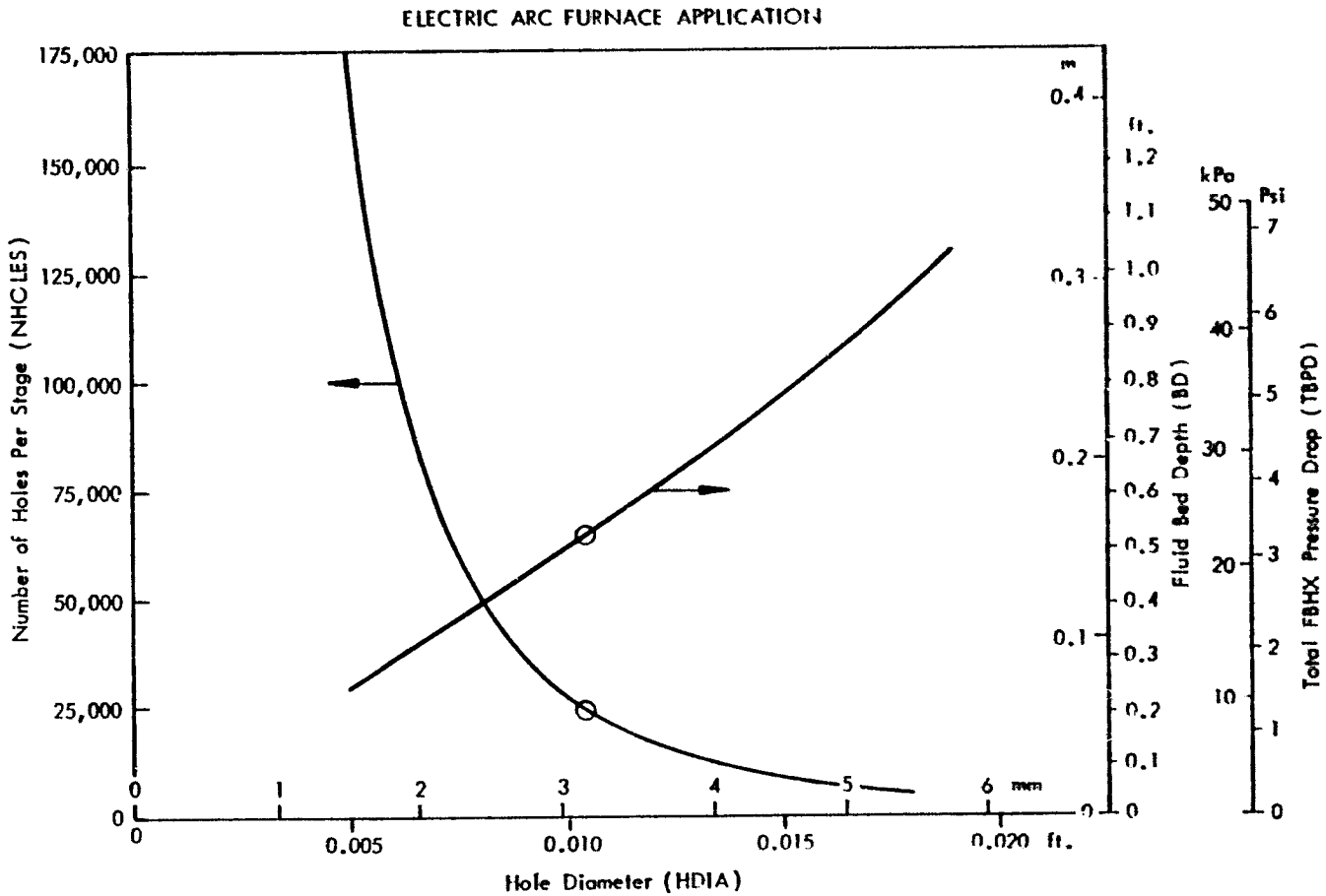

Figure 44 - Effect of Grid Hole Diameter on the Number of Holes Required, Bed Depth, and Bed Pressure Drop - Electric Arc Furnace Application

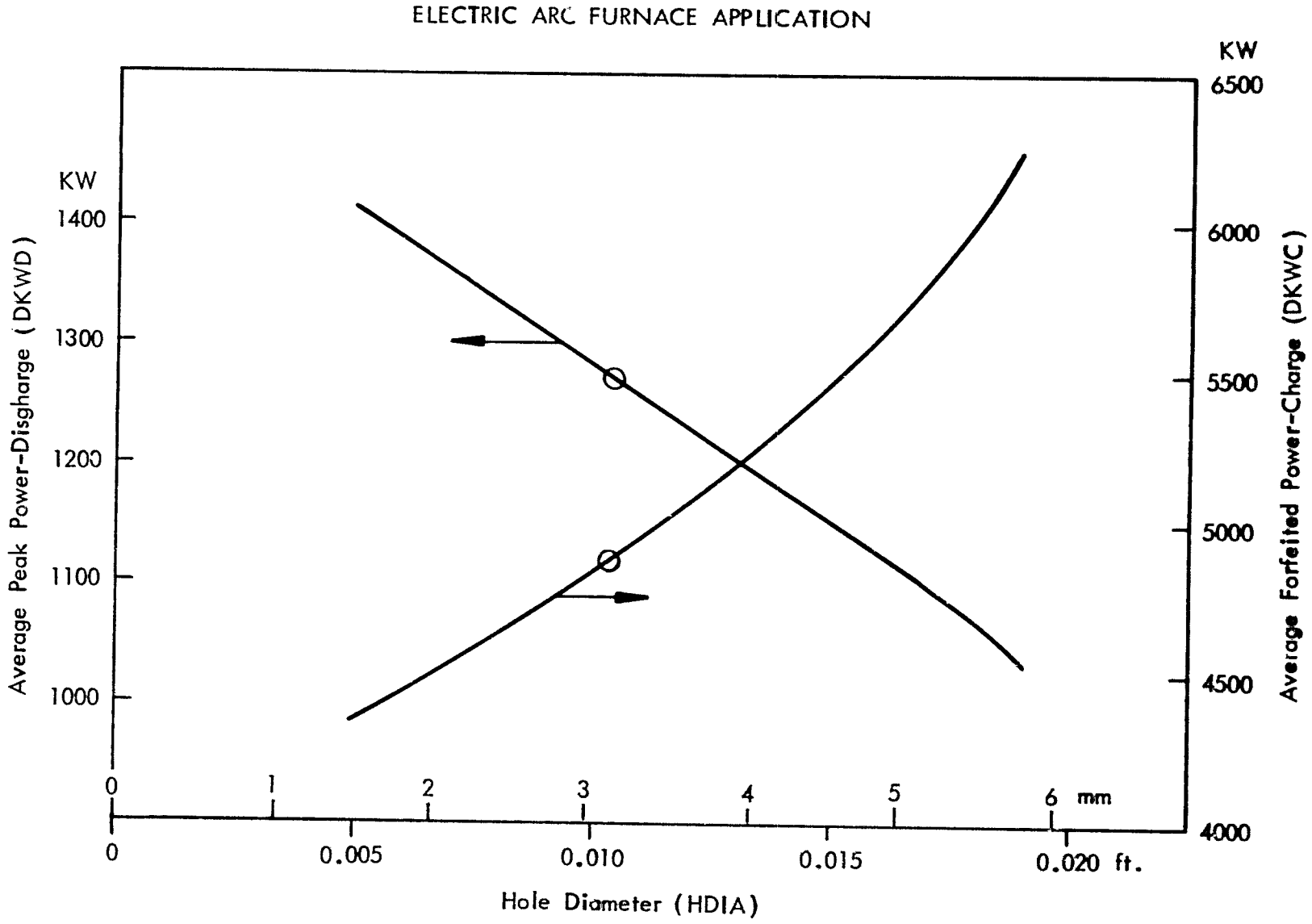

Figure 45 - Effect of Grid Hole Diameter on Average Peak Power and Forfeited Power - Electric Arc Furnace Application

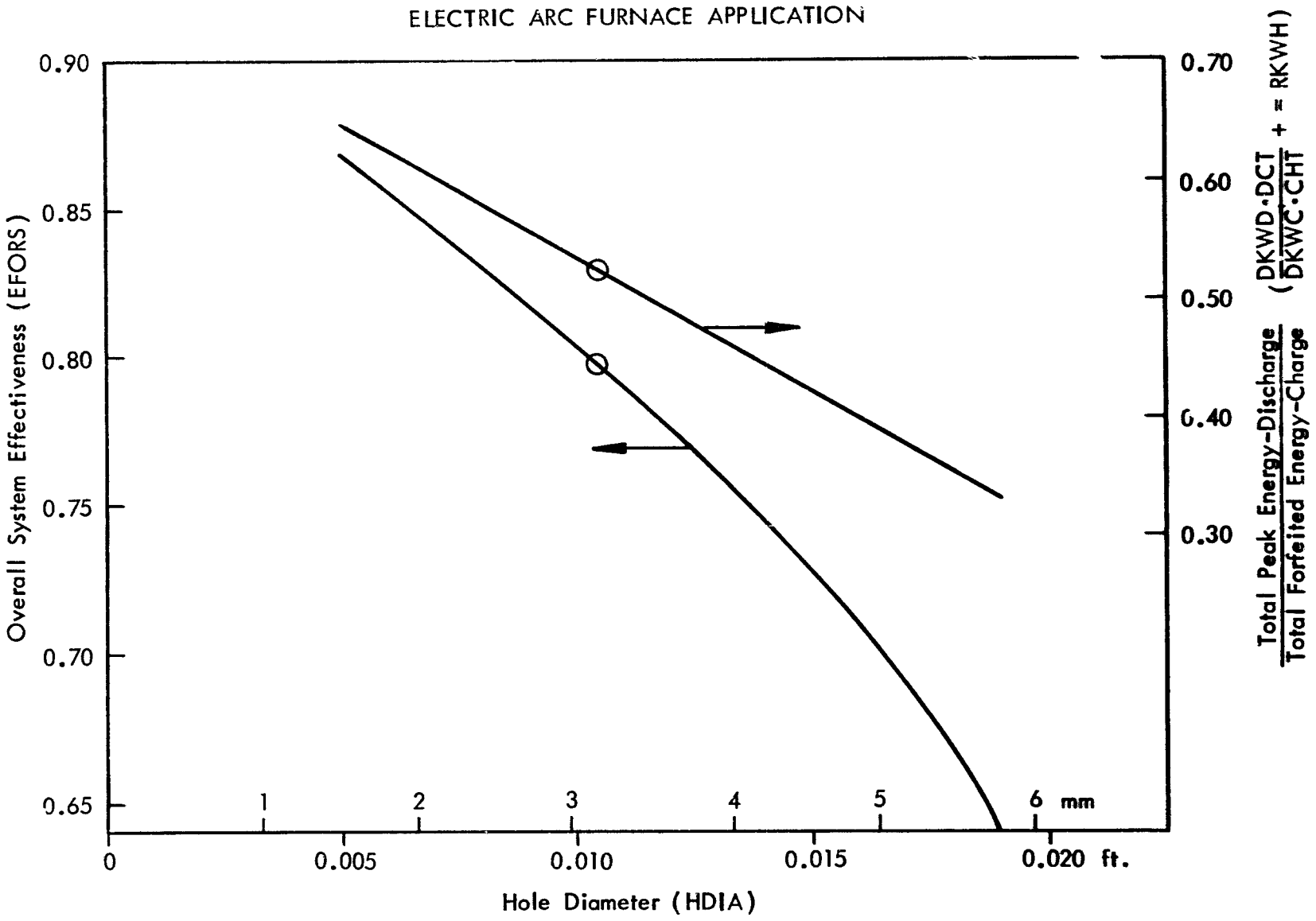

Figure 46 - Effect of Grid Hole Diameter on the Ratio of Peak to Forfeited Energy and the Overall System Effectiveness - Electric Arc Furnace Application

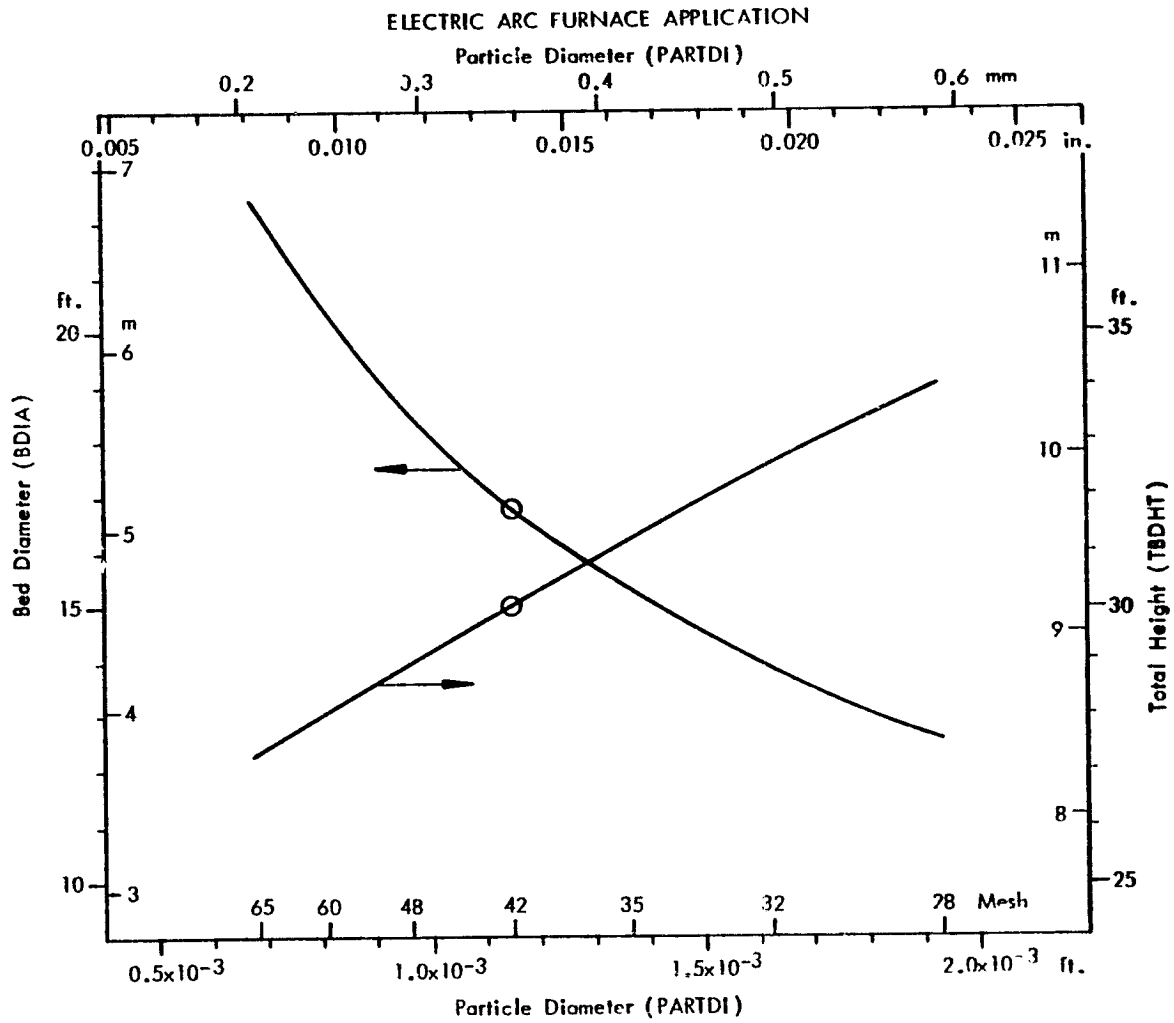

Figure 47 - Effect of Particle Diameter on Bed Diameter and Height - Electric Arc Furnace Application

Figures 43 to 46 show the effect of hole diameter on the FBHX size and overall energy balance. The results are very similar as for the cement kiln application, however, two things should be noted. First, the higher operating temperatures in the electric arc furnace result in higher superficial velocities at certain points in the system. This in turn results in greater jet penetrations which causes greater bed depths and pressure drops for a given hole diameter as shown in Figure 44. The second comment pertains to the overall system effectiveness shown in Figure 46. The model plant electric arc operating scenario has the waste heat boiler operating 16 hr/day which would result in a 66.7% overall system effectiveness with operation of the waste heat boiler on gases directly from the arc furnaces.

Figure 47 shows the effects of the particle diameter on the FBHX diameter and height which result in a trade off as discussed in the cement kiln application.

No other parameters of significant or practical importance were identified or evaluated for the electric arc furnace application.

4.0 ECONOMIC EVALUATION OF THE SELECTED APPLICATIONS

The objective of this portion of Task II was to estimate capital investment costs, annual operating costs, and unit energy costs to construct and operate each model system. Capital investment costs represent the total investment required to construct a new system and include direct costs, indirect costs, contractor's fees, and contingency. Annual operating costs represent the variable, fixed, and overhead costs required to operate the systems. Unit energy costs for each model system are the annual operating cost of the system divided by the annual energy savings.

The following sections describe the economic evaluation results by examining the basic economic options available, the capital and operating costs for the selected systems, the potential energy benefits of the selected systems, an examination of present utility rate structures with possible trends in future rate structures, and concludes with the potential economic benefits of the selected systems.

4.1 BASIC ECONOMIC OPTIONS

The economic analysis of the proposed FBHX/TES applications requires consideration of three basic options which the operators of individual industrial plants may consider.

In the first option, all of the electrical energy requirements are purchased with no attempt to recover and recycle waste heat that may be available. Process modifications and energy conservation may be utilized to reduce energy consumption which in turn may reduce the supply of waste heat available for recovery and recycle, but no specific recovery and recycle efforts are in use. This is most likely the current status of typical plants in the two industrial applications being considered.

In the second option, waste thermal energy is continuously recovered and recycled via a waste heat boiler and turbine-generator set to reduce the purchased energy demand and use requirements of the plant. In the cement plant application a very large proportion (80 to 100%) of the total plant electrical requirements could be satisfied in this manner, while in the electric arc furnace application only a small portion (15 to 25%) of the total plant electrical requirements could be satisfied. On-site electrical generation is most likely to be economically attractive where the utility supplying purchased power has a high energy use charge and/or the customer has a relatively high load factor. The waste heat recovery and recycle system will be attractive only if the net cost of on-site power generation is less than the cost of purchased power by a wide enough margin to pay for the system out of savings and provide the desired return on investment (ROI). Once a system is in place, it usually pays to maximize the run hours and kilowatt hours generated.

In the third option, the waste thermal energy is recovered, a portion is stored for use at a later time and the remainder (if any) is used for continuous power generation. When the stored energy is retrieved it is combined with the primary waste energy stream to provide increased power generation over that which could be generated from only the waste energy alone. The waste thermal energy utilized for direct generation during the storage mode of the system operation is economically similar to the second option described above. The energy stored and retrieved essentially provides peak-shaving capacity for load management. In general, peak shaving is most likely to be economically attractive where the utility has a high demand charge and/or the customer has a poor load factor. Each installation would have an optimum shaving level which will maximize the ROI. Typically, peak shaving can be used to reduce peak kilowatt demand by 10 to 20%, however, the total kilowatt hour of energy used remains nearly the same.

In the cement kiln application scenario, 80% of the waste thermal energy goes directly to the waste heat boiler and turbine-generator. The remaining 20% of the waste heat sent to the FBHX/TES system results in 12 to 13% peaking capability above the kilowatt demand which could be supplied if all the waste heat were used for continuous generation during the 12 hr discharge. In this application the economics of on-site continuous generation are expected to dominate the overall economic evaluation.

In the electric arc furnace scenario none of the waste thermal energy goes directly to the waste heat boiler and turbine-generator during the TES charge mode. This results in 30 to 35% peaking capability above the kilowatt demand which could be satisfied by direct power generation alone during 16 hr of discharge. In this application the economics of peak shaving are expected to be considerably more important than in the cement kiln application.

In order to determine the economic feasibility of the total system including the FBHX/TES, option three must be compared with option one. Option two must be compared with option one to assess the benefit of the waste heat boiler and turbine-generator without energy storage. Option three may be compared with option two to determine the incremental benefits of the FBHX/TES system.

Since the main emphasis of the investigation is the FBHX/TES system, the incremental costs and economic benefits of waste heat recovery due to energy storage were examined in detail. The cost and economic benefits of the waste heat boiler and turbine-generator without storage (option two) are examined in general.

4.2 CAPITAL COSTS FOR THE SELECTED APPLICATION

The capital investment costs of constructing new model fluidized bed heat exchanger TES system determined in this analysis were based on price quotations from manufacturers, index-corrected cost data from published literature, and MRI cost estimates. This method of estimating the capital investment costs is commonly referred to as a preliminary estimate, and usually has an accuracy of ± 20%.

Typical capital cost items are shown below:

Direct cost items:
- Sitework
- Buildings
- Fluidized Bed Heat Exchanger
- Waste Heat Boiler
- Process and Storage Tanks
- Pumps, Blowers, and Compressors
- Electrical Equipment
- Instruments and Controls
- Piping, Ductwork, and Insulation
- Materials Handling Systems
- Yard Improvements
- Service Facilities
- Miscellaneous Equipment

Indirect cost items:
- Engineering Design and Supervision
- Construction Overhead

Contractor's fee

Contingency

The capital invesment costs associated with the waste heat boiler system and the fluidized bed heat exchanger TES system were determined separately. The sum of these two capital investment costs equals the total cost of the model system.

4.2.1 Capital Costs of Systems Without FBHX/TES

Because the objective of this study was to evaluate the feasibility of thermal energy storage utilizing fluid bed heat exchangers only a cursory study was performed to determine the capital costs of the systems without storage.

The unit capital costs per kilowatt of generating capacity were found to vary greatly from about \$200/kw for diesel-electric peaking systems to about \$1,200/kw for nuclear base load plants. Cogeneration plants which would be very similar to the waste heat recovery systems were found to vary between \$300 and \$600/kw of capacity. Therefore, it was estimated that the capital investment for cement kiln application without TES would be $\$2.8 \times 10^6$ and the capital investment for the electric arc furnace application without TES would be $\$1.2 \times 10^6$.

4.2.2 Incremental Capital Costs of FBHX/TES

For this portion of the study the incremental capital costs were defined as the differences between a plant containing a waste energy recovery system without energy storage and an identical plant containing a waste heat recovery system with thermal energy storage. The plant with the energy storage is assumed to have no waste heat recovery system installed prior to conversion in order to eliminate retrofit expenditures from consideration.

Tables 25 and 26 show the estimated incremetal costs for adding a FBHX/TES system to the waste heat recovery systems in the cement kiln and electric arc furace applications, respectively. These costs were determined from price quotations of component manufacturers, cost data from published literature, and MRI estimates.

Note that the plants with storage will be capable of delivering a higher output during storage discharge than the plants which operate continuously, therefore the energy recovery and conversion (i.e., waste heat boiler and turbine-generator set) have been sized proportionately larger in the plant with energy storage and included as an incremental cost.

The cement plant with TES has an output during TES discharge which is 1,163 kw greater than a continuously operating plant. Therefore, the incremental unit capital cost of TES is $2,596/kw. Similarily, the electric arc steel plant, which has an output during TES discharge that is 1,269 kw greater than a continuously operating plant, results in a $4,183/kw incremental unit capital cost.

4.2.3 Total Capital Costs of Systems with FBHX/TES

The total capital cost of the systems with FBHX/TES are the sum of the capital costs of systems without FBHX/TES in Section 4.2.1 and the incremental capital costs of the FBHX/TES portion of the system in Section 4.2.2. Total system costs with TES are 5.8×10^6 to 8.5×10^6 for the cement kiln application and 6.5×10^6, to 7.6×10^6 for the electric arc furnace application.

Unit capital costs for the total systems with storage are $559/kw to $819/kw for the cement kiln application and $1,267/kw to $1,480/kw for the electric arc furnace application.

4.3 OPERATING COSTS FOR THE SELECTED APPLICATIONS

The annual operating costs for each model system are the sum of variable costs, fixed costs, and plant overhead. The annual operating costs associated with the waste heat boiler system and the fluidized bed heat exchanger TES system were determined separately. The sum of the two annual operating costs equals the total operating cost of each model system.

4.3.1 Operating Costs of Systems Without FBHX/TES

The unit variable operating costs for typical power generation systems were found to vary from approximately 0.2¢/kwh for base load central station power plant up to 1.0 to 2.0¢/kwh for diesel-electric peak shaving units. Cogeneration plants which would be similar to the system without FBHX/TES have unit maintenance and repair costs of approximately 1.0¢/kwh.

The fixed costs depend on the initial capital investment required, the cost of acquiring capital and the methods of depreciation and amortization utilized. The unit fixed costs were found to vary from 0.3 to 2.0¢/kwh for the cement kiln application and from 0.3 to 2.2¢/kwh for the electric arc furnace

TABLE 25

ESTIMATED INCREMENTAL COSTS OF FBHX/TES SYSTEM FOR CEMENT KILN APPLICATION

Cost	Description
$ 540,000	Incremental cost to increase basic waste heat boiler and turbine-generator capcity by 1,200 kw at $450/kw.
$ 100,000	FBHX/TES foundation-including minimal site work, forms, reinforcing steel--150 m^3 at $667/$m^3$ (200 $yards^3$ at $500/$yard^3$)
$1,084,000	FBHX-5 stages, carbon steel shell, stainless steel grid plates, refractory lining, system installation.
$ 50,000	Fans for FBHX and pneumatic transport
$ 20,000	Fan motors and installation.
$ 270,000	Hot and cold solids storage bins, 566 m^3 (20,000 ft^3), 6.1 m (20 ft) diameter x 22.9 m (75 ft) high, slip poured insulative concrete with 100 mm (4 in.) insulation.
$ 25,000	Pneumatic transport duct, 0.4 m (16 in.) diameter, 76 m (250 ft) total length, 12.7 mm (0.5 in.) wall, with 127 mm (5 in.) insulation.
$ 25,000	Pneumatic feeder valves and cyclones.
$ 50,000	Incremental control cost (assuming that FBHX control system is added to waste heat boiler and turbine-generator control panel in existing control room).
$2,164,000	Subtotal
$ 856,000	Miscellaneous capital costs, engineering design and supervision, contractor's fee, and contingency: 40% of subtotal.
$3,020,000	Total

TABLE 26

ESTIMATED INCREMENTAL COSTS OF FBHX/TES SYSTEM
FOR ELECTRIC ARC FURNACE APPLICATION

Cost	Description
$ 585,000	Incremental cost to increase basic waste heat boiler and turbine-generator capacity by 1,300 kw at $450/kw.
$ 200,000	FBHX/TES foundation-including minimal site work, forms, reinforcing steel--300 m^3 at $667/$m^3$ (400 $yards^3$ at $500/$yard^3$).
$1,702,000	FBHX-8 stages, carbon steel shell, stainless steel grid plates, refractory lining, system installation.
$ 586,000	FBHX-2 stage, carbon steel shell, stainless steel grid plates, refractory lining, system installation.
$ 60,000	Fans for FBHX and pneumatic transport.
$ 25,000	Fan motors and installatin.
$ 270,000	Hot and cold solids storage bins for TES peak system 566 m^3 (20,000 ft^3), 6.1 m (20 ft) diameter x 22.9 m (75 ft) high slip poured insulative concrete with 100 mm (4 in.) insulation.
$ 200,000	Hot and cold solids storage bins for TES buffer system 400 m^3 (14,000 ft^3), 6.1 m (20 ft) diameter x 16.0 m (50) high, slip poured insulative concrete with 100 mm (4 in.) insulation.
$ 40,000	Pneumatic transport duct, 0.4 m (16 in.) diamter, 122 m (400 ft) total length, 12.7 mm (0.5 in.) wall, with 127 mm (5 in.) insulation).
$ 50,000	Pneumatic feeder valves and cyclones.
$ 75,000	Incremental control cost (assuming that FBHX control system is added to waste heat boiler and turbine-generator control panel in existing control room).
$3,793,000	Subtotal
$1,517,000	Miscellaneous capital costs, engineering design and supervision, contractor's fee, and contingency: 40% of subtotal.
$5,310,000	Total

application. The lower unit costs would be for long plant life and low interest rates (i.e., 20 years at 6%) while the higher unit costs would be for short plant lifes and high interest rates (i.e., 5 years at 18%).

The sum of the variable and fixed unit operating costs could range from 1.3 to 3.0¢/kwh for the cement kiln application and from 1.3 to 3.2¢/kwh for the electric arc furnace application.

4.3.2 Incremental Operating Costs of FBHX/TES

Most of the variable operating costs would remain nearly the same when the FBHX/TES is added to the system. The maintenance, labor, and materials are the only variable operating costs expected to have significant incremental increases when FBHX/TES is added. The annual incremental maintenance costs are estimated to be approximately 5 to 10% of the incremental capital costs. This results in a unit incremental variable cost of 0.2 to 0.4¢/kwh for the cement kiln application and 1.0 to 2.0¢/kwh for the electric arc furnace application if the kilowatt base is the total kilowatt for the complete system with TES.

The incremental changes in fixed operating costs will depend on the increase in capital required to build a system with FBHX/TES. For the cement kiln application the FBHX/TES components increase the total capital cost by 60 to 107% while the parasitic losses with the FBHX/TES system reduce the usable system output energy 4.8%. These changes result in increased unit capital costs of 68 to 117% or 0.4 to 1.4¢/kwh. For the electric arc furnace application, the FBHX/TES components increase the total capital cost by 230 to 442% while the parasitic losses with the FBHX/TES system reduce the usable system output by 20.9%. In this case, unit capital costs increase 318 to 585% or 1.7 to to 7.0¢/kwh. Again the lower unit cost limits are for long plant lifes and low interest rates (20 years at 6%) while the higher unit cost limits are for shorter plant lifes and higher interest rates (5 years at 18%).

The sum of the incremental variable and fixed unit operating costs could range from 0.6 to 1.8¢/kwh for the cement plant application and from 2.7 to 9.0¢/kwh for the electric arc furnace application.

4.3.3 Total Operating Costs of Systems with FBHX/TES

The total operating costs of the systems with FBHX/TES are the sum of the operating costs of systems without FBHX/TES in Section 4.3.1 and the incremental operating costs of the FBHX/TES portion of the systems in Section 4.3.2. Resulting unit variable costs are 1.2 to 1.4¢/kwh for the cement kiln application and 2.0 to 3.0¢/kwh for the electric arc furance application. The unit fixed costs vary from 0.7 to 3.4¢/kwh for the cement kiln appliation and from 2.0 to 9.2¢/kwh for the electric arc furance application. The total unit operating costs then range from 1.9 to 4.8¢/kwh for the cement kiln application and from 3.9 to 12.2¢/kwh for the electric arc furnace application.

4.4 ENERGY BENEFITS OF THE SELECTED SYSTEMS

The implementation of the selected applications can either provide conservation through reject energy recovery and reuse or permit a shift in critical fuels such as oil and natural gas to other less critical fuels such as coal.

The energy savings and/or shifts associated with the waste heat boiler-turbine-generator system and the FBHX/TES system were determined separately. The sum of the energy savings and/or shifts then equals the total energy and/or fuel savings.

4.4.1 Energy Benefits of Systems Without FBHX/TES

In the technical analysis of the selected applications it was calculated that the waste heat recovered from the cement plant rotary kiln without TES has an equivalent electrical generating capacity of 9,214 kw and the heat recovered from the electric arc furnace without TES has an equivalent generating capacity of 3,863 kw. The resultant energy conservation potential are 132 kwh/ton of cement clinker produced in the cement plant application and 116 kwh/ton of steel produced in the electric arc furnace application. The model cement plant would have an energy savings potential of 364 barrels of oil per day or 92 tons of coal per day. The model electric arc furnace steel plant would have an energy savings potental of 152 barrels of oil per day or 38 tons of coal per day. The maximum potential energy savings with 100% of all plants participating is 16.3×10^6 barrels of oil or 4.1×10^6 tons of coal per year for the cement plant application and 5.7×10^6 barrels of oil or 1.4×10^6 tons of coal per year for the steel plant application.

Since the applications without TES operate continuously there would be no fuel shifting credit although a reduction in all fuels utilized would be obtained.

4.4.2 Incremental Energy Benefits of FBHX/TES

For the cement plant rotary kiln application operating scenario, it was calculated that 2,051 kw of generating capacity would have to be forfeited during the 12-hr charge period in order to provide 1,163 kw of peak capacity during the 12-hr discharge period. This results in an average decrease of 444 kw in generating capacity or a decrease of 6.3 kwh in energy saved per ton of clinker. Although the total energy savings are reduced 4.8% the FBHX/TES system allows a shift of 23 kwh/ton of clinker from TES charge to TES discharge which is 18% of the average output. If the peak power saved during the TES discharge is normally generated from critical fuels such as oil, the shift would allow substitution of approximately 32 barrels of oil during peak hours or 8 tons of coal during off peak hours.

Similar results are obtained for the electric arc furnace application. The energy calculations show that 4,882 kw of generating capacity must be forfeited during the 8 hr TES charge in order to gain 1,269 kw of peak generating

capacity during the 16 hr TES discharge. The average generating capacity decreases 781 kw and the energy saved per ton decreases 23 kwh/ton of steel, however, an energy shift of 124 kw/ton of steel during TES charge to 62 kwh/ton of steel during TES discharge occurs. This shift is equivalent to the substitution of 24 barrels of oil during peak hours or 6 tons of coal during off peak hours.

4.4.3 Total Energy Benefits of Systems with FBHX/TES

For the cement plant application, the combined results of Sections 4.4.1 and 4.4.2 give an average energy savings of 125 kwh/ton of cement clinker. Furthermore, an energy shift of 23 kwh/ton of cement clinker occurs from the TES charge mode to the TES discharge mode. The model cement plant would have an average energy savings potential of 345 barrels of oil per day or 88 tons of coal per day. The energy shift from TES charge to TES discharge is equivalent to 32 barrels of oil per day or 8 tons of coal per day. On a national level the potential energy savings are 15×10^6 barrels of oil per year or 4×10^6 tons of coal per year while the energy shift from TES discharge is equivalent to 1.4×10^6 barrels of oil per year or 0.4×10^6 tons of coal per year. For the electric arc furnace application the combined results of Sections 4.4.1 and 4.4.2 give an average energy savings of 92 kwh/ton of electric arc steel produced. Furthermore, an energy shift of 124 kwh/ton of steel during the 8 hr TES charge mode results in 62 kwh/ton of steel during the 16 hr TES discharge mode. The model electric arc furnace would have an average energy savings potential of 120 barrels of oil per day or 30 tons of coal per day. The energy shift from TES charge to TES discharge is equivalent to 54 barrels of oil per day or 14 tons of coal per day. One a national level the potential energy savings are 4.5×10^6 barrels of oil per year or 1.1×10^6 tons of coal per year while the energy shift from TES charge to TES discharge is equivalent to 3.0×10^6 barrels of oil per year or 0.5×10^6 tons of coal per year.

For convenience Table 27 summarizes the energy benefits of the system without TES, and the overall benefits of the total system with TES.

4.5 EVALUATION OF UTILITY RATE STRUCTURES

Before making a detailed economic analysis it is useful to briefly examine utility rate structures and to assess the potential impact of rates on the FBHX/TES applications.

4.5.1 Basic Rate Structures

Electric rates can be divided into two main classes with several subclasses:

Energy Rates	Demand Rates
Straight line	Flat demand
Step	Step demand
Block	Block demand

TABLE 27

SUMMARY OF ENERGY BENEFITS

	Energy Savings			
	System without FBHX/TES		System with FBHX/TES	
	Conservation Potential	Switching Potential	Conservation Potential	Switching Potential
Cement Kiln Application				
Model Plant Impact				
KWH/ton of cement	132	± 0	125	± 23
Equivalent barrels of oil/day	364	± 0	345	± 32
Equivalent tons of coal/day	92	± 0	87	± 8
Maximum National Impact				
Equivalent 10^6 barrels of oil/year	16.3	± 0	15.4	± 1.4
Equivalent 10^6 tons of coal/year	4.1	± 0	3.9	0.4
Electric Arc Furnace Application				
Model Plant Impact				
kwh/ton of steel	116	± 0	92	+ 62 (discharge) - 124 (charge)
Equivalent barrels of oil/day	152	± 0	120	± 54
Equivalent tons of coal/day	38	± 0	30	± 14
Maximum National Impact				
Equivalent 10^6 barrles of oil/year	5.7	± 0	4.5	± 2.0
Equivalent 10^6 tons of coal/year	1.4	± 0	1.1	± 0 5

There are also combination rates which interlace both demand and consumption:

Combination Rates

Wright

Hopkinson

Energy rates refer to the kilowatt hours of energy actually used by a customer. With a straight line energy rate the price charged per kilowatt hour used is constant regardless of how much energy is used. For step type energy rates a specified price is charged for the entire energy usage; however, the specified rate or price depends on which particular step within the rate ranges that the total usage falls. For block type energy rates, a specific rate is applied to all usage within the first block of kilowatt hours and progressively lower rates are applied to each succeeding block of kilowatt hours until the total energy used is accounted for.

Demand rates refer to the highest average kilowatts of power load measured during a specified demand time interval. For a flat power demand rate, the price charged per kilowatt of demand is constant regardless of the total kilowatt demand. For step type power demand, a specified price is charged for the entire demand, however, the specified price per kilowatt depends on the step which the total demand falls. For block type power demand rates, a specific rate is charged for the first block of kilowatt demand and progressively lower demand rates are applied to each succeeding block of kilowatt demand until the total power demand is accounted for.

The Wright combination rate structure considers the load factor or utilization of demand. High load factor (utilization) is rewarded with lower rates per unit of usage. Utilization of demand is determined by hours of usage of demand. The hours of usage are determined by dividing the total kilowatt hours of energy use by the maximum power demand load measured. Higher hours of usage are reflective of higher load factor (utilization), and are rewarded with subsequent lower rates. Seven hundred and twenty hours monthly usage of demand would equate to a 100% load factor, while 360 hr usage would means the load factor is 50%.

The Hopkinson combined rate structure consists of a demand charge and an energy charge. The energy rate structure used may be any of the aforementioned or a combination of same. Likewise, the demand rate structure may be one or a combination of any of the demand rate structures discussed herein.

All of the energy usage and power demand rates mentioned may vary with the time of day. Typically the time of day (TOD) rate variations apply only to the power demand portion of the utility bill. In recent years TOD pricing has been also increasingly applied to the energy use portion of the utility bill.

4.5.2 Typical Rate Structures Without Time of Day Pricing

To assess the effects that the utility rates might have on the FBHX/TES system economics, several rate structures were briefly examined.

The Kansas City Power and Light Company's rate for primary service to large industrial users is as follows:

Demand Charge:

$2,559.18/month for the first 1,200 kw of billing demand;
$ 1.68/month/kw for the next 98,800 kw of billing demand;
$ 1.65/month/kw for all over 100,000 kw of billing demand.

Energy Charge:

	Rate A First 1,200 kw (¢)	Rate B Next 4,800 kw (¢)	Rate C Next 19,000 kw (¢)	Rate D Next 75,000 kw (¢)	Rate E Over 100,000 kw (¢)
First 180 hr use per month at	3 2	2.83	2.70	2.56	2.53
Next 180 hr use per month at	2.76	2.56	2.43	2.36	2.27
Excess of 360 hr use per month at	2.27	2.13	2.12	2.12	2.12

In addition the minimum demand charge is the larger of 80% of the maximum summer demand or 50% of the maximum winter demand. There are no time of day energy rates, however, off-peak (11:00 PM to 7:00 AM plus all day Sunday) demand charges are two-thirds of the basic on-peak demand charges above. These rates are a typical Hopkinson combined rate structure and are representative of large industrial customers serviced by utilities which use coal-fired power plants for most of their generating capacity and which have ample reserve generating capacity available.

Most other utilities also use the Hopkinson combined rate format with the magnitude of the demand and energy charges appropriate for their generating facilities. Utilities with extensive hydroelectric power plants may offer considerably lower rates while utilities which rely on oil-fired power plants or have limited reserve capacity generally offer considerably higher rates.

By incorporating on-site power generation via a waste heat boiler it is possible for industrial users to reduce the energy charge portion of their bill. The effect on the demand charge depends on the difference, if any, which the utility makes in normal demand and standby demand charges. Presently, most utilities do not have reduced standby demand charges and the operator of a waste heat recovery system would have to pay the normal demand charge if the waste heat

system were temporarily out of service. The additional impact of installing a TES system will primarily be an incremental reduction in on-peak demand charges unless standby demand charges are the controlling factor. In the rate structure illustrated above, the demand charge is only approximately 10% of the total bill for a 1,500 kw industrial customer with 80% load factor and no energy recovery or storage system.

When the parasitic power requirements are considered, the incremental savings in demand charges may be offset or even exceeded by the increased energy use charges. For example, in the cement kiln application the FBHX/TES system results in a decrease of 1,163 kw during on-peak hours which could result in an incremental savings of approximately $2,000/month in demand charges. However, the total energy consumption increases 319,622 kwh/month due to the thermal losses and parasitic power needed to run the FBHX/TES system. This results in an increased incremental expenditure of approximately $9,000/month for energy charges or a net incremental loss of $7,000/month. Only if the demand portion of the rate structure were substantially higher or off-peak energy rates lower would the FBHX/TES system be economically profitable.

4.5.3 Typical Rate Structures with Time of Day Pricing

There is currently a trend toward time-of-day (TOD) pricing for the energy charge portion of some utility bills. TOD pricing by the utilities is an attempt to more accurately assess the cost of service by considering the marginal or incremental costs of providing service with intermediate and peak load generating facilities which are inherently less efficient and/or utilize more expensive fuels than base load generating equipment. Several TOD rate structures were examined via information supplied from EPRI. The following paragraph summarizes several typical TOD rates.

In an opinion and order examining the merits of applying marginal cost concepts to electric rates, the New York Public Service Commission ordered that each electric utility shall proceed to develop marginal cost data. As a result, time-of-use rates were approved for Long Island Lighting Company's (LILCO) 175 customers with maximum demand of more than 750 kw/month. LILCO's rate design calls for three pricing periods based on an examination of loss of load probabilities, marginal running costs, and potential for future load growth. The peak period, 10:00 AM to 10:00 PM occurs only during the summer months (June through September), Monday to Saturday. The intermediate period occurs during the hours of 7:00 AM to 10:00 AM and 10:00 PM to midnight in the summer and 7:00 AM to midnight for the remainder of the year (October through May). The off-peak period is midnight to 7:00 AM for all months. There are separate demand charges for on-peak and intermediate periods: no demand charge is assessed to off-peak demand. Although the marginal cost study showed that the ratio of on-peak demand charge to intermediate demand charge should be 20:1, the final order established a ratio of 4:1 ($5.60/kw: $1.40/kw at primary voltage). The energy charges were set equal to the marginal running cost for each of the three periods. Customers receiving their power at primary voltage pay 3.18¢/kwh for on-peak usage, 2.61¢/kwh for intermediate period usage, and 1.71¢/kwh for off-peak consumption, not including any cost of fuel adjustments.

Although the three pricing periods are not directly comparable to the two period operating scenario of the selected applications, some comparisons can be made. For example, the cement kiln application would have an incremental demand savings of $6,000/month during the summer peak months and $1,600/month during the remainder of the year. The incremental energy costs would be a savings of approximately $700/month during the summer peak months and additional expenditure of $1,600/month during the remainder of the year. The net incremental result of having a FBHX/TES is a savings of approximately $6,700/month during the summer peak months and break even operation the remainder of the year assuming that no standby demand charges are assessed.

At this rate the total savings will be $26,800/year (6,700 x 4) in contrast to a loss of $7,000/month with the previously determined rate structure. This result demonstrates the sensitivity of energy costs in an evaluation of the system.

For Wisconsin Power and Light Company the on-peak period selected extends from 8:00 AM to 10:00 PM Monday through Saturday. The approved on-peak energy charge is twice the off-peak emergy charge, and the billed demand is the larger of (a) the maximum 15 min demand measured in the on-peak period or (b) one-half the maximum 15-min demand measured in the off-peak period.

Southern California Edison's time-of-use rate schedule has an on-peak energy cnarge that is 1.5 mills larger than the intermediate energy charge and 3.0 mills larger than the off-peak energy charge. The nonseasonal on-peak demand charge is more than eight times greater than the intermediate demand charge; off-peak demand is not billed. Pacific Gas and Electric established a 2.0 mill difference between on- and intermediate peak energy charges and between the intermediate and off-peak energy charges. During summer months (May through September) the on-peak demand charge is about 12 times larger than the intermediate demand charge: the peak period demand charge is about eight times larger during winter months.

The rate design implemented by San Diego Gas and Electric (SDG&E) is extremely innovative because its customers are charged for their contribution to monthly system peak ($6.41/kw). The utility provides the customers on this rate schedule with nearly instantaneous system load data and forecasts of the peak load pattern. This information allows the customers to estimate roughly the probability of the monthly system peak occurring at any time. The customers can then decide to defer, accelerate, or shed some or all of their load during times of high system load. For the rest of the month they do not have to worry about their maximum demand. SDG&E's time-of-use rate also has an on-peak energy charge that is 4.0 mills larger than the intermediate energy charge and 6.0 mills larger than the off-peak energy charge.

No specific savings calculations were performed for these utilities because no specific charges were available. The demand charges probably would result in a net savings if standby demand is not the controlling demand factor. The incremental energy charges could result in either net savings or expenditures depending on the ratio of on-peak to off-peak energy use rates.

4.6 ECONOMIC BENEFITS OF THE SELECTED SYSTEMS

In order to determine the net economic savings which the selected applications can provide by energy conservation or by shifts of critical fuels to less critical fuels, the displaced power demand charges and energy use charges must be considered.

The sections which follow examine the economic benefits of the applications without the FBHX/TES system and the incremental economic benefits of the FBHX/TES system. The net economic benefit will be the sum of the individual benefits.

4.6.2 Incremental Benefits of FBHX/TES

It is unlikely that the present utility rate demand structures will result in an economic return if TES is included with the waste heat recovery and power generation. When no differentiation between normal and standby charges is made, the incremental economic benefits of additional demand reduction with a FBHX/TES system will be nullified. In addition, whenever the TES output is unavailable during an on-peak demand period load shedding or production cutbacks equivalent to the TES output would have to be implented or higher demand charges incurred. Since standby demand charges are the exception rather than the rule the incremental economic benefit from reduced on-peak demand was excluded from further consideration. This leaves the differentiation in energy charges for the accumulation of economic benefits.

4.6.1 Economic Benefits of Systems Without FBHX/TES

Waste heat recovery and on-site electrical energy generation are most likely to be economically attractive where the utility supplying the purchase power has a high energy use charge and/or the customer has a relatively high load factor. The waste heat recovery and recycle system will be economically attractive only if the net cost of on-site power generation is less than the cost of the displaced purchased power by a wide enough margin to pay for the system and provide the desired return on investment. Since the unit operating costs in Section 4.3.1 already include the fixed cost of capital recovery, the purchased electrical cost must exceed the on-site operating cost of electrical power by a sufficient differential provide a reasonable return. For example, if the cement plant rotary kiln application operates 7,200 hr/year and the effective tax rate is 50%, the after tax return on investment would be 6.3 to 11.8% for each 1.0¢/kwh difference between on-site operating costs of Section 4.3.1 and purchased electrical energy charges. Similarly, the steel plant electric arc furnace application would have on after tax rate of return of 6.0 to 11.3% for each 1.0¢/kwh difference between on-site operating costs of section 4.3.1 and purchased electrical energy charges.

If the utility which serves the selected plant applications charges the same rates for regular power demand as for standby power demand, there may not be any return due to the electrical utility demand charges. When no differentiation is made between normal power demand and standby demand, the operators of the industrial plants with waste heat recovery systems would either have to

shutdown the process whenever the heat recovery and/or on-site power generation equipment are out of service or forego the economic benefits of reduced demand charges. Since shutting down the process seems unlikely, the plants with heat recovery and power generation will most likely have to pay the same demand charges as a similar plant without energy recovery.

4.6.2 Incremental Benefits of FBHX/TES

It is unlikely that the present utility rate demand structures will result in an economic return if TES is included with waste heat recovery and power generation. When no differentiation between normal and standby charges is made, the incremental economic benefits of additional demand reduction with a FBHX/TES system will be nullified. In addition, whenever the TES output is unavailable during an on-peak demand period load shedding or production cutbacks equivalent to the TES output would have to be implemented or higher demand charges incurred. Since standby demand charges are the exception rather than the rule, the incremental economic benefit from reduced on-peak demand was excluded from further consideration.

In the technical evaluation, it was calculated that the ratio of peak energy during TES discharge to forfeited energy during TES discharge was 0.57 for the cement kiln application and 0.52 for the electric arc furnace application. In order for the energy charges to break even, the ratio of the energy cost per kilowatt hour during TES discharge to the energy cost per kilowatt hour during TES charge must be the reciprocal of the ratios above (i.e., 1.76 for the cement kiln application and 1.92 for the electric arc furnace application). To accrue economic benefits from the differences in on-peak and off-peak energy charges, the actual price ratios must exceed the break even ratios by sufficient margin to amortize the incremental investment required to install the FBHX/TES components and provide a reasonable rate of return.

In order to simplify the calculation of accured economic benefits, if any, the nomagraphs shown in Figures 48 and 49 were prepared for the cement kiln and electric arc furnaces, respectively. To use the nomagraphs it is necessary to first determine the on-peak and off-peak energy charges of the utility which would normally supply the power requirements. The annual savings in purchased power is then determined by drawing a straight line from the on-peak purchased energy cost on the far left scale through the off-peak purchased energy cost on the second scale from the left until it intersects the annual savings scale. For example, if on-peak energy costs 7¢/kwh and off-peak energy costs 3¢/kwh the annual savings as indicated by the dashed lines on the nomagraphs would be approximately $72,000 for the cement kiln application and $76,000 for the electric arc furnace application. It should be noted that the nomagraphs assume the plants operate 300 days/year. If the plants operate more or fewer days per year the savings would be proportionately increased or decreased.

The right half of the nomagraphs provide a method for determining the accumulated savings over the life of the FBHX/TES system or the time required for simple pay-back of the original cost. For example, if the useful life of the FBHX/TES system is 20 years the accumulated savings in the previous example

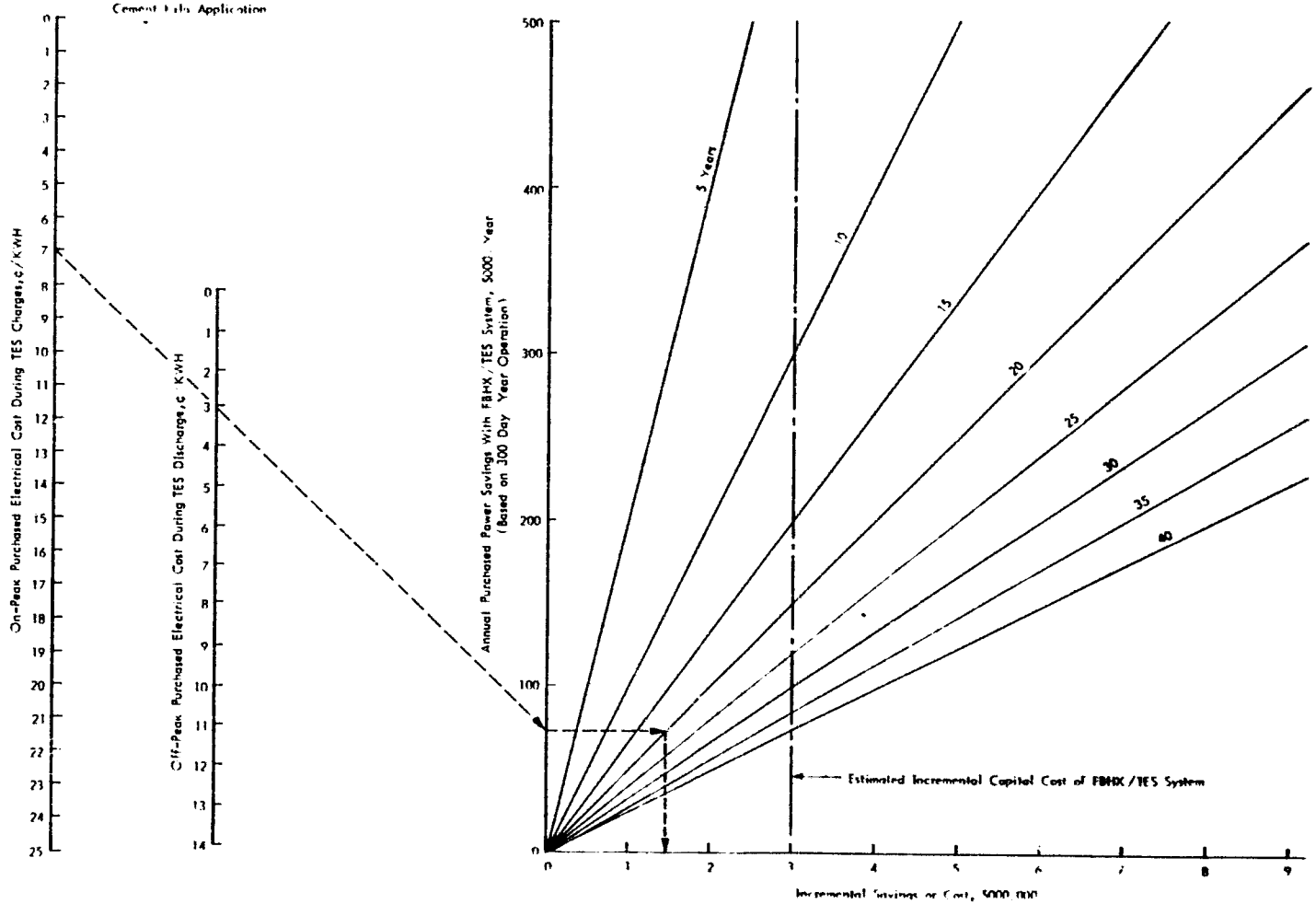

Figure 48 - Nomagraph for Determining Effects of On-Peak and Off-Peak Energy Costs on the Annual and Accumulated Incremental Savings with TES-Cement Kiln Application

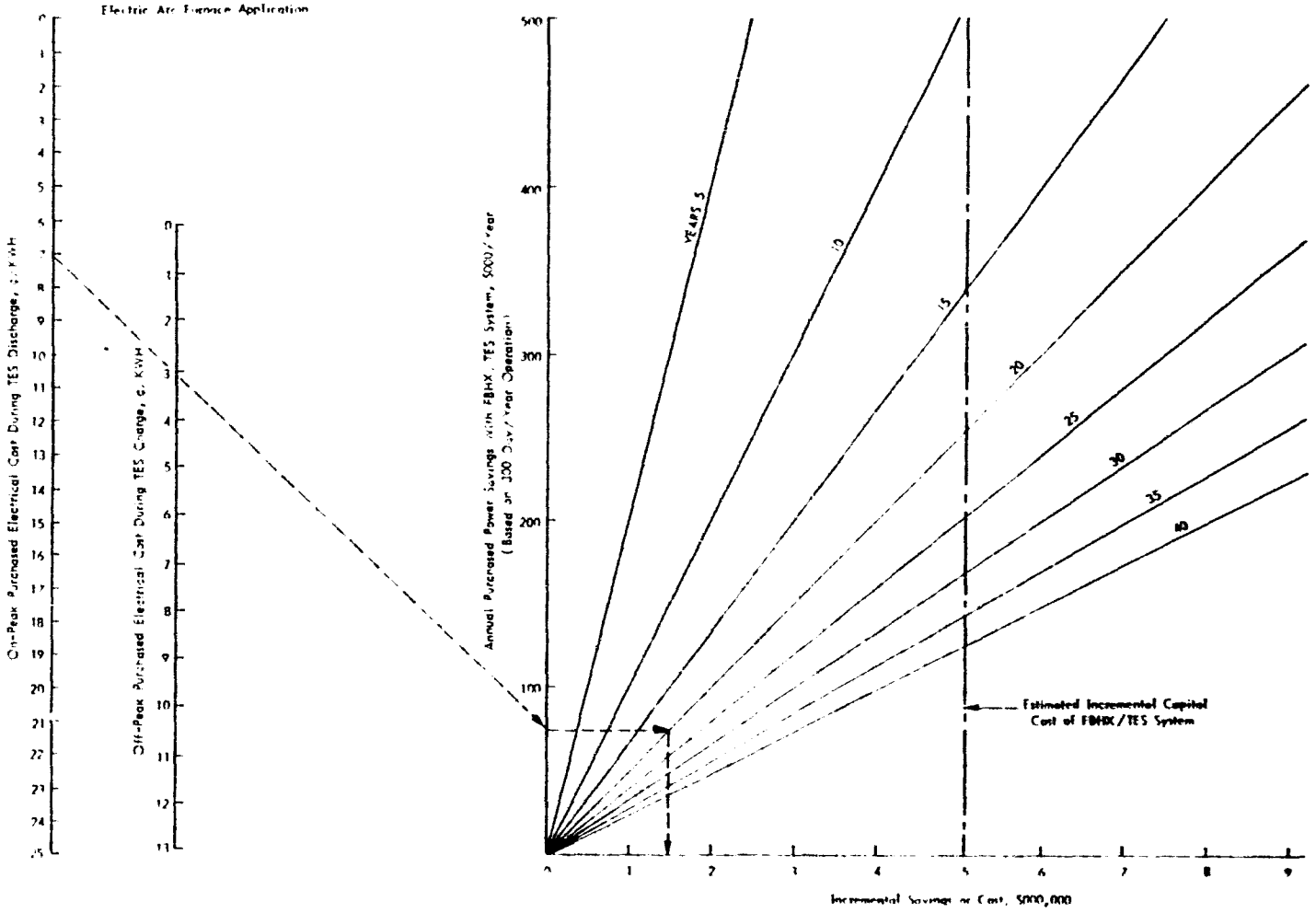

Figure 49 - Nomagraph for Determining Effects of On-Peak and Off-Peak Energy Costs on the Annual and Accumulated Incremental Savings with TES-Electric Arc Furnace Application

would be $\$1.4 \times 10^6$ for the cement kiln application and $\$1.5 \times 10^6$ for the electric arc furnace application. Since the incremental cost of the FBHX/TES systems are $\$3.0 \times 10^6$ and $\$5.3 \times 10^6$, respectively, the time required for simple pay back would be approximately 40 years for the cement kiln application and 70 years for the electric arc furnace application. Note these estimates are based on capital costs only and do not include allowances for annual operating costs.

The examples above are for illustrative purposes only. In reality, the present differentiation between on-peak and off-peak utility rates as discussed in the preceding section are such that little if any net savings would result. As the availability declines, the cost of premium fuels used by utilities for peak power generation could increase dramatically. If this occurs, the differentiation between on-peak and off-peak energy costs will increase. If the differentiation in on-peak and off-peak rates increased until the annual savings are greater than $250,000/year, the FBX/TES systems become economically attractive. Also if savings can be accrued from demand charges by separating normal demand from standby demand, then the combined annual savings would increase and the FBHX/TES system would be more economically attractive.

4.6.3 Total Economic Benefit of Systems with FBHX/TES

The economic benefits of the total system are extremely sensitive to the energy and demand rate structures of the utility which the energy recovery, storage and recycle system displaces.

When typical energy rates are considered the energy conservation potential of the total system may be attractive, but a detailed site-specific study would have to be performed for each potential installation.

If the cement kiln system operates 7,200 hr/year and the effective tax rate is 50% the after tax rate of return would be 3.8 to 5.4% for each 1.0¢/kwh difference between the on-site operating cost of Section 4.3.3 and the purchased electrical energy charges displaced. Similarly, in the steel plant electric arc furnace application, the after tax rate of return would be 1.4 to 1.7% for each 1.0¢/kwh difference between the on-site operating costs of Section 4.3.3 and the purchased power displaced.

The general lack of time-of-day in rate structures would results in a negative return for the thermal storage portion of the system at present. However, for those areas in which utilities now have time-of-day rates, the FBHX/TES begins to look attractive. If the price of critical fuels such as oil escalates faster than less critical fuels such as coal, the shift permitted by TES could result in significant economic benefits. If sufficient price differentiation occurs, the rate of return due to TES increases and the system rate of return would increase.

If reduction of demand charges for standby power are implented by utilities and regulatory agencies, then economic benefits would accrue and the rate of return would increase.

5.0 CONCLUSIONS

The technical feasibility of FBHX for TES systems has been verified by analysis of two selected conceptual systems. The basic energy recovery system results in favorable energy conservation. The inclusion of TES allows significant shifts in the charge/discharge modes and would allow alleviation of company or utility load peaks.

Initial results for the cement plant application indicate that the diversion of 20% of the kiln exhaust gases to a 5-stage FBHX/TES system during a 12-hr charge period allows power production to be increased 11% during a 12-hr discharge period. This results in a 5% net reduction in total energy recovered. However, the TES system allows 18% of the net energy to be shifted from the charge (off-peak) mode to the discharge (on-peak) mode of operation.

Similarly the diversion of 100% of the electric arc furnace gases during an 8-hr charge cycle of an 8-stage FBHX/TES system allows power production to be increased 34% during a 16-hr discharge perod. This results in a 20% net reduction in total energy recovered. However, the TES system allows 44% of the net energy to be shifted from the charge (off-peak) mode to the discharge (on-peak mode) with this application.

The reductions in net total energy recovered when TES is included in the waste heat recovery system are due to (a) the parasitic fan power losses required for fluidization and pneumatic transport; and (b) the thermal losses resulting from the limited heat exchanger effectiveness with a finite number of fluid bed stages.

The economic feasibility of FBHX for TES depends on the difference in the value of the displaced energy during the charge and discharge periods (i.e., time of day pricing is mandatory for the TES system to provide a return on investment). Currently utilities with time of day pricing do not have sufficient differentation between on-peak and off-peak energy rates to make FBHX/TES very attractive economically. The price differentiation could increase substantially if the cost of critical fuels (such as oil) used for peak power production by utilities increases faster than the price of fuels (such as coal) used for base load power production. Also, most utilities do not differentiate between the demand charge for normal industrial customers and the standby demand charge for industrial customers with waste energy recovery systems. Adoption of favorable standby demand charges would add to the economic benefits of the FBHX/TES system.

Due to the unique dependence that both the cement kiln and electric arc furnace TES applications have on the prevailing utility rate structures, it is difficult to recommend one application as being clearly superior to the other. At the present time, the cement kiln application appears more likely to become economically viable if sufficient differentiation between on-peak and off-peak utility rates occurs in the future. The electric arc furnace TES system capital

cost is considerably higher than the cement kiln TES system and would require greater differentiation between on-peak and off-peak utility rates to be competitive. In general, the cement industry appears to be economically stronger than the steel industry so that incorporation of new technologies might be more readily accepted.

An additional consideration which may favor the cement kiln application for TES is that the plant energy requirements are very nearly equal to the capacity obtainable from a waste heat recovery system. If the ability to store and recover energy could aid in making the plant self-sufficient, then the TES system might be justified. In this situation the energy used to charge the TES system during off-peak hours would ordinarily be wasted by venting to the atmosphere. Therefore, the value of the off-peak forfeited power would be reduced to zero regardless of the actual utility price at that time. Hence, the annual savings potential could be increased dramatically. However, the load profiles and total energy consumption of specific cement plants would have to be examined to evaluate this situation on a case-by-case basis.

One possible option in the steel industry would be to use only the TES buffer to attenuate the electric arc furnace gas stream temperature for direct use in a continuously operating waste heat boiler. This option would use the short-term storage capability of the buffer to condition the gas stream temperature for energy recovery. Without the buffer it might not be feasible to use conventional equipment to recover the waste energy from the exhaust stream with the widely varying temperatures encountered in the electric arc furnace off-gases.

6.0 RECOMMENDATION FOR FUTURE R&D EFFORTS

Limited R&D in three specific areas appears warranted before attempting a demonstration of FBHX/TES technology. These are:

1. Collection of data for the cement kiln application to determine the electrical load profile and waste heat available in specific plants which might be candidates for TES installation and demonstration. This activity may identify plants with high thermal energy availability and low power requirement, which TES would make self-sufficient.

2. Detailed technical and economic evaluation of the electric arc furnace application with only the TES/buffer. This option might make continuous generation of power feasible by mitigating the wide temperature variations in the exhaust gases.

3. Analysis of current utility rates and prediction of future trends in time of day and standby pricing which could make FBHX/TES more economically attractive.

Successful acquisition of favorable information on a candidate cement plant, verification of the electric arc furnace TES buffer or prediction of favorable utility rates would warrant establishment of a multiphase program leading to full-scale implementation of FBHX/TES technology. The implementation program would consist of the following major technical phases.

Phase I - Refinement of Conceptual Design and Costs

Phase II - Pilot Scale FBHX/TES Design

Phase III - Fabrication, Assembly and Test of Pilot Scale FBHX/TES Design

Phase IV - Full-Scale FBHX/TES System Design

Phase V - Fabrication, Assembly, and Test of Full-Scale FBHX/TES System Design

Phase VI - Long-Term Monitoring and Development of Commercialization

These technical phases would be accompanied by periodic updating of the energy and economic benefits derived from the use of FBHX/TES for energy conservation and/or fuel shifting.

APPENDIX A

PROCESS FLOW DIAGRAMS FOR SIX SELECTED APPLICATIONS

I. Introduction

Flow diagrams for the six selected applications are briefly discussed in this Appendix. To the extent possible, we have shown heat and mass flow characteristics in the various flow diagrams.

II. Cement Kiln Application

There are two processes used for manufacturing portland cement--the wet process in which crushed raw materials are ground with water, thoroughly mixed, and fed into the kiln in the form of "slurry," and the dry process in which the raw materials are ground, mixed, and fed into the kiln in their "dry" state. This is the only major difference between these two processes. Figure A-1 presents a typical flow diagram for the dry process. A cement kiln is normally made of steel, lined with firebrick or special fire-resistant material, and mounted in a slightly tilted position. A large kiln may have a diameter of 7.6 m (25 ft) and a length of 230 m (750 ft). The raw material fed from the high end of the kiln is gradually heated to 1500°C (2700°F) by a forced draft burner flame located at the low end. As the raw material moves slowly from the high end to the low end, certain elements are driven off by the flame becoming part of the exhaust gases. The remaining material, grayish-black pellets about the size of marbles, is called "clinker." The hot clinker discharged from the kiln is then cooled by a clinker cooler. The clinker is fed into grinding mills where gypsum is added in the grinding process. The final grinding reduces clinker to extremely fine powder which is called portland cement.

Significant quantities of thermal energy are rejected to the atmosphere each year from cement kilns. Two major sources of this rejected heat are the kiln exhaust and clinker cooler. Several combinations and/or configurations of fluidized bed heat exchangers/storage systems could be used to recover the waste thermal energy.

III. Iron Ore Sintering Application

Sintering is used to improve iron ore permeability, to improve gas-solid contact, and to decrease dust problems in the blast furnace. About one-third of the total iron ore burden in a typical blast furnace operation is sintered. The other form of iron ore agglomeration is pelletizing. Due to similarities in thermal treatment between sintering and pelletizing, a common heat recovery system could probably be used for both.

The sintering operation occurs on a traveling grate which conveys a bed of ore fines, limestone fines, and coke breeze. The bed (coke breeze) is ignited by gas burners. As the mixture moves along the grates, air is pulled down through the mixture to keep the breeze burning. The heat sinters the mixture at about 1400°C (2500°F) into pea-to-baseball size lumps. Combustion gas is normally passed through an electrostatic precipitator (ESP) to remove dust and then discharged to the atmosphere through a stack. Cooling of the sinter so that it can be handled is an important part of the process.

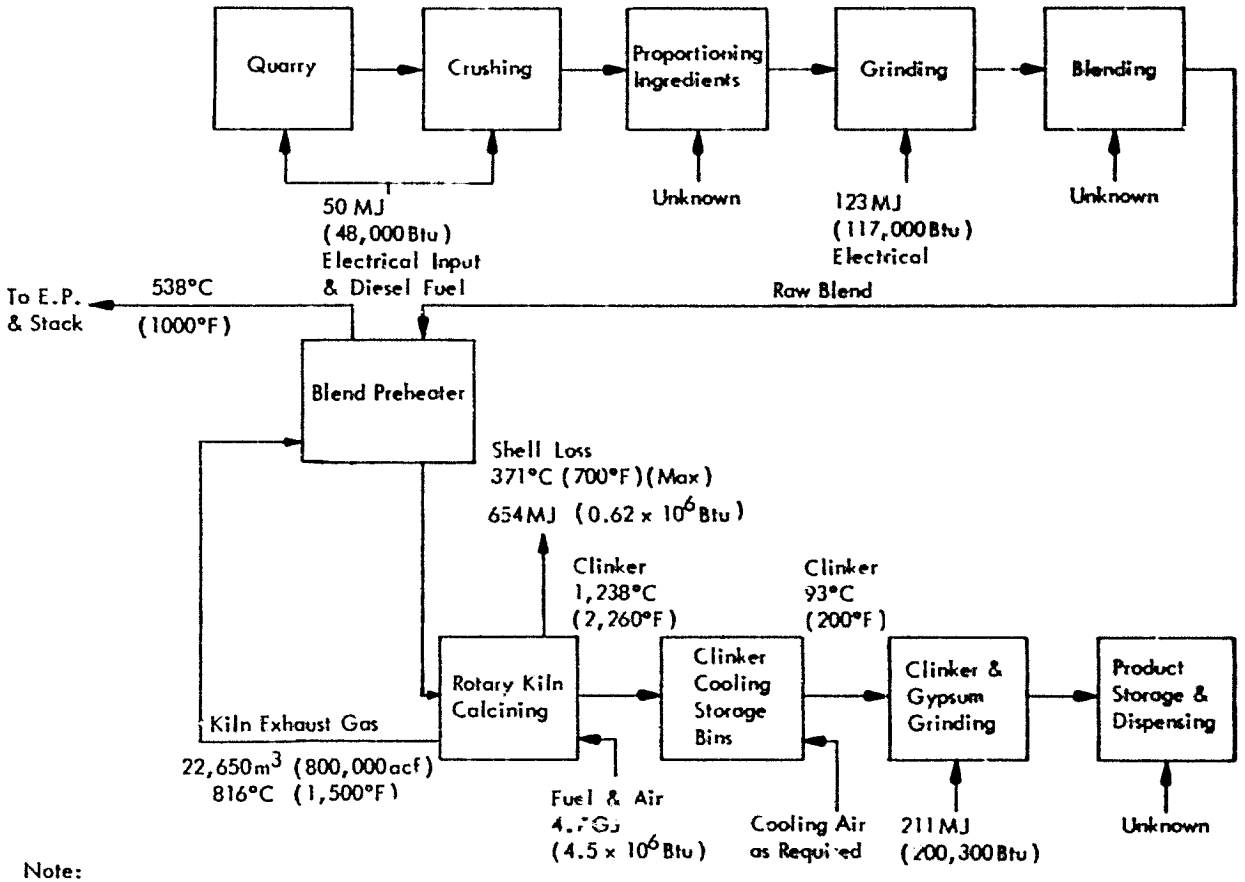

Note:
All energy values are based on the production of 907 Kg (1 Ton) of clinker.
Typical production rate is 64 Mg (70 tons) of clinker per hour.

Figure A-1 - Flow Diagram for Cement Kiln Process

A diagram of the sintering process is shown in Figure A-2.

IV. Electric Arc Furnace Application

Figure A-3 presents a flow diagram for an electric arc furnace. Electric arc furnaces are cylindrical refractory-lined vessels with carbon electrodes suspended from above which can be lowered to extend through the furnace roof. The charge for an electric arc furnace is 100% cold (nonmolten) scrap. With the electrodes retracted, the furnace roof can be rotated aside to permit the charge of scrap steel to be dropped into the furnace. Alloying agents and slag materials are usually added through the doors on the side of the furnace (some smaller or older furnaces are charged through these side doors). Current is then switched to the electrodes as they descend into the furnace. The heat, generated by the arc as it shorts between the electrodes through the scrap, melts the scrap. The slag and melt are poured from the furnace by tilting it.

The production of steel in an electric arc furnace is a batch process. Cycles of "heats" range from about 1-1/2 to 5 hr to produce carbon steel and from about 5 to 10 hr to produce alloy steel. Scrap steel is charged to begin a cycle and alloying agents and slag material are added for refining. Each cycle normally consists of alternate charging and melting operations, refining (which usually includes multiple oxygen blows of 1 to 5 min each), and tapping. Each heat requires approximately 500 kwh (1.7×10^6 Btu) per ton of molten metal. The gaseous effluent from the furnace, known as furme gas, is collected by a large furnace hood and quenched with a water spray. The fume gas temperature fluctuates from 27 to 1650°C (80 to 3000°F) during a complete processing cycle, and averages 700°C (1300°F) for the 3-hr period.

V. Coke Oven Application

One of the most important ancillary operations associated with iron ore smelting is the production of coke. Almost all the coal-based coke in the United States is produced by the "by-product" method. The by-product coke oven is a long, narrow chamber lined with refractory brick. Coke plants consist of a number of ovens, each of which operates intermittently in rotation to produce a continuous supply of coke oven gas. Crushed coal is fed into the oven which is then sealed. The exterior of the of the oven is then heated by combustion of previously produced coke oven gas. The coal starts to fuse at the walls, which are at about 2000°F. Coking proceeds gradually toward the center of the coal charge, while volatile products are removed in the vapor phase for subsequent recovery. The coking finishes about 17 hr later, at which time doors at the end of the oven are opened and a ram pushes the hot coke into a quenching car. The car takes the coke to a quenching station where it is sprayed with water. The coke is finally allowed to cool and is screened before being fed into the blast furnace.

There is a considerable amount of energy consumed in the coking process. A large amount of this energy is lost at the wet quenching stations where

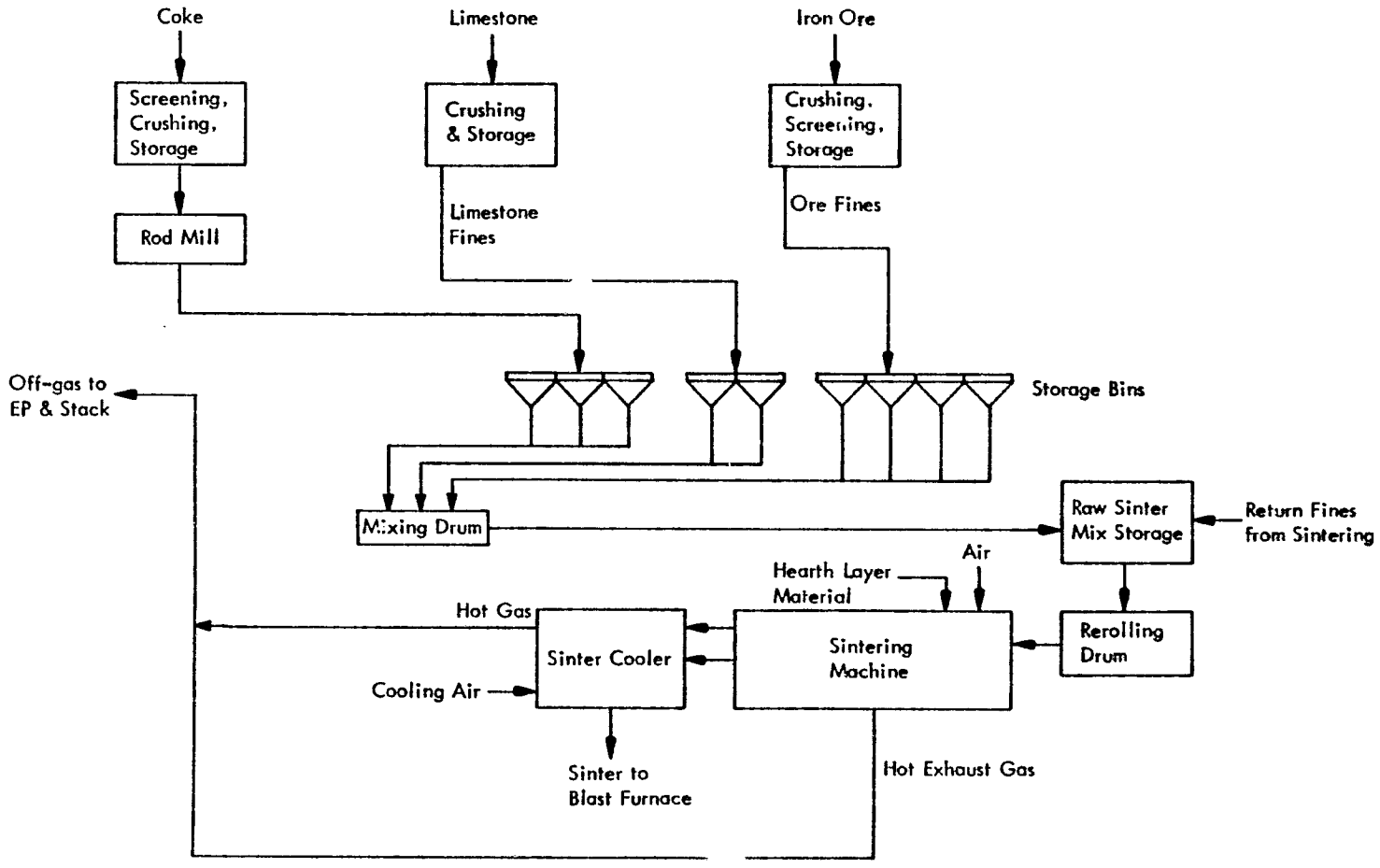

*A type of fluid bed heat exchanger

Figure A-2 - Flow Diagram for Iron Ore Sintering Process

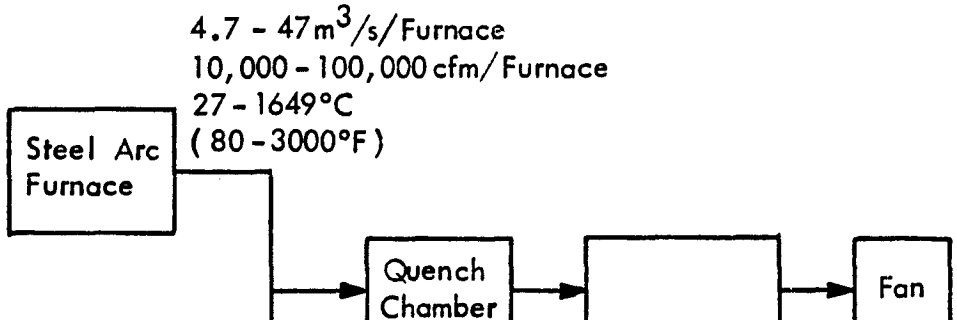

Figure A-3 - Flow Diagram for Electric Arc Furnace Operation

a large amount of water evaporates. One alternative technology to conserve energy is the dry quenching process in which the quenching is accomplished by circulating inert gases in a closed loop in conjunction with a heat recovery unit. The dry quenching process has been extensively applied in the U.S.S.R. and it is mandatory for all new installations. There are also installations found in Europe and Japan. There is no plant installation in the United States that uses dry quenching at the present time. However, as the energy picture changes, this technology may become more attractive in the United States.

Figure A-4 shows the process flow of a typical dry quenching coke plant. In dry quenching of coke, the hot coke pushed from the ovens is cooled in a closed system. Dry quenching uses "inert" gases to extract thermal energy from incandescent coke by direct contact. The energy is then recovered in waste heat boilers or by other techniques. The inert gases can be generated from an initial intake of air which reacts with the hot coke to form a quenching gas of the following composition: 14.5% CO_2, 0.4% O_2, 10.6% CO, 2% H_2, and 72.5% N_2. There might be slight variations from plant to plant, and cyclic fluctuations, but the given figures can be assumed to be average, representative values.

Except for the periodic introduction of hot coke with entrained gases, dry quenching is a closed-cycle operation on the gas side. Because oxygen is largely absent, the danger of explostion is minimized. Nevertheless, explosion precautions must be taken and the composition of circulating gases must be monitored and controlled by the addition of nitrogen.

When the hot coke is cooled from 1030 to 204°C (1900 to 400°F) in a dry quenching unit, about 1.3 kJ/g (1.1×10^6 Btu/ton) of coke are recoverable. Conceptually, the recovered energy can be put to a variety of uses. Possibilities of utilizing recovered energy are: (a) production of steam, (b) production of electricity, and (c) preheating of coking coal.

VI. Copper Smelter Application

Copper is obtained from copper ores by smelting. A general flow diagram is shown in Figure A-5. The term "smelting" can be used, in a wide sense, to cover the successive operations of roasting, reverberatory smelting, converting, and fine refining. Of these processes, the reverberatory furnace is the most energy-intensive.

The large, batch operated reverberatory furnaces are heated to about 1200°C (2200°F) during the smelting process. The heat input during smelting is required to melt the charge components; little heat is generated by chemical reaction during melting as presently conducted. Approximately 15% of the heat input is discarded with the slag and 5% is contained in the matte which is sent to the converter. Another 25% is lost by radiation, conduction, etc. Of the remaining 55%, discharged in the flue gases, about half is presently recovered by heat exchangers in the exhaust gas system for air preheating and waste heat boilers.

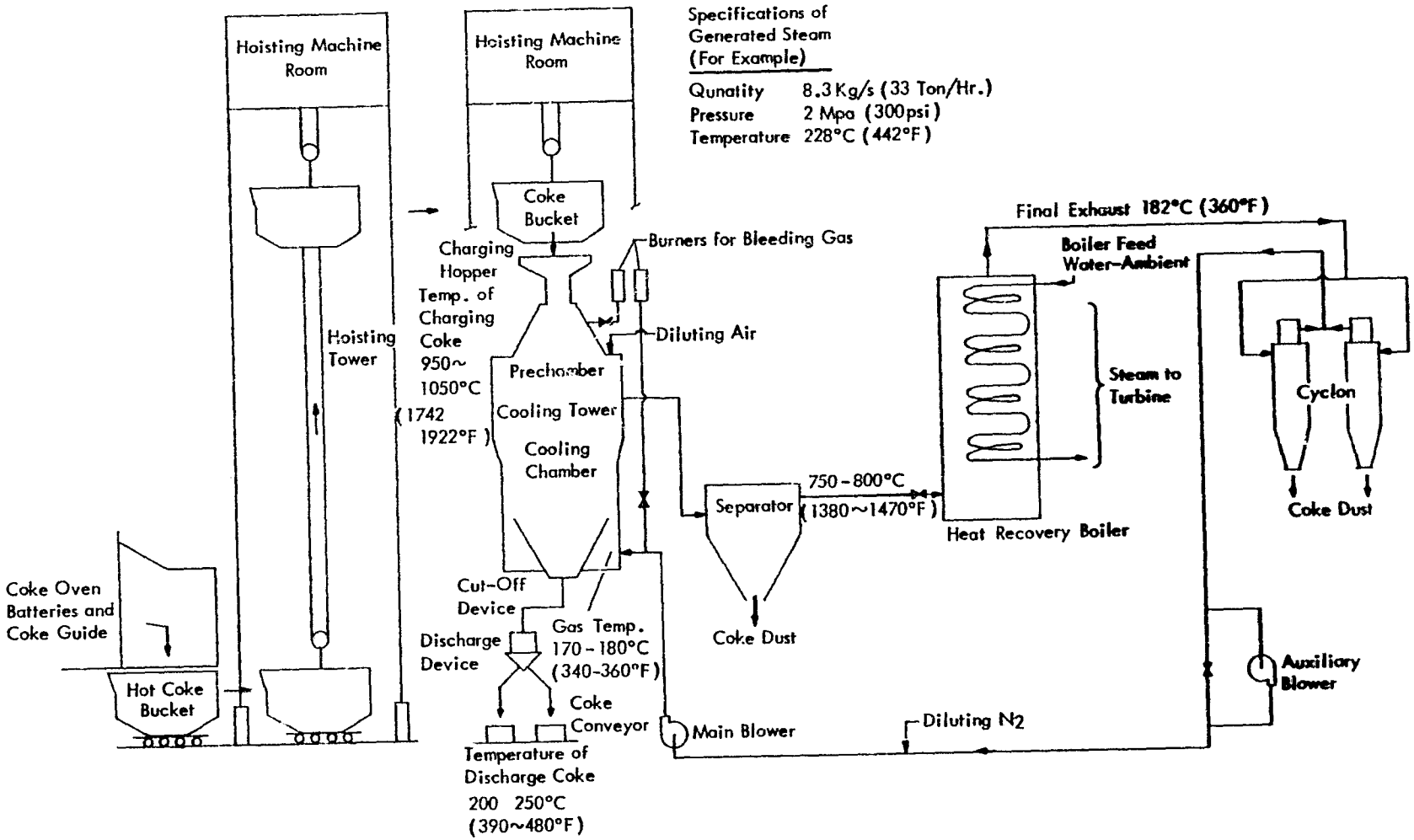

Figure A-4 - Flow Diagram for Dry-Quenched Coke

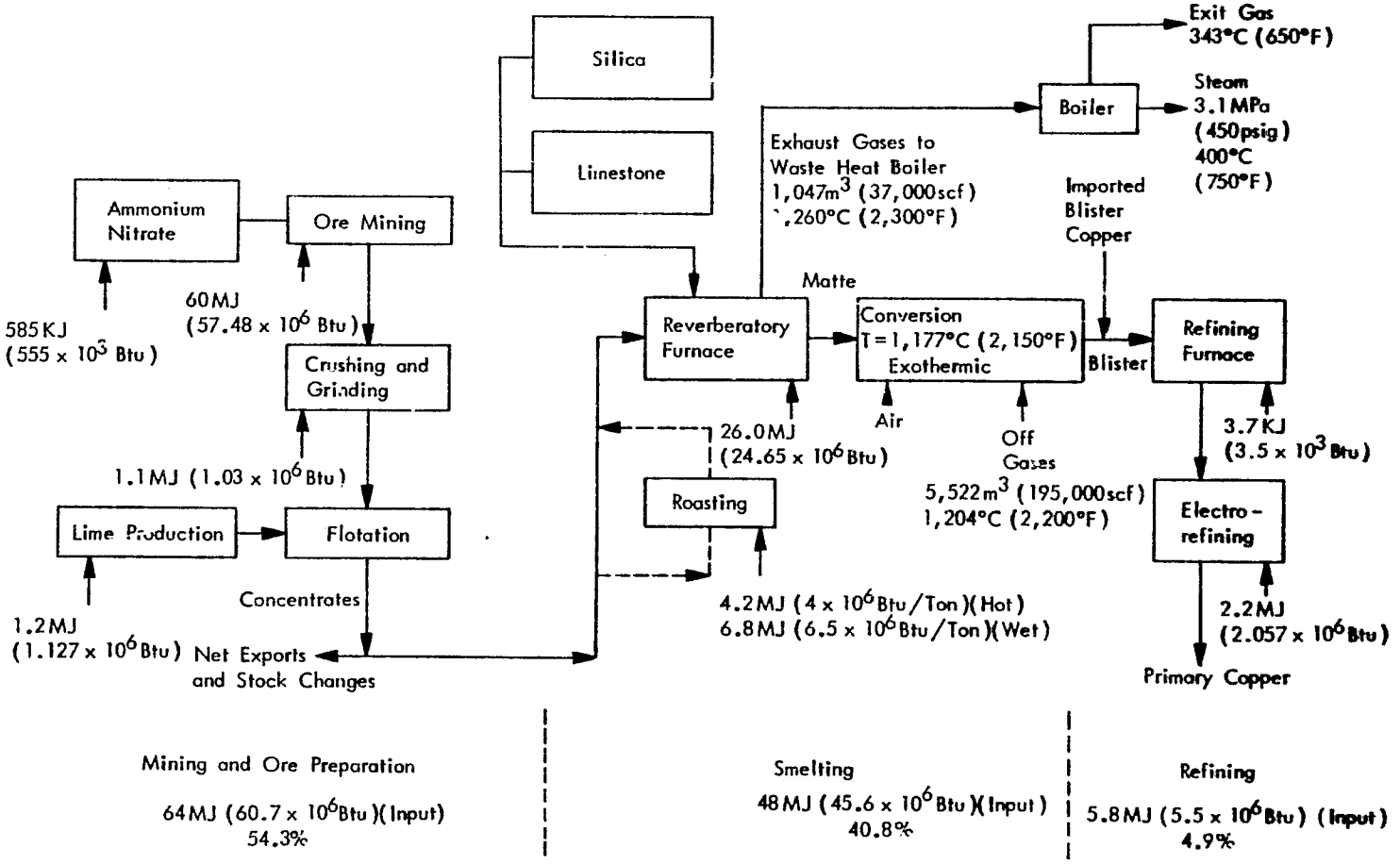

Note:
(1) Values given are for 907Kg (2,000) of Copper (99.9 Purity).

Figure A-5 - Flow Diagram for Copper Production

VII. Solar Brayton Power Plant Application

The reality of generating electrical power by solar Brayton systems for commercial consumption is probably a decade away. The available data pertain to preliminary design of proposed systems. However, values given for flow rates, temperatures, heat transfer rate, heat flux, interruption times, turbine sizes, etc., as well as proposed thermodynamic cycles and media are expected to be representative of final designs.

Two basic solar Brayton cycles are possible--open cycle systems such as shown in Figure A-6 which utilize ambient air as the working fluid and closed cycle systems such as shown in Figure A-7 which utilize an inert gas such as helium for the working fluid. Typical temperatures and pressures for various points in the closed cycle system are presented in Table A-1. These values may also be applicable to open cycle systems at selected points.

A representative daily plant operating power cycle is shown in Figure A-8. The upper curve shows the receiver heat input as it comes from the collector field. The curve below it is the amount of heat absorbed in the helium circuit. This heat is divided into components (also indicated) for direct use in the turbine generator cycle and to charge storage. The particular mode of operations shown uses the first few hours of insolation to charge storage while a limited amount of heat is used in the turbine-generator to produce the power to run the storage mode.

The generator is put on-line to furnish 50 MW_e to the grid at 8:00 AM. The plant module runs uninterrupted until approximately 4:00 PM when the 6-hr storage limit is achieved. From this time until 6:00 PM, the amount of heat from the collector field is excessive and some heat must be rejected (shaded region). At 6:00 PM, the storage system begins discharging as the receiver output drops off unitl finally the plant is running only on heat from the storage device. The daily cycle in the summer is completed shortly after midnight, the plant then having been operated for 16 hr.

The heat rejected due to storage limits represents lost energy for the summer insolation condition. For the winter, spring, and fall insolation conditions, the storage limit is not reached during the daily operating cycyle; consequently there is no rejected or lost insolation. Approximately 5% of the yearly insolation is rejected for the 6-hr thermal energy storage device in the baseline 50 MW_e power plant. Heliostat field size and storage time both affect this loss and consequently affect the energy output of the plant.

In contrast to the closed cycle system, the open cycle system, as shown in Figure A-6, utilizes fossil fuel combustion to supplement the energy supplied from the solar receiver. However, thermal energy storage could be incorporated in parallel with the solar receiver to reduce or eliminate the need for the fossil fuel back-up. The resultant system would then store and discharge the surplus solar energy much like the closed cycle system shown in Figure A-7.

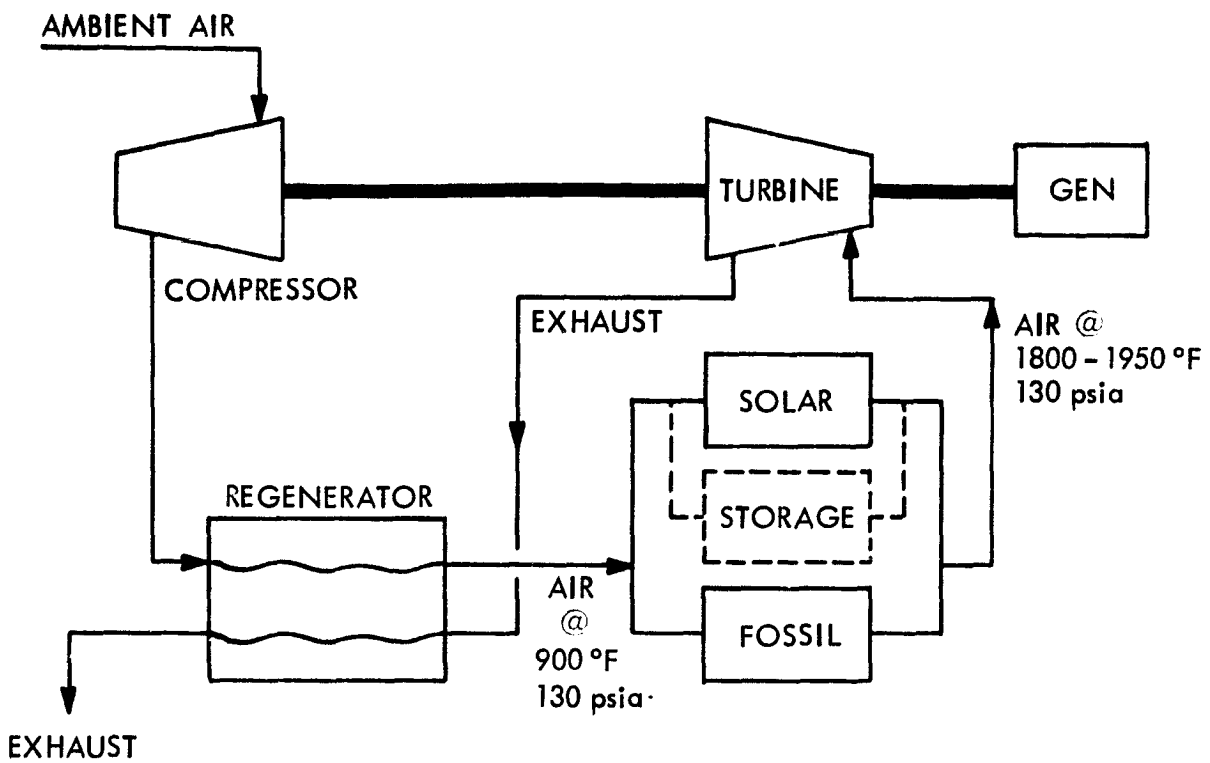

Figure A-6 - Schematic Flow Diagram - Open Brayton Cycle

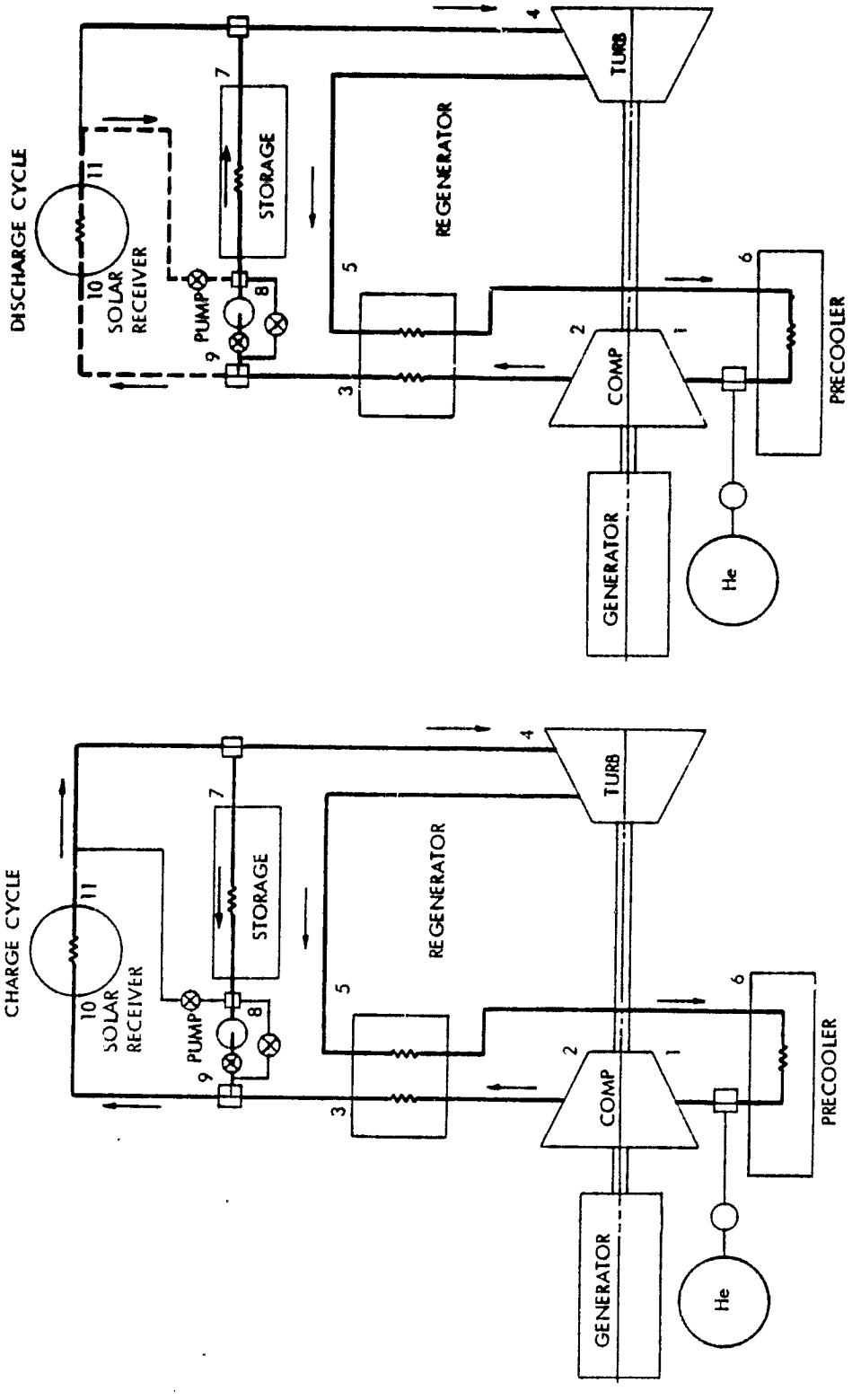

Figure A-7 - Solar-Brayton - Closed Cycle System

TABLE A-1

TYPICAL TEMPERATURES AND PRESSURES FOR SOLAR BRAYTON CLOSED CYCLE GAS TURBINE POWER PLANT WITH THERMAL ENERGY STORAGE

Charge					Discharge				
Max flow 173 kg/sec 22,836 lb/min					Max flow 197 kg/sec 26,009 lb/min				
State Point	Temperature (°C)	(°F)	Pressure (MN/m^2)	psi	State Point	Temperature (°C)	(°F)	Pressure (MN/m^2)	psi
1	49	120	1.6	232	1	49	120	2.0	290
2	152	306	3.0	435	2	143	289	3.5	508
3	581	1078	2.9	421	3	435	815	3.5	508
4	816	1501	2.9	421	4	598	1108	3.4	493
5	609	1128	1.6	232	5	454	849	2.1	305
6	179	354	1.6	232	6	165	329	2.0	290
7	816	1501	2.8	406	7	598	1108	3.4	493
8	699	1290	2.8	406	8	435	815	3.5	508
9	732	1350	2.9	421	9	435	815	3.5	508
10	663	1225	2.9	421	10	-	-	-	-
11	816	1501	2.9	421	11	-	-	-	-

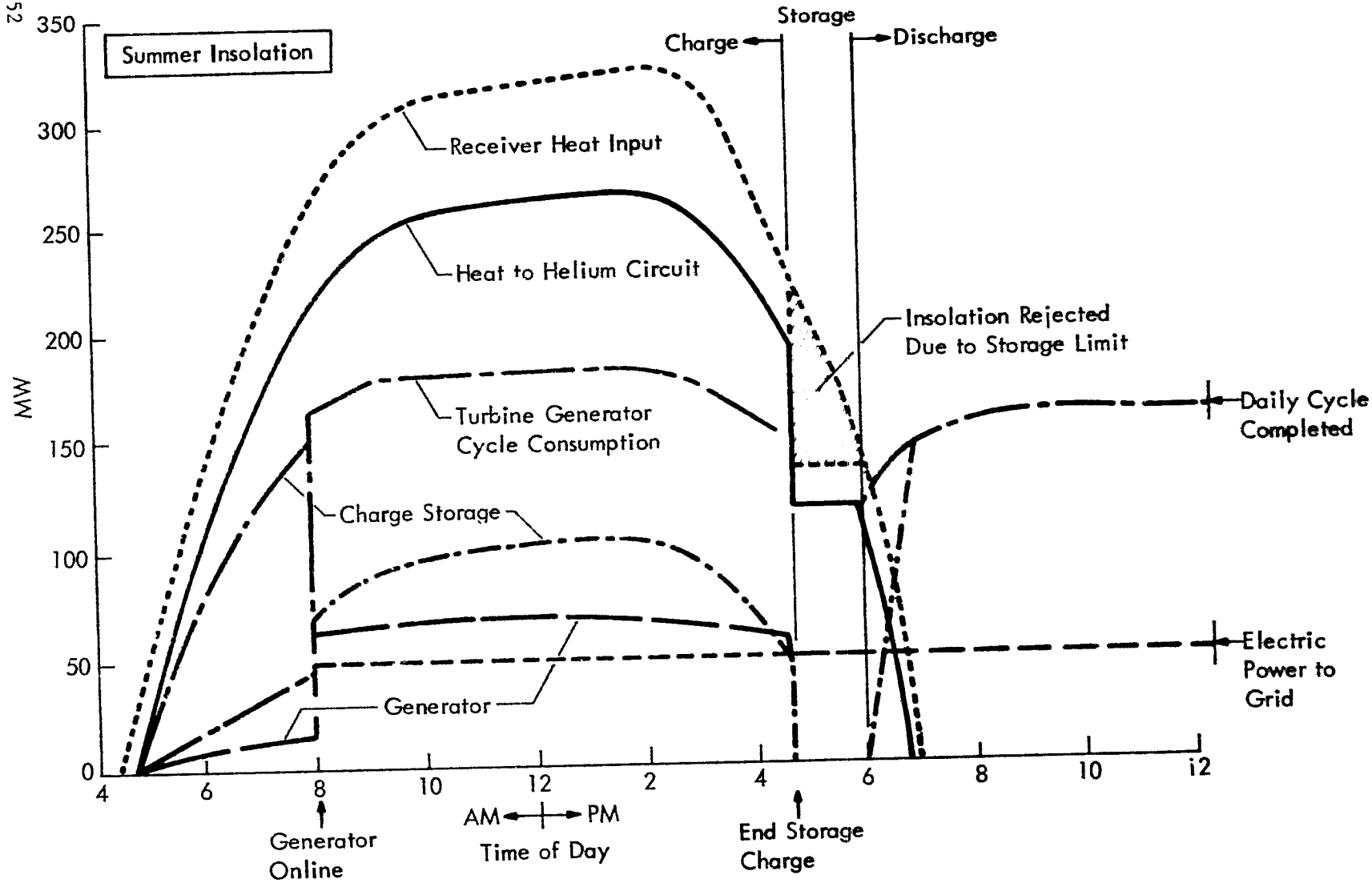

Figure A-8 - Plant Operation - Representative Operating Cycle

APPENDIX B

SAMPLE CALCULATIONS FOR THE TECHNICAL ANALYSIS OF THE CEMENT PLANT ROTARY/KILN APPLICATION

Design of Fluidized Bed Storage System for Cement Kiln

Charge time--to storage = 12 hr

Discharge time--out of storage = 12 hr

Kiln gas flow rate to fluidized bed = 20% of kiln exhaust

$= 1.07 \times 10^5$ lb/hr at 1000°F

For effective heat recovery, we assume:

$$(\dot{m}C)_s = (\dot{m}C)_g ,$$

i.e., solids flow rate x sp ht of solids = gas flow rate x sp ht of gas.

This gives solids flow rate $= \frac{1.07 \times 10^5 \times 0.28}{0.20}$

$= 1.498 \times 10^5$ lb/hr

Total amount of sand required = 898.8 tons

TES Charge Mode

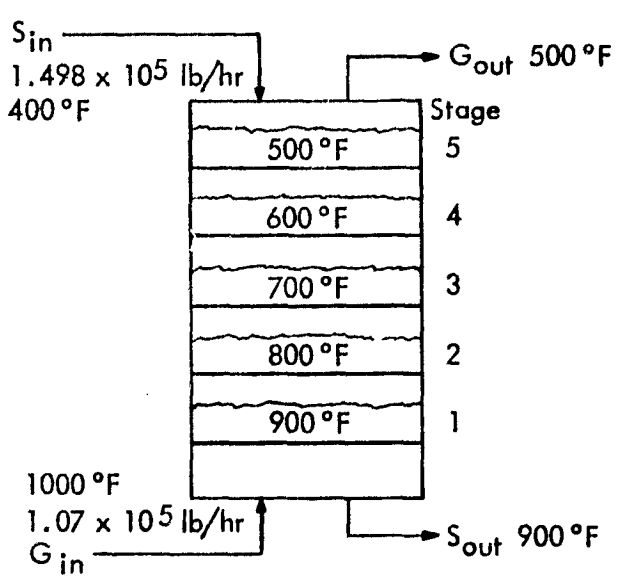

$$\eta_g = \frac{1,000-500}{1,000-400} = \eta_s = \frac{900-400}{1,000-400} = \frac{5}{6} = \frac{N}{N+1} = 83.3\%$$

TES Discharge Mode

The same fluidized bed is used, but the flow of heat is reversed--now from hot solids to cold gas.

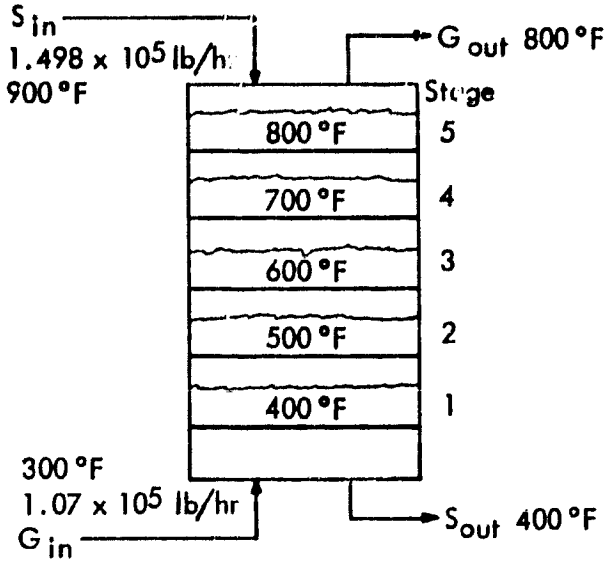

$$\eta_g = \frac{800-300}{900-300} = \eta_s = \frac{900-400}{900-300} = \frac{5}{6} = \frac{N}{N+1} = 83.3\%$$

In both charge and discharge operations, each stage of the fluidized bed is in complete thermal equilibrium, i.e.,

$$T_{s_{out}} = T_{bed} = T_{g_{out}}$$

The bed depth required to reach equilibrium is very small; the 'active section' was calculated to be about 2 in. This means that the bed can operate 'shallow' and the solids inventory in each stage can be kept as low as practically feasible, thus minimizing bed pressure drop. The only constraint is that the bed depth should be larger than the jet penetration depth to keep the bubbles from blowing holes through the bed.

During Charge

Stage 1

$\dot{m}_g = 1.07 \times 10^5$ lb/hr $\qquad \rho_{g_{1000°F,\ 18.8\ psia}} = 0.035$ lb/ft^3

$G = 51{,}224$ acfm (1000°F, 18.8 psia) $\qquad \mu_g = 0.036$ cp

$= 854$ acfs

Stage 5

$\dot{m}_g = 1.07 \times 10^5$ lb/hr $\qquad \rho_{g_{500°F,\ 14.7\ psia}} = 0.0414$ lb/ft^3

$G = 43{,}076$ acfm (500°F, 14.7 psia) $\qquad \mu_g = 0.027$ cp

$= 718$ acfs

During Discharge

Stage 1

$\dot{m}_g = 1.07 \times 10^5$ lb/hr (in order to keep $(\dot{m}C)_s = (\dot{m}C)_g$)

$\rho_{g_{300°F,\ 18.8\ psia}} = 0.067$ lb/ft^3

$\mu_g = 0.023$ cp

$G = 26{,}665$ acfm

$= 444$ acfs

Stage 5

$G = 56{,}537$ acfm $\qquad \rho_{g_{800°F,\ 14.7\ psia}} = 0.0315$ lb/ft^3

$= 942$ acfs $\qquad \mu_g = 0.033$ cp

If the entire bed is designed for 'Stage 1 - Charge' conditions, i.e., G = 854 acfs at 1000°F, 18.8 psia, the velocity at the extreme conditions will vary as follows:

$$\frac{942}{854} \text{ to } \frac{444}{854},$$

i.e., 1.11 to 0.52 times the design velocity.

For stable fluidized bed operation,

$$U_t > U_o > U_{mf}$$

For 42-mesh sand particles, U_t and U_{mf} values at the above four critical conditions are presented in Table B-1.

Selecting a velocity of $U_o = 4$ ft/sec for 'Stage 1 - Charge' condition gives a bed cross-sectional area of 854 ft^3/sec x 1/4 ft/sec = 213.5 ft^2.

U_o at the other three conditions are:

Stage 5 - charge: $U_o = 3.36$ ft/sec

Stage 1 - discharge: $U_o = 2.08$ ft/sec

Stage 5 - discharge: $U_o = 4.41$ ft/sec

These values of U_o satisfy the condition $U_t > U_o > U_{mf}$ as evidenced in Table B-1.

Diameter of bed = $\sqrt{\frac{213.5 \times 4}{\pi}} = 16.5$ ft

$$U_{mf} = \frac{\mu}{d_p \rho_g} \left[\left\{ 33.7^2 + d_p^3 \rho_g (\rho_s - \rho_g) g \times \frac{0.0408}{\mu^2} \right\}^{1/2} - 33.7 \right]$$

$$\text{(For 42 mesh sand)} = 870 \frac{\mu}{\rho_g} \left[\left\{ 33.7^2 + 2.98 \times 10^{-7} \frac{\rho_g}{\mu^2} \right\}^{1/2} - 33.7 \right]$$

$$U_t \text{ (in the relevant range)} = \left[\frac{4}{225} \frac{(\rho_s - \rho_g)^2 g^2}{\rho_g \mu} \right]^{1/3} d_p$$

$$= 8.54 \times 10^{-2} \left[\frac{1}{\rho_g \mu} \right]^{1/3}$$

Let bed depth: $z = 1$ ft

$$\Delta P \text{ bed/stage} = \frac{1 \text{ ft} \times 90}{144} = 0.625 \text{ psi}$$

ΔP grid/stage = 0.3 x 0.625 = 0.1875 psi

TABLE B-1

SUMMARY OF FLUID BED PARAMETERS

	Charge		Discharge	
	Stage 1	Stage 5	Stage 1	Stage 5
T_g =	1000°F	500°F	300°F	800°F
G =	854 acfs	718 acfs	444 acfs	942 acfs
P =	18.8 psia	14.7 psia	18.8 psia	14.7 psia
ρ_g =	0.035 lb/ft^3	0.0414 lb/ft^3	0.067 lb/ft^3	0.0315 lb/ft^3
μ_g =	0.036 cp	0.027 cp	0.023 cp	0.033 cp
U_{mf} =	0.16 ft/sec	0.21 ft/sec	0.244 ft/sec	0.173 ft/sec
U_t =	9.0 ft/sec	9.4 ft/sec	8.44 ft/sec	9.62 ft/sec

Total ΔP per stage = 0.8125 psi

ΔP of whole bed = 0.8125 x 5 = 4.0625 psi

Solids inventory/stage = 213.5 x 90 x 1 = 19,208 lb

$$\text{Residence time/stage} = \frac{19{,}208 \text{ lb}}{1.498 \times 10^5 \frac{\text{lb}}{\text{hr}}} \times 60 = 7.69 \text{ min}$$

Grid Design

U_o = 4 ft/sec; 854 acfs; 213.5 ft^2; 16.5 ft diameter

Assume a bed depth of 1 ft (unfluidized)

$$\Delta P_{bed} = \frac{1 \times 90}{144} = 0.625 \text{ psi}$$

$$\Delta P_{grid} = 30\% \text{ of } \Delta P_{bed}$$

$$= 0.30 \times 1.042 = 0.1875 \text{ psi}$$

$$V_{o_{min}} = 0.8 \sqrt{\frac{2g \, \Delta P \times 144}{\rho_g}}$$

$$= 178.3 \text{ ft/sec}$$

$$\text{Maximum hole area} = 854 \frac{ft^3}{sec} \times \frac{1}{178.3 \frac{ft}{sec}} = 4.79 \text{ ft}^2 = 2.24\% \text{ free area}$$

Try 3/16-in. hole - area/hole = 1.9175×10^{-4} ft^2

$$\text{No. of holes} = \frac{4.79}{1.9175 \times 10^{-4}} = 24{,}980 \text{ holes}$$

$$V_o \sqrt{\rho_g} = 178.3 \sqrt{0.035}$$

$$= 33.4$$

$$\frac{P}{D_o}\uparrow = 16$$

$$P = 16 \times \frac{3}{16} = 3 \text{ in.}$$

$$D_{Bo} = \frac{P}{2} = 1.5 \text{ in.}$$

Jet penetration depth P is less than bed depth, i.e., 3 in. < 1 ft.

Hence no blow-through occurs.

TDH

$U_o = 4$ ft/sec

Using the TDS versus U_o correlation (with bed diameter as parameter),

TDH = 168 in. = 14 ft

It is probably necessary to provide TDH only at the top stage. The bottom four stages can do with a small freeboard height, since we are not concerned about particle scrubbing the bottom surface of grid plates.

Allowing a plate-to-plate clearance of 2.5 ft,

(1 ft unfluidized → 2 ft fluidized, plus 0.5 ft freeboard),

between stages and 14 ft TDH above the top bed, the total height of the bed becomes =

$$\overline{4 \times 2.5} + \overline{14 + 2} + \overline{3} \text{ (at bed inlet)}$$

= 29 ft

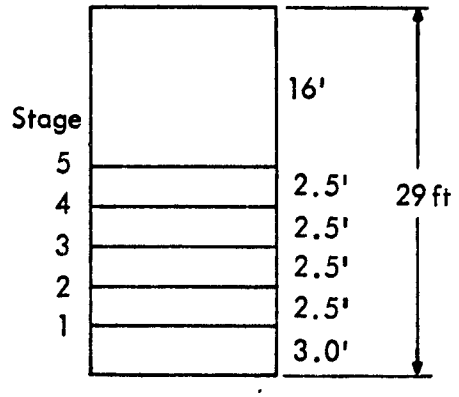

Pneumatic Transport of Solids

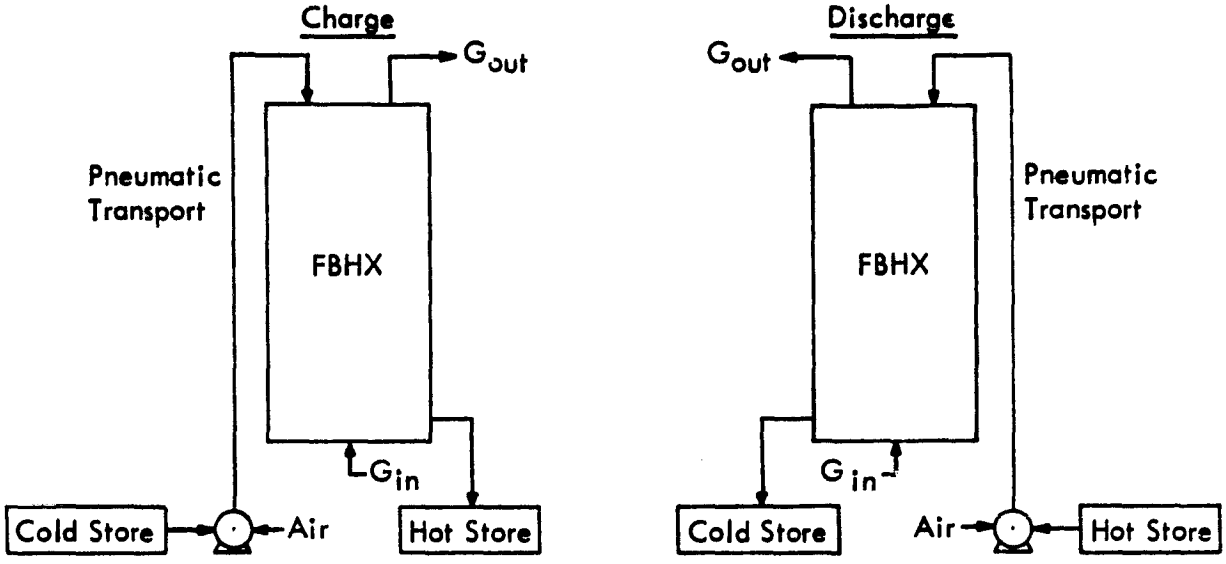

Total height of vertical transport = 29 ft bed height + 11 ft allowance above and below bed = 40 ft.

Mass flow rate of solids = 1.498×10^5 lb/hr,

i.e., $U_s \rho_s (1 - \epsilon)$. $A = 1.498 \times 10^5/3,600$

$\epsilon = 0.982$ for stable operation without choking (Figure 17, p. 386, Kunii and Levenspiel)

$$U_s \; 150 \; (1 - 0.982) \frac{\pi d_t^2}{4} = \frac{1.498 \times 10^5}{3,600}$$

$$U_s \; d_t^2 = 19.622$$

Saltation velocity > choking velocity

U_{cs} U_{ch}

U_o should be > U_{ch}

Safer if $U_o > U_{cs}$

U_{cs} was computed for 1 ft duct (d_t = 1 ft)

$U_{cs} = 29.5$

If $d_t = 1$ ft

$$U_s = \frac{19.622}{1^2}$$

$$= 19.622 \text{ ft/sec}$$

$$U_o = (U_s + U_t)\ \epsilon$$

$$= (19.62 + 6.06)\ 0.982$$

$$= 25.22 \text{ ft/sec}$$

is $< U_{cs}$, so not acceptable.

Try $d_t = 0.75$ ft

$U_s = 34.88$ ft/sec

$U_o = (34.88 + 6.06)\ 0.982 = 40.20$

$U_{cs} = 26.25$ ft/sec

$U_{cs} < U_o$, so acceptable.

Pressure drop in the transport line:

$$\Delta P = \frac{G_s}{G} \cdot \frac{U_o}{U_s} \cdot \rho_g L + \frac{U_s}{g_c} \cdot \rho_g U_o \frac{G_s}{G} + 2 f_s' \frac{U_o}{U_s} \cdot \frac{G_s}{G} \cdot \frac{\rho_g U_o^2 1}{g_c d_t}$$

$$\frac{G_s}{G} = \frac{U_s}{U_o} \cdot \frac{\rho_s}{\rho_g} \cdot (1 - \epsilon) = \frac{34.88}{40.20} \cdot \frac{150}{0.071} \cdot 0.018 = 33.0$$

L = vertical transport length = 40 ft

1 = total transport length = 40 ft + 10 ft, say = 50 ft

f_s' = friction factor $\simeq 0.02$

$$\Delta P = 33.0 \times \frac{40.2}{34.88} \times 0.071 \times 40 + \frac{34.88}{32.2} \times 0.071 \times 40.2 \times 33 + 2 \times$$

$$0.02 \times \frac{40.2}{34.88} \times 33.0 \times \frac{0.071 \times 40.2^2 \times 50}{32.2 \times 75}$$

$= (108.01 + 102.03 + 361.4)\ lb_f/ft^2$

$= 571.44\ lb_f/ft^2 = 3.97\ psi$

Adiabatic horsepower required for pressurizing the gas input to fluidized bed:

$$hp = \frac{P_1\ CFM_1}{33,000} \cdot \left(\frac{\gamma}{\gamma-1}\right)\left[\left(\frac{P_2}{P_1}\right)^{\frac{\gamma-1}{\gamma}} - 1\right]$$

Charge

$$= 14.7 \times 144 \times \frac{64,287}{33,000}\left(\frac{1.4}{0.4}\right)\left[\left(\frac{14.7 + 4.1}{14.7}\right)^{\frac{0.4}{1.4}} - 1\right]$$

$= 1,051\ hp$

$$\Delta T \text{ across compressor} = T_1\left[\frac{P_2}{P_1}^{\frac{0.4}{1.4}} - 1\right]$$

$$= 1,000\left[\frac{18.8}{14.7}^{\frac{0.4}{1.4}} - 1\right]$$

$= 72.8°F$

Discharge

$$hp = 14.7 \times 144 \times \frac{33,464}{33,000}\left(\frac{1.4}{0.4}\right)\left[\frac{18.8}{14.7}^{\frac{0.4}{1.4}} - 1\right]$$

$= 547\ hp$

$$\Delta T = 300\left[\left(\frac{18.8}{14.7}\right)^{\frac{0.4}{1.4}} - 1\right]$$

$= 21.9°F$

Power for Pneumatic Transport

$$\text{Gas velocity } U_g = \frac{U_o}{\epsilon} = \frac{40.2}{0.982} = 40.94\ ft/sec$$

$= 2,456.4\ fpm$

$$cfm = 1,717 \times \frac{\pi \times 0.75^2}{4} = 1,085.2\ cfm$$

$$\Delta P = 3.97 \text{ psi}$$
(allow 20% for bends)
$$= 4.76 \text{ psi} = 131.93 \text{ in. } H_2O$$

$$hp = \frac{cfm\ \Delta P}{6{,}356 \times \eta}$$

$$= \frac{1{,}085.2 \times 131.93}{6{,}356 \times 0.7} = 32.18 \text{ hp}$$

APPENDIX C

COMPUTER PROGRAM FOR ANALYZING FBHX/TES SYSTEMS

COMPUTER PROGRAM DESCRIPTION

This appendix describes the computer program used for the parametric analysis of the theraml energy storage system (TES). The computer program uses FORTRAN and consists of nine modules. The paragraphs below describe the algorithm and the function of each module, followed by the description of nomenclature used in the computer program. Subsequently, the computer program and the computed results from the base case simulations of the cement kiln and the electric arc furnace are presented.

Module 1: All the necessary input data are entered in this module. These input data include:

* Total gas flow rate from a particular process system
* Gas flow rate to the TES during charge
* Gas flow rate to the TES during discharge
* Inlet gas temperature to the TES during charge
* Charge and discharge times
* Outlet gas temperature from the TES during discharge
* Waste heat boiler exit temperature (WHBET)

All of these inputs are necessary for both cement kiln and electric arc furnace systems. However, if available, clinker gas flow rate, clinker production rate, and clinker gas temperature are required in the cement kiln system. Module 1 also set the initial gas inlet temperature during discharge (TITD) equal to 10°F higher than WHBET and the initial bed depth equal to 0.5 ft.

Module 2: Given the input data from Module 1, Module 2 computes the mCp ratios of solid to gas during charge and discharge (RC/RD). Thermal efficiency equations for the fluidized bed heat exhcanger (FBHX) and Newton's method of successive substitution are used in the computation with the convergence criterion of 0.01% for the value of RC. Module 2 minimizes the number of stages when more than one solution exist to satisfy the given operating conditions. After the computation of the feasible values of RC and RD and of the minimum number of stages, the gas and solid (storage media) temperatures at the four extreme-end conditions, which are the top and the bottom conditions of the FBHX during charge and discharge, are calculated.

Module 3: Based on the current value of bed depth, Module 3 calculates the pressure drop across the FBHX and avoids operating the FBHX at rarefied gas flow regions. Because a forced-draft fan is used in the TES system during discharge, GITD equals to the adiabatic discharge temperature, which is dependent upon the pressure drop across the FBHX. Module 3 computes a new value of GITD according to the pressure drop across the FBHX. With the pressure drop data and the gas temperature data, Module 3 calculates the gas operating velocities at the four extreme conditions and checks if all the velocity criteria of fluidization are satisfied. The bed diameter of the FBHX is determined according to the satisfactory gas operating velocities.

Module 4: Module 4 optimizes the bed depth. With the gas operating velocities computed in Module 3, and with the given grid hole diameter, the jet penetration depth in each stage is computed. A new bed depth is then determined by multiplying the maximum jet penetration depth by a factor of 1.1. However, if the absolute difference between the old and new values of GITD is larger than 0.05°F, the computation will go back to Module 2 and a new iteration is started from Module 2 with the new value of GITD; alternately, if the absolute difference is less than 0.05°F, the current parametric values are accepted.

Module 5: The height of the FBHX and the makeup rate of the storage media are computed in Module 5. The height of the FBHX is determined by both the number of stages and the transport disengaging height, and the makeup rate of the storage media is estimated by the attrition rate.

Module 6: The adiabatic horsepower requirements of the FBHX in charge and discharge modes are computed in Module 6.

Module 7: According to the operating condition of the FBHX, Module 7 designs the pneumatic transport system of the storage media. Both the carrier gas and storage media velocities are specified on the consideration of choking and saltation velocities. Pneumatic transport duct diameter and the horsepower requirement for the pneumatic tranpsort are determined in Moudle 7.

Module 8: Module 8 computes several parameters necessary for the energy efficiency assessment of the TES. These parameters include:

* Energy fed to the waste heat boiler (WHB)

* Energy required to operate TES

* Energy recovered from TES during discharge

* Total net energy from the process system with the WHB and the TES during charge or discharge

* Total energy recovered from the process system with the TES (TERS)

* Total energy recoverable from the process system without TES (TER)

* Energy efficiency of the TES (TERS/TER)

* Differential kilowatt forfeited by using TES during charge

* Differential kilowatt recovered by using TES during discharge

Module 9: The computed values of the relevant parameters in all of the previous modules are printed by Module 9. Detailed description of these parameters are presented in the nomenclature.

NOMENCLATURE USED IN THE COMPUTER PROGRAM

A1, A2, A3, A4, A5, A6, A7, A8, or A9 = dummy variable in the iterative computation of $\frac{M_s C_{ps}}{M_p C_{pg}}$;

where M_s = solid mass flow rate, lb/hr

C_{ps} = solid heat capacity, Btu/°F, lb

M_g = gas mass flow rate, lb/hr

C_{pg} = gas heat capacity, Btu/°F, lb

$AC0 = \frac{GOTD - GITD}{GITC - GOTC}$;

where GOTD = gas outlet temperature during discharge, °F

GITD = gas inlet temperature during discharge, °F

GITC = gas inlet temperature during charge, °F

GOTC = gas outlet temperature during charge, °F

$AC1 = \frac{N + 1}{N}$;

where N = number of stages in the fluidized bed

$AC2 = (RCO^{N+1} - 1)/(RCO^{N} - 1)$;

where RCO is an old trial value of $\frac{M_s C_{ps}}{M_g C_{pg}}$ during charge

AHPG(i) = adiabatic horsepower for pressurizing gas;

where i = 1, charge

i = 2, discharge

AHPGC = AHPG(1)

AHPDG = AHPG(2)

AK = a parameter to control the number of iterations

APH = area per hole, ft^2

APM = dummy variable in the iterative computation of $\frac{M_s C_{ps}}{M_g C_{pg}}$

ATTRT = attrition rate, lb/hr

B

B6(i) = empirical parameter at the i^{th} iteration of the pneumatic transport

B7(i) = empirical parameter at the i^{th} iteration of the pneumatic transport

BAREA = bed area, ft^2

BDIA = bed diameter, ft

BDO = assumed bed depth, ft

BLKDS = solid bulk density, lb/ft^3

BPD = bed pressure drop, psi

C

CFMP(i) = gas flow rate in pneumatic transport at i^{th} iteration, ft^3/min

CGE = clinker gas energy, Btu/hr

CGFR = clinker gas flow rate, lb/hr

CGT = clinker gas temperature, °F

CHT = charge time, hr

CP = clinker production rate, tons/hr

CPG = gas heat capacity, Btu/lb °F

CPS = solid heat capacity, Btu/lb °F

CST = cool solid temperature, °F

D

D = particle diameter, ft

DBN(i) = i^{th} new iterated value of a parameter in the computation of transport disengaging height

DBO(i) = i^{th} old iterative value of a parameter in the computation of transport disengaging height

DCT = discharge time, hr

DELPP(i) = pressure drop in the pneumatic transport;

where i = 1, charge

i = 2, discharge

DELPPT(i) = 1.2 x DELPP(i)

DELPPTC = DELPPT(1)

DELPPTD = DELPPD(2)

DELTQ = (GFRC) (GITC) (CHT) - (GFRD) (GOTD) (DCT);

where GFRC = gas flow rate during charge, lb/hr

GITC = gas inlet temperature during charge, °F

CHT = charge time, hr

GFRD = gas flow rate during discharge, lb/hr

GOTD = gas outlet temperature during discharge, °F

DCT = discharge time

DKWC = differential kilowatt by using storage during charge

DKWD = differential kilowatt by using storage during discharge

DPB7(i) = empirical parameter in the computation of saltation velocity at ith iteration

DTC = duct diameter during charge, ft

DTD = duct diameter during discharge, ft

DTN = new iterated value of duct diameter, ft

DTO = old iterated value of duct diameter, ft

DTP(i) = duct diameter at i^{th} iteration

DU(i) = i^{th} iterated value of the difference between operating and minimum fluidization velocities, ft/sec

E

EFORS = energy efficiency of the storage system, $\frac{TERS}{TER}$;

where TERS = total energy recovered from the system using storage, Btu/hr

TER = total energy recoverable from the system without storage, Btu/hr

ESC = bed thermal efficiency during charge, $\frac{GITC - GOTC}{GITC - SITC}$;

where GITC = gas inlet temperature during charge, °F

GOTC = gas outlet temperature during charge, °F

SITC = solid inlet temperature during charge, °F

ESD = bed thermal efficiency during discharge, $\frac{SITD - SOTD}{SITD - GITD}$;

where SITD = solid inlet temperature during discharge, °F

SOTD = solid outlet temperature during discharge, °F

GITD = gas inlet temperature during discharge, °F

ETESD = energy recovered from TES during discharge, Btu/hr

ETS(i) = energy required to operate the storage, Btu/hr;

where i = 1, charge

i = 2, discharge

EWHB(i) = energy available to waste heat boiler, Btu/hr;

where i = 1, charge

i = 2, discharge

G

G = acceleration by gravity, ft/sec^2

$GC = \frac{32.2\ lbm\ ft}{lbf\ sec^2}$

GFRC = gas flow rate during charge, lb/hr

GFRCR(i) = gas flow rate during discharge, lb/hr;

where i = 1, 2, charge

i = 3, 4, discharge

GFRD = gas flow rate during discharge, lb/hr

GIPC = gas inlet pressure during charge, psi

GIPD = gas inlet pressure during discharge, psi

GITC = gas inlet temperature during charge, °F

GITD = gas inlet temperature during discharge, °F

GITDN = new iterated value of GITD, °F

GOPC = gas outlet pressure during charge, psi

GOPD = gas outlet pressure during discharge, psi

GOTD = gas outlet temperature during discharge, °F

GOTDN = new iterated value of GOTD, °F

GPD = grid pressure drop, psi

GRLDGC = gas grain loading due to attrition during charge, gr/ft^3

GRLDGD = gas grain loading due to attrition during discharge, gr/ft^3

GSG(i) = parameter in the pneumatic transport, dimensionless;

where i = 1, charge

i = 2, discharge

H

HAMAX = maximum grid hole area, ft^2

HDIA = hole diameter, ft

HIGHN = the next higher number of stages, dimensionless

HPP(i) = horsepower for pneumatic transport, hp;

where i = 1, charge

i = 2, discharge

HPPC = horsepower for pneumatic transport during charge, hp

HPPD = horsepower for pneumatic transport during discharge, hp

HST = hot solid temperature °F

I

ICOUNT = a parameter to control the number of iterations

J

JPD(i) = jet penetration depth at i^{th} condition, ft

JPDMX = maximum of JPD(i), ft

K

KW(i) = kilowatt from the system with storage, kw;

where i = 1, charge

i = 2, discharge

KWC = KW(1)

KWD = KW(2)

KWHPT = kilowatt-hour per ton of clinker

KWHNSPT = kilowatt-hour per ton of clinker without storage

KWNS = kilowatt from the system with no storage, kw

M

MUG(i) = gas viscosity at i^{th} condition, lb/ft sec

MUGC(i) = MUG(i) at i^{th} iteration

N

N = number of stages, dimensionless

NHOLES = number of holes, dimensionless

O

OPTION = control parameter to select a particular system

P

P(i) = pressure at i^{th} condition, psia

P1 = GIPC

P2 = GOPC

P3 = GIPD

P4 = GOPD

PARTDE = particle density, lb/ft^3

PARTDI = particle diameter, ft

PCT = percent of gas to the storage, %

PCTFA = percent of free area, %

PCW = percent of gas to the waste heat boiler, %

PCWH(i) = percent of gas to the waste heat boiler, %;

where i = 1, charge

i = 2, discharge

PI = π, 3.1416

R

RC = iterated value of $\frac{M_s C_{ps}}{M_g C_{pg}}$ during charge;

where M_s = solid mass flow rate, lb/hr

C_{ps} = solid heat capacity, Btu/°F, lb

M_g = gas mass flow rate, lb/hr

C_{pg} = gas heat capacity, Btu/°F, lb

RCO = old iterated value of RC

RD = iterated value of $\frac{M_s C_{ps}}{M_g C_{pg}}$ during discharge

RDO = old iterated value of RD

RG = gas density, lb/ft^3

RHO(i) = gas density at i^{th} iteration, lb/ft^3

RHOG(i) = gas density at i^{th} iteration, lb/ft^3

RHOGC(i) = gas density at i^{th} iteration, lb/ft^3

RKW = DKWD/DKWC

RKWH = (RKW) DCT/CHT

$$RRCRD = \frac{GFRD}{GFRC} \cdot \frac{DCT}{CHT}$$

RS = solid density, lb/ft^3

S

SFR(i) = solid flow rate, lb/hr;

where i = 1, charge

i = 2, discharge

SFRC = solid flow rate during charge, lb/hr

SFRD = solid flow rate during discharge, lb/hr

SITC = solid inlet temperature during charge, °F

SITD = solid inlet temperature during discharge, °F

SOTC = solid outlet temperature during charge, °F

SOTD = solid outlet temperature during discharge, °F

SRPY = make-up solid per year, tons/year

T

T(i) = bed temperature at i^{th} condition, °F

T1 = GITC

T2 = GOTC

T3 = GITD

T4 = GOTD

TBDHT = total bed height, ft

TBPD = total bed pressure drop, psi

TCOUNT = a parameter to control the number of iterations

TDH(i) = transport disengaging height at i^{th} iteration, ft

TDHMX = maximum transport disengaging height, ft

TEEF = thermal electric efficiency, %

TEFRS(i) = thermal energy from the system with storage, Btu/hr

where i = 1, charge

i = 2, discharge

TER = total energy recoverable from the system without storage, Btu/hr

TERS = total energy recovered from the system with storage, Btu/hr

TGFR = total gas flow rate, lb/hr

TL = total length of the pneumatic transport system

U

UCS(i) = saltation velocity at i^{th} iteration, ft/sec

UCSM(i) = minimum saltation velocity at i^{th} iteration, ft/sec

UGP(i) = gas velocity in pneumatic transport at i^{th} iteration, ft/sec

UGR(i) = minimum gas velocity through the grid, at i^{th} iteration, ft/sec

UGRMIN = minimum value of UGR(i), ft/sec

UMAX = minimum terminal velocity, ft/sec

UMF, UMFU = minimum fluidization velocity (U_{mf}), ft/sec

UMFC = maximum value of U_{mf}, ft/sec

UMFU = minimum fluidization velocity at i^{th} condition/ ft/sec

UMF1 = UMFU(1)

UMF2 = UMFU(2)

UMF3 = UMFU(3)

UMF4 = UMFU(4)

UMIN = maximum value of minimum fluidization velocity, ft/sec

UMOP = gas operating velocity, ft/sec

UO(i) = superficial gas velocity at i^{th} iteration, ft/sec

UOP(i) = gas operating velocity in the fluidized bed at i^{th} condition/ ft/sec

UOP1 = UOP(1)

UOP2 = UOP(2)

UOP3 = UOP(3)

UPO4 = UOP(4)

US(i) = solid velocity in pneumatic transport at i^{th} iteration

USDT2(i) = i^{th} iterated value of solid velocity multiplied by the square of duct diameter, ft/sec

UT(i) = i^{th} iterated value of terminal velocity in pneumatic transport, ft/sec

UTC = minimum value of terminal velocity, ft/sec

UTPN(i) = i^{th} iterated value of terminal velocity in pneumatic transport, ft/sec

UTU(i) = terminal velocity at i^{th} condition, ft/sec

UTU1 = UTU(1)

UTU2 = UTU(2)

UTU3 = UTU(3)

UTU4 = UTU(4)

V

V(i) = volumetric gas flow rate at i^{th} condition, ft^3/min

V1 = V(1)

V2 = V(2)

V3 = V(3)

V4 = V(4)

VGFR(i) = volumetric gas flow rate at i^{th} condition, ft^3/sec

VGFRIC = VGFR(1)

VGFROC = VGFR(2)

VGFRID = VGFR(3)

VGFROD = VGFR(4)

VGFRM = maximum value of volumetric gas flow rate, ft^3/sec

VL = total height of the pneumatic transport, ft

VSR(i) = i^{th} iterated value of the square root of gas density multiplied by gas minimum velocity through the grid

W

WHBET = waste heat boiler exit temperature, °F

```
00100C
00110C
00120C
00130C     SIMULATION OF THERMAL ENERGY STORAGE(TES)
00140C     AND RECOVERY USING FLUIDIZED BED HEAT EXCHANGERS(FBHX)
00150C     FOR CEMENT KILN AND ELECTRIC ARC FURNACE APPLICATIONS.
00160C
00170C     DECEMBER,1979  -  MIDWEST RESEARCH INSTITUTE
00180C
00190C     BY  T. WEAST, V. RAMANATHAN, AND T.SUTIKNO
00200C
00210C     PROGRAM SEQUENCE, ARRANGED IN MODULES, IS AS FOLLOWS:
00220C
00230C MODULE (1): DATA INPUT: USER-PROVIDED DATA ON WASTE ENERGY
00240C     STREAM, WASTE HEAT BOILER/STORAGE FLOW SPLIT,
00250C     DURATION OF CHARGE/DISCHARGE, GAS OUTLET TEMPERATURE
00260C     DURING DISCHARGE, STORAGE MEDIA PRLPERTIES, AND GRID
00270C     HOLE DIAMETER
00280C
00290C
00300C MODULE (2): DETERMINATION OF FBHX NUMBER OF STAGES, GAS, SOLID
00310C     FLOW RATES DURING CHARGE AND DISCHARGE AND
00320C     TEMPERATURE DISTRIBUTION. THE FBHX SOLID/GAS M*CP
00330C     RATIOS DURING CHARGE AND DISCHARGE ARE COMPUTED
00340C     USING NEWTON'S METHOD
00350C
00360C
00370C MODULE (3): DETERMINATION OF OPERATING VELOCITY(UOP)
00380C     SUCH THAT TERMINAL VELOCITY(UTU) > UOP >
00390C     MINIMUM FLUIDIZATION VELOCITY(UMFU) AT ALL STAGES
00400C     DURING CHARGE AND DISCHARGE. BED DIAMETER IS THEN
00410C     CALCULATED USING FLOWRATE AND VELOCITY
00420C
00430C MODULE (4): FBHX GRID DESIGN CORRESPONDING TO THE
00440C     MINIMUM VOLUMETRIC FLOWRATE CONDITIONS.
00450C     ALSO A FINAL CHECK IS MADE ON DEPTH OF BED
00460C     WITH AN ACCURATE DETERMINATION OF JPD;
00470C     IF BD < JPDMX RETURN TO MODULE (3) WITH THE NEW BD
00480C
00490C MODULE (5): CALCULATION OF TRANSPORT DISENGAGEMENT HEIGHT(TDH)
00500C     AND ATTRITION RATE AND  YEARLY STORAGE MEDIA
00510C     REPLACEMENT NEEDS
00520C
00530C MODULE (6): DETERMINATION OF BLOWER HP FOR
00540C     PRESSURIZING GAS THROUGH FBHX DURING CHARGE AND DISCHARGE
00550C
00560C MODULE (7); DESIGN OF PNEUMATIC TRANSPORT SYSTEM
00570C     FOR MOVING THE STORAGE MEDIA BETWEEN FBHX AND
00580C     COLD/HOT STORES: TUBE DIAMETER, PRESSURE DROP,
00590C     AND HP DURING CHARGE AND DISCHARGE
00600C
00610C MODULE (8): PERFORM OVERALL RECOVERY AND STORAGE
00620C     ENERGY BALANCE CALCULATIONS
00630C
```

```
00640C MODULE(9): PROGRAM OUTPUT: FBHX NUMBER OF STAGES, TEMPERATURE
00650C    DISTRIBUTION,  SOLID/GAS M*CP RATIO FOR CHARGE AND DISCHARGE,
00660C    FLOW RATES, BED OPERATING PARAMETERS, VELOCITY, FBHX
00670C    DIMENSIONS, GRID DESIGN, JPD, TDH, ATTRITION RATE,
00680C    PNEUMATIC TRANSPORT SYSTEM DESIGN, OVERALL ENERGY BALANCE,
00690C    AND FBHX TES SYSTEM PERFORMANCE
00700C
00710C
00720C
00730     PROGRAM TES1(INPUT,OUTPUT)
00740     DIMENSION T(4),P(4),GFRCR(4)
00750     DIMENSION RHOGC(4),VGFR(4),UGR(4),UMFU(4),UTU(4)
00760     DIMENSION V(4)
00770     DIMENSION UOP(4),VSR(4),DBO(4),DBN(4)
00780     DIMENSION DU(4),TDH(4),AHPG(4)
00790     DIMENSION SFR(2),USDT2(2),RHO(2),UTPN(2),B6(2),B7(2)
00800     DIMENSION DPB7(2),UCSM(2),UCS(2),US(2),UO(2)
00810     DIMENSION DTP(2),GSG(2),DELPP(2),UGP(2),CFMP(2)
00820     DIMENSION DELPPT(2),HPP(2)
00830     DIMENSION PCWH(2),EWHB(2),ETS(2),TEFRS(2)
00840     INTEGER OPTION
00850     REAL MUG,MUGC(4),JPD(4),JPDMX,KW(2),KWHPT(2),KWNS,KWHNSPT
00860     DATA CPS,CPG,WHBET/0.2,0.28,300.0/
00870     DATA DT/100./
00880     DATA PI,G,GC/3.14159,32.18,32.2/
00890     DATA TEEF/30./
00900     RHOG(T,P)=29./359.*492./(T+460.)*P/14.7
00910     MUG(T)=1.254E-5+1.1342E-8*T
00920     UMF(U,D,RS,RG)=U/D/RG*((33.7**2+(D**3)*RG*(RS-RG)*32.2*
00930+    0.0408/U**2)**.5-33.7)
00940     UT(U,D,RS,RG)=((4./225.*((RS-RG)**2)*(32.2**2)/RG/U)**
00950+    (1./3.))*D
00960C
00970C     MODULE (1): INPUT DATA
00980C
00990     PRINT,/,/,/
01000   1 PRINT, *INPUT SYSTEM OPERATING CONDITIONS:*
01010     PRINT,*OPTION(0=STOP, 1=CEMENT KILN, 2=ELECTRIC ARC FURNACE) ? ?*,
01020     READ ,OPTION
01030     PRINT,/
01040     IF(OPTION.EQ.1) GO TO 4
01050     IF(OPTION.EQ.2) GO TO 3
01060     GO TO 280
01070   3 PRINT,/
01080     GO TO 5
01090   4 PRINT,*CGFR,CP(TONS/HR),CGT?*
01100     READ,CGFR,CP,CGT
01110   5 PRINT,*TGFR,GFRC,GITC,CHT,GFRD,GOTD,DCT*
01120     READ,TGFR,GFRC,GITC,CHT,GFRD,GOTD,DCT
01130     PCT=GFRC/TGFR*100.
01140     PCW=100.-PCT
01150     PRINT,*PARTDI(FT),PARTDE,BLKDS,HDIA(FT)*
01160     READ,PARTDI,PARTDE,BLKDS,HDIA
01170   6 CONTINUE
```

```
01180     BD=0.5
01190     GITD=WHBET+10.
01200     GITDN=GITD
01210C
01220C     MODULE (2): FBHX STAGES, FLOWS, TEMPERATURES
01230C
01240     DELTQ=GFRC*GITC*CHT-GFRD*GOTD*DCT
01250     IF((DELTQ/GFRC/GITC/CHT).LE.0.05) GO TO 276
01260     IF((GITC-GOTD).LE.50.) GO TO 277
01270     RRCRD=GFRD/GFRC*DCT/CHT
01280     TCOUNT=1.
01290   7 ICOUNT=0
01300     GITD=GITD+(GITDN-GITD)*.5
01310     N=1.
01320   8 RC=(1.+1./N/N)*((RRCRD+1.)/2.)
01330  10 RD=RC/RRCRD
01340  20 ESC=N/(N+1.)
01350     IF(RC.NE.1.0) ESC=(RC**N-1.)/(RC**(N+1.)-1.)
01360     ESD=N/(N+1.)
01370     IF(RD.NE.1.0) ESD=(RD**N-1.)/(RD**(N+1.)-1.)
01380     GOTDN=GITD+(GITC-GITD)*RD/(1./ESC+1./ESD-1.)
01390     IF(ABS(GOTDN-GOTD).LE.0.005) GO TO 77
01400     IF(GOTDN.GT.GOTD) GO TO 30
01410     IF(ICOUNT.EQ.0) N=N+1.
01420     IF(ICOUNT.EQ.0) GO TO 8
01430  30 IF(ICOUNT.EQ.0)N=N-1.
01440     IF(ICOUNT.EQ.0)HIGHN=N+1.
01450     ICOUNT=ICOUNT+1.
01460     ACO=(GOTD-GITD)/(GITC-GITD)
01470     IF(N.LT.0.99) N=N+1.
01480     IF(ICOUNT.EQ.1)RCI=RC
01490     IF(ICOUNT.GT.1) GO TO 31
01500     RC=.99
01510     IF((ACO-N/(N+2.)).GT.0.01) RC=1.01
01520  31 IF(ABS(ACO-N/(N+2.)).GE.0.01) GO TO 35
01530  33 RC=ACO*(1./ESC+1./ESD-1.)*RRCRD
01540     IF(RC.GT.2.0)N=HIGHN
01550     IF(RC.GT.2.0)RC=RCI
01560     IF(ICOUNT.LE.250) GO TO 10
01570     N=N+1.
01580     ICOUNT=1
01590     GO TO 8
01600  35 DO 80 I=1,250
01610     RCO=RC
01620     RDO=RCO/RRCRD
01630     IF(RDO.NE.1.0) GO TO 40
01640     AC1=(N+1.)/N
01650     A5=1./(N+1.)**2.
01660     GO TO 50
01670  40 AC1=(RDO**(N+1.)-1.)/(RDO**N-1.)
01680     A2=(RDO**N-1.)*(N+1.)*(RDO**N)/RRCRD
01690     A3=(RDO**(N+1.)-1.)*N*(RDO**(N-1.))/RRCRD
01700     A4=(RDO**N-1.)*(RDO**N-1.)
01710     A5=(A2-A3)/A4
```

```
01720 50 IF(RCO.NE.1.0) GO TO 60
01730    AC2=(N+1.)/N
01740    A9=1./(N+1.)**2.
01750    GO TO 70
01760 60 AC2=(RCO**(N+1.)-1.)/(RCO**N-1.)
01770    A6=(RCO**N-1.)*(N+1.)*(RCO**N)
01780    A7=(RCO**(N+1.)-1.)*N*(RCO**(N-1.))
01790    A8=(RCO**N-1.)*(RCO**N-1.)
01800    A9=(A5-A6)/A7
01810 70 A1=ACO-RDO/(AC1+AC2-1.)
01820    APM=(RDO*(A5+A9)-(AC1+AC2-1.)/RRCRD)/(AC1+AC2-1.)**2.
01830    RC=RCO-A1/APM
01840    IF(RC.LE.0.0) N=N+1.
01850    IF(RC.LE.0.0) GO TO 8
01860    IF(RC.GT.2.0) N=N+1.
01870    IF(RC.GT.2.0) GO TO 8
01880    IF(ABS(RC-1.0).LE.0.01) GO TO 33
01890    IF(ICOUNT.GE.200)N=HIGHN
01900    IF(ICOUNT.GE.200) RC=RCI
01910    IF(ICOUNT.GE.200)ICOUNT=1
01920    IF(ICOUNT.GE.200) GO TO 10
01930    IF(ABS((RCO-RC)/RC).LE.0.0001) GO TO 10
01940 80 CONTINUE
01950    IF(ICOUNT.EQ.1.)N=HIGHN
01960    RC=RCI
01970    GO TO 10
01980 77 SFRC=GFRC*RC*CPG/CPS
01990    TCOUNT=TCOUNT+1.
02000    SFRD=GFRD*RD*CPG/CPS
02010    GOTC=GITC-(GOTD-GITD)*RRCRD
02020    CST=GITC-(GITC-GOTC)/RC/ESC
02030    HST=GITD+(GOTD-GITD)/RD/ESD
02040    SITC=CST
02050    SOTC=HST
02060    SITD=HST
02070    SOTD=CST
02080    IF(TCOUNT.GE.50)GO TO 303
02090C
02100C     MODULE (3): FBHX OPERATING GAS VELOCITY, BED DIAMETER
02110C
02120  85 BPD=BD*BLKDS/144.*1.3
02130    TBPD=BPD*N
02140    P(1)=14.7
02150    IF(OPTION.EQ.2) P(1)=14.2
02160    P(2)=P(1)-TBPD
02170    IF(P(2).GT.7.)GO TO 88
02180    PRINT,*TBPD IS TOO HIGH FOR THE USE OF AN INDUCED-DRAFT FAN.*
02190    GO TO 280
02200 88 P(3)=14.7+TBPD
02210    P(4)=14.7
02220    T(1)=GITC
02230    T(2)=GOTC
02240    T(3)=((WHBET+460.)*(P(3)/14.7)**(.4/1.4))-460.
02250    GITDN=T(3)
```

```
02260      T(4)=GOTD
02270      GFRCR(1)=GFRC
02280      GFRCR(2)=GFRC
02290      GFRCR(3)=GFRD
02300      GFRCR(4)=GFRD
02310      DO 100 I=1,4
02320      RHOGC(I)=RHOG(T(I),P(I))
02330      MUGC(I)=MUG(T(I))
02340      UMFU(I)=UMF(MUGC(I),PARTDI,PARTDE,RHOGC(I))
02350      UTU(I)=UT(MUGC(I),PARTDI,PARTDE,RHOGC(I))
02360      VGFR(I)=GFRCR(I)/3600./RHOGC(I)
02370      IF(I.NE.1)GO TO 90
02380      UTC=UTU(1)
02390      UMFC=UMFU(1)
02400      VGFRM=VGFR(1)
02410      RHOGCR=RHOGC(1)
02420      VGFRMX=VGFR(1)
02430      GO TO 100
02440   90 IF(UTU(I).LT.UTC)UTC=UTU(I)
02450      IF(UMFU(I).GT.UMFC)UMFC=UMFU(I)
02460      IF(VGFR(I).LT.VGFRM)VGFRM=VGFR(I)
02470      IF(VGFR(I).LT.VGFRM)RHOGCR=RHOGC(I)
02480      IF(VGFR(I).GT.VGFRMX)VGFRMX=VGFR(I)
02490   100 CONTINUE
02500      UMIN=UMFC
02510      UMAX=UTC
02520      UMOP=(UMAX-UMIN)/6.+UMIN
02530      AK=1
02540   110 BAREA=VGFRM/UMOP
02550      IF(AK.GT.400)GO TO 275
02560      BDIA=(BAREA/PI*4.)**.5
02570      DO 120 I=1,4
02580      UOF(I)=VGFR(I)/BAREA
02590      IF(UOF(I).GE.UTU(I))GO TO 130
02600      IF(U   F(I).LE.UMFU(I))GO TO 140
02610   120 CONTINUE
02620      GO TO 150
02630   130 UMOP=UMOP*0.95
02640      AK=AK+1
02650      GO TO 110
02660   140 UMOP=UMOP*1.05
02670      AK=AK+1
02680      GO TO 110
02690C
02700C     MODULE (4): GRID DESIGN AND FINAL CHECK ON BED DEPTH
02710C
02720   150 GPD=BPD*.3/1.3
02730      UGRMIN=.8*(2.*G*GPD*144./RHOGCR)**.5
02740      HAMAX=VGFRM/UGRMIN
02750      PCTFA=HAMAX/BAREA*100.
02760      APH=(HDIA**2)*PI/4.
02770      NHOLES=HAMAX/APH
02780      DO 160 I=1,4
02790      UOR(I)=VGFR(I)/HAMAX
```

```
02800     JPD(1)=HDIA*.5.*((RHOGC(I)/(PARTDE-RHOGC(I))*
02810+    (UGR(I)**2)/G/HDIA)**0.187)
02820     IF(I.EQ.1)JPDMX=JPD(1)
02830 160 IF(JPD(I).GT.JPDMX)JPDMX=JPD(I)
02840     IF(ABS(1.1*JPDMX-BD).LE.0.0005) GO TO 170
02850     BD=1.1*JPDMX
02860     GO TO 85
02870 170 IF(ABS(GITDN-GITD).GT.0.05)GO TO 7
02880     GIPC=P(1)
02890     GOPC=P(2)
02900     GIPD=P(3)
02910     GOPD=P(4)
02920     DO 165 I=1,4
02930     V(I)=VGFR(I)*60.
02940 165 CONTINUE
02950C
02960C     MODULE (5): TDH AND ATTRITION RATE
02970C
02980     DO 180 I=2,4,2
02990     VSR(I)=VGFR(I)/HAMAX*RHOGC(I)**.5
03000     DBO(I)=HDIA/2.*(-95.09+73.0897*(ALOG10(VSR(I))))
03010     DBN(I)=DBO(I)*(.15*BD/DBO(I)+.85)
03020     DU(I)=UOP(I)-UMFU(I)
03030     TDH(I)=(EXP(3.245-.647*(ALOG(DU(I)))+5.499E-2*DBN(I)*12.))/12.
03040 180 CONTINUE
03050     TDHMX=TDH(2)
03060     IF(TDH(4).GT.TDHMX)TDHMX=TDH(4)
03070     TBDHT=(N-1)*(BD+2.)+BD+TDHMX+3.
03080     ATTRT=.00349/6./2.*((UGRMIN*(RHOGCR**.5))**2.5)*
03090+    HAMAX/454*60.
03100     GRLDGC=ATTRT/3600.*7000./VGFR(2)
03110     GRLDGD=ATTRT/3600.*7000./VGFR(4)
03120     SRPY=ATTRT*(CHT+DCT)*360./2000.
03130C
03140C     MODULE (6): BLOWER HP
03150C
03160     AHPG(1)=VGFR(2)*60.*P(2)*144./33000.*1.4/.4*
03170+    ((14.7/P(2))**(.4/1.4)-1.)
03180     AHPG(2)=GFRD/60.*(GITD+460)/39.7437*14.7*144./33000.
03190+    *1.4/.4*((P(3)/14.7)**(.4/1.4)-1.)
03200C
03210C     MODULE (7): PNEUMATIC TRANSPORT SYSTEM DESIGN
03220C
03230     SFR(1)=SFRC
03240     SFR(2)=SFRD
03250     T(1)=(SITC+GOTC)/2.
03260     T(2)=(SITD+GITC)/2.
03270     P=17.
03280     DTO=1.
03290     VL=TBDHT*1.2
03300     TL=VL+30.
03310     DO 260 I=1,2
03320     USDT2(I)=SFR(I)/3600.*4./PI/PARTDE/.018
03330     RHO(I)=RHOG(T(I),P)
```

```
03340     UTPN(I)=UT(MUG(T(I)),PARTDI,PARTDE,RHO(I))
03350     B6(I)=(4.*G*MUG(T(I))*(PARTDE-RHO(I))/3./
03360+    (RHO(I))*2)**(1./3.)
03370     B7(I)=(3.*(MUG(T(I)))**2/4./G/RHO(I)/
03380+    (PARTDE-RHO(I)))**(1./3.)
03390     DPB7(I)=PARTDI/B7(I)
03400     UCSM(I)=B6(I)*(.667-.135*DPB7(I)+.148*(DPB7(I))**2)
03410     DTN=DTO
03420 200 UCS(I)=(UCSM(I)*30.48*DTN/6.35)**.4
03430     US(I)=USDT2(I)/DTN**2
03440     UO(I)=(US(I)+UTPN(I))*(0.914+0.0291*PARTDE/62.4)
03450     IF(UO(I).GT.UCS(I))GO TO 210
03460     DTN=DTN-.05
03470     GO TO 200
03480 210 IF((UO(I)-UCS(I)).LE.(2.*UCS(I)))GO TO 220
03490     DTN=DTN+.05
03500     GO TO 200
03510 220 DTP(I)=DTN
03520     GSG(I)=US(I)/UO(I)*PARTDE/RHO(I)*.018
03530     DELPF(I)=GSG(I)*UO(I)/US(I)*RHO(I)*VL
03540+    +US(I)/GC*RHO(I)*UO(I)*GSG(I)
03550+    +2.*.02*UO(I)/US(I)*GSG(I)*RHO(I)
03560+    *(UO(I)**2)*TL/GC/DTP(I)
03570     DELPF(I)=DELPF(I)/144.
03580     UGF(I)=UO(I)/(0.914+0.0291*PARTDE/62.4)
03590     CFMF(I)=UGF(I)*PI*(DTP(I)**2)/4.*60.
03600     DELPFT(I)=1.2*DELPF(I)
03610     HPF(I)=CFMF(I)*DELPFT(I)*27.68/6356./.7
03620     IF(I.EQ.1)GO TO 240
03630     DTD=DTN
03640     HPFD=HPF(I)
03650     GO TO 260
03660 240 DTC=DTN
03670     DTO=DTC
03680     HPFC=HPF(I)
03690 260 CONTINUE
03700C
03710C     MODULE (8): OVERALL ENERGY BALANCE
03720C
03730     CGE=0.
03740     IF(OPTION.EQ.1)CGE=CGFR*CPG*(CGT-WHBET)
03750     FCWH(1)=FCW/100.
03760     FCWH(2)=1.
03770     ETESD=0.
03780     DO 250 I=1,2
03790     EWHB(I)=FCWH(I)*TGFR*CPG*(GITC-WHBET)
03800     ETS(I)=(AHPG(I)+HPF(I))*2546/(TEEF/100.)
03810     IF(I.EQ.2)ETESD=GFRD*CPG*(GOTD-WHBET)
03820     TEFRS(I)=EWHB(I)+CGE-ETS(I)+ETESD
03830     KW(I)=TEFRS(I)/3414.*TEEF/100.
03840     KWHPT(I)=0.
03850     IF(OPTION.EQ.1)KWHPT(I)=KW(I)/CP
03860 250 CONTINUE
03870     TER=(EWHB(2)+CGE)*(CHT+DCT)
```

```
03880     TERS=TEFRS(1)*CHT+TEFRS(2)*DCT
03890     EFORS=TERS/TER*100.
03900     KWNS=(EWHB(2)+CGE)/3414.*TEEF/100.
03910     KWHNSPT=0.
03920     IF(OPTION.EQ.1)KWHNSPT=KWNS/CF
03930     DKWC=KWNS-KW(1)
03940     DKWD=KW(2)-KWNS
03950     RKW=DKWD/DKWC
03960     RKWH=RKW*DCT/CHT
03970C
03980C     MODULE (9): PROGRAM OUTPUT
03990C
04000     PRINT,/,/,*OPTION  *,OPTION
04010     PRINT,/,/,*CHARGE CYCLE*
04020     PRINT,/,*RC,GFRC,SFRC,N,GITC,SITC,GOTC,SOTC*
04030     PRINT,RC,GFRC,SFRC,N,GITC,SITC,GOTC,SOTC
04040     PRINT,*TBPD,VGFRIC,VGFROC,AHPGC,TEFRSC,DELPPTC,HPPC*
04050     PRINT,TBPD,VGFR(1),VGFR(2),AHPG(1),TEFRS(1),DELPPT(1),HPPC
04060     PRINT,/,/,*DISCHARGE CYCLE*
04070     PRINT,/,*RD,GFRD,SFRD,N,GITD,SITD,GOTD,SITD*
04080     PRINT,RD,GFRD,SFRD,N,GITD,SITD,GOTD,SOTD
04090     PRINT,*TBPD,VGFRID,VGFROD,AHPGD,TEFRSD,DELPPTD,HPPTD*
04100     PRINT,TBPD,VGFR(3),VGFR(4),AHPG(2),TEFRS(2),DELPPT(2),HPPD
04110     PRINT,/,/,*GENERAL FLUID BED OPERATING CONDITIONS*
04120     PRINT,/,*T1,T2,T3,T4      P1,P2,P3,P4      V1,V2,V3,V4*
04130     PRINT,GITC,GOTC,GITD,GOTD,GIPC,GOPC,GIPD,GOPD,V(1),V(2),V(3),V(4)
04140     PRINT,*UMF1,UMF2,UMF3,UMF4, UOP1,UOP2,UOP3,UOP4, UTU1,UTU2,UTU3,UT
04150     PRINT,UMFU(1),UMFU(2),UMFU(3),UMFU(4),UOP(1),UOP(2),UOP(3),UOP(4)
04160     PRINT,UTU(1),UTU(2),UTU(3),UTU(4)
04170     PRINT,*UMOF,BD,JPDMX,TDHMX,PCTFA,NHOLES,TBDHT,BDIA*
04180     PRINT,UMOF,BD,JPDMX,TDHMX,PCTFA,NHOLES,TBDHT,BDIA
04190     PRINT,*ATTRITION/CARRYOVER:LBS/HR,GRLDGC,GRLDGD(GR/FT3),SRPY(T/YR)
04200     PRINT,ATTRT,GRLDGC,GRLDGD,SRPY
04210     PRINT,*DTC,DTD,UOC,UOD*
04220     PRINT,DTC,DTD,UO(1),UO(2)
04230     PRINT,/,/,*OVERALL ENERGY BALANCE*,/
04240     IF(OPTION.EQ.1)GO TO 265
04250     GO TO 270
04260 265 PRINT,*KWHPT DURING CHARGE, KWNSPT, KWHPT DURING DISCHARGE*
04270     PRINT,KWHPT(1),KWHNSPT,KWHPT(2)
04280 270 PRINT,*TER,TERS,EFORS(BTU BASIS)*
04290     PRINT,TER,TERS,EFORS
04300     PRINT,*KWC,KWNS,KWD*
04310     PRINT,KW(1),KWNS,KW(2)
04320     PRINT,*DKWC,DKWD,RKW,RKWH*
04330     PRINT,DKWC,DKWD,RKW,RKWH
04340     PRINT  ,/
04350     GO TO 1
04360 275 PRINT,*EXCESSIVE ITERATIONS, TRY ANOTHER VALUE OF HDIA.*
04370     GO TO 5
04380 276 PRINT,*REQUESTED OUTPUT ENERGY IS TOO LARGE--REENTER DATA*
04390     GO TO 5
04400 277 PRINT,*DISCHARGE OUTLET TEMPERATURE TOO LARGE--REENTER DATA*
04410     GO TO 5
```

```
04420 303 PRINT,*INPUT NEW GOTO*
04430     READ,GOTO
04440     GO TO 6
04450 280 STOP
04460     END
```

TABLE C-1

BASE CASE SIMULATION RESULT FOR CEMENT KILN

```
INPUT SYSTEM OPERATING CONDITIONS:
OPTION(0=STOP, 1=CEMENT KILN, 2=ELECTRIC ARC FURNACE) ? ? ? 1

COFR,CP(TONS/HR),COT?
 ? 1,70,400
TOFR,OFRC,GITC,CHT,OFRD,GOTD,DCT
 ? 535000,.07000,1400,12,147000,800,12
PARTDI(FT),PARTDE,BLKDS,HDIA(FT)
 ? 1.15E-3,154,90,.010417

OPTION                                :

CHARGE CYCLE

RC,OFRC,SFRC,N,GITC,SITC,GOTC,SOTC
       9.40741E-01        107000.00          140922.94                5
          1400.00           403.71             515.87            915.15
THPD,VGFRIC,VGFROC,AHPOC,TEFRSC,DELPPIC,HPPC
             1.32          1091.80             874.25            268.63
       31510210.80           1.22              10.84

DISCHARGE CYCLE

RD,OFRD,SFRD,N,GITD,SITD,GOTD,SITD
       9.40741E-01        107000.00          140922.94                5
           318.87           915.15             800.00            403.71
TBPD,VGFRID,VGFROD,AHPGD,TEFRSD,DELPPID,HPPTD
             1.32           534.51             942.29            195.13
       1.18100E+08       9.81091E-01             9.38

GENERAL FLUID BED OPERATING CONDITIONS

T1,T2,T3,T4      P1,P2,P3,P4       V1,V2,V3,V4
          1400.00           518.87             318.87            800.00
            14.73            13.38              16.02             14.73
         65511.38         49254.84           32470.57          56337.22
UMF1,UMF2,UMF3,UMF4, UOP1,UOP2,UOP3,UOP4, UTU1,UTU2,UTU3,UTU4
       1.01374E-01      2.08326E-01        2.35964E-01       1.79775E-01
             3.43             2.52               1.68              2.90
             9.94             9.75               8.59              9.74
UMOP,RD,UPOD,TDHX,PCTFA,NHOLES,IBDHI,HDIA
             1.08      3.24369E-01        2.95136E-01              4.52
             1.46            54438              17.14             24.14
ATTRITION/CARRYOVER:LBS/HR,GRLDGC,GRLDGD(GR/FT3),SHPY(T/YR)
       2.60971E-01      6.79139E-04        5.79049E-04              1.21
DTC,DTD,UOC,UOD
             1.15             1.30              22.52             20.00

OVERALL ENERGY BALANCE

KWHPT DURING CHARGE, KWNSPT, KWHPT DURING DISCHARGE
           142.33           131.63             148.26
TER,TERS,EFORS(BTU BASIS)
       2.51654E+09      2.30547E+09              93.19
KWC,KWNS,KWD
          7163.11          9214.41           10377.57
DKWC,DKWD,RKW,RKWI
          2051.30          1163.46        5.07182E-01       5.07182E-01
```

TABLE C-2

BASE CASE SIMULATION RESULT FOR ELECTRIC ARC FURNACE

APPENDIX D

DERIVATION OF EQUATIONS FOR SIZING OF THE ELECTRIC ARC FURNACE BUFFER WITHOUT SOLIDS STORAGE AND RETRIEVAL

In order to determine the mass of the electric arc furnace buffer, it is necessary to first consider the basic energy storage equation:

$$Q_{in} - Q_{out} = Q_{stored} + Q_{loss}$$

If it is assumed that the energy losses are minimal and that the exit gas temperature equals the fluid bed buffer temperature, the following differential equation results for a single stage buffer:

$$\dot{M}_g C_g (T_{gi} - T_B) = M_B C_B \frac{dt_B}{dt} \qquad (D\text{-}1)$$

or

$$\frac{dt_B}{dt} + \frac{\dot{M}_g C_g}{M_B C_B} T_B = \frac{\dot{M}_g C_g}{M_B C_B} T_{gi} \qquad (D\text{-}2)$$

$\dot{M}_g$, C_g, and T_{gi} are the gas mass flow rate, specific heat and inlet temperature, respectively; M_B, C_B, and T_B are the fluid bed material mass, specific heat and temperature, respectively; and t is time. It should be noted that the temperatures are measured relative to the average gas temperature (i.e., the actual bed temperature is T_B plus the average gas temperature and the actual inlet gas temperature is T_{gi} plus the average gas temperature). If the inlet gas temperature is assumed to vary periodically with time in a sinusoidal manner with an amplitude, A, and frequency, ω, the following equation for the inlet gas temperature results:

$$T_{gi} = A \sin (\omega t) \qquad (D\text{-}3)$$

Substituting this in the preceding differential equation and solving for the bed temperature which is also equal to the outlet gas temperature gives:

$$T_B = T_{GO} = \frac{\alpha}{\alpha^2 + \omega^2} [\alpha \sin (\omega t) - \omega \cos (\omega t)] + c_1 e^{-\alpha t} \qquad (D\text{-}4)$$

where $\alpha = \dfrac{\dot{M}_g C_g}{M_B C_B}$

and c_1 = an integration constant dependent on initial conditions

An alternate form of the equation for the bed temperature is the following:

$$T_B = T_{GO} = A\left[\frac{\alpha}{\sqrt{\alpha^2 + \omega^2}}\right] \sin\left[\omega t - \tan^{-1}\left(\frac{\omega}{\alpha}\right)\right] + c_1 e^{-\alpha t} \quad \text{(D-5)}$$

Comparing this equation with the inlet gas temperature equation shows that they are very similar. The amplitude of the outlet gas temperature has been reduced by the factor $\alpha/\sqrt{\alpha^2 + \omega^2}$. The frequency of the periodic temperature variation remained the same; however, the occurrence has been delayed by a phase angle shift equal to $\tan^{-1}(\omega/\alpha)$. The term containing the integration constant is a transient which approaches zero if the system has been operating for any length of time and can be neglected for continuous operation of the buffer.

Following the development of the equation for the single stage buffer, two stage and multiple stage buffers were examined. The equation for a multiple stage buffer is:

$$T_{GO} = G_{B_N} = A\left[\frac{\alpha_1\alpha_2\ldots\alpha_N}{\sqrt{(\alpha_1^2 + \omega^2)\ (\alpha_2^2 + \omega^2)\ldots(\alpha_N^2 + \omega^2)}}\right] \sin\left[\omega t - \tan^{-1}\left(\frac{\omega}{\alpha_1}\right) - \tan^{-1}\left(\frac{\omega}{\alpha_2}\right) - \ldots\tan^{-1}\left(\frac{\omega}{\alpha_N}\right)\right] \quad \text{(D-6)}$$

If it is assumed that $\alpha_1 = \alpha_2 = \ldots\alpha_N = \alpha$, then the equation can be simplified to:

$$T_{GO} = T_{B_N} = A\left[\frac{\alpha^N}{(\alpha^2 + \omega^2)^{N/2}}\right] \sin\left[\omega t - N \tan^{-1}\left(\frac{\omega}{\alpha}\right)\right] \quad \text{(D-7)}$$

If the new variable, r , is defined as the bed attenuation or the ratio of the output amplitude to the original input temperature amplitude, then:

$$r = \frac{\alpha^N}{(\alpha^2 + \omega^2)^{N/2}} \quad \text{(D-8)}$$

Solving for α as a function of r , N , and ω gives:

$$\alpha = \frac{\omega}{\sqrt{\frac{1}{r}^{2/N} - 1}} \quad \text{(D-9)}$$

From the definition of α the mass of each fluid bed stage may be determined by:

$$M_B = \frac{\dot{M}_g C_g}{\omega C_B} \sqrt{\left(\frac{1}{r}\right)^{2/N} - 1} \qquad \text{(D-10)}$$

To obtain the total mass, it is necessary to multiply by the number of stages, N, which results in the following equation:

$$M_{B_T} = \frac{N\dot{M}_g C_g}{\omega C_B} \sqrt{\left(\frac{1}{r}\right)^{2/N} - 1} \qquad \text{(D-11)}$$

If the electric arc furnace exit gases have a periodic temperature variation which differs from the sinusoidal temperature assumed in Eq. (D-3), the previous solutions may still be utilized if the temperature variation can be represented by a Fourier series expansion. For example, the Fourier series for temperature variation in the form of a square wave with an amplitude A relative to the mean temperature and a period of L for each cycle is the following:

$$T_{gi} = A \frac{4}{\pi} \sum_{n = 1,3,5\ldots} \frac{1}{n} \sin (n\omega t) \qquad \text{(D-12)}$$

If each term of the Fourier series expansion is integrated separately and the transient term with the integration constant is neglected, the following solution results for a single stage bed:

$$T_{GO} = T_B = A \frac{4}{\pi} \sum_{n = 1,3,5\ldots} \frac{1}{n} \left[\frac{\alpha}{\sqrt{\alpha^2 + n^2\omega^2}}\right] \sin \left[n\omega t - \tan^{-1}\left(\frac{n\omega}{\alpha}\right)\right] \qquad \text{(D-13)}$$

For a multistage fluid bed with N identical stages, the solution for a square wave input temperature variation is:

$$T_{GO} = T_{B_N} = A \frac{4}{\pi} \sum_{n = 1,3,5\ldots} \frac{1}{n}\left[\frac{\alpha^N}{(\alpha^2 + N^2\omega^2)^{N/2}}\right] \sin \left[n\omega t - N \tan^{-1}\left(\frac{n\omega}{\alpha}\right)\right] \qquad \text{(D-14)}$$

Because Eqs. (D-12), (D-13), and (D-14) are series, no direct calculation of the bed mass such as in Eqs. (D-8) through (D-11) is possible. Therefore, a bed mass would have to be assumed and the outlet gas temperature calculated at different times. Because the phase shift for each

term is different, the periodic form of the outlet gas temperature would no longer be a square wave and the maximum temperature would have to be determined by trial and error.

Solutions for other wave forms, such as ramps and saw-tooths, which can be replaced with Fourier series expansions would be similar to Eq. (D-13) and (D-14).